2017

Where does the Oxygen go? – Pathways and Partitioning in Autothermal Pyrolysis

Ross David Mazur
Iowa State University

Where does the oxygen go? – Pathways and partitioning in autothermal pyrolysis

by

Ross David Mazur

A thesis submitted to the graduate faculty

in partial fulfillment of the requirements for the degree of

MASTER OF SCIENCE

Co-Majors: Mechanical Engineering; Biorenewable Resources and Technology

Program of Study Committee:
Robert Brown, Major Professor
David Laird
Dave R Raman
Travis Sippel
Mark Mba-Wright

Iowa State University

Ames, Iowa

2017

DEDICATION

I would like to dedicate my thesis work to my sister, Elise, my father, Peter, and my mother, Helene, who are omnipresent for support, bouncing ideas off of, and critical feedback.

TABLE OF CONTENTS

LIST OF FIGURES

LIST OF TABLES

GLOSSARY OF TERMS

- Mercerization - A process in which spun lignocellulosic fibers are rapidly impregnated with a chemical lye, allowed to swell, then are overstretched lengthwise along the fiber's length (causing axial shrinkage), followed by crosswise stretching then rolling ("fixing"), and washed to remove the lye solution. Mercerization has the effect of increasing sheen and softness of the fibers, by partially separating and tearing whole fibers into their macrofibrils subunits [1]
- Micropyrolyzer – refers to a vertical microfurnace manufactured by Frontier Labs. It operates in batch with continuous flow of sweep gas. Used for high throughput testing of pyrolysis experiments in a well-controlled, reproducible environment.
- Oxidation
    - Oxidation (Chemistry; as opposed to reduction)
        - loss of electrons from substance of interest to oxidizing agent (oxidizing agent is reduced, gains electrons) [2]
        - "A reaction that results in a loss of electron density by carbon, caused either by bond formation between carbon and a more electronegative atom – usually oxygen, nitrogen, or a halogen –or by bond-breaking between carbon and a less electronegative atom –usually hydrogen. Note that *oxidation* often adds oxygen while a *reduction* often adds hydrogen" [3]
    - Oxidation State/Number
        - "A measure of the degree of oxidation of an atom in a substance. It is defined as the charge an atom might be imagined to have when electrons are counted according to an agreed-upon set of rules: (l) the oxidation state of an oxidation state of -1 in hydrides of active metals, e.g. LiH, and oxygen has an oxidation state of -1 in peroxides, e.g. H_2O_2; (4) the algebraic sum of oxidation states of all atoms in a neutral molecule must be zero, while in ions the algebraic sum of the oxidation states of the constituent atoms must be equal to the charge on the ion. For example, the oxidation states of sulfur in H_2S, S_8(elementary sulfur), SO_2, SO_3, and H_2SO_4 are, respectively: -2, 0, +4, +6 and +6. The higher the oxidation state of a given atom, the greater is its degree of oxidation; the lower the oxidation state, the greater is its degree of reduction" [4]
        - "Oxidation state (OSfree element (uncombined element) is zero; (2) for a simple (monatomic) ion, the oxidation state is equal to the net charge on the ion; (3) hydrogen has an oxidation state of 1 and oxygen has an oxidation state of -2 when they are present in most compounds. (Exceptions to this are that hydrogen has) is defined using ionic approximation of bonds. Two principal algorithms are outlined for OS determination in a chemical compound described by a Lewis formula or bond graph… The oxidation state of an atom is the charge of this atom after ionic approximation of its heteronuclear bonds." [5]
    - Oxidation (Thermochemistry; equilibrium oxidation) – In the case of combustion under excess oxygen, equilibrium oxidation of a carbonaceous material refers to oxidation to an extent such that all of the carbon is in the form of CO_2. In the case of

oxygen-starved processes, refers to oxidation to the extent that all molecular oxygen is consumed and reactive oxygen species have undergone chain termination reactions [6].

- Oxygen Electronic State
  - Triple Oxygen – normal gaseous oxygen (O_2, formally named 1,2-dioxidanediyl), having an electronic degree of degeneracy of three, resultant from the sum of its orbital angular momentum (*l=1*) *and* total electron spin angular momentum (2**S*), or (2*S*+1 for the various oxygen states) [7]. Since gaseous oxygen has two valent electrons with parallel spins, its total electron spin angular momentum is (2*(½ + ½) = 2), and thus has an electronic degree of degeneracy of 3, making it triplet oxygen [8] Because of two valent electrons, gaseous oxygen is often termed a diradical, which because of the parallel spins makes gaseous oxygen non-reactive with most substances (in the singlet state) at ambient conditions, other than radical species (often in the doublet state), found commonly at elevated temperatures or in the presence of catalyst [9] Gaseous oxygen is relatively unique in having a triplet ground state, most diatomic gases has singlet ground states [10]
  - Singlet Oxygen – a higher energy form of diatomic oxygen, occurs in two forms; delta singlet oxygen and epsilon singlet oxygen, both of which have two valence electrons of opposite spin. These differ by occupation of antibonding orbitals; epsilon's occupying two separate antibonding orbitals (unpaired), making it higher in energy and less stable than delta singlet oxygen (paired) [11] Singlet oxygen often found in the environment as a product of photochemical degradation of ozone and various organic compounds (such as turpentine), additionally is the product of some biochemical processes such as photosynthesis [12]
  - Molecular Oxygen -

- Combustion
  - (General definition) -"Combustion**,** a chemical reaction between substances, usually including oxygen and usually accompanied by the generation of heat and light in the form of flame. The rate or speed at which the reactants combine is high, in part because of the nature of the chemical reaction itself and in part because more energy is generated than can escape into the surrounding medium, with the result that the temperature of the reactants is raised to accelerate the reaction even more**...** Properly ignited, the heat from the flame raises the temperature of a nearby layer of the matchstick and of oxygen in the air adjacent to it, and the wood and oxygen react in a combustion reaction. When equilibrium between the total heat energies of the reactants and the total heat energies of the products (including the actual heat and light emitted) is reached, combustion stops. Flames have a definable composition and a complex structure; they are said to be multiform and are capable of existing at quite low temperatures, as well as at extremely high temperatures. The emission of light in the flame results from the presence of excited particles and, usually, of charged atoms and molecules and of electrons" [13]

  - (Complete Combustion) –"For complete combustion with the theoretical amount of air, the products consist of carbon dioxide, water, sulfur dioxide, the nitrogen accompanying the oxygen in air, and any nitrogen contained in the fuel" [6]
  - (Stoichiometric Combustion/Theoretical Air) –"The minimum amount of air that supplies sufficient oxygen for the complete combustion of all of the carbon, hydrogen, and sulfur present in the fuel" [6]
  - (Air-to-Fuel Ratio) –Simply the ratio of the amount of air in a reaction to the amount of fuel, expressed on either a molar ($\overline{AF}$) or mass (AF) basis, conversion between the two accomplished by division of the ratio of molecular weights of air and fuel [6]
  - (Equivalence Ratio) – "is the ratio of the actual fuel-air ratio to the fuel-air ratio for complete combustion with the theoretical amount of air. The reactants are said to form a *lean* mixture when the equivalence ratio is less than unity. When the ratio is greater than unity, the reactants are said to form a *rich* mixture" [6]
- Reactive Oxygen Species (ROS) – "are chemical constituents with oxygen atoms that are highly reactive in the ambient air … defined to include oxygen-centered or related free radicals such as hydroxyl (·OH), hydroperoxy (HOO·), alkoxy (RO·), and organic peroxy radicals (ROO·); ions such as superoxide (O_2^-), hypochlorite (ClO^-), and peroxynitrite ($ONOO^-$); and molecules such as hydroperoxide (ROOH) and organic peroxide (ROOR′)." [14]

NOMENCLATURE

- AAEM Alkaline and Alkaline Earth Metals
- ATR Autothermal Reformer
- CFP Catalytic Fast Pyrolysis
- DFT Density Functional Theory
- ER Equivalence Ratio
- FID Flame Ionization Detector
- FP Fast Pyrolysis
- GC Gas Chromatography
- GPC Gel Permeation Chromatography
- HPLC High Performance Liquid Chromatography
- HRP Horseradish Peroxidase
- HTL Hydrothermal Liquefaction
- LCC Lignin-Carbohydrate Complex
- MFSP Minimum Fuel Selling Price
- MS Mass Spectrometry
- PEV Plug-in Electric Vehicle
- PPDU Pyrolysis Process Development Unit
- Py-GC/MS Micropyrolyzer over GC-MS
- SF Stage Fraction (multi-stage fractionation bio-oil collection system)
- SLPM Standard Liters Per Minute
- SP Slow Pyrolysis
- TCD Thermal Conductivity Detector
- TEIC Total Equipment Installed Cost
- TGA Thermogravimetric Analyzer

ACKNOWLEDGEMENTS

I would like to thank my committee chair and major professor, Dr. Robert Brown, and my committee members, Dr. David Laird, Dr. Mark Wright Dr. Raj Raman, and Dr. Travis Sippel for their guidance, support, and inspiration throughout the course of this research.

In addition, I would like to thank my lab-colleagues and staff of the Bioeconomy Institute, friends in the Agronomy, Biorenewable Resources and Technology, and Mechanical Engineering departments, Graduate Program in Sustainable Agriculture, and roommates over the past two years for making this a memorable experience (and presumably those to come with future studies).

ABSTRACT

Autothermal fast pyrolysis (AFP), a variation of fast pyrolysis (FP) admitting a small amount of oxygen to provide process heat, has notable merit as a biomass-to-biofuels conversion process. As a result of heat transfer and product collection advantages over standard non-oxidative FP, it has the potential to generate a higher quality product in a more economically competitive manner. Initial investigation and process development efforts, first led by Kwang Ho Kim, and Joseph Polin, respectively, at the Bioeconomy Institute, generated many further questions about the process. One notable question was "where does the energy come from to support autothermal pyrolysis" – to which the obvious answer is *exothermic reactions*, but beyond that is not well understood. This work explored the chemistry underlying autothermal (partial oxidative) pyrolysis, as distinguished from standard non-oxidative pyrolysis of whole biomass. A critical literature review was carried out to develop a theoretical mechanistic framework which was then applied to a process base case, and experimentally tested.

Key findings of the literature review included reaction mechanisms for the oxidation of: lignin interunit linkages, lignin monomers (and their functionalities), cellulose dimers and monomers, *and* hemicellulose units and functionalities. As discussed in the cellulose oxidation section, oxidation could occur by means of assisting glycosidic bond hydrolysis (either at a chain end (*unzipping*) or mid-chain (*cracking*)), effectively increasing levoglucosan yield, *or* by oxidation of ring functionalities. If cellulose's substituents were to measurably react with Reactive Oxygen Species (ROS), the C_6 primary alcohol would be the likely candidate, oxidizing to a C_6 aldehyde or carboxylic acid, yet theoretically possible for ring-hydroxyls to oxidize.

Similarly to celluloses, hemicellulose might be oxidized by four means; polymer-end-wise chain scission initiation (*primary peeling*), mid-chain scission, end-chain unit degradation (*secondary peeling*), or side-chain oxidation. Because of its branched and heterogeneous nature, and tendencies for decomposition of monomeric units following complete depolymerization during non-oxidative pyrolysis, fewer hemicellulose hexoses and pentoses would likely be recovered during oxidative pyrolysis.

Lignin, also structurally diverse, has many possible routes for oxidation. From linkage studies, it is apparent that oxidation of the β- or γ-hydroxyl (in the case of a β-O-4' linkage), or the α-hydroxyl (for α-*O*-4' linkages) greatly weakens ether linkages, making susceptible to cleavage. Lignin's phenolic substituents are prone to oxidation to aldehydes, carboxylic acids and ketones. Those side chains with reactive double bonds could be oxidatively cleaved or encourage a concerted decomposition reaction. Because products of oxidation can be further oxidized themselves, care must be taken in extrapolating out composition trends to scaled-operation. Even considering these routes which would effect a change in product composition, the most significant effects might come simply due to improved reaction conditions (heat transfer, heating rate, and ventilation (due to greater gas production)).

Experimental work identified reactor limitations, and explored partial oxidation of a number of model compounds, representative of cellulose, hemicellulose, as well as lignin monomers and linkages. It is important to note that the findings of the micropyrolyzer studies are not directly applicable to continuous reactor chemistry due to the fundamentally different hydrodynamics and heat transfer. Additionally, biopolymer characteristics and interaction effects are not accounted for in the monomer and dimer model compound studies, as would be seen with whole biomass.

CHAPTER 1.
GENERAL INTRODUCTION

Background

Biomass-based economies and societies have prevailed for much of human civilization, declining with the advent of coal and oil-exploration. The implications and meaning of a *strong bioeconomy* have changed with time. For thousands of years it pertained to sourcing foods fuels and fibers from natural sources. Recently, it has more to do with the ability to provide the feedstocks and fuels which supply an industrial society; specifically, those compatible with existing conversion and production technology [15]. Although often not receiving dedicated efforts, there is a well-voiced desire for the modern bioeconomy to provide for new and not yet developed environmentally sensitive alternatives. For example, the six main synthetic polymers (polyethylene terephthalate (#1, PE), high density polyethylene (#2, HDPE), polyvinyl chloride (#3, PVC), low density polyethylene, (#4, LDPE), polypropylene (#5, PP), and polystyrene (#6, PS)), have become standards for which products and processes must be compatible. Thus much attention goes to converting biomass into these true compounds or making biobased compounds with comparable physical and chemical properties, when tasks might be better accomplished with biomaterials whose properties are incompatible with the six polymers. An example would be the application of the short rotation woody biomass crop kenaf for novel biocomposites or replacement of synthetic fiber products, [16]. Although there is great potential for these undeveloped materials, the urgency of addressing climate change makes plug-and-play solutions (compatibility with the 6 commercial polymers, for example) more attractive, and often more impactful.

When the desired application of a conversion process is to provide energy for the transportation sector, a decision must be made about the energy source which it would displace, as well as the locomotive technology which it would power. Electric vehicles appear to be the way of the future, although there seems to be uncertainty about how far into the future this will be. Since 2008, more than 520,000 plug-in electric vehicles (PEV's) were sold in the U.S. [17]. Even with this many PEV's on the road, the real question is when affordable 'long-range" passenger PEV's, capable of traveling the benchmark 200 miles on a single charge, will be on the market [18]. Even though this goal has received much attention, a large bulk of energy used by the transportation sector is used for non-passenger transport, often with greater power demands, longer distances traveled and tighter constraints for vehicle weight and volume. Thus, if affordable long-range PEV's are a decade or two from market, it is perceivable that it will be many decades before tractor trailers, cargo tankers, and jet-propelled airplanes could feasibly be powered this way. If the status quo of the world's globalized free-market is maintained, there will be continued demand for heavy transport and passenger air travel, which will be incompatible with stationary power generation, as justified above. With greater flexibility for stationary power generation feedstocks and technologies, it would seem that liquid fuels, particularly "drop-in" (i.e. directly compatible with current grades of diesel, jet, and fuel oils) for non-passenger vehicles, would seem to be the highest priority end-goal product from biomass resources.

Another important consideration is the scale of available biomass resources. According to the 2011 billion ton study; as of 2011, 470 million tons of agricultural and forestry residues were available on an annual basis (representative of that obtainable at $60/dry ton) [19]. The study

predicted 1.4-1.6 billion tons available annually by 2030 if yield increase goals are met. Even though all of this material is theoretically sustainably available for regular use, it is not enough to provide for all of the fuels and chemical feedstocks which we consume. The study states that one-billion tons (double the currently available resource, and two thirds the 2030 prediction) would be sufficient to displace only **a third** of the country's petroleum demand [19]. Keeping this in mind, it is important that we are strategic with how use of the resource is partitioned. We must weigh the relative importance of producing biobased fuels with biobased chemicals. Often the choice of what chemical or fuel to replace or offset is not obvious, from the perspective of which will provide the greatest environmental relief. Even if this was straight forward, economics preclude the implementation of most processes because they cannot outcompete conventional petroleum-fed processes. Because this is the major hurdle to overcome, the characteristics of biomass and waste resources must be studied in depth to leverage their small advantages over petroleum resources.

The approach to gathering, processing, converting, and distributing must be well meditated if a process is to successfully scale. The billion ton update's predictions for progressive increases in production follows assumptions that crop scientists and geneticists will continue to make breakthroughs enabling greater yields. Many techniques are employed here to modify plant phenotype (morphology and growth habit), a number of which improve one characteristic at the expense of another. For example; corn geneticists might find a way to make the corn cob larger and shrink the stalk to reduce the plant's fertilizer requirements, which would reduce stover yield. Again, economics usually establishes the priority of these items.

There are a wide variety of conversion technologies which might be used depending on type of feedstock, desired product, value of product, and scale of production to name a few. The two main classes of these technologies are thermochemical and biochemical. As the names might suggest, thermochemical are generally those involving heat, catalyst, and pressure, while biochemical are those involving microorganisms, enzymes, and catalyst. Both have their pros and cons; biochemical processes generally have high selectivity but are unable to achieve a high yield due to a toxic limiting concentration (sort of like swimming in your own feces). The great diversity of microorganism metabolic pathways enables are diversity of compounds (secondary metabolites) to be produced such as alcohols (ethanol, butanol), carboxylic acids, fatty acids and bioplastic precursors, to name a few [20]. If true fuels (gasoline, diesel, and jet) are desired, thermochemical processes are often desired as they have the tendency to convert with low selectivity in non-catalytic environments, yielding a mixture of compounds which resemble an oxygenated version of the mixture of hydrocarbons comprising a true fuel. A benefit of thermochemical conversion is that the process generally takes seconds to minutes, rather than hours to days, as is the case for biochemical conversion. This benefit often means smaller reactors can handle the same amount of material, and that facility capital costs can be lower.

Although many post-processing technologies would fall into the thermochemical category, thermochemical conversion, by the classical definition encompasses a few technologies, those being combustion, torrefaction, pyrolysis, gasification, and solvolysis. There are numerous other terms such as *thermoloysis* or *carbonization* which fall into this category, but are more of descriptors of a material's conversion behavior than a set of process conditions [21]. Torrefaction is the slow heating of carbonaceous material in an inert environment to "low" temperatures in a relatively minimally-ventilated environment. Torrefaction leads to production of charred or torrefied solids, condensable volatiles (termed *tars*), and some non-condensable volatiles (light gases). Torrefaction, generally taking place in the range of 200-300°C, is often used as a biomass pretreatment method to increase the density, higher heating value, and ease with which it can be reduced to a powder (for

use in fluidized bed combustors and gasifiers) [22]. The process occurs on the timescale of minutes to hours. As early as the 1930's, the French researched application of torrefaction as a wood pretreatment for gasification and combustion [23].

Pyrolysis is the process of devolatilization of carbonaceous materials under "rapid" heating in a well-ventilated oxygen-free environment, producing predominantly condensable vapors in addition to some char and non-condensable gases. The term *rapid* is relative. In the case of slow pyrolysis, heating could occur on the order of a few degrees (Celsius) per minute. With FP, this occurs on the order of 100-1000°C per minute, and in flash pyrolysis, it occurs at even greater rates [24]. Even over this entire range, pyrolysis heating rate and maximum temperature are more severe than occur during torrefaction. The term *pyrolysis* is used to describe both the process and the feedstock transformation which occurs. The latter usage generally refers to the decomposition of a carbonaceous feedstock, but can also specifically mean depolymerization; in the case of bio- and synthetic polymers, dissociation; in the context of light hydrocarbon combustion, and devolatilization; in the context of slow pyrolysis of feedstocks which readily carbonize. Slow pyrolysis of resinous woody materials was historically carried out under the name "dry distillation" for the production of pitch, creosote, and turpentine [25]. Additionally of common reference is the historical use of pyrolysis char as a soil amendment to ancient Amazonia, termed *terra preta* or the Amazonian dark earths [26]. Low-technology applications of slow pyrolysis in earthen, brick, or steel kilns had been used to produce charcoal for various combustion or heating purposes for centuries. Smoke and pollution released by these simple kilns have left pyrolysis and biochar technologies ill reputed where education efforts on advances in pollutant treatment and air handling have not occurred [27]. Due to the high liquid yields achievable by FP, its application to biofuels production is of great interest. The pyrolysis dynamics governing yields and properties of the various phases will be elaborated upon in chapter 2.

Gasification is the next most severe process; occurring at even greater temperatures and pressures than pyrolysis. Gasification is the heating of carbonaceous material to "high" temperatures, on the order of 800-1200°C, converting to predominantly non-condensable gaseous products, on the order of seconds to minutes. When compared to pyrolysis, gasification utilizes longer residence times in order to approach reaction equilibrium, whereas pyrolysis seeks to quench the reaction as soon as primary products are formed to maximize condensable product yield. In fact, pyrolysis is generally considered a step in the gasification process (following heating and drying, and prior to secondary decomposition and residue oxidation) [28]. A brief history of gasification is reviewed below.

Solvolysis is generally the thermal depolymerization of a carbonaceous material in a hot, compressed solvent. A variety of solvents with different solubility or solvation properties are used, generally classified as polar or non-polar, and further polar-protic or polar-aprotic [29]. When the solvent is water, and when process conditions are such that predominantly liquid products are formed, the term hydrothermal liquefaction (HTL) is used. HTL has the benefits of utilizing a very-low cost solvent, as well as being able to handle high-moisture feedstocks. A drawback of HTL is the severity of the process required to sufficiently liquefy the feedstock, generally occurring at supercritical conditions. Constructing and operating a full-scale HTL reactor, capable of achieving these conditions, historically has been prohibitively expensive. When other solvents, such as tetralin or gamma-valerolactone are used, although mild process conditions can be used, high cost of solvent necessitates highly effective recovery. The technical challenges associated with product-solvent separation processes have prevented commercial implementation. An additional challenge associated with the use of solvents other than water is the use of feedstock having high residual

moisture content has been shown to inhibit the conversion process [30]. The scope of solvolysis challenges complimented with the potential for high product selectivity suit it well for high-value, low-volume specialty chemical production [30]. Although finding biobased replacements for petrochemicals is critically important, it could be considered secondary to replacing heavy transportation fuels.

To return to the goal of producing liquid drop-in fuels from biomass, if constrained to thermochemical conversion methods, pyrolysis is a better solution than torrefaction or gasification. A pyrolysis system can convert a feedstock to predominantly liquid products which could be separated and upgraded to a drop-in fuel with a few relatively-simple unit processes. When assessing whole-system costs from agricultural field to pump, much of the cost can be attributed to items other than the reactor itself, such as feedstock cultivation, gathering, transport, and pre-processing of the feedstock, and the separation and upgrading of the liquid pyrolysis products [31]. According to a techno-economic analysis of a FP to liquid fuels-platform, the pyrolysis reactor itself would account for 1/8-1/6th of the total capital costs, and on the order of 1/5th of the operating costs (when accounting for depreciation) [32]. Even though these may seem small, they are still substantial when considering the total capital costs for a 2000 ton per day facility are on the order of $150M and operating costs are on the order of $120M per year [32].

Upon analyzing a FP reactor; how it operates; what constrains it; and what inputs it requires, there are two areas with room for improvement commonly focused on. Those two being; heat transfer to the biomass particle, *and* rapid removal of primary pyrolysis products. From an economics perspective, increasing feedstock throughput could enable a smaller reactor to handle the same amount of material, although would likely harm heat transfer. Increasing sweep gas flow would improve removal of products, but would also likely harm heat transfer. If production (and sale) of char was a goal, electric or natural gas heaters, for example, would need to replace char combustors to supply process heat. All of these modifications have both a major benefit and drawback. One idea, contradictory to the definition of pyrolysis, yet free of major drawbacks, would be to admit oxygen into the system to provide heat.

Introduction to Autothermal Pyrolysis

Autothermal process operation is premised on a steady-state thermally self-powered system. By *thermally self-powered*, a system in which thermal energy is internally supplied to an otherwise endothermic process, is meant. Autothermal process operation should be distinguished from other thermally self-powered systems, such as an incinerator or compost pile. Even though pyrolysis occurs alongside combustion in an incinerator, because the system boundary includes the feedstock and flame, this system is simply considered *exothermic*. Two examples of autothermal processes are autothermal reforming (ATR) of methane, and autothermal gasification.

To provide context; early gasification technologies used to produce the so-called *town gas* or *manufactured gas* operated with small amounts of air (or steam) added, allowing for exothermic partial oxidation of the primary gaseous products to supply required process heat [33]. Later systems controlled equivalence ratio to achieve autothermal operation. In the early 20th century, methane was reformed to carbon monoxide and hydrogen (collectively syngas) to fuel the Fischer-Tropsch process [34]. Two operation regimes developed for this process, termed ATR and partial oxidation (POX), used air (and or steam) and oxygen, respectively to partially oxidize the methane to supply process heat in the same manner as described above, during air-blown gasification. Both ATR and POX reactors enable higher H_2 concentrations in the product stream and supply process

heat at the expense of some product yield [35], and could be considered autothermal and exothermic, respectively.

The concept of applying autothermal operation to a FP system has possibly been avoided due to the concern of oxidizing (consuming) desired condensable product. Kim, Bai, Polin, and Brown have shown that the benefits of carefully-controlled autothermal operation far outweigh the concern for consumption of product. Since FP is only slightly endothermic, only a small fraction of the air required for stoichiometric combustion would be required to achieve adiabatic operation. Specifically, Daugaard and Brown [36] found that the enthalpy of pyrolysis for red oak was 1.61 MJ/kg, while Spearpoint et al. [37] found the heat of gasification of red oak to be 5.1—9.5 MJ/kg. Incropera et al. [38] as well as Harper et al. [39] were in agreement about hardwood heat of gasification to be 3.07 MJ/kg. Since gasification is a more severe process proceeding further towards equilibrium, it is logical that it would require more heat. In order to operate autothermally, this (~2MJ/kg) supply of heat must be provided through exothermic oxidation reactions. This may sound like a lot of heat energy, although to put it into perspective; both the bio-oil and biochar have a higher heating value on the order of 25 MJ/kg, and the gaseous products have a heating value on the order of 17MJ/kg [40]. In other words, very little condensable product would need to be oxidized (reacted exothermically) to balance the endothermic pyrolysis reactions. Other benefits have been cited such as improved heat transfer, monosaccharide yield and selectivity towards *mono*phenols [41]. Heat transfer to the feedstock particles entering the system occurs at or near the particle surface (at the locale of the oxidation reaction), rather than needing to be transferred from the reactor wall or the heat carrier particle to the biomass particle. Since a pillar of FP is obtaining very high heating rates, heat transfer has traditionally been a bottleneck for scaling of these systems. Additionally, feedstock throughput has been limited by the capacity of a reactor to heat that mass flow-rate of incoming ambient-temperature feedstock. Autothermal operation of a reactor greatly reduces this barrier, enabling significant increase in potential process throughput. This not only enables the reactor to scale quite large without the use of bed internals (heat exchange tubing internal to the bed), but also enables a facility of specified throughput to utilize a smaller reactor, reducing facility capital costs.

If autothermal operation was adopted, the combustor described in the Wright et al. [32] TEA study above would not be required, and additional marketable product would be available for sale. Because in this study the minimum fuel selling price (MFSP) accounts for capital costs only on a depreciation basis, not requiring a char combustor does not dramatically reduce operating costs, rather it only significantly reduces facility capex. Using this study's definition of MFSP, autothermal operation would likely only reduce MFSP by 10-15 cents per gallon. Capital costs would be reduced to ~112M for the hydrogen-production scenario and ~$65M for the hydrogen-purchase scenario. It should be noted that these estimates of cost savings are conservative, as they don't account for process intensification (increased biomass throughput) allowing for a smaller facility. Although this might not be competitive with petroleum-based fuels for the hydrogen-production case, cost reductions on this scale are substantial. Because most of these process technologies have been in developed for many decades, process modifications achieving improvements on this scale are few and far between.

Although the economic and technical logistics of autothermal FP are of great practical interest, they are not the core focus of this thesis. This thesis investigated the chemistry underlying partial oxidative pyrolysis in attempt to describe the discrepancy in product composition between non-oxidative and autothermal pyrolysis. Additionally, the major reaction pathways occurring in partial-oxidative pyrolysis, *not* occurring during standard pyrolysis, were hypothesized. The goal of

a subsequent degree is to investigate the relative contribution of these reaction pathways towards autothermal pyrolysis heat generation.

CHAPTER 2.
LITERATURE REVIEW: PYROLYSIS AND OXIDATION – APPLICATIONS TO AN OXIDATIVE PYROLYSIS MECHANISTIC FRAMEWORK

Introduction

Utilization of waste streams and dedicated energy crops for energy and fuels applications have been demonstrated time and again, although significant process improvements are needed to undercut natural gas, coal, and petroleum. A recent thermochemical conversion improvement was made with respect to fluidized bed FP, at Iowa State University's Bioeconomy Institute which makes the process much cheaper than it has historically been. Termed *autothermal pyrolysis*, the process modifies fast pyrolysis by replacing an inert, anoxic sweep gas with one containing small amounts of oxygen. Partial oxidation reactions supply heat for endothermic pyrolysis reactions.

Autothermal pyrolysis has a multitude of benefits, such as reducing requirements for process support infrastructure, and classical scale-up bottlenecks [41]. These are achieved through improved reactor heat transfer, resulting from *in situ* heat release; improved reactor biomass throughput (mass loading), resultant of increased gas production; and improved bio-oil quality, possibly due to reduced vapor phase residence time with increased gas velocity. Even though these are established, the underlying chemistry distinguishing it from non-oxidative pyrolysis is poorly understood. The premise for this chapter was that sufficient precedents exist to build a mechanistic model describing autothermal pyrolysis to some degree of realism.

Studies on the chemistry of oxidation and fuels combustion phenomenon could be viewed as the first major source of organized knowledge applicable to this field. The following are a few examples of narrative-style reviews which walk through a history of the body of knowledge; Smith's 1982 review of coal combustion kinetics and mechanisms [42], a 1992 review by Solomon et al. on coal pyrolysis kinetics and mechanisms [43], Hucknall's 1985 chemistry of hydrocarbon combustion text [44], and Glassman's combustion textbook series [45].

In addition to coal combustion reviews, a number of biomass pyrolysis reviews have been published since 2000. Collinson et al. [46] reviewed the catalytic depolymerization and oxidation of biomass. Collard and Blin [47] reviewed the pyrolysis of the three biomass fractions (lignin, cellulose, and hemicellulose). Mohan et al. [48] reviewed biomass pyrolysis, focusing effects of feedstock properties on bio-oil composition. Dickerson and Soria [49] reviewed biomass catalytic fast pyrolysis (CFP), focusing on catalysis for hydrodeoxygenation and production of aromatics. A few reviews of lignin pyrolysis and oxidation exist, supported by the wealth of lignin literature. Brebu and Vasile [50] reviewed pyrolysis, "thermal depolymerization", of lignin. Crestini et al. [51] reviewed oxidative upgrading of lignin.

Although a number of quality reviews and prior investigations into pyrolysis have been undertaken, none of these focused on oxidative pyrolysis. The existing oxidative pyrolysis studies provide a number of product composition references as a function of oxygen/air concentration for which the mechanistic framework can be compared with. When comparing findings of these studies, variability in experimental apparatus and definitions of terminology, *autothermal operation* for example, must be considered [52-66]. Findings from this body of literature are summarized below.

Amutio et al. [52,67] investigated the effect of oxygen on pine waste pyrolysis kinetics and product composition in a conical spouted bed, reporting a fairly comprehensive set of measurements, finding 2.7% O_2 by volume enabled autothermal operation, and that with oxygen, devolatilization initiated at lower temperatures and char oxidation occurred within a narrower

range. Boukis et al. [53,68] investigated "air-blown flash pyrolysis" of pine in a circulating fluidized bed two-part study focusing on operation logistics, experiencing challenges with char accumulation, once no longer consumed in the char combustor (for process heat), yet achieving high bio-oil yields (61.5 wt. %-maf-biomass). Butt carried out a three-part study on Radiata pine bubbling fluidized bed oxidative pyrolysis, looking at effects of oxygen, moisture, and bed parameters on product composition, claiming monophenol yield benefits from increased substrate moisture as well as bed mass [54,69,70]. Possibly the most applicable prior work is that of Kim et al. [71].

Kim investigated effects of oxygen (ER = 0.034 – 0.539) on red oak bubbling fluidized bed pyrolysis (and a further study on combining alkaline and alkaline earth metal (AAEM)-passivation with autothermal pyrolysis to achieve 67% hydrolysable sugar yield [56]), suggesting vinylphenols and methoxyphenols are oxidized to aldehyde and ketone-containing compounds. Li et al., also investigating bubbling fluidized bed oxidative pyrolysis, achieved autothermal operation at 0.08g-O_2/g-biomass, and similarly to Kim et al. [71], observed high reactivity of acetic acid, hydroxyl-propanone, LG, and methoxy/vinylphenols [66]. Additionally, Li quantified a ¼ - ⅓ reduction in bio-oil energy density, possibly due to the high oxygen concentrations used (here, autothermal was defined as inclusive of parasitic heat loss from bed to surrounding environment) [66].

More focused on chemical mechanisms than scale-up logistics, Lofti et al. [57] looked at oxidative catalytic pyrolysis of solubilized lignin in a microfluidized bed, comparing aluminum-vanadium-molybdenum- with vanadium-pyrophosphate-catalysts, finding improved selectivity towards lactic acids (by hydration of acetic acid, from aldehyde side chain cleavage) and maleic anhydride (by catalyzed ring opening), respectively. Mesa-Pérez et al. [58] pyrolyzed sugar cane "straw" in a bubbling fluidized bed reactor (ER = 0.14 – 0.23), noting decreased oxygen content of bio-oil under oxidative pyrolysis conditions. Persson et al. [59] investigated the activities of a variety of bifunctional catalysts on cellulose "staged-autothermal" *ex-situ* catalytic pyrolysis, cracking bio-oil compounds primarily to flammable gases and aromatics, deoxygenation occurring by decarbonylation and dehydration rather than decarboxylation.

In one of the earlier studies, Rovero and Watkinson [61] pyrolyzed coal in a two-stage spouted bed-combustor (in the low temperature gasification regime), finding excess spent char (ash) suppressed tar yields, and that low-rank coals were not as hydrodynamically compatible with standard depth (low char-holdup) spouted beds. Scott et al. [62] filed a patent in 1995 on production of anhydrosugars from lignocellulosic biomass by partial-oxidative pyrolysis, claiming possibility for selective oxidation of lignin, "destroyed and removed as oxidation products such as CO_2, CO, and H_2O", allowing for collection of concentrated anhydrosugars.

Suárez et al. [63] looked at effect of high equivalence ratios (in excess of stoichiometric, such that parts of the reactor outside of the bed, such as the collection train, could be heated) on Cuban pine fluidized bed decomposition, finding high gas yields and low liquid yields (primarily water-soluble). Wey et al. [64] pyrolyzed waste tire in a 10 cm fluidized bed (ER = 0.07 – 0.35) for the catalytic production of gasoline and diesel, whose yield peaked at the ER = 0.21 level, although lower than achievable by vacuum pyrolysis, and proposed a mechanism of catalytic activity to yield observed products. Collectively this body teaches much about process behavior and product tendencies under oxidative FP conditions.

Physiochemical Model of Lignocellulose

Overview

Before discussing pyrolysis mechanisms of biomass fractions, their physical structures and native chemistry (in isolation and whole biomass form) should be reviewed. Red Oak, a lignocellulosic biomass is comprised of cellulose, lignin, and hemicelluloses in major quantities, as well as extractives (such as resins, phytosterols, and fatty acids), and ash (mineral content) in minor quantities [72]. Cellulose, often referred to as the structural fiber, comprising roughly 50% of red oak heartwood and sapwood by mass [73]. Hemicellulose, often referred to as the plant biopolymer-adhesive, comprises almost 30% of the mass of red oak heartwood and sapwood [73]. Lignin, referred to as the plant's primary physical protection, comprises roughly 10% of red oak by mass [73]. Although responsible for less than 1% by weight in red oak, the ash content present is sourced mostly from soil minerals, containing silica, aluminum, magnesium, and iron, often in the forms of thermally-instable salts or oxides [73,74]. Extractives make up the balance (less than 10%) of the whole biomass [73].

Although all of these fractions will be characterized independently below, their interactions with other fractions (inter-fraction bonding and forces) should be considered when studying whole biomass. The covalently (ester or ether) bonded interface between lignin and hemicellulose units is often physically modeled as what is termed a lignin-carbohydrate complex (LCC) [75]. The term LCC uses the word *carbohydrate*, because a variety of hemicellulose units (xylose, glucose, galactose, arabinose, uronic acids (carboxylic acid-containing sugars), as well as small amounts of rhamnose) could be present in the complex [76]. These linkages, between carbohydrates and lignin units, are thought responsible for many of the pyrolysis interaction effects observed, affecting the relative yields of guaiacols and the final form of monosaccharides [77]. Of particular interest is yield of the monosaccharide product of cellulose depolymerization; levoglucosan. Zhang et al. [78] demonstrated lower yields of levoglucosan occurred when cellulose is in native whole biomass form rather than when isolated, due to covalent LCC linkages between cellulose and lignin (elaborated below). Although much of the chemistry of interest occurs at this level, early pyrolysis processes are more strongly dependent on larger-scale structural features.

On the sub-cellular level, the superstructure of biopolymers within a plant cell wall can be thought of as crystalline cellulose macrofibrils (small fibers) enveloped in a sheath of LCC's, loosely bound to one another by Van der Waals forces (specifically attracting cellulose and hemicellulose units) and occasional covalent linkages [79]. Cellulose microfibril units are superstructures of polymer chains bound by inter-molecular hydrogen bonds into sheets, attached to one another through inter-sheet hydrogen bonding [80]. The degree of polymerization refers to the number of glucose units comprising a single polymer within a fiber. A cellulose "fiber" unit consists of a number of macrofibrils, each of which is comprised of a number of microfibrils [81]. It is due to this model, where lignin physically obscures cellulose, that lignin is thought of as a physical barrier to chemical and microbial attack, and cellulose is considered a structural agent. It is important to note that this physical model is highly idealized and would vary dramatically with plant part and species, as well as environmental factors. For example, even though a minor portion of the plant's mass; leaves, contain greater quantities of extractives and structures (rather than lignin, as is the case for stems) enabling then to respond to stresses by production of secondary metabolites with herbivore-repelling effects [82].

The macrostructure of lignocellulose can be generalized as the differentiated cells produced by the vascular cambium meristem (tissue of actively dividing cells) of a dicotyledonous plant. In a given cambial cell file, a perpetual meristematic cell (collectively termed *initials*) divides to produce

the primary cell wall (hemicellulose framework) of what will become either an axially-elongating fusiform cambial cell (FCC) or a radially (isodiametrically)-elongating ray cambial cell (RCC) [83]. FCCs go on to differentiate into vessel elements (of xylem), fibers, or axial parenchyma, while contact or isolation ray cells can form from RCCs [84]. Following formation; fibers, axial parenchyma and contact ray cells experience a period of radial expansion, "development displaces cambium outward, necessitating extension in stem girth" [84]. Following this, a period of secondary cell wall deposition ensues, working from the middle lamella (space between cells), inward, laying down the cellulose microfibrils with orientations and arrangement specific to the cell region [84]. In the outer region, S1, described as thin or flat, microfibrils are oriented transverse to the cell cross-section, arranged in a "loose helicoidal pattern" (collectively macrofibril). In the next region, S2, described as thick, microfibrils are oriented longitudinally to the cell section. In the inner-most section, S3, the fibrils return to the orientation and approximate arrangement of S1 [85]. Following secondary wall formation, a number of cell biology tasks, generally powering up the cells, occurs, succeeded by lignification of those cells which underwent radial expansion (notably vessel elements and contact ray cells), and simultaneous lignification and secondary wall formation of those that did not (notably isolation ray cells), both proceeding inward from middle lamella [86]. Lignification is a multiphase process occurring over the time scales of earlywood, latewood, and subsequent seasons. Due to changing modes of lignification and because the differentiated cells are displaced radially over time (xylem inward and phloem outward), cells located close to the cambium contain greater H- and G-unit lignin content , but further away are more S-unit-rich [87].

While hardwoods have fibers, vessels, and parenchyma tissue; softwoods have parenchyma, and tracheids rather than fibers but no vessel cells. In softwoods, tracheid cells form a roughly honeycomb-like structure [88]. In hardwoods, fibers have a honeycomb-like structure. In both hardwoods and softwoods, parenchyma have a roughly box-like structure [88]. Although highly dependent on density, parenchyma cells tend to be weaker than fiber cells [89]. This might be because fiber cells are denser, due to greater degree of lignification. Thus fiber cells might be more resistant to milling or conversion.

Cellulose

Cellulose, the common fibrous structural biopolymer, is a comprised of chains of 1,4-glycosidic bond-linked β-D glucopyranose monomers with an widely-varying degree of polymerization, dependent on genetics of the feedstock and pretreatment modification, from ~1000 for native sugar cane bagasse to 5000 for native jack pine [90]. It is due to the described superstructure that the majority of cellulose chains are precluded from bonding with the other fractions. Even though this is the case, cellulose is described as exhibiting Van der Waals intermolecular forces, and covalent linkages with lignin-carbohydrate-complexes which surround individual fibers [91]. The specific adhesion forces vary depending on the locale of the interface. Because cellulose's crystalline structure varies with location (generally possessing both highly ordered "crystalline" and "fringed-fibril amorphous" regions), and plant type/treatment polymorph, so does the extent with which it meshes with an LCC at the interface [92]. Cellulose is described to exhibit five crystalline polymorphs; I_α, common of native algal cellulose, I_β, common of native herbaceous and woody cellulose, *II*, resultant from the mercerization (solubilization) process (technical fiber spinning)), *III*, resultant from treatment by an organic amine, such as liquid ammonia or ethylenediame, and *IV*, resultant from high temperature treatment in glycerol for example [92]. The LCC-amorphous region interface, in bamboo for example, forms poorer contact than an LCC-crystalline interface, which has 2-3 times the adhesive strength [91]. The different crystalline polymoprhs arise from differences in resonances of the glucose ring's C_1 carbon, which

leads to differences in hydrogen bonding patterns between polymers, also influencing the polymer's strength [92].

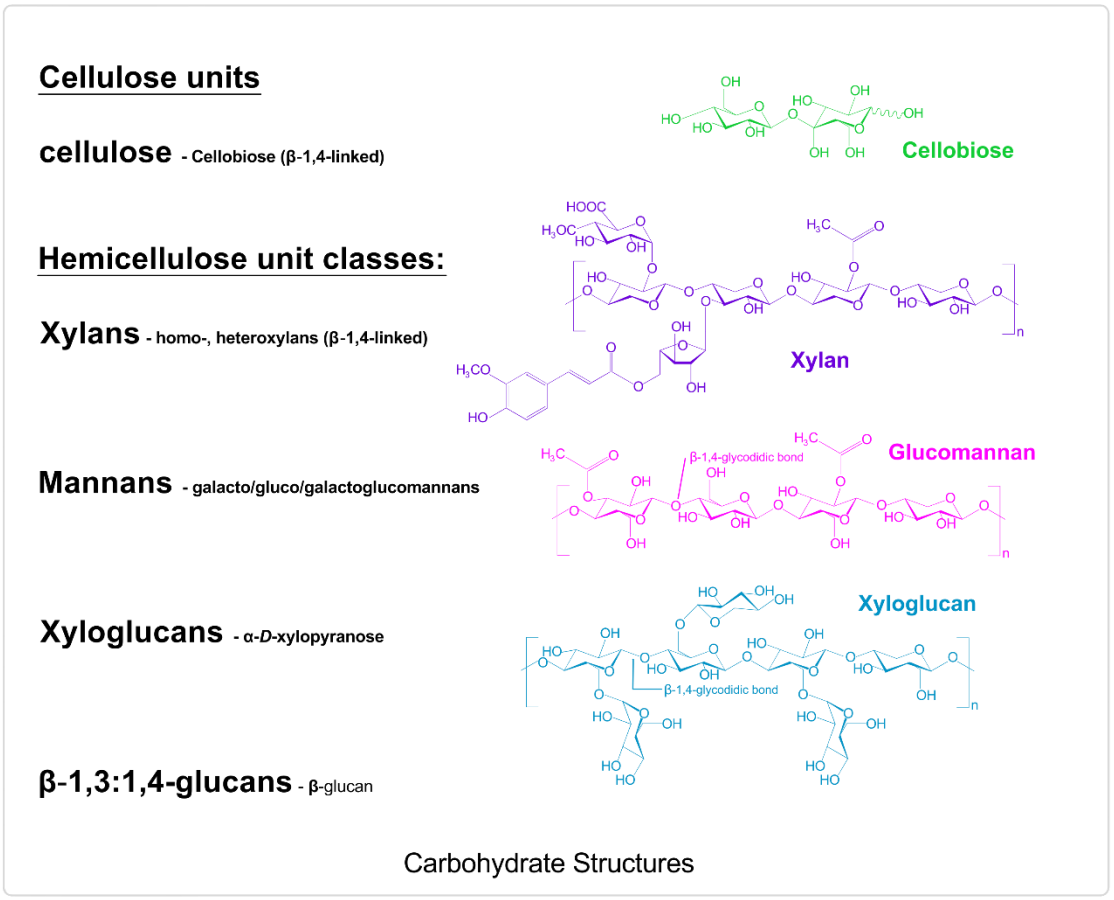

Figure 1. Carbohydrate structural units.

Dry isolated cellulose is described to exhibit thermoset polymer behavior in that it forms permanent bonds "stable" in heat and many solvents, depolymerization occurring before fiber dissociation [93]. The polarity and hydrogen bonding propensity of cellulose is attributed to its oxygen and hydroxyl content. The lack of solubility of cellulose is certainly not resultant from its hydrogen bonding (as this should trait should theoretically increase solubility), but rather the balance between intermolecular hydrogen bonding and Van der Waals forces, and amphiphilic (containing both polar and non-polar regions) nature confounded by a stiff crystalline structure (hindering conformational changes normally allowing separation of hydrophobic parts) [94]. Solubilization of cellulose in non-derivitizing solvents such as ionic liquids and non-aqueous salt solutions is possible, breaking hydrogen-bonds being the predominant mode of solubilization [95].

Hemicellulose

Hemicelluloses are the clade of readily-hydrolyzed then solubilized (degraded) plant polysaccharides, distinct from pectic polysaccharides (a class of extractive which is also readily extractible) by alkali-solubility [96]. A biopolymer of predominantly xylose monomeric units, hemicellulose units are generally of low degree of polymerization. Hemicellulose, accounting for 1/5 – 1/3 of biomass's dry weight, is comprised of a wide variety of oligomeric to polymeric structures whose presence and prevalence depend on plant type, plant part, season, among other

factors [97]. Although xylose is the most common monomeric unit, mannose, galactose, arabinose, and rhamnose are also commonly found [98]. The four common structural units include; xylans, mannans, xyloglucans, and β-1,3;1,4-glucans, of which are predominantly β-1,3 and β-1,4-glycosidically linked [98]. Hemicellulose is distinct from pectic plant polysaccharaides, a class of plant extractives, those readily extracted by chelation, weak acids, or hot water [98].

Xylose-derived xylans, already mentioned most prevalent, can comprise as much as 50% of the tissues of some grasses and cereals [99]. In general, xlyans are comprised of a β-1,4-linked D-xylopyranose backbone with short chain branches comprised of D-glucuronic acid, D-xylose, and L-arabinose. They are classified into homo- or heteroxylans. Of the heteroxylans are; glucuronoxylans, arabino-glucuronoxylans, glucurono-arabinoxylans, arabinoxylans, and "complex heteroxylans" [98].

Mannans are generally cladded galactomannans or glucomannans, made up of mostly straight chain β-1,4-linked D-mannopyranose units, and a mixture of β-1,4-linked D-mannopyranose and D-glucopyranose, respectively, both with galactopyranose branches [98]. Although uncommon, galactomannans with minimal branching, have been observed in ivory nut, date nut, and Arabica coffee beans [100,101]. The more common, highly-branched, galactomannans are commonly found in storage tissue of seed cell wall, particularly in leguminous plants [102]. Galactomannans are often characterized by their mannose: galactose ratio, ranging from 1 – 5.7: 1 for most leguminous plants, having implications on solubility and hydrolyzability [103]. Although found to a lesser extent in hardwoods, Glucomannans and galactoglucomannans are some of the more common hemicellulose units in softwoods, making up a significant component of softwood secondary cell walls [104], and suggested present in primary cell walls in structures containing glucans and xylan [105].

Xyloglucans, having cellulose (β-1,4-linked D-glucopyranose units) as a backbone, contain α-D-xylopyranose as branching units linked at the pyranose 6-position [106]. Xyloglucans are a "major" building block of hardwood primary cell walls, comprising up to 25% by mass in sycamore, although are much less prevalent in grasses and herbaceous plants [99]. Xyloglucans in hydrogen-bonding coordination with cellulose are thought responsible for the resistance to cell rupture under turgid osmotic stress [107].

1,3- and 1,4-β-D-glucans have been observed primarily in grasses, bromeliads, and sedges, collectively the taxonomic order Poales, [98]. β-glucans are of industrial importance as they act as gellants, hindering membrane filtration of beer wort (introduced via barley in the mash) [108]. Also of interest to the commercial food industry, β-glucan located in the bran of cereals is thought responsible for lowering cholesterol [109]. The proposed mechanism of action being β-glucans binding (followed by excretion, thus preventing reabsorption) with bile acids, stimulating production of bile acid by converting both plasma-based and liver-based cholesterol [110]. Whereas galactomannans are commonly characterized by mannose: galactose ratios, 1,3-: 1,4-linkage ratios are also common for characterizing β-glucans. Commonly 30% : 70%, the alkali-extractable β-glucan-rich fraction of barley, for example, was shown to have higher 1,4-linkage content [111].

Compression wood, a distinct tissue in softwoods, is formed on the underside of branches or stems at the node exerting compressive stress to support the weight of the limb, contains hemicellulose of enriched β-1,4-glucan content and reduced galactoglucomannan (and cellulose), compared to normal wood [112]. Opposite wood, that tissue under tension at a node, located opposite compression wood, is of greater galactose, mannose, and cellulose content than normal wood [113,114].

Lignin

The potential to valorize technical lignin (lignin-rich industrial by-product) has been a major driver for research in this area. Lignin valorization and conversion has been reviewed extensively, to say the least [46,115-128], identifying many routes, few of commercial viability. Although many valorization efforts are geared towards conversion to liquid fuels, another goal is production of potentially valuable platform chemicals such as BTX, 1,4-butanediol and adipic acid by way of catalytic pyrolysis, suppressing inherent methoxy and hydroxyl-based reactivity and inducing ring-opening (in the case of the latter two) [116].

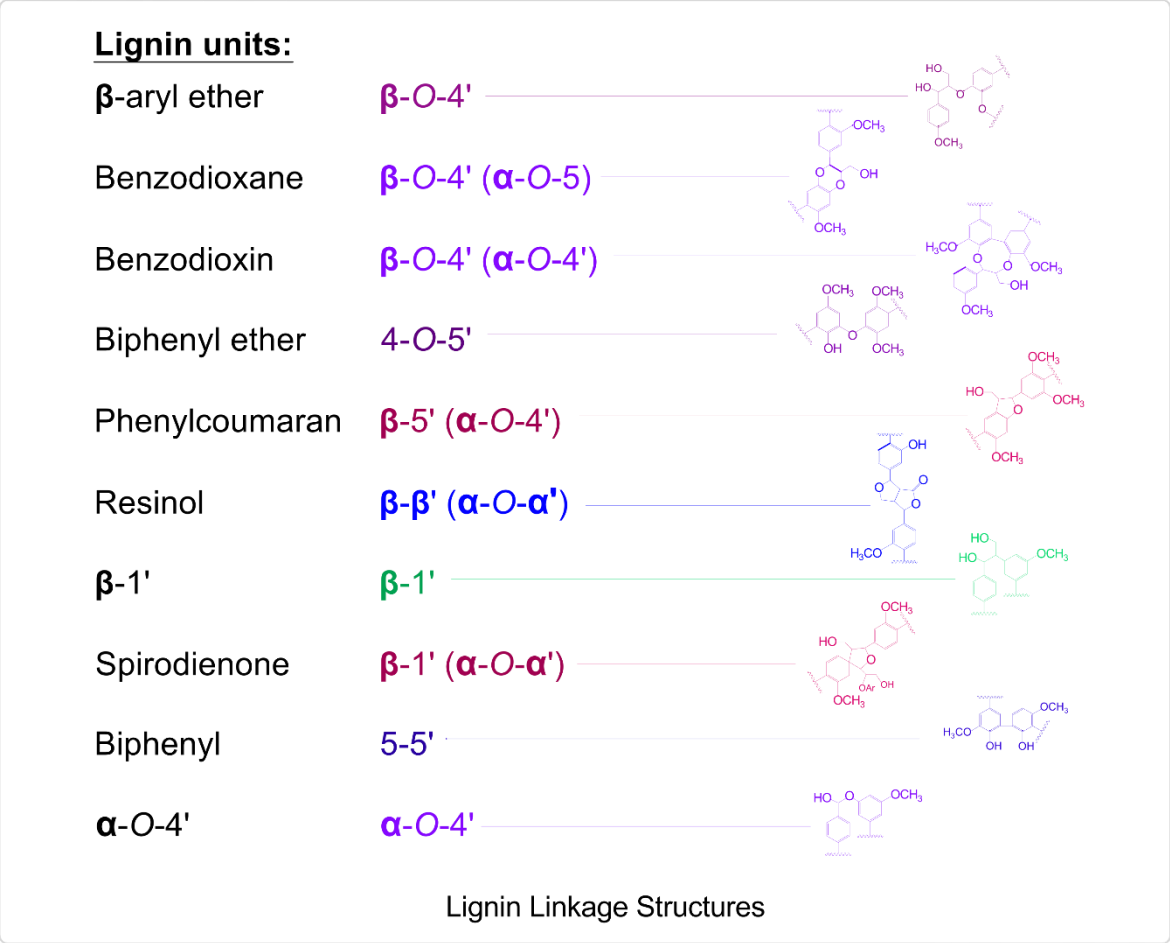

Figure 2. Lignin structural units.

Lignin, an amorphous biopolymer of phenylpropane units with a variety of monophenol interunit linkage types, provides protection and strength to the plant cell wall. Although amorphous and heterogeneous, lignin has been characterized by the monolignol units (phenylpropanoids), as well as its linkage structures from which it was biologically synthesized. Beyond the structures and relative prevalence of interunit linkages, the collective structure of lignin cannot be absolutely defined [114]. The three main monolignols are *para*-coumaryl alcohol (associated with the lignin H-unit), coniferyl alcohol (associated with the lignin G-unit), and sinapyl alcohol (associated with the lignin S-unit) [129]. What distinguishes the three lignin monomer units is the number of methoxy substitutions located *ortho* to the phenolic hydroxyl; 0, 1, and 2, for *H*, *G*, and *S-units*, respectively. The three units, differing in reactivity, are incorporated into lignin uniquely. In general; the lesser-

lignified (only 13 - 19% lignin by mass) tissues of herbaceous plants contain H, G, and S-units, while woody deciduous plants (20 - 26% lignin by mass), contain primarily G with some S-units, and coniferous plants (27 – 33% lignin by mass) contain predominantly G-unit lignin [130,131]. The most prevalent lignin interunit linkages are β-*O*-4', α-*O*-4, α-1', β-*O*-5', 5-*O*-4', β-β', β-1', β-5', and 5-5', see Figure 1. Although present, the condensed C-C linkages are less common than the ether linkages. When comparing deciduous and coniferous; deciduous have a greater proportion of β-*O*-4' linkages, comparable amounts of 5-*O*-4' and condensed β-1', but lesser relative amounts of β-5' and 5-5' condensed linkages [132]. Relative to normal wood, compression wood contains lignin of increased H-unit content. The proportion of H-units has been suggested as a means for indicating compression wood severity, which could be compared with brittleness [133]. Smith et al. [134] claimed G-units associated with both covalent ether/ester linkages and condensed linkages did not notably vary in concentration when traversing the section of a stem (at the node) from compression wood to opposite wood. Contrarily, Suckling et al. [135] claimed greater condensed linkages in compression wood. Even though relative abundance of these units or their bonding patterns was not notably different between a given compression wood and normal wood, as compression wood severity increased, so did content of condensed-linkages [135]. This was shown by molecular weight distributions of thioacidolysis products (a process which more readily decomposes covalent bonds), regardless of age [135]. Applying these concepts; lignin derived from lower quality, knotty wood might contain fewer methoxy functionalities and exhibit a greater condensed C-C linkage structure, making it less reactive and more resistant to depolymerization, and likely producing more char.

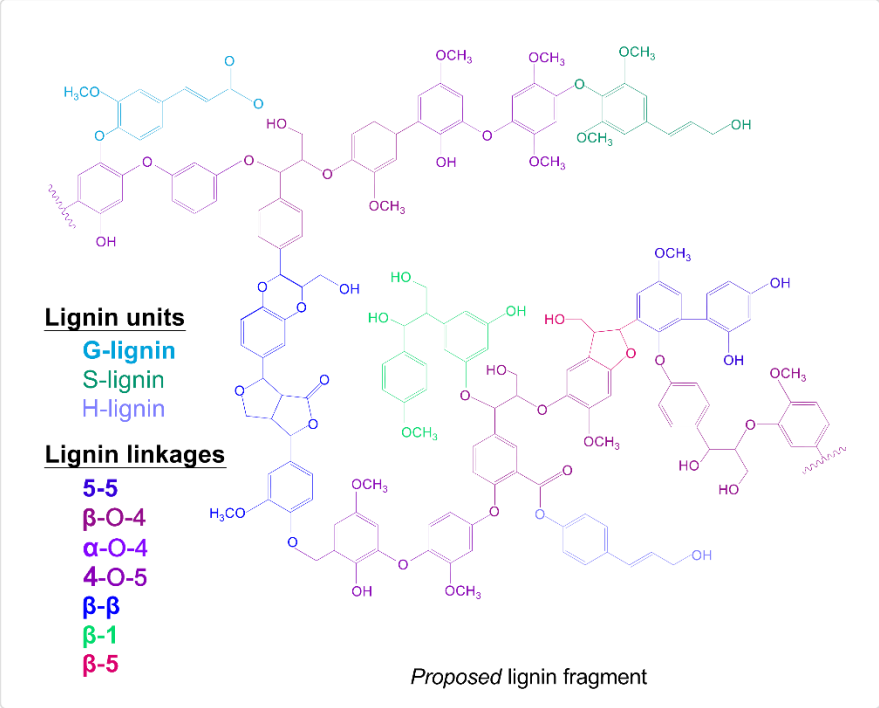

Figure 3. Proposed hardwood lignin fragment structure with representative units and linkages.

Biochemists have studied the metabolic mechanisms describing the formation of lignin, and have developed an intimate understanding of the structures which might be present in native lignins. Starting with one of the three photosynthetic pathways (C3, C4, CAM), plants are able to utilize CO_2 and sunlight to produce adenosine triphosphate (the plant's chemical potential energy)

and NADPH (termed the *transport molecule*) [136]. The Calvin (Calvin-Benson-Bassham, CBB) cycle, utilizes these along with CO_2 and water to produce organic precursors, thanks to the enzyme RuBisCo [137,138]. Eventual formation of compounds such as erythrol-4-phosphate and quinate supply the shikimate pathway producing chorismate (in addition to other species) [139]. Chorismate mutase converts chorismate into phenylalanine and tyrosine, which is where classical lignin (phenylpropanoid) biosynthesis begins [140].

Phenylalanine is deaminated to trans-cinnamic acid (and ammonia) via the phenylalanine ammonia lyase (PAL) enzyme. The same enzyme also catalyzes conversion of tyrosine although might be termed tyrosine ammonia lyase (TAL) [141]. Utilizing NADPH, hydrogen ions and gaseous oxygen, cinnamate 4-hydroxylase (C4-H) hydroxylates trans-cinnamic acid into 4-hydroxycinnamate (*para*-coumaric acid) [142]. *P*-coumaric acid is the precursor to all of the hydroxycinnamic alcohols (the *monolignols*); *p*-coumaryl alcohol (the methoxy-deficient base unit of H-lignin), caffeyl alcohol (the hydroxylated H-lignin unit), coniferyl alcohol (the monomethoxy base unit of G-lignin), 5-hydroxyconiferyl alcohol (the hydroxylated G-unit lignin), and sinapyl alcohol (the dimethoxy base unit of S-lignin) [114]. The pathway from *p*-coumaryl alcohol to any of the hydroxycinnamic alcohols can be generalized by a series of functionalization reactions, and conversion of the side chain end groups to alcohol groups. Functionalization reactions generally hydroxylation from the coumaryl unit to caffeoyl unit via an enzyme so-called "*p*-coumaric acid 3-hydroxylase" [143], which is then methylated to a feruloyl/coniferyl unit via caffeoyl-coenzmye-A *ortho*-methyl transferase (CCoAOMT) [144], which is then again hydroxylated by ferulate 5-hydroxylase (F5H) to a hydroxyferuloyl/hydroxyconiferyl unit [145], which is again methylated via CCoAOMT to a sinapyl unit [144]. Side chain reactions, starting with *p*-coumaric acid (having a carboxylic acid end group), for example, involve forming an ester of Coenzyme A (by way of 4-coumarate CoA ligase) [146], the CoA-ester end group is reduced to an aldehyde via cinnamoyl-CoA reductase (CCR) [147], which undergoes a dehydration reaction to alcohol (the final monolignol form) via either cinnamyl alcohol dehydrogenase (CAD) for H and G units or sinapyl alcohol dehydrogenase (SAD) [140].

Once the monolignol units are formed, the lignification process, polymerization by dimerization and cross-linking, can begin. Broerjan et al. [114] shows a schematic describing some of lignin's polymerization tendencies, regarding the formation (or lack thereof) of certain linkage types and morphologies. In short, coniferyl alcohol cross linked with G-lignin can form a β-*O*-4' or β-5' (but not 5-5', 5-*O*-4', or β-β'), cross-coupling of G-lignin oligomers can form 5-5' or 5-*O*-4', sinapyl alcohol dimerization can form β-β' or β-*O*-4' (but not 5-5'), crosslinking of S-lignin with either a coniferyl or sinapyl alcohol can only form β-*O*-4', and cross-coupling of G-lignin with S-lignin oligomers can form 5-*O*-4' linkages [114].

Aside from feedstock-based monomer and linkage variability, it should be noted that much variation in reported values could be attributed to the lignin isolation method used. Technical (industrial by-product) lignins isolated during pulping through the sulfite, Kraft (sulfate), or organosolv processes, have very different properties from those isolated during a cellulosic ethanol process, which might resemble an acid hydrolysis (acidolysis) lignin, or an enzymatic hydrolysis lignin (such as enzymatic mild acidolysis lignin (EMAL)). Increasing ethanol organosolv lignin (EOL) extraction intensity is described to reduce molecular weight and aliphatic hydroxyl content, as well as increasing syringyl content and condensed-linkage content [148]. The proposed mechanism involves action of acetic acid derived from hydrolysis of xylan's acetyl groups, protonating C_α hydroxyls, leaving radical lignin units susceptible to condensation (combination) reactions [148]. Although it is described in greater detail below, during Kraft pulp oxidative

delignification (the Kraft lignin extraction process), increases in pH leading to ring fragmentations (mainly of guaiacyl units), and condensation reactions. Increases in temperature was correlated with increase in carboxylic acid content, and increasing reaction time did not have a significant effect [149]. When comparing milled wood lignin (MWL), cellulolytic enzyme lignin (CEL), and EMAL; EMAL removed the greatest fraction (was most effective at extraction) of lignin, yet also had the highest residual carbohydrate content, and had the highest weight- and number-average molecular weight, while MWL had the lowest average molecular weight [150]. The three extraction methods did not seem to yield different residual β-aryl ether linkage content, carboxylic acid content, or erythro : threo ratios, when comparing Douglas fir, giant redwood, Colorado white fir, or blue gum (*Eucalyptus*) [150]. CEL appeared to slightly yield slightly lower condensed and uncondensed-hydroxyl content for Colorado white fir, giant redwood, and Douglas fir [150].

Lignin Carbohydrate Complexes

As introduced prior, LCC's are the structures binding hemicellulose polymer units with lignin. In herbaceous feedstocks, the term LFP (lignin-ferulate-polysaccharide) complex can be used as hemicellulose units have been shown to bond to lignin via ferulic acid (the G-monolignol) [151]. LFP might not be a comprehensive term, as one group identified *para*-coumarate ester linkages in corn stover LCCs [152]. In woody materials, it is understood phenyl glycoside bonds, phenyl esters, and benzyl ethers are the main LCC linkage classes [153]. Monlau describes LCC formation as occurring in herbaceous plants during phenolic coupling (during lignification), and in both herbaceous and woody plants by way of nucleophilic attack of C_α substituents of a quinone methide intermediate (hydroxyls, carboxylic acids) resultant of lignin polymerization [154]. A variety of hydrolysis methods have been used to attempt to quantify by extraction [155]. Arguably, extraction methods are potentially inaccurate due to modification during the process, leading to wider use of quantification by 2D NMR integration methods. Two examples are; integration of HSQC chromatogram areas, assuming total chromatogram area correlates with 100% of the structures [156,157] or more rigorously, the use of standards and ^{13}C-NMR to calibrate HSQC areas [158]. Analysis of woody biomass LCC's pose a challenge because their low native prevalence requires extraction and or concentration (usually through a lignin extraction method) for quantitation, possibly modifying the structure [153]. Conversely, because LCC-extraction methods are common to those used for lignin isolation, when working with "isolated lignins" consideration must be given to the small residual carbohydrate content, generally in the form of LCCs. CEL appeared to degrade the LCC structures less than MWL, suggesting they were affected by shearing forces at macroscopic length-scales [159].

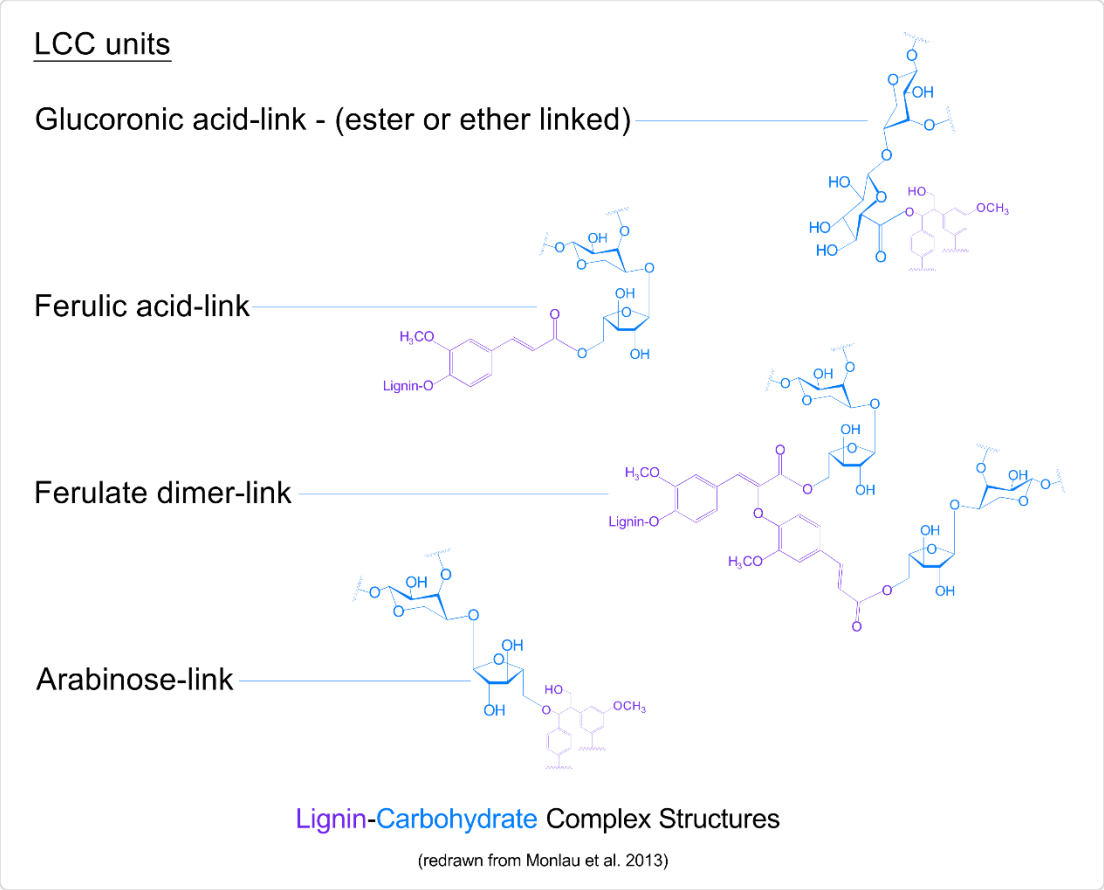

Figure 4. Lignin-Carbohydrate Complex structural units.

"Extractives"

In addition to cellulose, hemicellulose and lignin, other structures are ubiquitous in plant materials. Although found in small quantities or predominantly in certain plant parts, they often play critical roles in plant cell function [160]. Common classes of plant extractives include; resins, triglycerides, fatty acids, phenolics, and phytosterols [15]. Resins, commonly known by their fossilized form, amber, can be defined as; "primarily mixtures of terpenes or phenolic compounds, which may be produced in internal ducts or in special surface glands of plants" [161]. Resins are distinct from sap; aqueous solution transported through phloem, and gums; polysaccharide excretions produced as a result of bacterial infections [161]. Specifically, the terpenoid resins (oligomers of isoprene units) can be classified into volatile; such as monoterpenes, sesquiterpenes, and diterpenes, and non-volatile; such as di- and triterpenoid acids [162]. The fossilization process involves polymerization, cross-linking and isomerization to highly stable structures. Additionally, conifer-emitted monoterpenes have been suggested as important players in the nitrogen biogeochemical cycle as they inhibit growth of soil bacteria responsibly for nitrification, and are leached from soils in marine environments where they are broken down [163].

Chemically, plant and animal lipids are defined by four characteristics; they are water-insoluble, soluble in organic solvents (such as chloroform or benzene), they contain long-chain hydrocarbon groups, and they are present in- or derived from organisms, [164]. Lipids can be characterized as simple; composed of fatty acids and alcohol components and include acylglycerolds, ether acylglycerols, sterols, and their wax esters, *or* complex; multi-component

lipids including glycerophospholipids (phospholipids), glycerolglycolipids (glycolipids), and sphingolipids [165]. Common lipids are often referred to by a shorthand naming convention *A*:*B*ω*C*, where *A* is the number of carbons in the fatty acid main-chain, *B* is the number of double bonds present in the structure, and *C* is the location of the closest double bond relative to the methyl end, hence ω, end (of alphabet) [165]. Further, fatty acids can be more comprehensively be categorized as; saturated (those beginning with a formic acid unit), unsaturated (most ubiquitously oleic acid, containing most common fatty acids), acetylenic (as the name suggests, contain one or more triple bonds), *trans* (any unsaturated fatty acids containing an E (*trans*) configuration), branched, cyclic, hydroxyl and epoxy, and furanic (all as their names might suggest, contain that structural feature) [165]. Most plants produce fatty acids or triglycerides (functionally found in plants as membrane lipids or storage lipids), although usually concentrated in the seeds (or other propagules). Composition of individual oil compounds is highly sensitive to geography (associated climate and soils), cultivar, individual plant genetics, which plays out in erucic acid content in rapeseed oil, which has been observed to vary from 1 – 58% (canola oil is a common name for low-erucic acid rapeseed oil) [166]. Fatty acid synthesis involves conversion of acetyl-CoA to malonyl-CoA by acetyl-CoA carboxylase (in the presence of a divalent cation and ATP), followed by a combination of modifications; elongation (occurring in the cell ER via a multi-enzyme complex, involving either long-chain fatty acid elongase or the fatty-acid synthase complex, termination of which involves acyl-ACP thioesteraces (in storage lipids) or acyl-APC:glycerol-3-phosphate acyl transferase (in membrane lipids)) , desaturation, hydroxylation, and wax formation [167].

Phytosterols, or plant steroid alcohols, are a class of 250 compounds structurally classified into 4-desmethyl sterols and their precursors (present in minor quantities); 4α-monomethyl sterols, and 4-4-dimethyl sterols [168,169]. Sitosterol is the most prevalent in plants, although stigmasterol and campesterol are also present in many plants, all of which are 4-desmethyl sterols. Distinct from cholesterol (the common animal sterol) by differences in side chain, plant sterols having a more highly branched side chain. Both plant and animal sterols are based upon a tetracyclic cyclopenta[a]phenanthrene ring, characterized by the large side chain at the C_{17} location [169]. In the dietary (i.e. whole food) form, plant sterols have been shown to reduce absorption of cholesterol (lowering serum and liver cholesterol levels) [170]. Although in isolated, concentrated form they didn't seem to exhibit the same benefits, while concentrated plant stanols (with a saturated C_5 bond, where a double bond is present in sterols), such as those present in wheat and rye, were more effective [170,171]. Phytosterols, notably campesterol, are precursors to some plant growth factors (collectively brassinosteroids) in meristem tissue [172]. Additionally, phytosterols play a role in cell membrane function; becoming incorporated in the form of steryl glycosides or esterified acetyl-containing steryl glycosides, [173]. Verleyen et al. [174] measured sterol composition and content in a number of agricultural and horticultural crops, listing sterol mass-fraction in decreasing order, of the unrefined (whole plant) form. The list was ordered as follows; corn, rapeseed, cotton, sunflower, soybean, peanut, olive, walnut, palm, and coconut, where olive, cotton, soy and sunflower had the lowest esterified (as opposed to free-) sterol content [174].

Proteinaceous, Oleaginous, and Synthetic Polymeric Materials

Although it was not a primary focus of this study, there is significant interest in thermochemical conversion of many waste and byproduct streams. These materials are substantially comprised of fractions not present in lignocellulosic biomass, such as amino acids (collectively proteinaceous material), fatty acids and triglycerides (collectively lipids), and hydrocarbon polymers (collectively synthetic polymers). Because the properties of these materials

differ so much from cellulose, lignin, and hemicellulose, it seemed necessary to write a section on their general properties and postulate about their partial oxidation behavior.

α-amino acids, particularly the 20 standard biological amino acids, whose amino group is bonded to the C_α, often simply referred to as *amino acids*, are the most common class found in nature. Other than β-alanine, β-amino acids, those with the amino group bonded to the C_β, are not formed in nature. When pyrolyzing proteinaceous wastes, consideration must be given the nitrogen and very high reactive oxygen content, which could produce bio-oil unfit for transportation fuel (if out of compliance with emission standards) [175]. Approaches to handling the nitrogen content are discussed in the pyrolysis and oxidation section below. Common proteinaceous waste streams include; waste water- and lagoon-biosoilds, some food processing wastes and a number of materials also classified as oleaginous. Oleagenous materials will not be elaborated upon here as they were described above, in the extractives section. Synthetic polymers, are generally classified as *thermosets*; generally having primary bonds between chains, or *thermoplastics*; having secondary bonds between chains. Among the thermoplastics are thermoplastic polymers; including crystalline polymers (such as HPDE, PP, polyesters, acetyls, polyamides, PTFE, and PEEK), and amorphous polymers (such as PVC, PS, PMMA, ABS, PC, and polyethersulfone), and thermoplastic elastomers (such as polyureas, polyurethanes, and SBR's); exhibiting properties of both elastomers and thermoplastics comprised of two unique polymers [176]. Thermosets are highly cross-linked polymers, applied where thermal and mechanical stability is required, and include polymers such as aminos, phenolics, polyurethanes, polyesters, epoxides, and rubbers [176]. Greater volumes of thermoplastics are produced, thus these polymers might be a bigger target for conversion and process design.

Fast Pyrolysis and Oxidation Mechanisms

A FP model combining many recent and fundamental perspectives will be described with respect to pyrolysis phase, biomass fraction, interactions between fractions, and interactions between products and fractions. In this review, pyrolysis will be considered to occur in four phases; 1. Heating and drying, 2. Early pyrolytic cleavage, 3. Rapid pyrolytic cleavage and intermediate formation, 4. Late pyrolysis (Tight-gas liberation), subsequent fragmentation of intermediates, and secondary reactions. The first phase occurs as the feedstock is heated from ambient to a temperature above the boiling point of water (100°C), but not extending much above 200°C. Initiation of the second phase can be characterized by initial fragmentations and pyrolytic cleavage events, usually associated with the hemicellulose fraction. The second phase could be considered to end slightly prior to the feedstock reaching reactor temperature. The third phase encompasses the bulk of pyrolysis reactions, although may occur over a very short duration [177]. The duration of the fourth phase depends greatly on the operation conditions, and the experimental setup, but could be the longest phase if the char precursor has significant residence in the reactor (such as the base case scenario, in a bubbling fluidized bed). Oxidation during oxidative pyrolysis has not been described much prior, but could be proposed to initiate with ROS (radical pool) formation through interactions with the condensed phase and early gases. Subsequently, oxidation of lignin oligomers and monomers might occur followed by oxidation of volatiles, char, and to a minor extent the carbohydrate fraction, collectively consuming remaining oxygen. Fast pyrolysis and thermal depolymerization of biomass have been reviewed expansively [23,47-50,118,178-183]. Findings of theirs and others will be abridged below.

Cellulose

Non-oxidative Fast Pyrolysis

Cellulose pyrolysis has been investigated in depth since the 1950's, particularly from the context of conversion kinetics. Cellulose has been proposed to rapidly depolymerize over the temperature range of 250 - 340°C [184]. Although reactor context-specific, Koufopanos and Papayannakos demonstrated that in a 38 mm diameter tubular reactor, particles smaller than 2mm in diameter behaved isothermally, thus could be considered to behave in a thermally-thin regime, [185].

Over the years, a wealth of semi-global kinetic models intended for thermal analysis model-fitting have been developed. Serbanescu compiled and compared 17 of these models, noting the inapplicability of the Arrhenius parameters (of which these models are fit to) to the system of condensed-state reactions occurring [186]. Further, *model-free* (or *isoconversional*) kinetic models (assuming isothermal constant conversion, and exclusively temperature-dependent reaction rates) have allowed for better fitting of Maxwell and Boltzmann's energy distribution functions, thus allow for a better physical description of the process [187]. A number of models, stemming from first principles of Stamm et al. 1956 and Madorsky et al. 1956, followed by Kilzer and Broido 1965, Shafizadeh 1968, Broido and Nelson 1975, Lewellen et al. 1977, Shafizadeh and Bradbury 1979, Agrawal 1988, Diebold 1994, Di Blasi 1996, Varhegyi et al 1997, are considered canonical (although not exhaustive), and deserve mention [188]. Because kinetic parameters are sensitive to reaction conditions and feedstock properties, this study does not go as far as comparing reaction kinetics among potential pathways. Thus these models have limited applicability beyond those with more sophisticated mechanisms, such as those of Lewellen et al. 1977, Ranzi et al. 2008 (elaborating on elementary reactions of light oxygenates), and Garcia-Perez 2008 (informed by a literature review on PAH and dioxin formation during cellulose pyrolysis and combustion) [188]. Garcia-Perez's model involves fast depolymerization to low DP "active cellulose" which can either fragment to light oxygenates, further depolymerize to levoglucosan, or cross-link to char (low temperature/slow). Levoglucosan can undergo retro-ene reaction to acetaldehyde or other light oxygenates, could repolymerize to polysaccharides ("lignin-inhibited"), or could undergo alkali-catalyzed oxidation to levoglucosenone which could further dehydrate to furans [189], verified by the work of Bai et al. [190].

Comprehensive cellulose pyrolysis models have been developed, such as the early review by Molton and Demmitt [191] (in 1977), and more recently; Lin et al. [192] (in 2009), Agarwal et al. [193] 2012's *ab initio* model, Vinu and Broadbelt [194] (in 2012), and Mayes and Broadbelt [195] (in 2012). Molton and Demmitt identify possibilities for cellulose direct decomposition to light products (in addition to the default convention involving a levoglucosan intermediate), through direct ring scission to furans and light oxygenates, for example [191]. Detailed arrow pushing mechanisms were also shown for the production of 1,6-anhydro-β-glucofuranose (a levoglucosan decomposition precursor to levoglucosenone), decomposition of 1,6-anhydro-β-glucofuranose, and formation of levoglucosenone repolymerization products, to name a few [191].

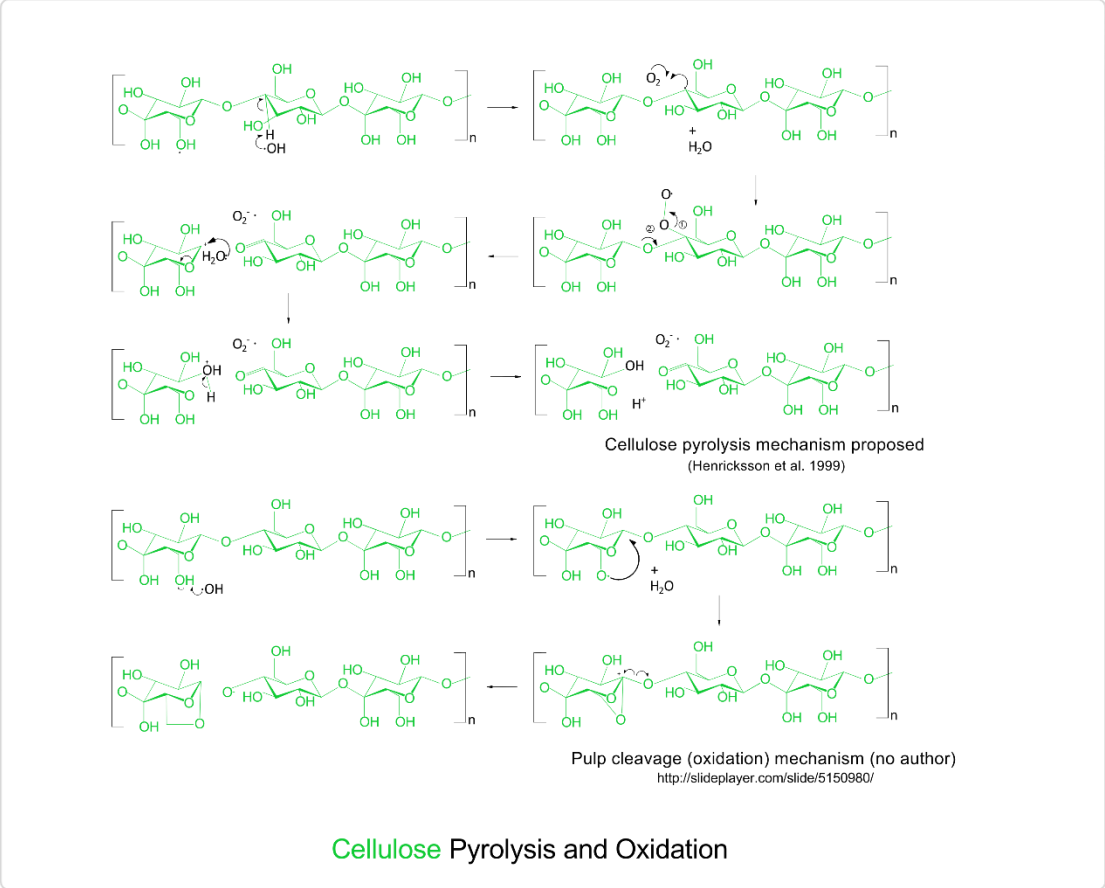

Figure 5. Pyrolysis and oxidation mechanisms of cellulose

Lin et al., define "active cellulose" as cellobiosan through septaosan. They propose all reactions pass through a levoglucosan intermediate, but that levoglucosenone can form directly from levoglucosan by double dehydration. Alternately proposing levoglucosan decomposition to either anhydro-α-glucopyranose (through isomerization) or dianhydro-β-glucofuranose (through a single dehydration) as double and single dehydration precursors to levoglucosenone, respectively, [192].

At low temperatures (327°C), Agarwal et al., propose depolymerization occurs driven by a concerted ring-contraction (reduction of glucopyranose to glucofuranose) and cleavage of the end unit. Additionally, they propose both neighboring group participation and hydrogen bonding involvement in formation of the levoglucosan precursors, which could possibly support observations of lower levoglucosan yields when "active cellulose" is diluted by other pyrolysis intermediates, during the pyrolysis of whole biomass [196]. Although supporting this observation, the prevailing theory has to do with inhibition of levoglucosyl formation due by lignin carbohydrate complex covalent linkages (oxygen at the C_6 position physically precluding formation of the levoglucosan bridge) [197].

Vinu and Broadbelt generally categorize reactions as occurring within the cellulose chain leading to cleavage, or reactions among low molecular weight products. They also mention the three general cellulose pyrolysis schools of thought; a gas-phase free radical mechanism, a condensed-phase concerted reaction mechanism, and an ionic reaction mechanism. Among the condensed-phase concerted reactions, five possible routes (termed *initiation*, *depropagation*, two

called *end-chain initiations*, and *thermohydrolysis*) are discussed. Glycoaldehyde is said to result from a mid-chain ring-hydroxyl dehydration to form a double bond making the ring susceptible to a retro-diels alder ring-opening reaction. A comprehensive mechanism for the conversion of glucose (as an intermediate) into all of the commonly observed low molecular weight decomposition products is proposed [194].

Mayes and Broadbelt propose a revision to Strati et al. 2002's density functional theory (DFT) study, identifying a set of cellobiose conformations with lower energies. These new conformations allow them to identify a new set of kinetic constants and reaction coordinate energies, which "better align with experimental values" to be generated [195].

In 2014, Mayes et al. [198] investigated 5-HMF and levoglucosan formation in greater depth through a computationally-supported experimental study. Findings suggest α-D-glucose in addition to the common intermediate beta-D-glucose are "accessible" to further react under standard non-oxidative pyrolysis conditions.

Oxidative Pyrolysis

Cellulose oxidation methodologies have been developed and employed industrially for nearly 150 years, starting with the advent of camphor-plasticized nitrocellulose (used as a synthetic polymer), followed by a wide range of products made from cellulose acetate, nitrocellulose, methyl-,ethyl-,hydroxyethyl-, hydroxypropyl-, and sodium carboxymethyl-cellulose, all making use of native cellulose's concentration of hydroxyl functionalities [199]. Komen et al. [199] reviewed the history of pulp oxidation technologies listing numerous applications of catalysts for improving pulping process compatibility, wet fiber strength, and fiber resilience during hypochlorite bleaching, a number of which utilize TEMPO catalyst. Further, TEMPO combined with a variety of oxidants has been explored for development of various commodity chemicals (markedly; carboxylates, aldehydes, and esters) [200]. Thanks to all of this work, mechanisms for a variety of cellulose oxidation reaction conditions have been published. Komen's 2002 patent on the production of stable carboxylated cellulose shows what might be the most energetically favorable oxidation pathway; oxidation of the C_6 primary alcohol, Figure 6 [199]. Oxidation at this site leads to hydrogen abstraction from the hydroxyl, leaving an aldehyde, or further oxidized to a carboxylic acid.

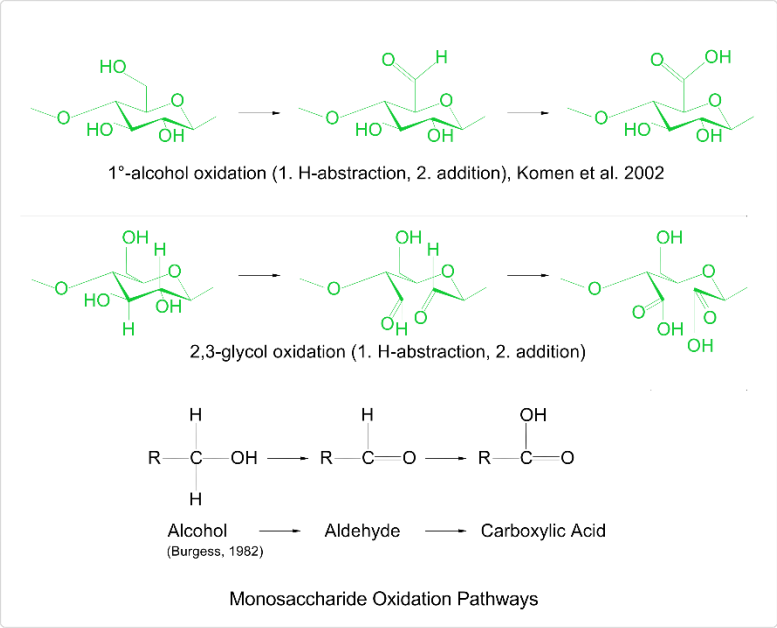

Figure 6. Monosaccharide oxidation pathways. (Top) primary alcohol oxidation, (middle) 2,3-glycol oxidation, (bottom) generalized secondary hydroxyl oxidation, [199].

Alternatively, cellulose units can be oxidized at the 2,3-glycol group. In a two-step oxidation (periodate acid oxidation, and subsequent reaction with the Girard reagent) dialdehyde modified cellulose was produced from hairy cationic nanocellulose [201]. Yang and van de Ven propose the periodate leads to the ring-opening at the C_2-C_3 bond, leaving two carbonyls where hydroxyl groups were present (as well as reducing the periodate and forming water) [201]. Very recently, Yuldoshov et al. [202], also oxidizing cellulose using a periodate acid, proposed the formation of a cyclic periodate (dioxetane) intermediate. Another group reported oxidation at this site through the use of ammonium cerium(IV) nitrate as a microfibrillated cellulose oxidant, proposing ring-opening with a single hydroxyl-hydrogen abstraction (leaving a radical which further reacts with the Girard reagent) [203].

The last oxidation which might possibly commonly occur is that leading to the cleavage of the glycosidic interunit bond. Most depolymerization mechanisms involve hydrolysis by dehydration; requiring vapor-phase water, two hydrogen atoms, or a hydrogen peroxide-sourced hydroxyl radical. Since all of these could be liberated by molecular oxygen oxidation reactions, this is a plausible step to occur during oxidative pyrolysis. If not driven by these energetic species, heat from nearby exothermic oxidation reactions could simply induce homolytic or heterolytic cleavage of the linkage [204]. During oxygen bleaching, carbohydrates have been observed to be undesirably slightly degraded by hydroxyl radicals, leading to cleavage of glyosidic bonds, during oxygen bleaching [205].

Hemicellulose

Non-oxidative Fast Pyrolysis

Hemicellulose is often the first fraction to begin to decompose due to the large amount of covalent bonding, and the reactivity of functional groups which it contains, generally considered to devolatilize between 220 - 315°C [206]. As described above, most hemicellulose is built of glycosidically bonded xylose, mannose, galactose, arabinose and rhamnose, of which are found in units with a degree of polymerization generally less than 100 [207]. Patwardhan et al. [208] used

xylan to develop a hemicellulose pyrolysis mechanism, as distinct from cellulose. While levoglucosan forms during cellulose pyrolysis, no anhydrides form during hemicellulose pyrolysis due to xylose's lack of a secondary alcohol, inhibiting bridge bond formation of the xylosyl cation intermediate (possible with cellulose's glucosyl cation intermediate). Xylose rather dehydrates to furans and anhydroxylopyranoses (AXP, DAXPI, and DAXP2), DAXP2 (xylose's double-dehydration product) being the major product [208]. Also notably, hemicellulose forms greater amounts of light oxygenates (ring-degradation products) than cellulose, postulated consequent from hemicellulose's degree of branching and overall amorphous structure [208]. Ponder et al. Investigated the role of linkage position on pyrolysis of glucans (a class of polysaccharides containing the secondary alcohol required for levoglucosan formation), finding that linkage location did not substantially affect levoglucosan yield, while other factors, such as AAEM content, were more influential [209].

Oxidative Pyrolysis

Thermal degradation of xylan (the common hemicellulose surrogate) under varying oxidative conditions (0, 7, 20, 60%-by volume) under slow heating, and long residence times lead to the formation of furfural, 1-hydroxypropanone, acetic acid, acetone, water, formaldehyde, CO, and CO_2 [210]. Similar to other biopolymers, thermogravimetric analysis of xylan shows two periods of mass loss, the first associated with pyrolysis and oxidation of saccharide-related molecules, the second shows oxidation or combustion of the char residue. Greater oxygen concentrations lead to more abrupt pyrolysis peaks at the lower end of normal devolatilization temperatures, and at high concentrations dramatically reduced the char oxidation temperature (peaking at 467°C, and 409°C for 7% O_2, and 60% O_2, respectively), as would follow flammability limit logic [210]. As oxygen concentration increased, yields of furfural, 1-hydroxypropanone, acetic acid, and acetone decreased while formaldehyde, water, CO and CO_2 increased [210,211]. Under alkaline hydrolysis pulping conditions, the hemicellulose fraction is degraded by way of depolymerization from the reducing-end (termed *primary peeling* by the Kraft industry), mid-chain scissions, monosaccharide degradations (termed *secondary peeling*), and hydrolysis of substituents (such as acetyl groups) [212]. Hemicelluloses were more susceptible to degradation during pulping than cellulose because of lower degree of polymerization (containing more, reactive reducing-end's), and lesser extent of crystallinity. Given this, even solubilized fragments of some hemicellulose units are resistant, such as those of xylan, due to glucuronic acid substituent stabilization (requiring greater temperatures to decompose), while others (such as galactomannan) are readily degraded [212]. The peeling reaction mechanism involves keto-enol tautomerization weakening the reducing-end hemiacetal, allowing β-alkoxy scission to an aldehyde and monomer (forming a new reducing end in the process) [213]. Peeling continues until left with a metasaccharinic acid [212]. Wetterling outlines a number of other potential premature termination reactions, such as C_3 (rather than C_4) β-elimination [212]. Xylan has also been described to peel to xylose and 4-*O*-methylglucoronic acid under *alkaline* hydrolysis conditions, or xylose and hexenuronic acid under *acid* hydrolysis conditions [214].

Lignin

Non-oxidative Fast Pyrolysis

Lignin pyrolysis is distinct from that of cellulose or hemicellulose, characterized by a broad temperature range of devolatilization, encompassing those of the other fractions. Many different ranges are proposed, but generally include 180°C to 750°C [50,67,206,215-218], reported extending to as high as 900°C [219]. Below 350°C pyrolytic cleavage of interunit linkages to monomers through fragments is thought to predominate, whereas above 500°C ring fragmentation

to acids and oxygenates (aldehydes, and ketones) is thought to become significant [215]. More specifically, propane side chains of H-acids, and S- and G-acids have been shown to breakdown between 230-260°C and 240-260°C respectively [220]. Aryl-ether bonds have been shown to decompose at temperatures below 310°C [221], or in some cases as low as 250°C [222]. Condensed linkages in a similar, slightly higher range of 275-350°C [220]. Formation G-unit derivatives, notably methylguaiacol, ethylguaiacol, and guaiacol are favored at low temperatures whereas S-unit derivatives catechols and phenol) are favored at higher temperatures [223]. This was supported by the work of Rover et al. [224], who showed greater yields of alkylated phenols, where mono- and dimethoxyphenols had maximum yields at 400°C and 350°C, respectively.

An area of continued debate revolves around the mechanism of lignin-derived aerosol or oligomeric pyrolytic lignin formation. The peculiarity is the collection of products with boiling points greater than that of the reactor, thus the question is; "how do they get out?" Patwardhan et al. [225] discusses the two prevailing theories premising on thermal ejection (allowing for entrainment of liquid-phase products) and pyrolysis to monomers followed by rapid recombination reactions. Rapid, possibly uneven, heating and initiation of boiling has been suggested to induce large shear stresses in the condensed phase exceeding the surface tension forces, allowing for small droplets to become ejected and entrained in the sweep flow. This phenomenon has been demonstrated in some pyrolysis experiments, although the applicability to continuous flow systems has been questioned due to differences between unidirectional heating and omnidirectional heating [225]. The second theory postulates that pyrolysis of lignin at 500°C fully depolymerizes the lignin structure to monomers able to vaporize at reactor conditions, which repolymerize to oligomers that coalesce into aerosols prior to collection [225].

Regarding the mechanism of lignin pyrolysis, two common approaches are to investigate how the inter-unit linkages behave, and how monomer units themselves behave under pyrolysis conditions. Choi et al. [226] demonstrated the role of functionalities on β-*O*-4' model compounds. When no functionalities were present, homolysis of the C_β-O bond leaves reactive fragments which could abstract hydrogens to form phenol or toluene, which could recombine to form bibenzyl or benzylphenols. Presence of an α-hydroxyl allowed for dehydration to a conjugated linkage (minor), or a retro-ene to form cyclohexadienone or phenylethenol intermediates (major), which further demethylated and tautomerized, tautomerized , hydroxylated and dehydrated, or just tautomerized to form benzaldehyde, acetophenone, phenylacetaldehyde, or phenol, respectively [226]. Presence of both α- and γ-hydroxyl (γ-hydroxyl being synonymous with β-primary alcohol), was proposed to react by similar means, but yielding products containing an extra primary alcohol and or double bond [226]. Nakamura et al. [227] demonstrated the reaction pathways which different linkage types might undergo. They used highly substituted models representative of native cellulose; the β-*O*-4' model containing both the α-hydroxyl and γ-hydroxyl, for example [227]. For the β-*O*-4' model, C_β-O cleavage (by concerted retro-ene according to Choi et al. [226]) to cinnamyl alcohol structures was predominant, while in the β-5' model C_α-C_β cleavage to methoxy-styrene and methoxybenzaldehyde structures was predominant, for both; γ-hydroxyl elimination was observed, leaving stilbene-type structures for example, when the β-5' was not cleaved [227]. In the case of α-*O*-4' models, C_α-O cleavage lead to formation of guaiacols, and condensed 5-5' linkages, stable at standard pyrolysis temperatures (not yielding any low molecular weight fragments) [227].

Lignin monomer pyrolysis reaction pathways can be described on the basis of phenolic side chains. Scheer et al. [228] looked at the pyrolysis of methoxyphenols (guaiacols), showing a general series of reactions; 1. demethylation (leaving a carbonyl intermediate), 2. decarbonylation (leaving a hydroxylcyclopentadienyl radical), 3. dehydrogenation to cyclopentadienone, and incompletely; 4.

decarbonylation degradation to vinylacetylene compounds. Observation of phenol as a major product prompted the additional step; recombination of cyclopentadienone with a methyl radical, proceeding through a carbene intermediate to phenol [228]. Anisole (guaiacol minus a hydroxyl) has been shown to undergo the same route, and form similar products without the hydroxyl, initiated by either a hydroxyl O-H scission or tautomerization to a carbonyl [229]. Dimethoxybenzene's pyrolysis path appears dependent on methoxy relativity; *ortho-* leading to hydroxybenzaldehyde, *meta-* leading to cyclopentadienone, *para-* leading to 1,4-benzoquinone [229]. Syringol appears to undergo demethylation, undergoing resonance to a form conducive of demethoxylation, leaving catechol [229].

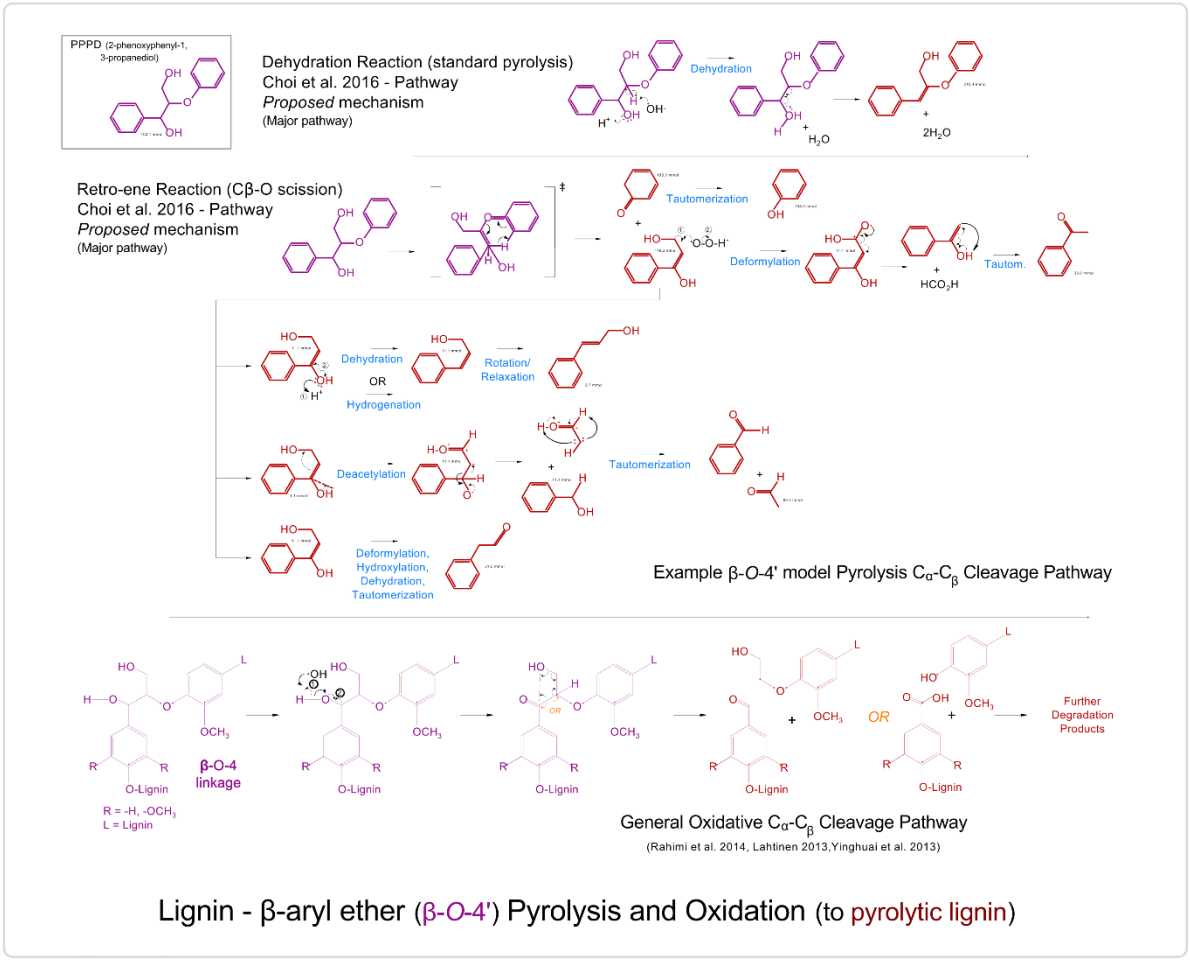

Figure 7. β-O-4' Lignin linkage pyrolysis and oxidation reaction mechanisms.

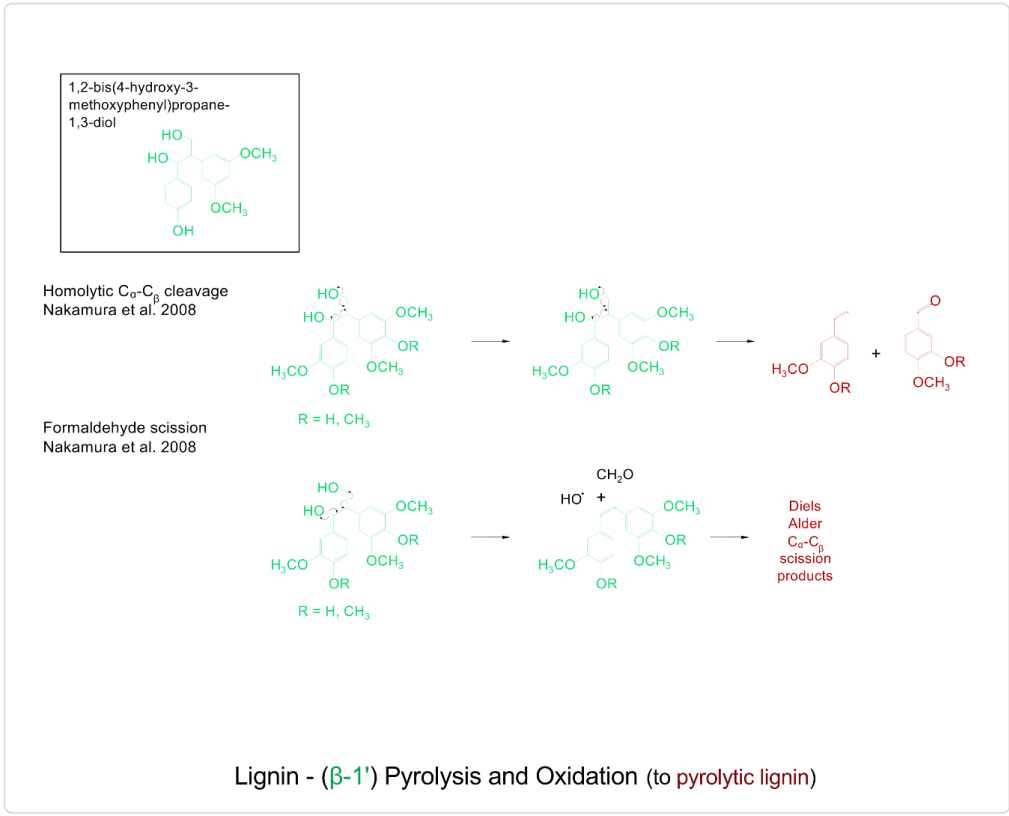

Figure 8. β-1' Lignin linkage pyrolysis and oxidation reaction mechanisms.

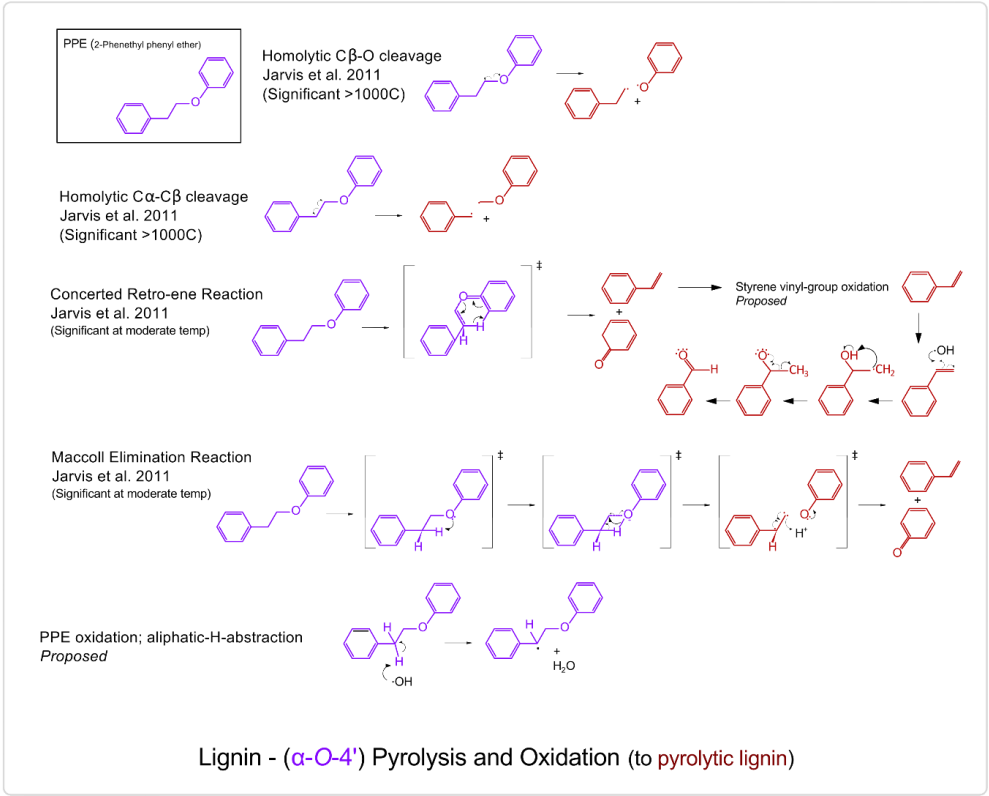

Figure 9. α-O-4' Lignin linkage pyrolysis and oxidation reaction mechanisms.

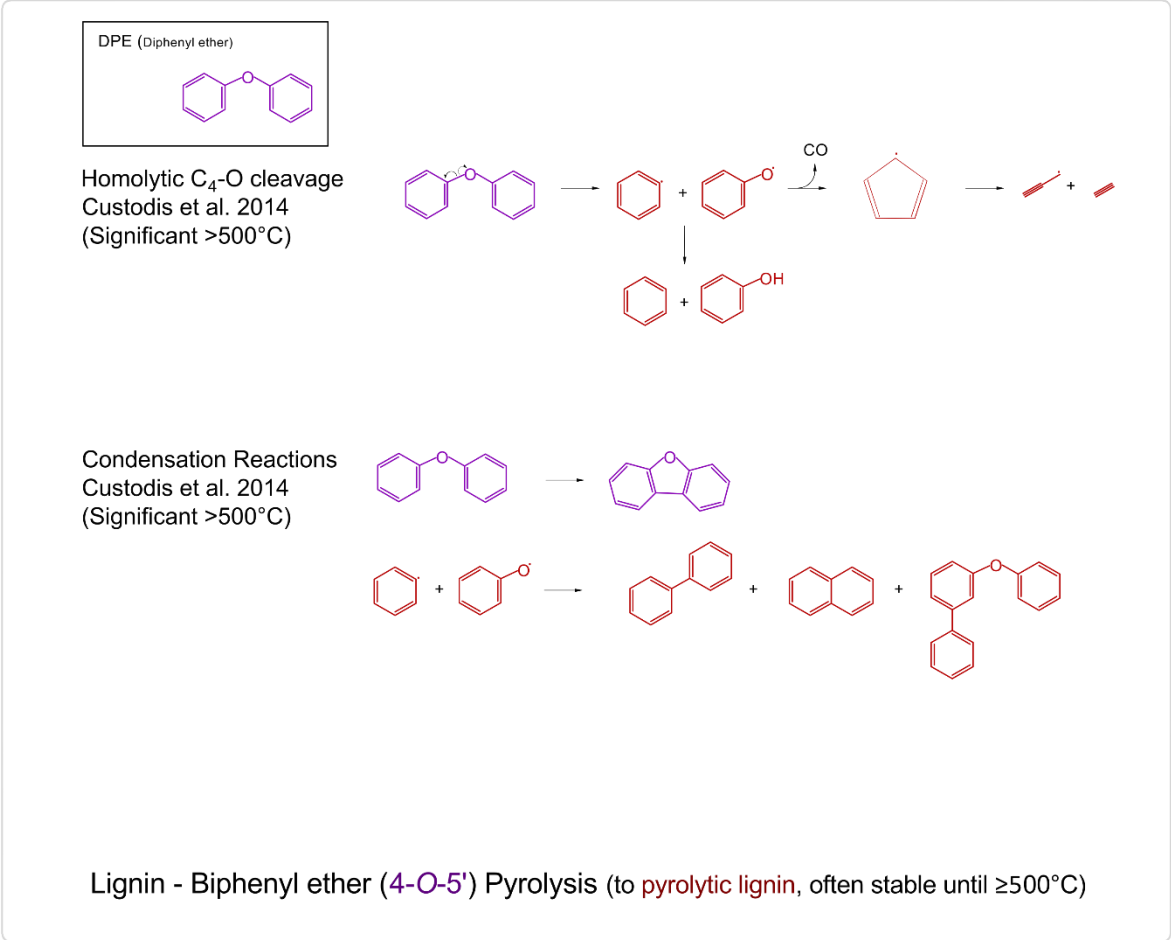

Figure 10. 4-O-5' Lignin linkage pyrolysis and oxidation reaction mechanisms.

Oxidation

Since little work has been done characterizing the mechanisms of high temperature thermal, molecular oxygen-oxidation of lignin in the condensed phase, few *directly* analogous precedents exist. Most existing studies on molecular oxygen-oxidation are either limited to small compounds (vapor-phase) or low-temperature, long residence conditions. Some additional classes of related mechanistic precedents are in the areas of enzymatic-, organometallic-, biomimetic-, or aqueous phase-catalyzed conditions. Further; solid-state oxidizer, and gaseous (molecular oxygen or ozone)-oxidation of lignins have been studied. Combustion research of the 1940's-1980's resulted in the publication of a number of gas phase oxidation analytical studies, although generally limited to ethylbenzene, styrene or smaller [230-235]. The pulp industry has investigated a diversity of oxidative delignification methods, some of which involve molecular oxygen-oxidation. A text reviewing oxidative delignification was edited by Argyropoulos in 2001 [236]. Additionally, Lange et al. [117] and Crestini et al. [51] reviewed lignin upgrading pathways involving various modes of oxidation (unrelated to the pulp industry).

From a theoretical standpoint, the relative reactivity should not be uniform across different lignin monomeric units or interunit linkages. Northey reviewed structure-reactivity effects, as well as reaction pathways, in lignin models under oxygen bleaching (gas-phase oxidation) conditions,

elaborated upon below [237]. In their lignin oxidation chapter, Chang and Allan also acknowledge structure-reactivity effects, such as lack of a phenolic hydroxyl group, *para* to a propyl side chain, associated with a lesser amount of oxidation products [238]. A classical oxidation pathway of aromatic aldehydes to aromatic acids, designated the Cannizaro reaction, follows similarly to the alcohol, aldehyde, carboxylic acid pathway described to occur with carbohydrate side chains [239]. Chang and Allan remark that aromatic aldehydes with hydroxyl groups are relatively stable and resistant to nucleophilic attack by a hydroxyl radical, "stability of vanillin, syringaldehyde, and *p*-hydroxybenzaldehyde reflects the resonance stabilization of the carbonyl group by the phenolate anion", justifying the high yield (lack of degradation) of these species [238].

Gas phase-oxidant Oxidation

A product of base-catalyzed oxidation by air, vanillin has been one of the few lignin valorization products to make it to market, having been commercially produced since the 1940's, [123]. The mechanism of formation involves cleavage of a guaiacyl-unit's ether linkage to form a guaiacyl oxy-radical, shifting resonance forms to a stable ketone, followed by dihydroxylation then dehydration to convert the alcohol side chain into an aldehyde, leaving vanillin [118,240].

Pulp is arguably the other major commercial product of lignin oxidation. The primary goal of a pulp mill is to isolate cellulose from a woody lignocellulosic feedstock. The pulping process could also be described as delignification of lignocellulose. Since the widespread adoption of the Kraft (sulfate) pulping process, supplanting the sulfite process, the use of pulp bleaching technologies have greatly increased [241]. This is due to the greater effectiveness of the sulfite process to delignify lignocellulose, directly generating relatively bright pulps, while the Kraft process generates Kraft pulp (known for being of higher Kappa number, darker in color). Many secondary delignification (pulp bleaching) processes make use of oxidation reactions to selectively partially decompose (and allow for separation of-) residual lignin and hemicellulose. Initially, in the 1940's, a variety of chlorine-containing methods were developed. Later in the 1960's and 1970's oxygen bleaching was developed in Sweden and Japan (and later adopted in North America) to replace chlorine bleaching as a more environmentally sensitive approach [242]. In the oxygen bleaching method, pulp and white liquor (alkali source) are pumped into a low pressure mixer in the presence of steam and oxygen, then conveyed in a reactor where the pulp maintains residence for 20-60 minutes at 90-110°C and at 80-125 PSI [241]. The mode of action here is "ionization" (radicalization) of phenolic hydroxyl groups via reaction with the alkaline white liquor leading to ability to react with gaseous triplet state oxygen, forming superoxide anion oxygen, hydroperoxy radicals, and possibly some hydrogen peroxide and/or hydroxyl radicals if residence allows [205]. Lignin units are modified by hydrogen abstraction to form quinones, ring opening to form aldehyde and carboxylic acids, side chain cleavage to benzophenones and various other substitutions [205].

Reactive oxygen species (ROS) become involved in both unassisted gas-phase and enzyme-catalyzed oxidations. From the perspective of metal-ion catalyzed oxypulping; superoxide, hydroxyl and hydrogen radicals all play a role in the lignin-oxidation process [243]. If in a solvent, phenolate ions can reversibly lead to solvent-caged superoxide radicals, which could further form hydroperoxy in presence of metal catalyst [243].

Northey investigated the role of ROS in bleaching, and relative reactivity of lignins to molecular oxygen-oxidation, similarly to the way food compounds are compared with antioxidant bioassays, but in the context of relative effectiveness of delignification. When looking into reactivity of functionalities, a single hydroxyl group was far more reactive than a single methoxy group, a catechol group was far more reactive than a syringyl which was slightly more reactive than a guiacyl, slightly more than a *para*-hydroxybenzene group, and an alkyl group was slightly more

reactive than one with an α-hydroxyl, which was far more reactive than a carboxylic acid, which was slightly more reactive than α-carbonyl [237]. Stilbene structures (a β-5' linked dimer with a C_α-C_β double bond) reacted two orders faster than vinyl-ether linkages, both considered highly reactive relative to β-1', β-5', α-5', β-*O*-4' (with α-carbonyl/hydroxyl), and 5-5' linkages considered "somewhat" reactive. Even less reactive were non-phenolic β-*O*-4' (hydroxyl replaced with methoxy) and cross-linked β-*O*-4' structures [237]. A more comprehensive study comparing specific activities of more than 50 phenolics identified proton-coupled electron transfer (PCET, resulting from homolytic O-H cleavage of active hydroxyls), and sequential proton loss electron transfer (SPLET, initial loss of proton to a free radical, strongly base-catalyzed) as the two predominant mechanisms [244]. Radicals present during alkaline hydrolysis include hydroxyl, superoxide and hydroperoxide, formation elaborated below. Hydroxyl radicals were proposed to form an adduct intermediate, by addition to an aromatic pi-bond, resulting in disproportionation (hydroxylation; cleaving linkage and replacing an aromatic hydrogen), demethoxylation (leaving a benzoquinone), dihydroxylation (cleaving linkage), or demethylation (cleaving linkage and replacing methoxyl), phenolic coupling reactions, side chain oxidations, and C_α-C_β cleavages [237]. Presence of superoxide lead to ring cleavage, oxirane formation, or side chain cleavage forming an aldehyde. Hydroperoxy behaves distinctly from other ROS due to nucleophilicity with carbonyl groups leading to formation of mono- and dicarboxylic acids in cleavage products (when ring-quinones are attacked), or *para*-quinones following side chain eliminations [149].

Combustion research of the 1930's-70's identified mechanisms for gas phase oxidation of some aromatic compounds. In 1935, Newitt and Burgoyne investigated combustion of benzene, toluene, and ethyl benzene, identifying that with substituted benzenes (toluene and ethyl benzene in this study), oxygen attacks the C_α [234]. Toluene oxidized to benzaldehyde and benzoic acid at atmospheric pressure, and benzyl alcohol at elevated pressure [234]. Also noted was increased phenol yield at lower equivalence ratios [234]. In 1955 and 1956 Norrish and Taylor published on the same three aromatics, identifying acetophenone as an additional product, noting its pyrolytic stability "requiring oxidation to form benzaldehyde, positing that acetophenone oxidation was a significant source of benzaldehyde [232,233]. In 1965, Barnard and Ibberson revisited the combustion of toluene, confirming Norrish and Taylor's suspicion of a correlation between formaldehyde concentration and reaction rate (or conversely phenyl radical oxidation [245]) [235]. More recently, Glassman described hydroquinone and pyrocatechol to form dioxetane intermediates with molecular oxygen, bonding at the hydroxyl-carbons, setting the stage for concerted ring-degradation to ethylene and maleic or ethylene and oxalic acids, respectively [45].

Enzyme-catalyzed Oxidation

Although developed for enzymatic oxidations, Perazzini's four-pathway summary of lignin oxidation is applicable to all modes of lignin oxidation. The pathways include; side-chain oxidation (possibly associated with depolymerization), aromatic ring cleavage, phenolic oxidative coupling (or cross-linking), and alkyl-arylether bond cleavage (commonly associated with depolymerization) [246]. While both side-chain oxidation and aromatic ring cleavage are associated with an increase in carboxylic acid content; side-chain oxidation is also associated with a decrease in aliphatic hydroxyl content [246]. Phenolic oxidative coupling is associated with a decrease in guaiacyl hydroxyl and an increase in condensed phenolic hydroxyl content, and an increase in guaiacyl hydroxyl content could be attributed to alkyl-arylether cleavage [246]. In addition to pathways, enzymatic oxidations can be classified by general reaction conditions required. Reitberger classified enzymes as either *oxygenases*; those involving an oxygen-atom transfer requiring close interaction between lignified material and the enzyme, or *cytochromes*; involving one-electron concerted

intermediate-stabilizing steps, less reliant on substrate conditions, the mode of common lignin-oxidizing enzymes [243].

Numerous studies have been carried out on the behavior of extracellular digestive enzymes of saprophytic fungi, ubiquitous decomposers of decaying lignified tissues, chemically decomposing lignocellulose materials to provide access to lignin-protected carbohydrates. These enzymes induce various oxidation reactions by way of electron transfers, hydrogen abstractions, or cleavage events. Three main classes of enzymes are responsible for the degradation of lignin; laccases, peroxidases, and immobilized enzymes.

Laccases and laccase-mediated reactions are well studied in natural decompositions and controlled environments, such as oxidative delignification. Laccases have been shown to substantially oxidize non-condensed C_5 lignin structures (linkages and side chains), cleaving linkages and oxidizing propanoid side chains to carboxylic acids, having little effect on condensed structures [247]. Laccases readily oxidize hydroxyl groups of semiquinones into carbonyls of hydroquinones through superoxide hydrogen abstractions [248]. With the absence of these hydroxyls (such as in non-phenolic substrates), virtually no degradation occurs due to low reaction rates [249]. In addition to *ortho*- and *meta*-quinones; radical coupling products, and ring-opening products were observed from vanillyl alcohol and Kraft lignin [249].

Welinder et al. [250] classifies peroxidase (heme-containing) enzymes into three "superfamilies"; those found in animals (such as glutathione peroxidase), catalases found in animals, plants, bacteria, and fungi, and third, peroxidases found in animals, plants, bacteria, and fungi. The third group is sub-classified into intracellular or membrane-bound, fungal-secreted (extracellular), and plant-secreted peroxidases [251]. Commonly studied in this context are fungal extracellular peroxidases (namely lignin peroxidases (LiP), manganese peroxidases (MnP), and versatile peroxidases (VPs)) [252] Hydroxyl radicals are understood to readily depolymerize lignin and the products of this reaction are also observed during enzymatic oxidation, but when constrained to the ingredients present in a biological context (substrate (lignin), aqueous media (hydrogen peroxide source), enzymes (peroxidases)), hydroxyl formation is not so obvious. Superoxide, whose reaction rate increases with pH, yet is still nominal at high pH, reduces hydrogen peroxide to hydroxyl radicals. Production at rates compatible with observed degradation requires presence of metals (such as Mn, Cu, Li, all in alkaline conditions) to catalyze a Fenton-type reaction, such is the proposed mechanism [253]. Although hydroxyl radical production is desired, excessive superoxide can lead to carbohydrate decomposition (undesired in bleaching processes), which in theory should necessitate passivation or leaching of metals from fibers, but in practice is not a significant issue if magnesium is present, not to mention some fiber loss is accepted in exchange for brighter pulp [243]. LiP and VPs are able to oxidize non-phenolic lignin, while MnP's requires accessible hydroxyl content to achieve Mn-chelation [252]. LiP, with its iron-centered heme, converts phenolics into phenoxy radicals leading to side chain cleavage, demethylation, isomerizations and radical recombinations (and ring-hydroxyls to aldehydes or carboxylates), and non-phenolics by one-electron benzylic cation-forming oxidations followed by C_α-C_β cleavage to radicals and aldehydes [254]. MnP, notably its Mn(III) chelator complex, is termed a *diffusible* mild oxidant, behaving similarly to LiP in presence of phenolic lignin. Although unable to directly oxidize non-phenolics, studies have shown it capable of doing so in the presence of a secondary mediator, often thiols or lipids, in which case β-aryl and C_α-C_β cleavage occur [255]. VPs, a class of glycoproteins, behave similarly to LiP and MnP, but generally are less active than LiP, other than the case of hydroquinones and substituted phenols which are only efficiently oxidized indirectly by LiP and MnP [252].

Cellobiose dehydrogenase (CDH), named after its role in cellulose degradation, has been shown to; assist LiP by preventing radical repolymerization, reduce quinones (toxins in biological systems) to phenols, and assist in transport of Mn(III) complex during MnP delignification [256]. In some cases, CDH has even been shown to slightly depolymerize lignin models on its own [257].

Enzymes are often immobilized, affixed to a substrate, and often treated, for improved activity and post process separation [258]. When a horseradish peroxidase (HRP) was immobilized using the layer-by-layer (layers of HRP and polyelectrolyte of alternating charge) method, it showed improved activity over the "free" enzyme, allowing further lignin depolymerization through the same proposed mechanism (notably the four main lignin oxidation pathways outlined by Crestini et al. [51]) as the free enzyme [259]. When repeating the experiment with a laccase, similar benefits were observed, those being improved conversion efficiency and stability [246]. Laccase stability in commercial processes is of concern due to concern of denaturing in low pH and high ion-concentration environments, justifying immobilization [260].

Organometallic Oxidation

Methyl rhenium trioxide (or methyltrioxorhenium, (MTO)), falling into the chemical class of perrhenates (and more specifically, organohenium(VII) oxides), catalyzes aqueous oxidation by hydrogen peroxide (or molecular oxygen). Apparently having been synthesized for the better part for four decades, MTO processing has become quite developed, allowing for catalyst recycling, [261]. MTO is used in its pure form, or on supports such as polymer or encapsulations [117]. When interacting with monophenols, can form *ortho*/*para*-quinones, products of ring-opening such as conjugated diacids or bicyclic furan structures [117]. When interacting with methoxybenzenes, forms *ortho*/*para*-quinones and methoxyphenols [117]. In the presence of substituted β-*O*-4' dimers, cleavage occurs leaving phenolic acids and some furanic products of ring-opening, [262]. α-1' dimers were less reactive, if cleavage occurred resulting in phenolic esters or carboxylic acids [263]. Overall, MTO enables weak oxidizers (such as molecular oxygen and hydrogen peroxide) to oxidize reactive aromatic structures strongly, and more resilient structures (such as condensed-linkage structures) to a lesser extent [263].

Salen complexes are a class of compound used as catalyst in ligand coordination chemistry containing both aryl-amine (imines) and phenolic aldehyde groups, which readily coordinate with numerous metals of varying oxidation state [264]. Hydroxycinnamic ester side chains were cleaved at the side chain-double bond to form phenolic aldehydes and esters [265]. In the presence of substituted β-*O*-4' dimers, Co(salen) and molecular oxygen lead to phenolic acids and phenoxyacrylaldehydes [266]. Side chains and linkages of β-5' dimers are oxidized by the Co(salen) complex, to poly-acid structures and monophenol acids and esters [117]. Another study showed reaction with phenylcoumarin (a β-5' dimer) caused furan-ring (C_4-*O* bond) opening and ipso-C_α cleavage to coumarin and monophenols [266]. Díaz-Urrutia compared behavior of a variety of vanadium and copper catalysts, showed that relative to an oxovandium catalyst, salen-vanadium consistently lead to low product selectivity yet very high conversion of β-*O*-4' models of varying degrees of functionalization [267].

Polyoxometalates (POMs) are a catalyst which can be categorized into two groups; isopolyanions (with the general formula $M_xO_y^{m-}$, M = Mo, W (common)) and heteropolyanions (with the general formula $X_zM_xO_y^{n-}$, X = P, Si, B, Ge, M = Mo, W, V), distinguished by their metal-oxide polyhedral structures (commonly octahedral, pentagonal pyramidal, or square pyramidal, commonly categorized by structure as Keggin-, Dawson-, or sandwich-type) [268]. Gaspar et al. [269] reviewed application of POMs to pulp delignification, highlighting unique characteristics; recalcitrance to oxidative degradation, acting as electron pools, inclusion of metals at their highest

oxidation state into the structure, solubility well-suited for liquid-phase reaction environments, and the ability to tune redox properties through selection of polyhedral structure. When a silicon-tungsten-vanadium-oxide POM was used with a functionalized β-*O*-4' model, the α-hydroxyl was oxidized, weakening the linkage, to some extent leading to its cleavage (of which the catalyst assisted in subsequent oxidation of monophenol fragments to quinone structures) [269]. Another review citing a similar study [270], utilizing a phosphorous-molybdenum-vanadium-oxide showed similar pathway and products [117].

Biomimetic Oxidation

Metalloporphyrins, a class of metal-centered porphyrins (large symmetric heterocycles generally based on four pyrrole subunits), are classified as biomimetic catalysts because some porphyrins are found in nature, such as heme, a co-factor and pigment of hemoglobin (not directly responsible for containing diatomic oxygen through the vascular system, rather playing a crucial role in its delivery by inducing conformational changes in the oxygen-receiving protein, or heme-peroxidases (described above) [271]. Crestini et al. [272] (in 2003) reviewed metalloporphyrin-catalyzed oxidations of lignin and lignin model compounds. Comparison of lignin peroxidase (LiP), manganese peroxidase (MnP) and metalloporphyrin-mediated oxidation of veratryl alcohol demonstrated similar effects, yielding verartaldehyde and *para*-quinone as major products, but proposed to occur by different means. The peroxidases both aid hydrogen peroxide oxidation; LiP by side chain oxidation to veratraldehyde, and one-electron oxidation leading to a temporary ring opening, eventually forming a quinone. MnP oxidizes ring-hydroxyls and α-oxo lignin keto acid groups, allowing formation of both veratraldehyde and quinones. The metalloporphyrin was described to form veratraldehyde and quinones by "benzylic oxidation followed by C_5 position hydroxylation followed by C_3 position demethoxylation" [272]. Horseradish peroxidase appeared to operate similarly, but having a greater selectivity towards veratraldehyde, conversion forming veratryl alcohol enhanced through the use of ionic liquids and Horseradish Peroxidase (HRP) immobilization [273]. When testing a beta-1 model, similar occurred but yielding *ortho*-quinone rather than *para*. For the C_α-C_β cleavage the proposed mechanism involved a benzylic oxidation (ring electron attack) followed by resonance of the radical to the C_β which then lead to cleavage upon interaction with another radical fragment and kicking off of an alcohol-hydrogen to stabilize the ring's positive charge (see scheme 17 in [272]). Additionally, C_β-C_1 oxidation lead to small amounts of muconic acid derivatives forming from ring-opening. Workup of the porphyrin with 5-5' model compounds oxidized aldehyde functionalities to carboxylic acids and some extent of ring-opening occurred. In another 5-5' model (with methoxy functionalities rather than aldehydes), one of the rings oxidized to a quinone (without cleaving from the other). In short, oxidation of lignins with porphyrins proceeded through side-chain oxidation, formation of *ortho*- and *para*-benzoquinones, and small amounts of aromatic ring cleavage to muconic acid derivatives [272]. Immobilized (supported) metalloporphyrins, are supported for the purpose of physical shielding from the harsh conditions of a commercial process. Support substrates which have been published on include; silica gels, clays, and synthetic polymers [274-276]. There have also been proposals for use of ionic liquids as a metalloporphyrin catalysis media [277-279]. Dendron-encapsulation of metalloporphyrins in a 3,5-dihydroxybenzyl alcohol-based dendrite, similarly to immobilized enzyme catalysts showed improved catalytic efficiency and resilience [280].

Catalyzed Aqueous-phase Oxidation

Hydrogen peroxide and peroxy acids are common aqueous oxidizers, generally considered mild when not catalyzed. Under strong alkaline conditions, peroxides become reactive nucleophiles,

reacting with carbonyl and conjugated compounds, whereas under acidic conditions, behave as electrophiles, reacting with unsaturated compounds (notably aromatic rings and vinyl- or double-bond containing side chains) [281]. Under alkaline conditions, they behave as electrophiles, readily undergoing addition reactions, epoxidation and hydroxylation), whereas in acidic conditions, becoming proxy anions (a conjugate base), peroxides readily undergo reactions involving electron pair transfer [281]. Alkaline hydrogen peroxide has the tendency to cleavage β-*O*-4' models at the C_1-C_α bond by way of Dakin-reaction (formation of epoxide intermediate followed by hydrolysis and bond cleavage) , [282]. Non-phenolic side chain structures have the tendency to cleave at the C_α-C_β bond following formation of an dioxetane intermediate [283]. Alkaline hydrogen peroxide oxidation of a 5-5' lignin dimer was investigated by Jurasek et al. [284] who identified dimer-rearrangement reactions (leaving a 5-*O*-4' linked system) and dioxetane-intermediate induced ring-opening, which subsequently either underwent lactonization or muconate scission to a lactone monophenol, or methylmaleate and a monophenol as predominant initial steps, respectively. If residence time allowed, monophenolic species proceeded to a hydroxymethoxybenzoic acid [284].

Rahimi et al. [285] compared effects of zinc, aluminum, magnesium, iron, and manganese on the aqueous formic acid-induced aerobic depolymerization of lignin and two β-*O*-4' models; one with a primary alcohol on the C_α, the other with a carbonyl on the C_α (as might be formed during pulping, resultant of oxidation). Although functionalities were further oxidized, no C_β – O cleavage products were produced from the first model, whereas the carbonyl model did majorly cleave [285]. With zinc; *O*-formylated products were minor (6%) and large amounts of dimethoxy-aryl-ethyl ketone phenol product and guaiacol (69%) were observed. With the other three metals, a di-ketone product replaced the monoketone product [285]. Davis et al. [123] reviewed lignin oxidation and cited usage of metal salts, Co(II)/Mn(II) acetate, to cleave beta-aryl ether linkages of phenolic and non-phenolic β-*O*-4' models, consistently cleaving the C_α-C_β bond.

Although primarily applied to cellulose systems, TEMPO catalyst has been used with lignin compounds to catalyze oxidation. One group using TEMPO as a part of a TEMPO/CuCl/bpy/NMI liquid-phase system showed monophenol benzylic hydroxyl underwent retro-aldol reaction then dehydration to form aldehydes and enals, and that C_α and C_γ hydroxyl groups in β-*O*-4' models had hydrogen abstracted leading to the formation of a 1,3-dicarbonyl TEMPO-adduct [286].

Inorganic-Oxidant Oxidation

A final class of lignin oxidation analogs are often catalyzed inorganic oxidizer-oxidation of lignin, taking place in the solid and liquid phase. Manganese oxide (MnO_2) is commonly discussed in the context of manganese peroxidase, due to its presence in decaying woody materials [287]. Traditional bleaching technologies utilize chlorine and chlorinated compounds (such as chlorine solutions and sodium hypochlorite) as oxidizers to delignify. Sarkanen described how chlorine-oxidations (in the case of Cl_2 solutions) occur by four main routes; aromatic substitution yielding a chlorinated phenol and HCL, electrophilic displacement yielding RCl and a chlorinated phenol, chlorine-catalyzed hydrolysis (and dehydration), and oxidation (a double-abstraction) yielding a benzoquinone and 2HCL given hydroquinone as an reagent [288].

Lignin Carbohydrate Complexes

Thermal Depolymerization

A study by Min et al. 2014 showed that mild-temperature alkaline hydrolysis of corn stover LCC's lead to a decrease in ether linkage content (presumably cleaved), and an increase in condensed linkages (notably β-5') increased (treatment allowing for condensation or cross-linking) [152].

Adhesion forces are one way to characterize the stability of LCC linkages, and how likely they might be to cleave under a thermal dissociation environment. Youssefian and Rahbar computed adhesion forces between faces of crystalline cellulose *and* hemicellulose, LCC's, and lignin units, reporting 38, 57, 58 MJ/m^2 and 44, 76, 95 MJ/m^2, for electrostatic and Van der Waals forces respectively [91].

Oxidation

Due to the prevalence of ester and ether LCC linkages, cleavage may occur by hydrolysis reactions. Thus a number of the studies looking at enzymatic and catalytic oxidation noted degradation of LCC linkage, [76,153,154,289-295]. One study showed preferential polymerization of oxidized units, rather than depolymerization of the Lignin associated with these structures [292]. Another study investigated the use of a Co(salen)-catalyzed hydrogen peroxide (discussed above, strictly in the context of lignin) decomposition of LCC's, for application in pulp bleaching [293]. Even at mild conditions (90°C for 5 hours), the complex indiscriminately oxidized the LCC; leading to LCC-linkage cleavage, lignin β-*O*-4' cleavage, phenolic ring-opening, side chain oxidation, and demethoxylation, according to fragments observed [293]. Because of the harsh nature of Co(salen), it is likely a poor model for LCC behavior during oxidative pyrolysis. Nguyen 2008 (thesis) synthesized then oxidized LCC's, notably 4-methoxyphenyl-β-D-glucopyranose and coniferin, in hydrogen peroxide, superoxide, as well as in the presence of photolysis-generated ROS [294]. Observed ether cleavage was proposed to occur by hydroxyl attack at the ipso (lignin-C_1) position leading to homolytic cleavage. The glucoxy radical was thought to abstract hydrogen from the hydrogen peroxide and further oxidize to gluconic acid or arabinose [294]. Superoxide was thought to attack at the same position, leaving a phenyl peroxyl anion rather than a 4-methoxyphenol (as during hydrogen peroxide oxidation). UV radiation during photolysis was thought to cleave the phenolic side chain of coniferin while the ROS generated were thought responsible for ether cleavage (by modes similar to the prior oxidants) [294].

Extractives

Thermal Depolymerization

Terpene thermochemistry has been studied in depth, for the better part of 70 years [296]. Stolle et al. [296] reviewed monoterpene, monoterpenoid "thermal rearrangements", used pinane, carane, and thujane as fully-saturated surrogates for the three main structural classes of monoterpenes, which generally undergo ring-opening reactions. These saturated structures (without a double bond C_α to the cyclobutane) behave similarly to other cyclobutane structures, whereas unsubstituted relatives (α-pinene and β-pinene for example) behave similar to other vinylcyclopropane species, generally undergoing ring-opening reactions or concerted reactions to branched linear structures, respectively [296]. If conditions, such as residence allow, acyclic primary pyrolysis or pinane-type species undergo ene-cyclization reactions [296]. Pyrolysis of the long-chain linear terpenes solanesol, squalene, phytol, and β-carotene at 600°C and short residence times (<1s) lead to chain scission and cyclization reactions, initiating PAH (polyaromatic) formation (3-5 ring structures, and growing to macroscopic PAH's (soot) at longer residence times, [297]. Additionally, a significant portion (notably greater than sterols which have been shown to more predominantly convert to PAH's) of lighter compounds; isoprene, toluene, and xylenes, were shown to form (resultant from the cyclization of chain cleavage products) [297]. During torrefaction of woody biomass, sterols and other lipophilic structures are described to be "emitted" between 150-200°C [298]. Although dehydration can lead to ether formation when maintained at 250°C for multiple hours, Moldoveanu describes sterols as stable until 400-450°C, at which point begin to

undergo rapid dehydration and dehydrogenations as well as double bond migrations, to unsaturated aliphatic hydrocarbons [299]. Under flash vacuum pyrolysis, stigmasterol completely converted by 650°C [300]. At higher temperature, fragmentations and dehydrogenation favor initialization of PAH formation [299]. The thermal degradation of lipids is covered below in the *proteinaceous, oleaginous and polymeric materials* section.

Oxidation

The single (ring) double bond in phytosterols is readily oxidized by radicals, ROS or enzymes [169]. The relatively mobile and highly substituted side chains (often carboxylic acids) are also prone to attack. Radical oxidation of the double bond leads a concerted reaction (similar to those of unsaturated lipids), while ROS and enzymes might abstract a hydrogen from C_7 leading to 7α- and 7β-hydroxyperoxide intermediates, eventually forming 7-hydroxy and 7-keto compounds as major products [301]. It is postulated that due to incompatibility of phytosterols as enzyme substrates, autoxidation of phytosterols predominate enzyme-catalyzed hydroxyl-oxidations [302]. Phytosterol thermal oxidative degradation leads to the production of a few characteristic groups (7-hydroxy-, 7-keto-, 5,6-epoxy-, and 3,5,6-triol-), associated any given sterol [303]. Among free plant sterols, plant sterol esters, and plant stanol esters; plant sterol esters were most sensitive to oxidation during long term storage and heat treatment [304].

Interaction among Fractions (Cellulose, Hemicellulose, and Lignin)

Non-oxidative Fast Pyrolysis and Thermal Depolymerization

Due to the extent of intermolecular forces binding biomass fractions, relative to true bonds, biomass fraction interactions occurring during pyrolysis might have less to do with the native chemical interactions and more to do with the "high" concentrations of reactive pyrolytic intermediates in close proximity to those of other fractions. Hosoya et al. [305]found that cellulose-lignin pyrolysis interactions occurred to a much greater extent than did cellulose-hemicellulose interactions. Wu et al.'s DFT study [306] complimented by a thermogravimetric analyzer (TGA) study on the isolated versus co-pyrolysis of lignin and cellulose found significant interactions in mass loss rate. In a fluidized bed study complimented by TGA, bio-oil yields were lower than predicted by summing bio-oil yields of the biomass fractions, for all mixtures tested (cellulose: hemicellulose: lignin of 6 : 1.5 : 1.5, 5 : 3 : 1, and 5 : 1 : 3), suggesting that hemicellulose and lignin melt inhibit release of volatiles of cellulose, also interaction of the three promote NCG formation [307]. Zhang et al. [308] compared multiple-feedstock components and their interactions, proposing a number of reaction mechanisms, such as the levoglucosan inhibition mechanism described in the cellulose section above.

Proteinaceous, Oleagenous, and Polymeric materials

Non-oxidative Fast Pyrolysis and Thermal Depolymerization

The thermochemical conversion of these materials requires an entirely different set of considerations due to the content of nitrogenous and sulfurous molecules which behave very differently from lignocellulose at elevated temperatures or pressures. Additionally, human and environmental toxicity of products must be accounted for when designing a process, through either production minimization, or post-process handling and or destruction. Examples of these are production of ammonia, as well as oxides of nitrogen and sulfur from proteinaceous or oleaginous materials, and production of HCl or possibly dioxins from PVC or chlorinated materials [309].

α-amino acids are decomposed over a range of 400-800ºC depending on the specific amino acid. For example, glutamic acid completely depolymerized at 400ºC, whereas alanine remained

partially intact at 800ºC. Two common pathways are total fragmentation to alkenes or hydrocarbons, and decarboxylation followed by dehydration and or intramolecular condensation reactions. Due to the complexity and diversity of amino acids, there are many other less common possible decomposition pathways [299]. For comparison, β-alanine decomposes at lower temperatures than does α-alanine [310]. Whereas with lignocellulose decarbonylation and decarboxylation are common, deamination occurs with amino acids, yielding ammonia gas [311].

Similarly to proteins, *lipids* are diverse and decompose at temperatures ranging from 200ºC to 750ºC. Triglyceride cracking forms free radicals; $RCOO^{\cdot}$ and $RCH_2O^{\cdot}$, accelerating breakdown. Decarboxylation of these radicals leads to the formation of alkanes and alkenes, which then undergo subsequent disproportionation and ethylene elimination [299].There are many possible subsequent processes, more than 15 are described by Maher and Bressler 2007, including carbonium ion abstraction, Diels-Alder ethylene addition to form aromatics [312]. Catalytic cracking of triglycerides for deoxygenation of bio-oil is common practice. Two common mechanisms are β-elimination and γ-hydrogen transfer to produce carboxylic acid and alkenes, respectively. Wang et al. [313] demonstrated the potential of algae catalytic pyrolysis for high conversion to aromatic compounds with an ammonia co-product, although noted a small yield of HCN which could be treated through use of a metal-catalyst packed bed.

Polymers are often cracked over a range of 400-800ºC, depending on desired products. Temperatures >700ºC are used to crack to C-1 through C-4 olefins and aromatics such as BTX (benzene, xylene, toluene) [314]. Lower temperatures (400-500ºC) are used to form higher molecular weight condensable oils and waxes [314]. Hydrocarbon pyrolysis is said to be reversible radical reaction-dominated, generalized by homolytic cleavage, radical disproportionation, and β-scission, and their reverse; radical recombination, molecular disproportionation, and radical addition at unsaturated sites, respectively [315]. Additional pathways include; isomerizations (such as 1,5-H or 1,2-aryl shifts) and hydrogen abstractions [315,316]. Since some polymeric materials (collectively *polyolefins*, comprising almost two-thirds of MSW polymer streams) are non-oxygenated and non-aromatic, they are good candidates for catalytic pyrolysis to straight-chain hydrocarbons compatible with drop-in liquid fuels [317]. Polyolefins are depolymerized by a radical chain mechanism; hydrogen abstraction followed by β–scission [318]. Interest in blending of polymeric waste streams with biomass for reduced feedstock costs, and potential improved bio-oil quality has led to a number of co-pyrolysis studies on the topic. Xue et al. [319] highlights the findings of a few of these; a common observation was increased bio-oil yield due to synergistic effects between the two streams.

Oxidation

Proteinaceous materials (amino acids and proteins) were thermally oxidized in air, showing reactions between free primary amino acids and their own carbonyl oxidation products to form Schiff bases, where lysine (rather than tryptophan, as observed in ROS-oxidation) oxidized to chemilluminscence-exhibiting advanced glycosylation end-products (AGE's) [320]. Metal-catalyzed oxidation of hydroxyaminovaleric and hydroxyaminocaproic acids ("model proteins") by Cu(II) and ascorbate *in situ* (in rats) lead to the formation of glutamic and aminoadipic semialdehydes [321]. These products were also observed for a range of other proteins [321]. Boguszewska-Mańkowska described the oxidation of proteins (amino acid proteolysis) resulting from plant cell oxidative stress from ROS (hydroxyl from Fenton-type hydrogen peroxide dissociation), suggested amino acids with greater side-chain sulfur content (thus cysteine, or others with a methionine side chains) were more readily oxidized [322]. Additionally, irreversible amino acid carbonylation is capable of oxidative cleavage, side-chain conversion to aldehydes or ketones [322].

Plant lipids are understood to oxidize by hydroperoxy-driven "autoxidation", oxidizing by addition to double bonds or sulfur atoms, or abstracting hydrogen to further unsaturated polyunsaturated fatty acids (PUFA) [323]. In living systems a number of classes of chemicals suppress autoxidation, collectively antioxidants, are classified as *primary*; free-radical scavengers, oxygen-absorbers, and alkaline chelators (including butylated hydroxyanisole (BHA), butylated hydroxytoluene (BHT), mono-tert-buty-hydroquinone (TBHQ), propyl gallate (PG)), or *secondary*; acid chleators or sequestrants (including citric, tartaric, oxalic, malic, and succinic acids) [323]. Many methods have been developed to quantify extent of oxidation, operating by quantification of structural features characteristic of oxidations. Some measurement methods examples are; residual peroxide content, hydroperoxide (notably malondialdehyde) content, measuring conjugated dienes, and measurement of oxirane and epoxidized species [324]. Robards et al. [325] also reviewed measurement of rancidity and proposed a general oxidation mechanism; starting with triglycerides which either oxidize (via enzymatic-, photo-, or autoxidation) to triglyceride hydroperoxides, and further hydrolyze to free fatty acids hydroperoxides (or directly to secondary products) further to secondary products, *or* initial hydrolysis to free fatty acids and glycerol which oxidize to free fatty acid hydroperoxides [325].

Fast pyrolysis of waste tires has been investigated to the extent that even oxidative pyrolysis studies have been published on [326]. Lee et al.'s 1995 findings [326] complimented those of other autothermal pyrolysis studies; gas (predominantly CO_2) yield increased while gas heating value decreased with increasing oxygen concentration. Additionally, operating at an equivalence ratio of 0.065 was ideal, below which primarily char was oxidized [326]. Results of low temperature (200-300°C) oxidative pyrolysis of polypropylene showed first order behavior with oxygen partial pressures above 4.2 kPa, and reduction in activation energy (from 230 at 0 kPa-O_2 to 65-75 kJ/mol at 16.7 kPa-O_2) attributed to, "agreed well with", peroxide-intermediate formation on tertiary carbons [327]. Peroxides were thought to lead to secondary-tertiary cleavage leaving a carbonyl and a hydroxyl radical [327]. Zhu et al. 1998 [328] compared thermal-oxidation with ammonium sulfate (sulfuric acid and sulfur trioxide in oxidized form)-catalyzed oxidation, showing production of double bonds at chain ends when modified by sulfur, and double bonds conjugating styrene units throughout the main-chain when oxidized by air. Achilias reviewed advances in chemical recycling of polymers, and cited examples of aqueous oxidations of polymer materials, such as PVC dehydrochlorinations, leading to HCl, oxalic acid, benzene-carboxylic acids an CO2 [329]. In another example, mild (150-260°C) alkaline solutions were used to degrade rigid-PVC, allowing for extraction of tin while generating standard products of dehydrochlorination [329].

Role of Ash and Mineral Content

Non-oxidative Fast Pyrolysis

Ash content, notably alkaline and alkaline earth metals (AAEMs) have shown to act detrimentally to FP, notably of biomass feedstocks. These metals catalyze ring scission of carbohydrates and aromatic structures, leaving light oxygenates, diminishing bio-oil yield. AAEM's can be ranked by increasing detrimental catalytic activity as follows; Mg^{2+}, Ca^{2+}, Na^{2+}, K^{2+} [330]. Wang et al. [330] successfully demonstrated two pretreatments to reduce the ill-effects of AAEMs; sulfuric acid infusion (converting AAEM's into thermally-stable and relatively inert salts), *and* washing with dilute nitric acid (to physically strip the biomass of AAEM content). Another group utilized a sulfuric acid (2.0 wt.%) infusion for a carbohydrate feedstock, dramatically increasing sugar yield (from 4.5 – 16.2 wt%-switchgrass), but lead to increased char yield (increasing by 65 and 30 wt.% for red oak and switchgrass respectively) [331]. Another study tested a variety of

mineral acid pretreatments to investigate effects of AAEM on levoglucosan yield, showing sulfuric and phosphoric were most effective, and claiming "AAEM passivation contributes to 80% increase in LG yield while the buffering effect of the acid salts contribute to the balance of the enhancement" [332].

Oxidation

In the field of combustion, the role of metal ions has been investigated, notably from the perspective of fuel soot-formation tendencies [333]. Colcote cites Haynes et al. 1979, noting addition of metals seems to have a non-linear effect on total soot formation (initially increasing, but decreasing with further increased concentration), attributed to ion-concentration effects [333]. They describe how two competing mechanisms, "nucleation" and "coagulation" control this. Colcote cites Bulewicz et al. [333], who describes these as "anti-sooting"; charge transfer from chemi-ion (substrate) to a metallic ion, thus reducing ion pool required to polymerize soot (*or* by increasing electron concentration by thermal ionization of "easily-ionized" metals, quoted as originally described by Addecutt and Nutt 1969), and "pro-sooting". This having to do with reaction rates being too low at low metal concentrations, to proceed the charge transfer reaction, in fact reversing it. This hinders potential for substrate dissociation reactions which also reduces the pool of soot-forming intermediates [333].

Role of the Condensed Phase

Non-oxidative Pyrolysis

The combustion process is often categorized into four steps; heating and drying, pyrolysis, flame-front combustion of flammable pyrolysis-released volatiles, and glowing char combustion. At some point during pyrolysis, following heating and drying, there is what will be termed a *condensed phase* [15]. The condensed phase is a film of molten pyrolysis intermediates comprised of biopolymer fragments small enough that they are molten at their elevated temperature, but have either not yet depolymerized far enough to a molecular weight low enough to boil off, *or* they have not yet reached reactor temperature (assuming this is above the product's boiling point). During standard non-oxidative pyrolysis, even under ideal conditions, where well ventilated, the sweep gas is assumed inert. Therefore the sweep gas should not become chemically involved in condensed phase processes, let alone any part of the process. Even still, much pyrolysis chemistry does occur in the condensed phase. Dente et al. [334] described condensed phase radical chemistry; "Unlike in the case of gas phase, the entropy change is related to the fact that when two radicals are formed, they remain "caged" and cannot fully develop their translational and external rotational degrees of freedom (internal rotations and vibrational frequencies remain more or less the same in the reactant and in the transition state). Rate constants of propagation reactions can be evaluated as in the case of the gas phase because the "caging effect" previously mentioned is negligible" [334]. In other words, reaction coordinate is less of a driving force in the condensed phase (due to comparable free energies of reactant and intermediate), allowing for a greater extent of reversibility, relative to gas phase radical reactions where free energy rapidly drops off with interactions.

Oxidation

An area which could be further clarified is the relative extent of condensed- and gas-phase oxidations occurring during sub-stoichiometric combustion. Classical combustion theory of liquid droplets describes the fuel to vaporize and continue to heat up, not reacting until reaching flame front temperature and locale, thus negligible oxidation occurs at the droplet surface [45]. Biomass

combustion is described to proceed in the four steps listed above (also with devolatilization distinct from oxidation) [335]. These cases might be viewed as a mass transfer-limited scenario, limiting extent of condensed-phase reaction. Atmospheric organic (acid) aerosol oxidation (occurring at ambient conditions on the timescale of days) theory suggests that oxidation reactions occur primarily in the condensed phase, yielding condensed-phase aldehydes, ketones, and some carboxylic acids without notable change in aerosol size [336-338]. These mild conditions establish reaction kinetics as limiting. During autothermal pyrolysis biomass, there is not consensus on the extent of condensed-phase reaction. One study suggests its prevalence; "thermal pyrolysis and heterogeneous oxidation occurring over comparable timescales" followed by char combustion [339]. Another suggests they are distinct, "sequential occurrence of oxidation and pyrolysis processes, which are separated spatially and therefore temporally" [68].

Oxidizing Environment and Mode of Action

It is important to recognize, that oxidations are not all equal. There is more distinguishing them than just the extent of oxidation. The chapter on oxidation in the 1971 lignin text by Sarkanen and Ludwig (by Chang and Allan) simply categorizes oxidations into those which "degrades lignin to aromatic carbonyl compounds and carboxylic acids, those degrading aromatic rings…and those in which exotic oxidants are employed in structural elucidation" [238]. In the first category; aqueous oxidation of methylated lignin via nitrobenzene, molecular oxygen, metal oxides, and permanganate. The second category, "strong oxidants", includes peracetic and nitric acid, chlorine, chlorine dioxide and the oxidizing anions of hypochlorous and chlorous acid [238]. As mentioned earlier, oxidations could be categorized as done by Perazzini (side chain, ring cleavage, phenolic oxidative coupling, and alkyl-arylether bond cleavage), although only context provided is distinguishing between horseradish peroxidase (HRP) leading primarily to ring cleavage but some of all four, and laccases tendency for specificity to side-chain oxidation [246]. In the context of a β-*O*-4' lignin linkage (containing α-hydroxy and a β-primary alcohol), Zhang et al. 2016 describes four oxidation pathways, each markedly associated with a separate reaction regime. Those reactions being loss of α-hydroxyl leaving a benzylic carbocation through a thermo-solvolysis route (EMAL being the type example), a dehydration reaction leaving a quinone methide intermediate through a thermal depolymerization pathway [78]. Additionally, thermal depolymerization could form an oxirane intermediate, or could support a purely free radical-driven cleavage [78]. An overarching message being; different oxidants and catalysts will react with a given species by different means, and to differing extents.

Summary of Review

Topics covered in this review include; physiochemistry, non-oxidative pyrolysis, and oxidative thermal depolymerization of the constituents of biomass and organic materials. Although chemistry of many similar processes has been described, little work directly-related to autothermal pyrolysis exists. Given this, sufficient similar work exists that potential pathways and products could be proposed for autothermal pyrolysis conditions.

During autothermal pyrolysis, admission of small sub-stoichiometric amounts of air into the reactor leads primarily to the oxidation of flammable gases, secondarily to that of the char particles, and *presumably* minimally to the bio-oil (condensable) vapors and aerosols. The non-condensable gases likely oxidize by dehydration, decarbonylation, and decarboxylation reactions. Char particles likely react in gas-solid reactions with reactive oxygen species, leading to CO and CO_2. Oxidation of bio-oil vapors and aerosols is chemically complex and poorly understood. Understanding chemistry in related regimes was the focus of this review. Chemical principals are described in the

applications of oxidation mechanisms section below. In general, mild oxidation reactions lead to the oxidation of side chains to aldehydes, ketones, and carboxylic acids, or cleavage of reactive double bonds via concerted reaction mechanisms. In the case of the carbohydrate fractions, this would result in oxidation of primary alcohol groups, glycosidic linkages, and possibly secondary ring alcohols. In the case of lignin, propanoid side chains, methoxy groups, and linkage functionalities would be primary targets. Oxidation of linkage functionalities would weaken linkages, increasing susceptibility to cleavage events, resulting in further depolymerization. In the case of more severe oxidations, carbohydrates might experience ring-opening; at the 2,3-glycol group in the case of monosaccharides, or of the phenolic ring in the case of the lignin fraction.

Exothermic partial oxidation of the condensed phase, and lignin intermediates *could* be responsible for the thus-far unaccounted for fraction of heat generated during autothermal pyrolysis. Before this can be concluded, identifying the reactions occurring during the process, and the relative extent to which they occur, via theoretical means, should support observed changes in product composition.

CHAPTER 3.
CRITICAL ANALYSIS AND BASIS FOR EXPERIMENTAL WORK

Process Specifics

In order to critically interpret findings of the literature review for application to mechanistic framework, a set of boundary conditions should be specified. The process is defined as steady state autothermal FP in an industrial scale bubbling fluidized bed reactor. By *autothermal*, admission of a small amount of oxygen (or air), sufficient in quantity to enable adiabatic operation of the bed, *not* accounting for any stray heat loss, is insinuated. Oxygen required for adiabatic operation is a quantity which should remain constant for a given feedstock, fluidization, and process conditions. Because of variability of heat loss from reactor to reactor, the reactor could be thought of as well-insulated or heated by auxiliary source. The bed material and heat carrier would be a standard-sized silica sand suited for operation in the bubbling fluidization regime. The feedstock is northern red oak (*Quercus rubra* or *Quercus borealis*, depending on preference). The oak is processed as it realistically might be at scale (green wood, milled down to 1/8" spec.), having the implication of conduction-limited operation (thus presence of mild thermal lag or thermally-thick behavior). Application of chemical dynamics experimentally derived under idealized conditions (isothermally, kinetically-limited) to this regime might be controversial, although is necessary in order to attempt to describe observations at scale. The bed will be operating at the standard "optimal" FP temperature of 500°C and the feedstock residence time, on the order of 1-5 seconds, common of industrial fluidized beds. Char and heat carrier are separated from volatiles with a post-freeboard cyclone. Non-condensable gases (NCG's) and volatile products are assumed to have short residence in the collection system prior to collection. Specifics of the condensation and collection system are should not significantly affect product composition, although condensers, impingers/bubblers, for vapor collection, and electrostatic precipitators in addition to physical filters, for removal of entrained particulate are commonly applied [340].

Application of Oxidation Mechanisms to Fluidized Bed Pyrolysis

If the vapor residence time in the bed is on the order of a few seconds and if particles experience some degree of thermal lag, one might assume that there was time sufficient for oxidation reactions occur to a small extent to not only the condensed phase, but to the char as well. Considering the superstructure of lignocellulose (remaining chemically "intact" during milling to reactor-compatible particle size, where cellulose fibrils are somewhat engulfed in an amalgamated lignin-carbohydrate complex) loosely representative of the condensed phase; lignin and hemicellulose might initially be selectively oxidized. If mass transfer was not limiting, meaning lignin and hemicellulose depolymerization products were removed *and* ROS could contact cellulose; cellulose might also be partially oxidized during the process.

As discussed in the cellulose oxidation section above, oxidation could occur by means of assisting glycosidic bond hydrolysis (either at a chain end (*unzipping*) or mid-chain (*cracking*) [341,342]), effectively increasing levoglucosan yield, or by oxidation of ring functionalities. If cellulose's substituents were to measurably react with ROS, the C_6 primary alcohol would be the likely candidate, oxidizing to a C_6 aldehyde or carboxylic acid, yet theoretically possible for ring-hydroxyls to oxidize. It does not seem likely that hydroxyls at the 2,3-glycol group would be oxidized to the extent of ring opening, as this only seemed to occur in strongly catalyzed conditions or when carbohydrates were significantly oxidized.

Similarly to celluloses, hemicellulose might be oxidized by four means; polymer-end-wise chain scission initiation (*primary peeling*), mid-chain scission, end-chain unit degradation (*secondary peeling*), or side-chain oxidation. Because of its branched and heterogeneous nature, and tendencies for decomposition of monomeric units following complete depolymerization during non-oxidative pyrolysis, fewer hemicellulose hexoses and pentoses would likely be recovered during oxidative pyrolysis. In the reactor, this might play out through further conversion of hexoses and pentoses to furans and light oxygenates from monomers, light oxygenates from furans, or CO_2 from light oxygenates.

Lignin, also structurally diverse, has many possible routes for oxidation. From linkage studies, it is apparent that oxidation of the β- or γ-hydroxyl (in the case of a β-O-4' linkage), or the α-hydroxyl (for α-*O*-4' linkages) greatly weakens ether linkages, making susceptible to cleavage. Lignin's phenolic substituents are prone to oxidize to aldehydes, carboxylic acids and ketones. Those side chains with reactive double bonds could be oxidatively cleaved or encourage a concerted decomposition reaction. Because products of oxidation can be further oxidized themselves, care must be taken in extrapolating out composition trends to scaled-operation. **Even considering these routes which would effect a change in product composition, the most significant effects might come simply due to improved reaction conditions** (heat transfer, heating rate, and ventilation (due to greater gas production)). These would cause the condensed phase to react faster; reducing extent of char forming processes, and preventing secondary gas-phase reactions; by reducing time at temperature.

When comparing these concepts to Kim et al. [71] and Amutio et al.'s [52] observed changes in product composition, Table 1, it appears that a combination of intermediate/primary pyrolysis product oxidation and improved process condition-based changes participate, the former occurring to a lesser extent. Kim observed linear reduction in pyrolytic (oligomeric) lignin yield with increasing oxygen content. Because the bulk of heating rate improvements are seen with addition of *smaller* amounts of oxygen (up to around the autothermal equivalence ratio), lignin oxidation is likely responsible to some extent for this reduction in pyrolytic lignin yield. Kim also observed slight increased yields of oxidized monophenols (such as vanillin), and slight decreases in monophenols containing reactive double bonds in side-chains (such as 2-methoxy-4-vinyl phenol), possibly described by minor oxidation of primary pyrolysis products. Overall reduction in acids and light oxygenates is likely primarily an artifact of exothermic oxidation of these species to CO_2, and secondarily to than decreased monomer degradation (the source of these species) resultant from improved process conditions. Finally, Kim's observed increase in monosaccharides might be primarily due to improved process conditions (notably higher heating rate and reduced vapor phase residence).

The rule of thumb FP temperature is commonly defined as 500°C, although for red oak in a fluidized bed, 450°C attained a maximum bio-oil yield [224]. Polin has shown that due to the enhanced heating rates achieved through the *in situ* heating enabled by feedstock partial oxidation, a slightly lower temperature (possibly in the range of 350-475°C) might be optimal for maximum bio-oil yield during autothermal pyrolysis [41]. If operating at these lower temperatures, decomposition of monosaccharides and monophenols might occur to a lesser extent. This would have the consequence of reduction of aqueous phase (water-soluble acids, furans, and aldehydes, for example) and light oxygenate products, increasing yield of heavy-ends bio-oil fractions. If biofuels production, either by hydrodeoxygenation to naptha-range drop-in fuels, or by separation and fermentation of sugars to ethanol, were the goal, this would be a favorable adjustment.

Studies of Pyrolysis in Micropyrolyzers

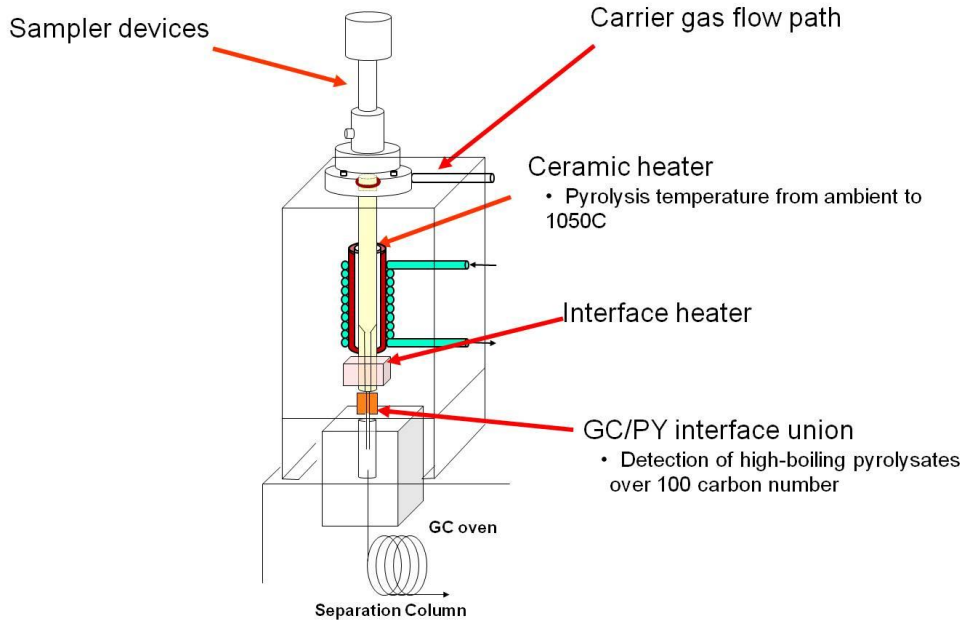

Figure 11. Frontier Micropyrolyzer reactor cut-away showing insulated furnace [343].

Limitations of Micro-scale and Continuous Reactor-based Experiments

The capabilities and operational characteristics of each type of reactor must be considered when designing pyrolysis experiments. For example, in a fluidized bed, changing a single operation condition has the potential to change the hydrodynamics and heat transfer of a process, due to their dynamic nature. If the research question involves investigating the effect of a single operation parameter (in isolation) on yield of a single product species, a continuous reactor such as the fluidized bed might not provide as useful as a micropyrolyzer. Although if the research question required accurate mass balance of the product streams, a fluidized bed might serve greater utility. An additional benefit of micropyrolyzers is the ability to rapidly setup for either online (direct injection into Gas Chromatograph (GC)) or offline (manual bio-oil collection) experiments.

Vertical micro-furnace pyrolyzers, commonly referred to as micropyrolyzers are generally considered to operate free of mass-transfer limitations, although this turns out to be "free" in the relative sense. The manufacturer recommends a sample size range of 0.2 – 0.5 mg in order to achieve quoted heating rates of 1000°C/s [343]. Even in this sample size range, cellulose powders undergo mass transfer limitations, as demonstrated by observed secondary reactions [78]. Both Zhang et al. [78] and Proano-Aviles et al. [344] modified pyrolysis cups in response to their findings, to mitigate poor ventilation-induced secondary reactions. These modifications were subsequently adopted by the manufacturer, Figure 12.

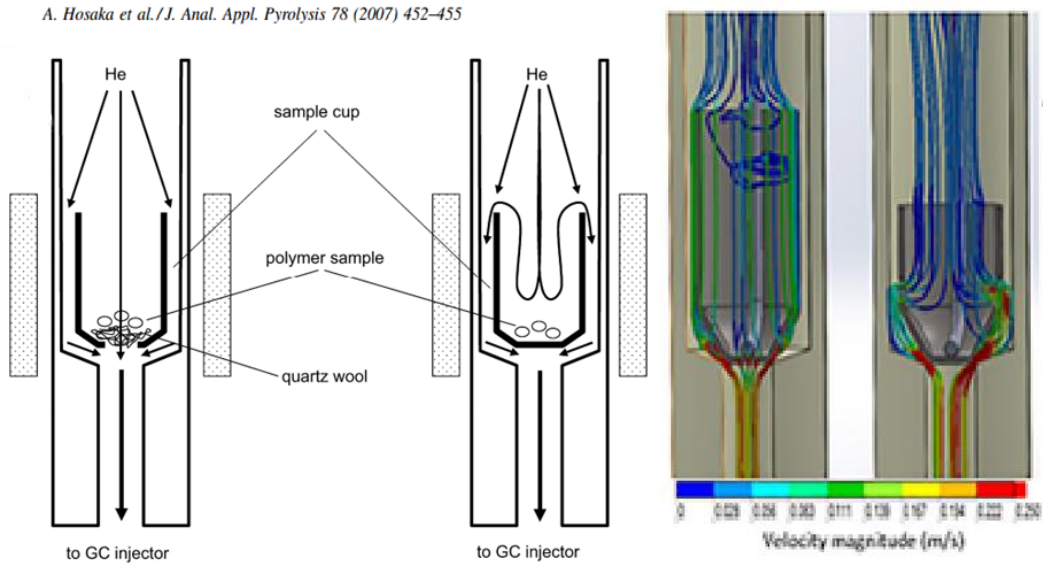

Figure 12. Modifications addressing flow effects of micropyrolysis sample holders. ((Left) Pyrolysis cup with perforations on bottom developed by Hosaka et al. [345], to mitigate vertical micro-furnace mass transfer limitations (targeting reduction of secondary reactions); (right) Lagrangian CFD snapshot showing improved ventilation in pyrolysis cup with perforations on opposing sides, borrowed with permission of Juan Proano-Aviles [344]; the manufacturer subsequently added two new sample holder designs incorporating these modifications [343].)

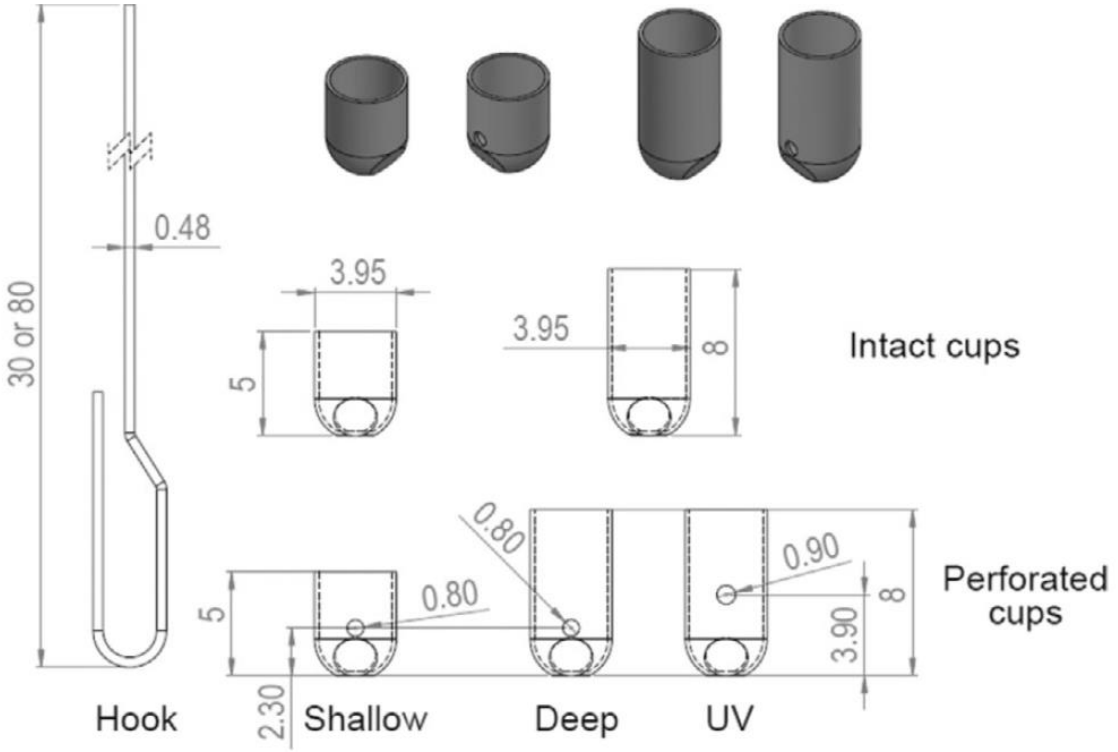

Figure 13. Sample holders utilized in the micropyrolyzer. Dimensions in mm, figure borrowed with permission from Proano-Aviles [344].

The effect of sample size on mass-transfer limitation was experimentally tested to verify findings of Proano-Aviles [344], Hosaka [345], and Zhang et al [78]. See Figure 20 below for findings.

Aside from residence time and sample size effects, if using the size of the sample holders (almost 4 mm wide) as a constraint, a variety of particle sizes could physically be tested in these systems. Varying particle size has also been shown to be associated with characteristic time variation [344]. Variation in characteristic time indicates that larger particle sizes might experience either slower heating rates or greater thermal lag. Studies of coal pyrolysis showed that a 500 μm diameter particle experienced 30°C thermal lag between the surface and center of a particle during 600°C pyrolysis [43]. Effects of both sample size and particle size on characteristic time were investigated, see Figure 21 and Figure 22 for findings.

It was hypothesized that the larger particle size of red oak (250-500 μm) behaves more so in a thermally-thick, conduction-limited regime than a kinetically-limited isothermal regime, where mass transfer would not be the reaction rate limiting factor. Mettler et al. [346] use a Biot number vs. Pyrolysis number plot to compare the thermal operation regime of thin-film cellulose and powdered microcrystalline cellulose pyrolysis. The Biot number is the ratio of conduction to convection characteristic times, the Pyrolysis I number (also known as the *internal* pyrolysis number) is the ratio of reaction characteristic time to the conduction characteristic time, and the Pyrolysis II number (also known as the *external* pyrolysis number) is the ratio of the reaction characteristic time to the convection characteristic time [347]. A large Biot number is associated with a conduction-limited process, conversely a small Biot number is associated with a convection-limited process. In general, a large pyrolysis number is associated with a well-mixed process with good heat transfer, limited by reaction kinetics. For a small Pyrolysis I number, the process is heat (conduction)-limited, and for a small Pyrolysis II number, the process is specifically convection-limited. Below is a recreated figure overlaid with the thermal regime of the small (75-150 μm) and large (500-750 μm) particle sizes of red oak utilized, Figure 14. The theory shows that the smaller particle size is on the boundary of the convection-limited regime, while the larger particle size was closer to the conduction-limited region (and clearly outside of the convection-limited regime). The combination of this and the findings of Proano et al. 2016 lead to the exclusive use of the smaller particle size red oak for the remainder of the research program.

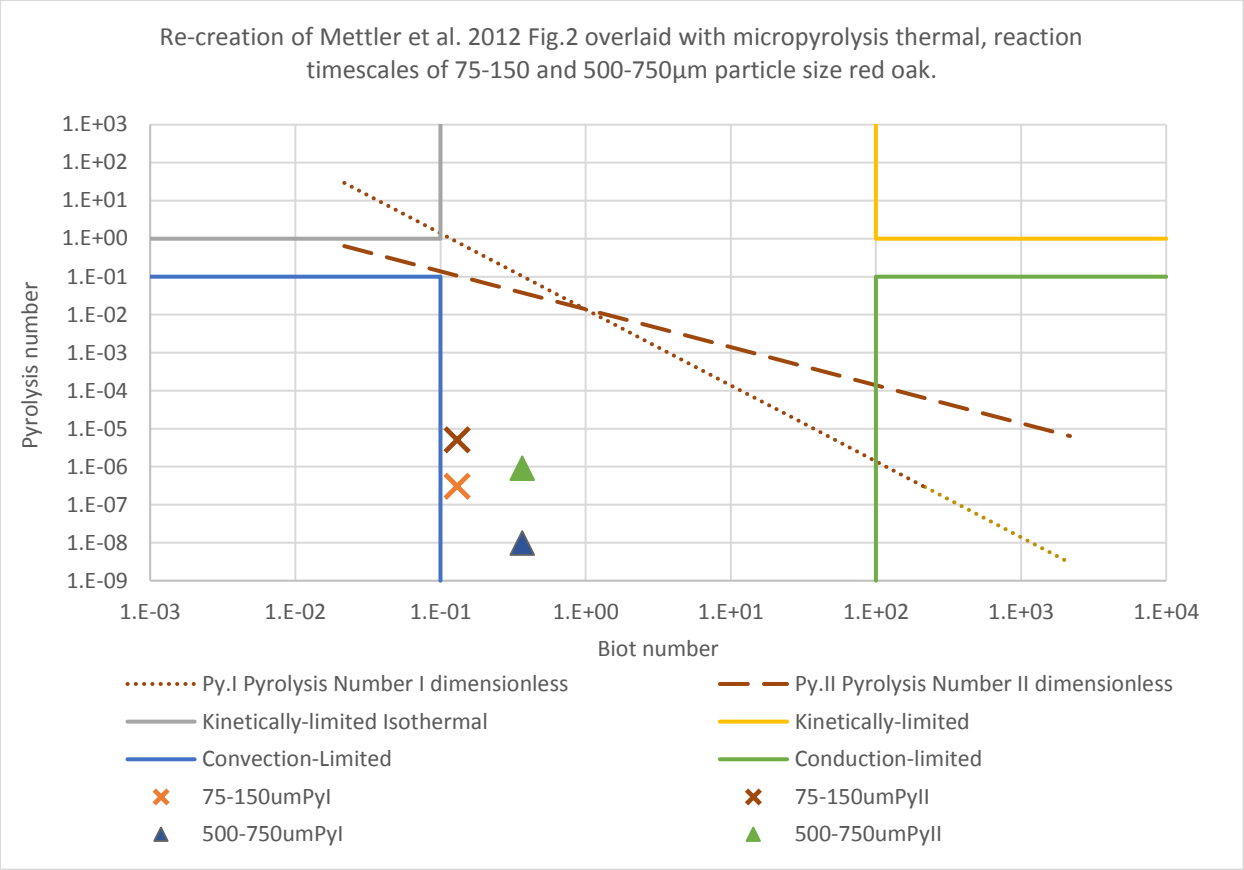

Figure 14. Smaller particle size red oak more closely resembles convection-limited regime. (Re-creation of Mettler et al. 2012 Fig. 2 (comparing pyrolysis of micron-scale thin-film cellulose with mm-size cellulose particles) overlaid with micropyrolysis regimes of 75-150 and 500-750µm particle size red oak; dotted and dashed lines represent Pyrolysis Number I and II (Internal, and External Pyrolysis numbers, respectively) thermal regime of cellulose particles ranging from 0.1µm (left) to 0.1m (right); boxes denote ideal regimes (counter-clockwise from top right; kinetically-limited, kinetically-limited isothermal, conduction-limited, convection-limited).)

In the case of partial oxidation experiments, controlling interaction of the gas with the sample and primary pyrolysis products is an additional consideration. In fluidized bed reactors, whenever oxygen is limiting (relative to stoichiometric combustion), the oxygen is assumed to be fully consumed or reacted because the reactor is considered “well mixed”. In this case the quantified equivalence ratio is relatively well correlated with extent of oxidation of the feedstock, on a carbon-basis. In a plug-flow type reactor, such as a free-fall reactor or an entrained-flow reactor, if oxygen is introduced at a single point near the beginning of the reactor (in an oxygen-limiting concentration), it is not consumed uniformly along its length. Rather, the oxygen is consumed rapidly near the injection location, leading to a hotspot and associated thermal gradient along the length of the reactor. Hotspots are undesirable because they drive the process further from idealized adiabatic operation, thus the concepts of heating rate, residence time, and reaction rates become unclear. This becomes the case as any two given points along the reactor are no longer comparable in terms of process conditions. In a ventilated non-continuous microscale reactor (such as a vertical micro-furnace pyrolyzer), because the sample size is so small and the heats of oxidation are so small, a hotspot is not of primary concern. Extent of oxidation and interaction of the oxygen fed into the reactor are rather the main concern. In a fluidized bed, autothermal operation can be achieved at an equivalence ratio of roughly 0.06.

Feeding an equivalence ratio of 0.06 (as defined by the ratio of sweep gas fed to the sample mass), to a micropyrolyzer leads to an entirely different process. Due to primary pyrolysis product entrainment mass transfer limitations imposed by the sample holders (pyrolysis cups), and the relatively short residence time of the sweep gas advecting through the reactor; even in oxygen-limiting concentrations, oxygen is not fully consumed.

In order to reproducibly observe differences in product composition, for a 500 μg sample size of red oak under 500°C 100ml/min pyrolysis, a minimum oxygen concentration of 10% by volume was required. For reference, the theory showed a concentration of 0.75% by volume should be required to achieve an ER = 0.06 for the same conditions. In order to have a clear difference in product composition, sweep gas with 20% by volume oxygen was often used. This follows logic since it is understood that the oxygen in the sweep gas does not interact substantially with the sample (there is substantial sweep gas (oxygen) by-pass), whereas it is fully consumed in a continuous reactor. Once this was established, biomass partial oxidation could be studied in the context that excessive oxygen concentrations might be required.

Investigating Partial Oxidation

Partitioning and Relative Reactivity

There are two questions which might arise when investigating partitioning of oxygen; how it is partitioned among biomass fraction, and how it is partitioned among product phase. Studying the relative reactivity of fractions and phases is one approach to understand this. Biomass fractions were proposed to have relative reactivity shown in Figure 15. *It was hypothesized that lignin's radical intermediates make it more reactive than either crystalline cellulose's hydroxyls or the amorphous (easily-degraded) hemicellulose functionalities*.

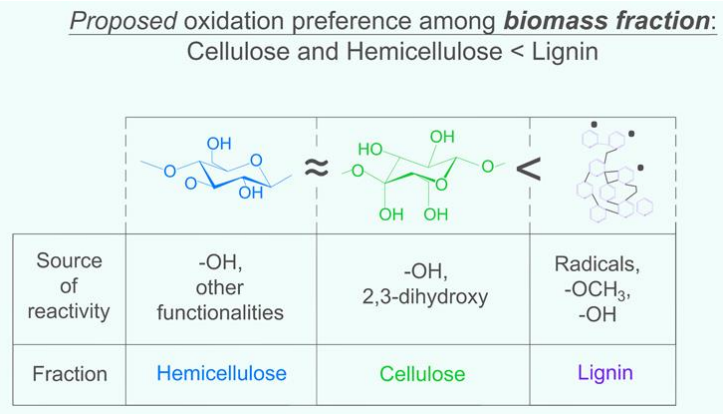

Figure 15. Relative reactivity of biomass fractions with oxygen (proposed). Lignin's radical chemistry is thought to make it more reactive.

To learn about partitioning among phase, the relative reactivity of primary pyrolysis products could be tested. This would show what might have a greater propensity for reacting with oxygen or reactive oxygen species. Food scientists study oxidation of phenols from an inverse perspective; activity of phenols to passivate unrestrained radicals in the human body, also commonly known as the *antioxidant activity* of a substance or food item. Since it is difficult to directly measure this activity *in situ*, a number of bioassays have been developed as proxies. An example is ORAC (oxygen radical absorbance capacity); measuring the oxidative degradation of a fluorescence-exhibiting biomolecule following incubation with the antioxidant and peroxy radical-forming azo-indicators, quantified by flourometer [348]. Others include TEAC (Trolox equivalent

antioxidant activity), a colorimetric assay comparing antioxidant activity to that of a standard referred to as *Trolox*, SOD (superoxide dismutase), which measures the consumption of a reducing agent, and HOSC (hydroxyl radical scavenging capacity) a reputed flourimetric *in vitro* assay based on hydroxyl radicals produced at constant concentration for non-lipophilic antioxidants [60,349]. Because antioxidant studies have generally involved phenolic acids, this theory was applied only to lignin pyrolysis, as lignin is a phenylpropane polymer. Because antioxidant capacity has been so widely studied by food scientists, a number of the monophenols produced during pyrolysis of lignin have been published on. Comparing the relative antioxidant activities of a number of primary pyrolysis products could provide a crude estimate of which are more reactive with molecular oxygen (or ROS) than others. Specific methods are detailed below.

Supporting the antioxidant body of literature are computational chemistry studies, a number of which investigate pyrolysis regime chemistry [55,350-353]. Observations by food scientists and predicted by computational chemistry can be summarized in a few statements, also depicted in Figure 16. Oxygen scavenging activity increases with; increase in number of hydroxyl and methoxy functionalities, more so than it increases with acetyl and methyl groups, more so than it increases with number of aldehyde or carboxylic acid groups [354]. Aldehydes have greater oxygen scavenging activity than carboxylic acid groups [354]. Hydroxycinnamates (aromatic acids with a propanoic acid side chain) have greater antioxidant activity than do hydroxybenzoates (aromatic acids with a carboxylic acid side chain), likely due to the reactivity of the C_2-C_3 double bond [348]. Findings of these studies were used to inform hypotheses testable under oxidative pyrolysis conditions. *Monophenols with greater theoretical ROS-reactivity, as quantified by antioxidant activity and computational chemistry, were hypothesized to oxidize more readily under oxidative pyrolysis conditions*. Experiments investigating this are described below.

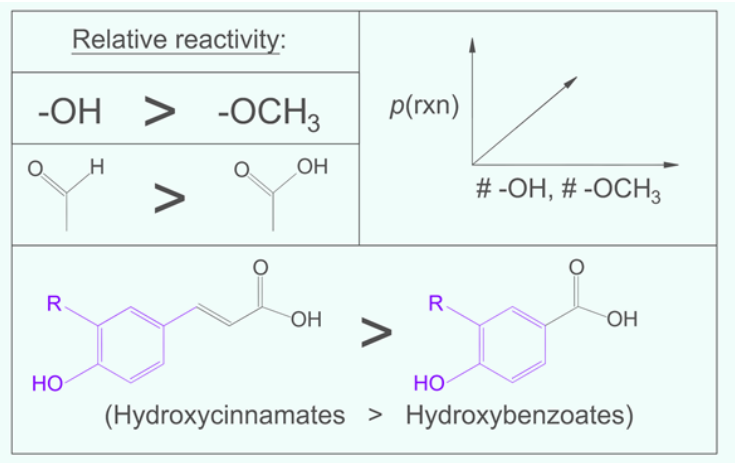

Figure 16. Relative reactivity of monophenols as described by Cirillo et al. [354], Yu et al. [348].

Lignin Side-chains and Interunit Linkages

To get to the crux of the changes which might result from oxidative pyrolysis of lignins, the behavior of phenolic side chains and interunit linkages might be investigated. *It was hypothesized ROS-oxidation increases the yield of aldehyde, ketone, and carboxylic acid-containing species, and decreases the yield of vinyl-containing species*. More specifically, because aldehyde-, ketone-, and carboxylic acid-containing compounds are non-oxidative pyrolysis products, *and* because oxidation reactions can decompose these as well, an increase in selectivity towards all species containing these functionalities is not expected. Rather, changes in the total combined yield of species containing these functionalities is anticipated.

Interunit linkages must be cleaved in order to release monomers and fragments small enough to vaporize. **The first goal of studying effects of oxygen on linkage reactivity was to see if observed increased in monophenol yield during autothermal pyrolysis, was resultant purely from decreased vapor residence time (limiting repolymerization), *or* if condensed-phase lignin depolymerization was enhanced by oxidation**.

Thanks to a sizeable body of literature in the area of lignin dimer model compound pyrolysis, non-oxidative pyrolysis mechanisms have been proposed for all of the common linkage types; β-*O*-4' ([222,226,227,355-361]), α-*O*-4' ([226,227,359,361,362]), 4-*O*-5' ([363]), β-5' ([227,361,364]), β-β' ([227]), 5-5' ([227]). The second goal was to build off of this series of mechanisms using observed differences in product composition among standard and oxidative pyrolysis. Experimental approaches to these goals are described below.

Pyrolytic Lignin Yield of Technical (isolated) Lignin

Isolated or technical lignins are notoriously difficult feedstocks to convert thermally, due to tendency to form a highly viscous melt-phase, and readily form char under FP conditions. One topic of interest to the thermochemical conversion community is improving pyrolytic lignin yield. If the mechanism driving char formation was better understood it might be more effectively suppressed. Empirical evidence suggests that pyrolytic lignin yield in from whole biomass pyrolysis is greater than that of an isolated lignin. In 2011 Wang et al. [307] showed decreasing volatiles yield with increasing lignin concentration more dramatically than would be expected if char yield increased linearly with lignin concentration.

This discrepancy was hypothesized to occur due to lignin-carbohydrate complex (LCC) linkages, assisting lignin's pyrolytic cleavage fragments in evaporation/ejection to the aerosol phase by preventing melt-phase coalescence. Further; the diversity of products present in the vapor phase prevent vapor-phase repolymerization by physical displacement or dilution of reactive lignin intermediates.

In order to improve the prospects of lignin pyrolysis, physical process improvements must be developed. Pretreatment technologies and process modifications are two approaches to this. *It was hypothesized that pretreatment with fumed silica and partial oxidative pyrolysis enable a greater pyrolytic lignin yield by prevention of melt-coalescence, and prevention of radical repolymerization in the gas phase due to radical capping reactions, respectively*. Experiments investigating pyrolytic lignin are described below.

CHAPTER 4.
EXPERIMENTAL METHODS

Materials

This thesis work made use of whole biomass, isolated biomass fractions, and model compounds. The two whole biomass materials used were red oak heartwood sawdust, and switchgrass (possibly hammer-milled) from Renmatix Inc. Biomass fractions included 50 μm Sigmacell cellulose from Sigma-Aldrich Co., beech wood xylan (used as a hemicellulose proxy), of unknown source, milled wood lignin prepared in-house from red oak sawdust, and switchgrass lignin, produced by the Renmatix Inc. supercritical hydrolysis process. Model compounds used include; benzyl phenyl ether (CAS: 946-80-6), 1-benzyloxy-2-methoxybenzene (CAS: 4125-43-3), diphenyl ether (101-84-8), bibenzyl (CAS: 103-29-7), 2-Phenoxy-1-phenylethanol (CAS: 42487-73-0), sourced from Sigma-Aldrich Co., The Chemistry Research Solution LLC., and Alfa Aesar Inc. A number of compounds were used to calibrate analytical chemistry for internal comparison across conditions, and for pyrolysis product quantification. The following compounds were used as calibrants; 2-methoxy-4-methylphenol, 2-methoxy-4-vinylphenol, 2-methoxyphenol, 4-methyl-2,6-dimethoxyphenol, 4-vinylphenol, 2,6-dimethoxyphenol, phenol, acetic acid, levoglucosan, furfural, 2-(5H)furanone, 5-hydroxymethyl furfural, propionic acid, acetol, Isoeugenol, vanillin, 2,6-dimethoxy-(1-propenyl) phenol, 4-hydroxy-3,5-dimethoxybenzaldehyde, 1,2,4-trimethoxybenzene, 4-hydroxy-3-methoxyacetophenone, and phenanthrene was used as an internal standard.

Sample Preparation

Oven-dried red oak sawdust, with initial particle size of 250-750 μm, was directly used for an initial round of experiments, but was also ball-milled down to a fine powder and sieved to within a particle size range of 75-150 μm. Switchgrass and switchgrass lignin were also ball-milled and sieved to within this size range. All other biomass fractions, model compounds, and calibrants were used as-received because were fine powders initially. Prior to massing out samples, regular maintenance was performed on analytical instruments and micropyrolyzers. This included running GC-column cleaning bake-out methods, replacing inlet liners, inlet septa, various seals and ferrules. The micropyrolyzer reactor tube and injector needle (in the case of online analytical analysis) were cleaned with acetone then dried. Sample holder cups and hooks used to suspend the sample holders were sonicated in acetone, then manually cleaned one at a time with acetone to ensure prior pyrolysis products were fully removed (unless new holders were used). Microgram analytical balances (with precision of ±1μg) were used to mass out samples into pyrolysis cups.

For preparation of calibrations; calibrants were massed out into small Nalgene bottles to prepare stock solutions (usually using methanol as the solvent), which were serially diluted into High Performance Liquid Chromatography (HPLC) vials to form a calibration series.

For use of non-volatile liquids, diluted solutions of the liquid were prepared in acetone, allowing for repeater-pipette transfer of small-enough masses of the compound into a pyrolysis cup. Acetone was allowed to evaporate prior to pyrolysis, or a solvent delay was used to protect the detector. For use of volatile solids, samples were prepared one at a time directly before the experiment to minimize mass loss.

General Experimental Operation Conditions

The micropyrolyzer was usually operated with an ultra-high purity helium sweep gas, flowing at 100 ml/minute. The micropyrolyzer has two heater zones; termed the *furnace* (the active

pyrolysis zone) and *interface (*the zone downstream of the furnace, and upstream of the gas chromatography-mass spectrometry (GC-MS)). For all of the experiments presented here, these were operated at 500°C and 350°C respectively. As is shown in Figure 13, there were multiple sample holder geometries available, of which shallow cups were used for most experiments, other than the lignin side-chain and partitioning experiments which used deep cups to induce greater residence time of pyrolysis products in the presence of an oxygenated sweep gas. For the case of most oxidative pyrolysis conditions, either 10 or 20ml/min of pure O_2 was fed into the standard 100ml/min of helium. For the case of the lignin side-chain and partitioning experiments, a custom gas mix (of 10% O_2, 90% helium, by volume) was used. Early oxidative micropyrolysis experiments made use of custom mixed gas cylinders with oxygen concentrations more closely resembling that required for autothermal operation in a fluidized bed for red oak and corn stover, containing0.75% and 0.50% oxygen by volume, respectively. These quantities were determined using a process shown in Figure 17. Elemental composition for red oak and corn stover, obtained from published ultimate analyses, were used to calculate stoichiometric oxygen requirements. This quantity of oxygen was multiplied by 0.06, the equivalence ratio understood to allow for red oak autothermal operation to yield a theoretical oxygen to biomass mass ratio. A 20 second pyrolysis time was assumed based on experiments carried out by fellow graduate students identifying that lignin pyrolysis was complete following a 10-20 second pyrolysis time. By multiplying the calculated mass ratio by the pyrolysis sample mass divided by 20 seconds, normalizing by oxygen's density as well as the sweep gas flow rate, a theoretical volumetric oxygen concentration could be determined to achieve the desired equivalence ratio for a particular feedstock. Experiments testing this theoretical concentration were tested by manually co-feeding helium and oxygen using a mass flow controller and needle-valve rotameter showed that there were no significant difference in product composition between non-oxidative and oxidative pyrolysis (using this calculated equivalence ratio). Because of the nature of micropyrolyzer sweep gas flow, designed to rapidly remove volatile products, a small fraction of the sweep gas passing through the pyrolyzer enters the pyrolysis cup (most flows around the outside of the cup). Quasi-kinetic diffusion calculations (of oxygen in hydrogen gas) were used to estimate what is termed a "fudge factor" in Figure 17, or an oxygen interaction factor. This calculation made use of an equation used to calculate the bulk fluid (sweep gas) oxygen concentration to achieve the theoretically required concentration at the particle surface;

$$\dot{m} = 4 * \pi * r_s * \rho * \mathcal{D} * \ln((1 + Y_{O_{2,\infty}}/\boldsymbol{v}_I)/(1+Y_{O_{2,S}}/\boldsymbol{v}_I))$$

Where; $\dot{m} = mass\ flow\ rate$

$r_s = average\ particle\ radius$

$\rho = gas\ density$

$\mathcal{D} = gas\ diffusivity$

$Y_{O_{2,\infty}} = bulk\ fluid\ oxygen\ mass\ concentration$

$\boldsymbol{v}_I = gas\ velocity$

$Y_{O_{2,S}} = oxygen\ mass\ concentration\ at\ particle\ surface$

The application of this equation resulted in a fudge factor of ~5, meaning one fifth of the oxygen would interact in the sample, under highly idealized conditions. This was used to calculate the oxygen concentration specifications for the mixed gas cylinders. It turned out that even a fudge factor of 5 was not conservative enough, as no statistical difference was observed when using these gases. Following this, a large round number concentration of 10% by volume was applied, allowing for significant differences to be observed, and to learn about the products produced when pyrolysis intermediates were partially oxidized. It was determined much later that this concentration was over-oxidizing the samples, as monosaccharide yields of levoglucosan decreased when pyrolyzing under these conditions, see results chapter for details.

Since the sample-suspending device which was used allowed for raising and lowering of the sample holder into the furnace (rather than one which could only drop the sample into the furnace, i.e. did not have the capability to remove from the sample from the furnace), 20 second pyrolysis time was applied to both online-and offline CPD-Q experiments.

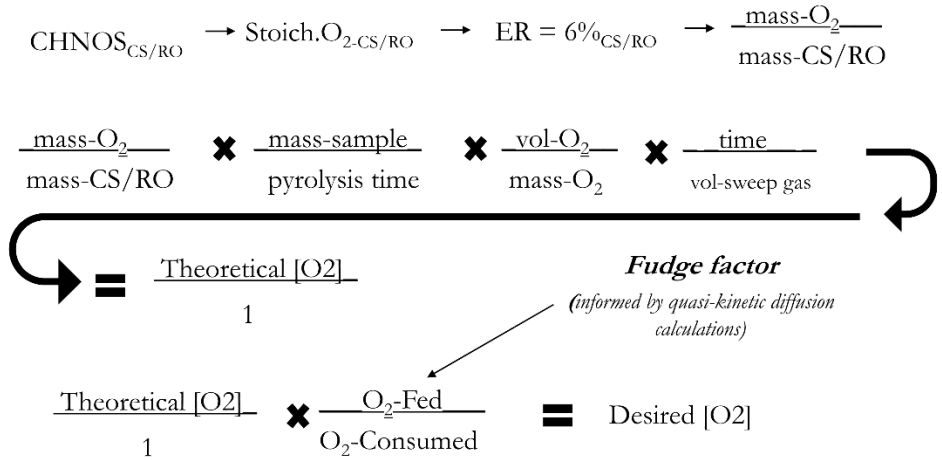

Figure 17. Method applied for determination of mixed gas oxygen concentrations.

Investigating Sample Size and Particle Size Effects (online analysis)

Using the micropyrolyzer, 100 µg and 500 µg sample sizes of red oak powder (75-150 µm) in short sample holder cups, Figure 13, were pyrolyzed in triplicate. To see effect on composition, flame ionization detector (FID) peak areas from the 16 compounds of highest selectivity were compared. Recorded sample masses were normalized to 100 or 500 µg to account for minor variability in actual masses, Figure 14.

A separate experiment used a short-column in the FID to show the effect of sample size on pyrolysis characteristic time. This involved the use of a py-GC/FID where instead of a standard 60m capillary column, a column of ~40cm was used, with the column oven starting at the maximum temperature. With this setup, all of the pyrolysis products passed directly to the detector, and the signal output was likened to the instantaneous rate of pyrolysis product vaporization, allowing for the descending toe slope (and reaction characteristic time) to be calculated. A similar experiment showed the effect of particle size. Short-column FID experiments were repeated in triplicate, see Figure 21 and Figure 22.

Attempt at Equivalence Ratio Quantification (offline analysis)

An attempt to quantify the equivalence ratio used a proxy feedstock which pyrolyzed or oxidized in a neat manner. Carbon lamp-black, a pure carbon material, which among many other

uses, is applied analytically in TGA leak-testing. In this application, carbon lamp-black is loaded into the TGA, which is ramped up to 800°C and set to dwell for 60 minutes. If air enters the TGA, the sample is oxidized, detectable by mass loss. So for example; if applied to a micropyrolyzer, and the sample lost 30% of its mass in the specified pyrolysis time, a claim could be made that the sample reacted with 30% of its theoretical air.

This experiment was carried out offline; rather than on a GC/MS, it was mounted on a set of scissor jack-stands on the lab-bench. Whenever the pyrolyzer was tested offline, a modified reactor tube (serving as both a reactor tube, and condenser vessel) was used, submerged in a dewar of liquid nitrogen to prevent harmful condensable vapors from entering the lab, Figure 18. In the case of this experiment, bio-oil analysis was not of interest, so condensed products were not analyzed.

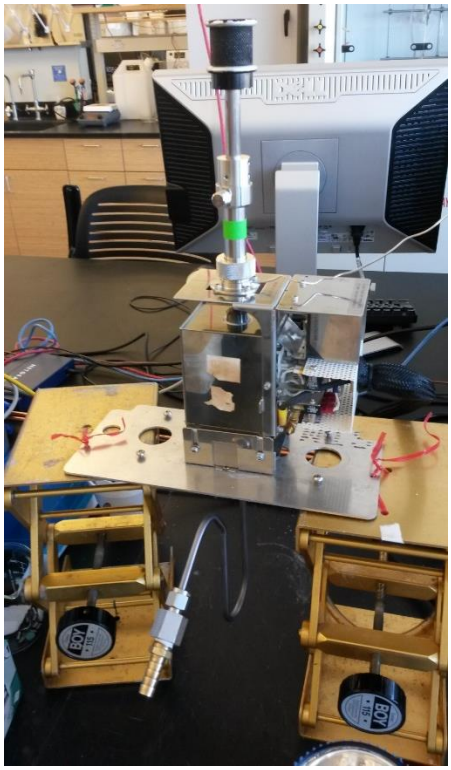

Figure 18. Frontier micropyrolyzer setup for offline analysis.

Relative Reactivity with Oxygen (online analysis)

Relative reactivity of biomass fraction was tested through the pyrolysis of cellulose, milled wood lignin and xylan in standard and oxidative conditions and comparing the decrease in total FID chromatogram area (i.e. conversion to light gases). Decrease in total chromatogram area was termed *change in conversion*. Relative reactivity of the fractions was designated based on increase in conversion observed with the addition of 20 ml-O_2/min to the non-oxidative pyrolysis 100 ml-He/min (those fractions with the greatest increase in conversion were the most "reactive" with oxygen). In other words, if addition of oxygen caused the unconverted yield of a biomass fraction (measured during non-oxidative pyrolysis) to decrease by the greatest portion, the model was considered most reactive with oxygen. These experiments were carried out in triplicate at standard pyrolysis conditions, Figure 23. This experiment was repeated with the following lignin model monophenolics; vanillin, syringaldehyde, and acetosyringone, see Figure 24 below.

When comparing bio-oil on instruments other than GC/MS, an offline semi-automated apparatus, termed the *controlled pyrolysis duration-quench reactor* (CPD-Q), was used. This allowed for collection of bio-oil from micropyrolysis. Bio-oil from pyrolysis of 20-60 samples run in series for a specified *pyrolysis duration* prior to *quenching* in a solvent bath, was collected with solvent from a condenser tube for a single run, then analyzed by GC/MS, GPC (gel permeation chromatography), HPLC (high performance liquid chromatography), GFC (gel filtration chromatography), FTIR (fourier transform infrared spectroscopy), or other. In the case of this experiment, the relative reactivity of cellulose pyrolysis intermediates was investigated by running 20x 500 μg samples of Sigmacell Cellulose for a pyrolysis duration of 20 seconds, using the custom gas mix for the oxidative condition, and pure helium for the non-oxidative condition, tested in duplicate, then analyzed by water-soluble sugar HPLC, Figure 25.

Lignin Side-chains and Interunit Linkages (online and offline analysis)

Red oak, red oak milled wood lignin (MWL), lignin monophenols, and lignin linkage representative dimer model compounds were pyrolyzed using Py-GC/FID, and subsequently Py-GC-MS/FID.

When testing red oak and red oak MWL, the GC was calibrated for red oak bio-oil compounds to allow quantification of oxygen concentration effects on major product yields. Specifically, enough species were calibrated to serve as a proxy for total yield of compounds containing functionalities of interest. These experiments were carried out in triplicate, so that non-calibrated MS-identified, FID-quantified peak areas could be statistically related to increases or decreases in yield as a result of the presence of oxygen in the sweep gas.

In the case of an earlier experiment, CPD-Q was used to pyrolyze red oak. This experiment required running three sets of 30 samples, and combining the collected oil from the three runs to generate a sample a great enough concentration to detect using a sensitive GC/MS, Figure 26.

Linkage-representative model dimer compounds were pyrolyzed in tall cups, to increase vapor residence time in the presence of the sweep gas (prior to quenching in the GC). Because a number of the model compounds are thermally stable or did not produce many different products, a sample size of 100 μg was used in order to prevent wear on the MS detector. After loading up the sample and prior to pyrolyzing, the headspace of the sample holder was purged for 2.5 minutes in the case of non-oxidative pyrolysis. In the case of oxidative pyrolysis, 4.5 minutes was allowed; additional time was needed to purge the FID and MS columns of pure helium. Directly following the 20 second pyrolysis time, the sweep gas was switched back to helium (in the case of the oxidative pyrolysis) to prevent excessive oxidation of the FID and MS columns. Data processing involved normalizing peak areas to a 100 μg sample mass. This was done so that a comparison could be made between the two conditions on a constant-mass basis. Further, in order to account for matrix (sweep gas composition) effects, a correction factor was used to normalize the peak areas from oxidative pyrolysis to the peak areas of non-oxidative pyrolysis. Determination of this correction factor involved the calibration of 7 model compounds in both non-oxidative and oxidative conditions to develop calibration curves for each case. Ratios of calibration curve slope for each compound ($m_{Non\text{-}oxidative}/m_{Oxidative}$) were averaged to develop a single correction factor. See Figure 19 for specifics of the analysis. These experiments were repeated with biomass fractions (Sigmacell cellulose, xylan (hemicellulose), and red oak milled wood lignin) to investigate their behavior as well. These biomass fractions were pyrolyzed in 500 μg samples in order to have good resolution since they have dozens of peaks. Thresholds defining major and minor peaks (for a given model)

were defined arbitrarily based on an assessment of which peak areas were large and which were small.

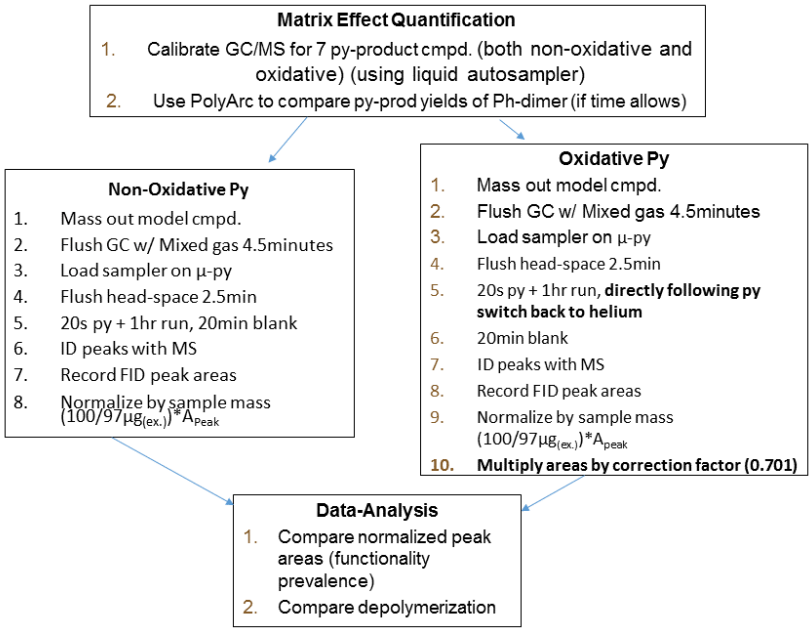

Figure 19. Lignin linkage-representative model compound experimental approach.

Pyrolytic Lignin Yields of Technical (isolated) Lignin (online analysis)

By investigating the yield of monophenolics on a lignin-basis from pyrolysis of whole biomass and isolated lignin, pyrolytic lignin yields could be compared. This was tested using a Py-GC-MS/FID/thermal conductivity detector (TCD), comparing Renmatix© switchgrass with Renmatix© switchgrass lignin. In order to quantify the pyrolytic lignin yield, the GC was calibrated with a representative portion of the lignin-derived pyrolysis products. Subsequently-calculated concentrations were normalized on a lignin-mass basis. Renmatix© switchgrass lignin was pretreated by mixing with fumed silica 1:1 by mass in agitated in isopropyl alcohol to ensure good mixing, prior to desiccation in a drying oven. Additional comparison of red oak, red oak-MWL, and fumed silica-pretreated red oak-MWL were testing using the same approach, Figure 31.

CHAPTER 5.
RESULTS

A series of experiments were carried out to learn about the constraints of using the micropyrolyzers. Once these limits were understood, oxidative and non-oxidative pyrolysis were compared from multiple perspectives. Results of these tests are discussed below.

Sample Size and Particle Size Effects

Statistically significant, using 3-sample 95% confidence intervals, differences in yields of the products with greatest selectivity were observed with changes from 100 to 500 microgram sample sizes, Figure 20.

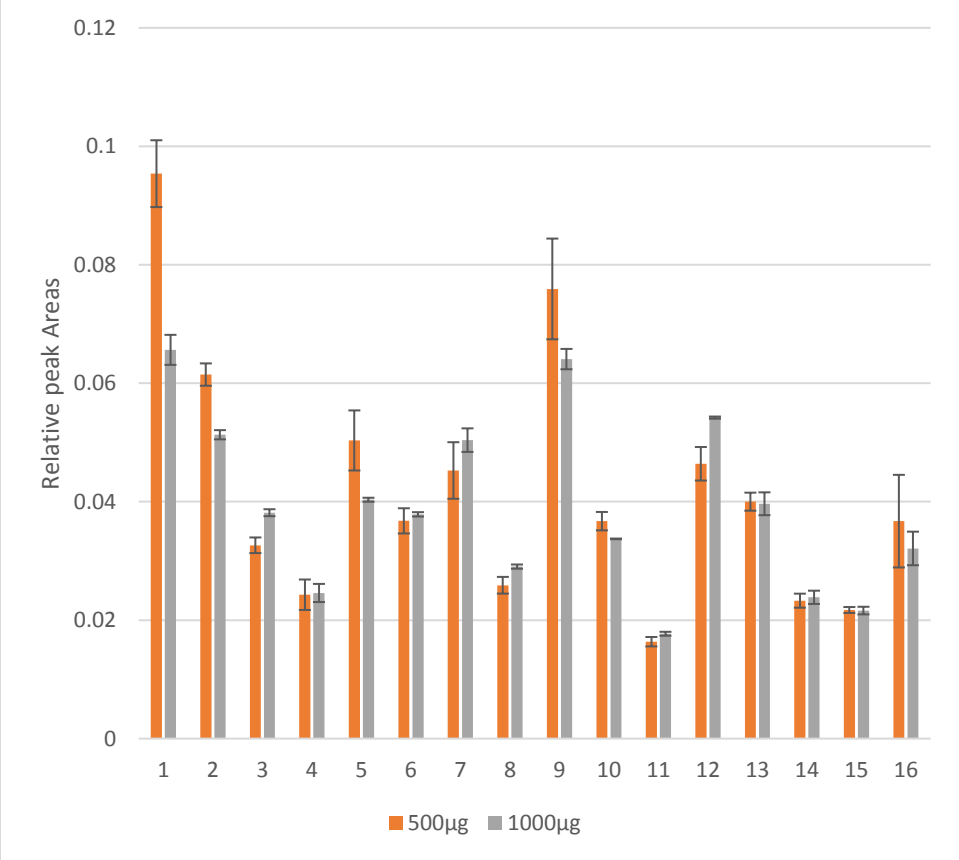

Figure 20. Doubling RO-MWL sample size changes pyrolysis product distribution. Py-GC/FID of 500, 1000 µg RO-MWL, 500°C, 100ml/min He. Peaks shown are the 16 largest relative areas (unidentified due to use of FID rather than MS, and lack of time for calibration of all major eluting compounds). Relative peak areas = ((peak area)/(tot. chromatogram area)) Error bars show 95% confidence intervals of three replicates.

When designing experiments, this result implies sample size should be considered for all conditions to be tested. Some factors influencing choice of sample size are number of pyrolysis products (if a substance is thermally stable, its signal will be contained in a single peak, whereas if the substance pyrolyzes into one hundred of species, its signal will be diluted one hundred-fold), the GC-split ratio; if a GC was calibrated using a split ratio of 10:1 rather than 200:1, a much greater portion of the sample (20X the 200:1 case) will pass through the column and hit the detector. In the case that a bio-oil collection experiment is being carried out, the product of sample size, number of

samples run, and bio-oil yield (diluted by some volume of solvent) must be greater than the minimum concentration detection limit of the instrument which will be used to analyze the bio-oil.

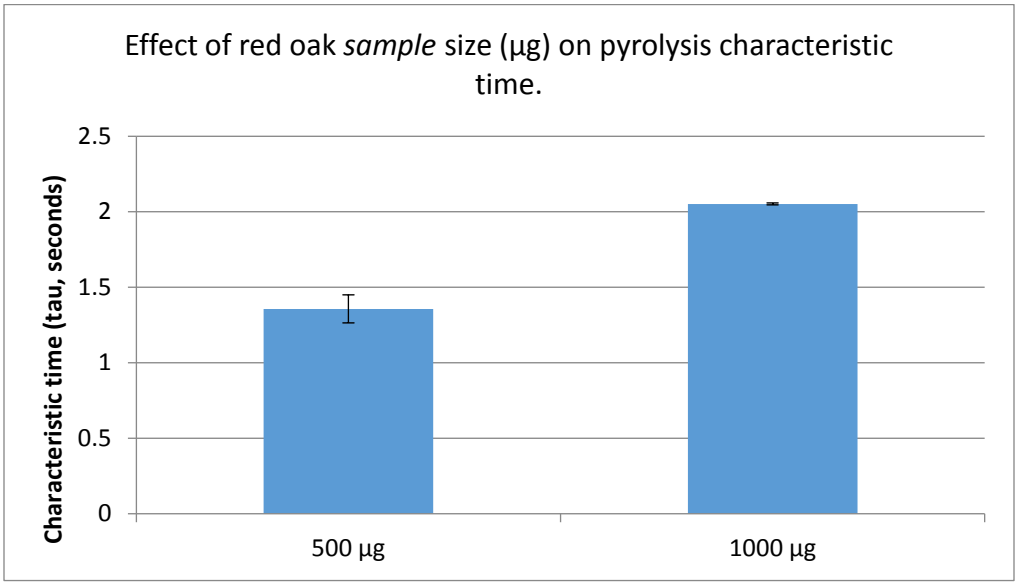

Figure 21. Doubling red oak sample size increases characteristic time.
(500°C, 100ml/min He, red oak-milled wood lignin ~<75 µm, Py-short column FID; error bars show 95% CI of three, two replicates, for 500, 1000 µg respectively.)

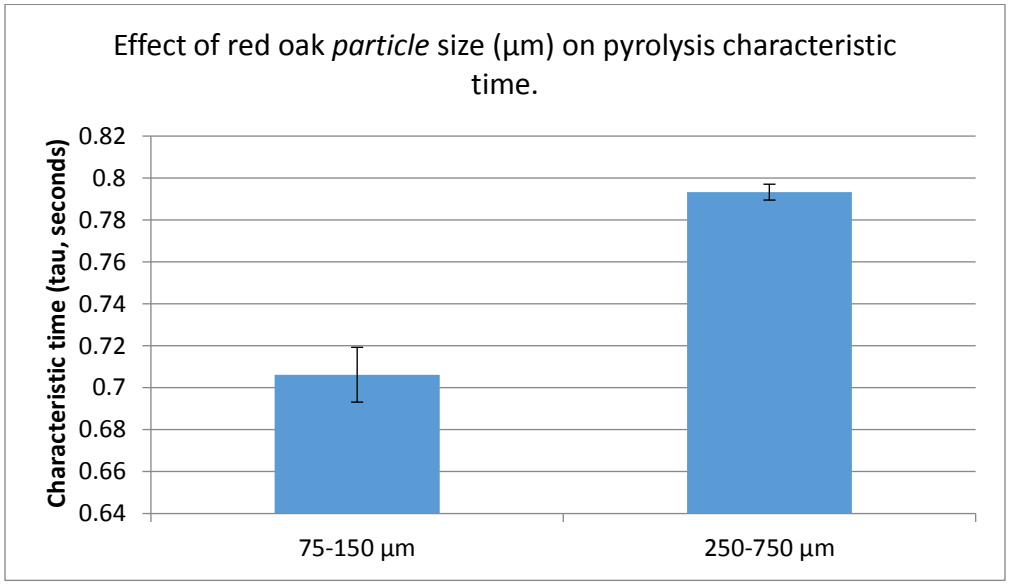

Figure 22. Increasing red oak particle size increases pyrolysis characteristic time.
(500°C, 100ml/min He, 500 µg red oak sample size, Py-short column FID; error bars show 95% CI of three replicates. Size ranges represent the variation in particle sizes of two samples (sieved to specified bounds).)

Equivalence Ratio Quantification

An attempt to quantify the equivalence ratio used a proxy feedstock (carbon lamp-black) which pyrolyzed or oxidized in a neat manner. The issue with this was the kinetic incompatibility of whole biomass and a nearly graphitized carbon material. In order to have appreciable mass loss during a standard pyrolysis time (10-20 seconds) with a 20% oxygen stream, the temperature needed to be increased to 800°C, whereas the biomass was clearly oxidized at lower temperatures.

It was thus determined that it would be impractical to attempt to use equivalence ratio as an absolute indicator of extent of oxidation. Instead, equivalence ratio was used only as a basis on which to compare sweep gas oxygen concentrations. It was also established that use of the term *autothermal pyrolysis in a micropyrolyzer* would be misleading, since the extent and modes of oxidation were not directly related to the fluidized bed-autothermal equivalence ratio. Instead *partial oxidative* (or just *oxidative*) *pyrolysis* was used.

Relative Reactivity with Oxygen

Reactivity of biomass fractions did not fully agree with the hypothesized reactivity. Hemicellulose conversion was not anticipated to increase comparably to lignin, rather it was thought it would convert comparably to cellulose. Analysis of sugars using HPLC might provide a more insight. Because hemicellulose and cellulose have similar functionalities, the polymeric structures might be responsible for the differences in conversion.

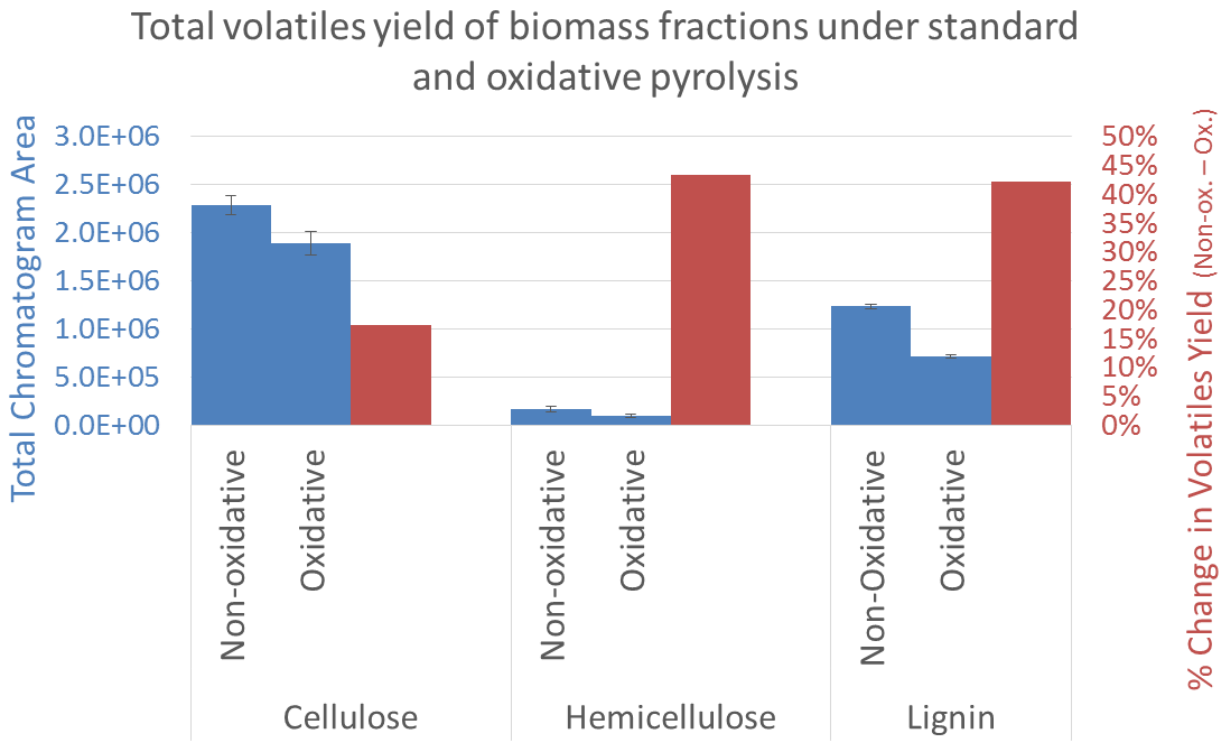

Figure 23. Lignin and hemicellulose are more reactive with oxygen than cellulose.

Monophenol reactivity tests agreed with reported reactivity rules of thumb described above, determined on both the basis of antioxidant activity and DFT studies. When looking at the structures of the three compounds tested, syringaldehyde has one more (reactive) methoxy group than vanillin, and acetophenone replaces syringaldehyde's aldehyde with a more reactive acetyl, Figure 24.

These results show some agreement with Amutio et al. [52], who tested ER = 0, 0.15, 0.25. Amutio observed decreased yield of methoxy containing (more reactive) guaiacol, and increased

yield of cresols, yet also observed increased yield of eugenol (having both methoxy and vinyl functionalities), Table 2.

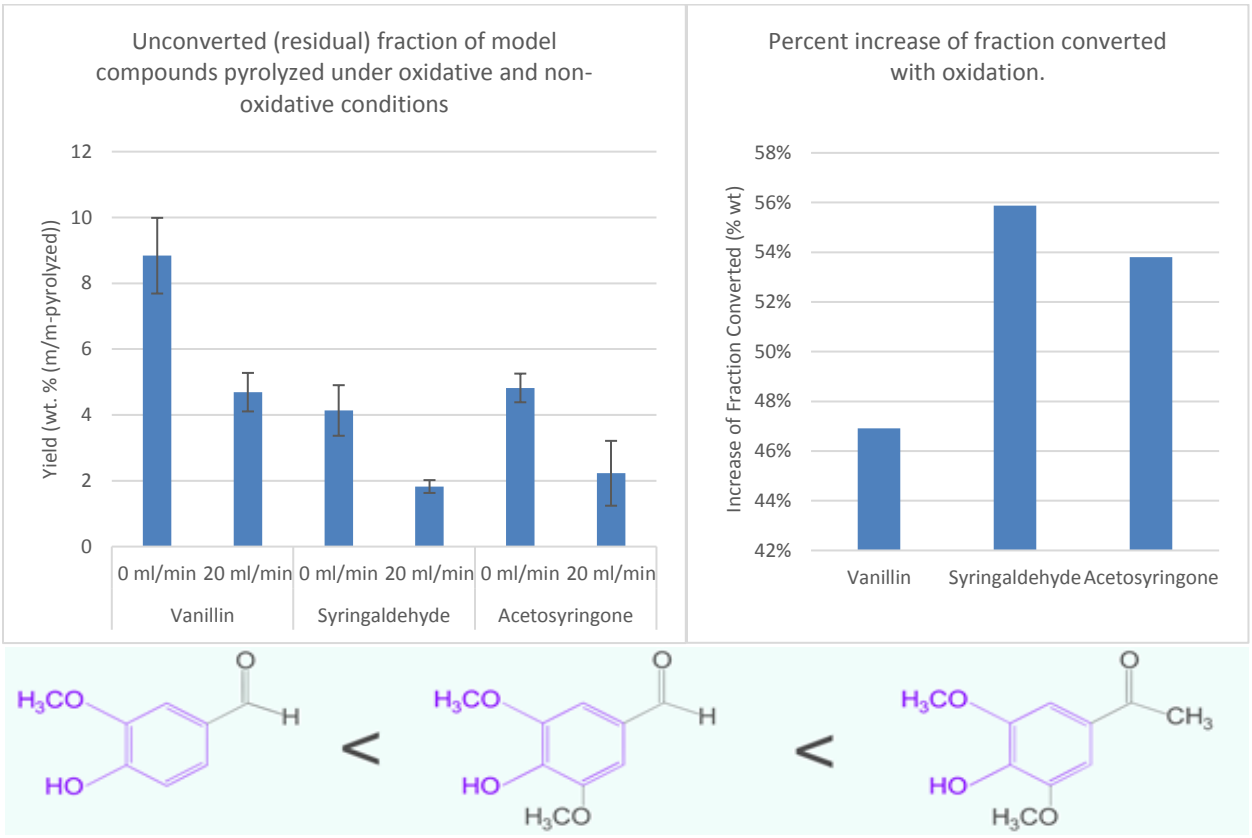

Figure 24. Relative reactivity of monophenols with different substituents.
((Left) (0, 20 ml/min O_2 over 100 ml/min He); error bars show 95% CI of three replicates. 75 µg of model compound directly in cup; (right) oxidation increased from 0 to 20ml/min O_2; (bottom) observed reactivity; vanillin < syringaldehyde < acetaldehyde.)

Cellulose bio-oil was collected by CPD-Q to compare sugar yields during non-oxidative and oxidative pyrolysis, Figure 25. Decrease in levoglucosan yield might have to do with the bridge-bonded oxygen being relatively minimally hindered.

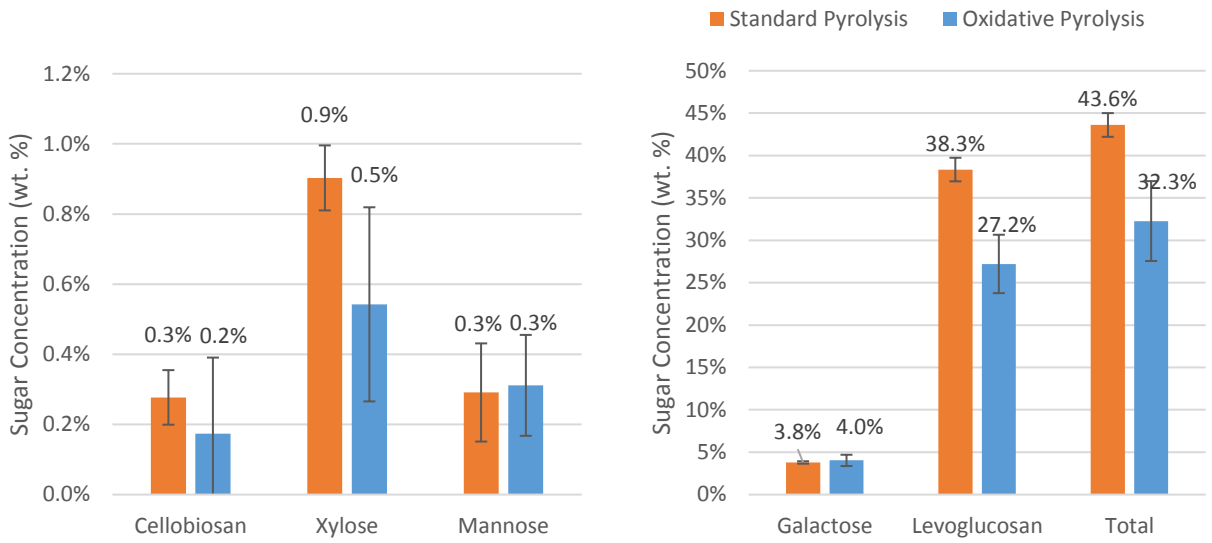

Figure 25. Oxidative pyrolysis (10% O_2 by vol.) preferentially consumes LG and possibly xylose. (CPD-Quench; 20x 500µg samples Sigmacell cellulose, run in duplicate for each condition, WSS-HPLC analysis of collected bio-oil tested in duplicate, error bars show 95% CI of four sub-replicates (2 experimental replications x 2 HPLC replications).)

Lignin Side-chains and Interunit Linkages

The results from the red oak experiment, when carried out for the first time during summer of 2016, Figure 26, showed increased yield of some aldehyde and ketone species, with admission of oxygen into the reactor. Examples of these compounds include; acetaldehyde, syringaldehyde, and vanillin (aldehydes), and acetosyringone (ketone). The only vinyl-containing compound calibrated for was 2-methoxy-4-vinylphenol, whose yield notably decreased. Yield of most other calibrated-for compounds decreased. Inconsistent results during later experiments brought earlier findings into question, Figure 26.

Comparing these results to the findings of others, Kim et al. [71] fluidized bed experiments showed similar trends; decreased yield of 2-methoxy-4-vinyl phenol and increased yield of 4-hydroxy-3-methoxyacetophenone as well as 4-hydroxy-3,5-dimethoxybenzaldehyde, Table 1.

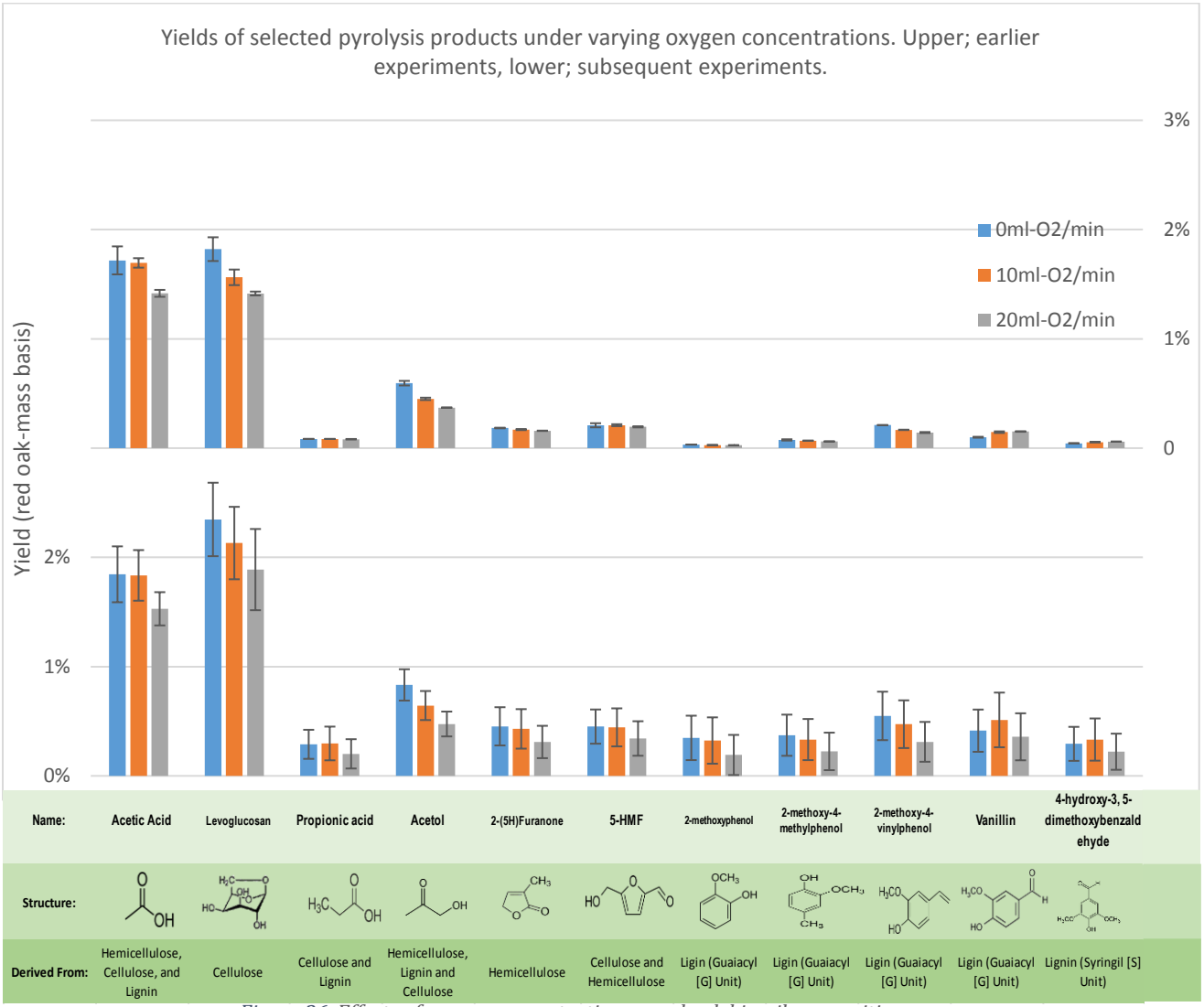

Figure 26. Effects of oxygen concentration on red oak bio-oil composition.
(Yields of selected compounds after 20 second, 500°C pyrolysis of 500 µg red oak, 100 ml/min sweep flow, under varying oxygen concentrations, note balance of sweep flow is helium, error bars show the 95% confidence intervals of three replicates, (upper panel) earlier experimental findings showing clear trends, (lower panel) later experiments showing inconclusive trends.)

Controlled pyrolysis duration-quench reactor results, Figure 32, partially support the findings of calibrated GC/FID. Decrease of 2-methoxy-4-vinyl phenol, and increase in; syringaldehyde, vanillin, and acetosyringone were all in agreement. The major discrepancy was observed increase in levoglucosan yield with the CPD-Q experiment.

The lignin dimer model compound study introduced many complications. When using the custom mixed gas, peaks of thermally stable compounds eluted differently, yielding different areas for the same quantity of a compound passing through the column. It is possible this effect had to do with increased density and decreased diffusivity of oxygen (relative to helium). This was adjusted for by developing a correction factor ($0.665*A_{oxidativePeak} = A_{standardPeak}$), based on the ratio of standard: oxidative peak areas of a series of phenanthrene and diphenyl ether calibrations, yielding 0.6580 and 0.6698, respectively. See relative standard-oxidative product distribution comparisons

below, Figure 33. It also turned out that a few of the dimer models were thermally stable at 500°C. During an earlier round of experiments, higher temperatures were applied to learn how the compound would pyrolyze if forced to, although subsequent tests used 500°C for all trials. Another challenge was incompatibility between observed product composition and species reported in pyrolysis mechanisms. This limited the applicability of some of the mechanisms.

The two goals of the lignin dimer model experiment were still able to be achieved, even given these constraints. It was shown that diphenyl ether (the 4-*O*-5' model), at 700°C, and 2-phenoxy-1-phenylethanol (the β-*O*-4' with α-OH), at 500°C, both converted (presumably by cleavage of linkage) further in the presence of oxygen. Additionally, product compositions from benzyl phenyl ether and 2-phenoxy-1-phenylethanol allowed for logical extensions of prior-published mechanisms, Figure 27 and Figure 28. Further, thermal stability of some linkages suggests important role of reactive intermediates in assisting linkage cleavage.

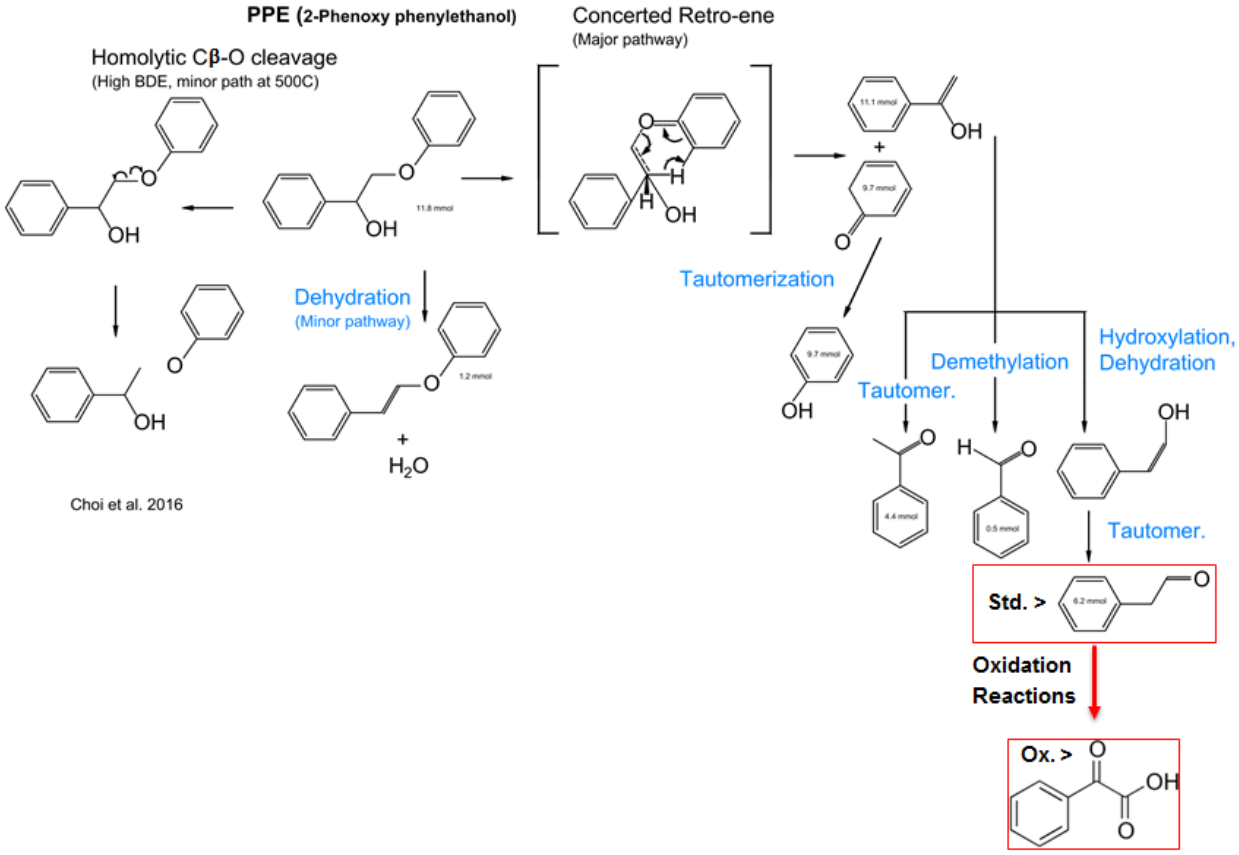

Figure 27. Expansion of published PP-EOL pyrolysis mechanism with proposed oxidation pathway [226].

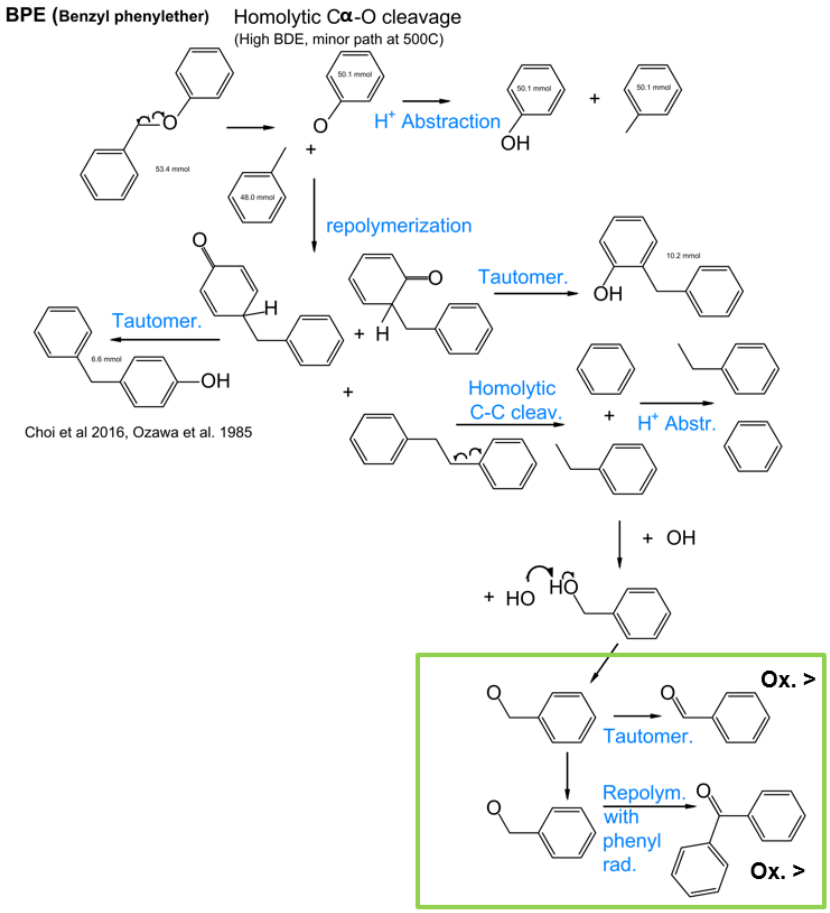

Figure 28. Expansion of published BPE pyrolysis mechanisms with proposed oxidation pathway [226,231].

The results presented in Figure 33 and Table 5 show all of the processed data from the non-oxidative versus oxidative pyrolysis py-GC experiments using lignin model compounds and biomass fractions. Oxidative pyrolysis, using the mixed gas (10% O_2, 90% He by volume), generally seemed to "over-oxidize" the compounds being tested. Relative to fluidized bed autothermal pyrolysis, where improved bio-oil composition has greater monomer content, monomers appeared to be partially degraded in the oxidative pyrolysis trials (note increased yields of acids and light oxygenates, Figure 33. Given this, a number of observations can be made such as in the case of cellulose, where cellobiose (glucose dimer) yield decreased during oxidative pyrolysis; indicating increased extent of depolymerization, in addition to increased monosaccharide degradation.

A propagation of error analysis was carried out to attempt to quantify all of the sources of error and uncertainty which are part of the micropyrolysis experimentation process. The results of the analysis nullify many of the findings from non-oxidative and oxidative pyrolysis comparisons of individual species. See Figure 29, Figure 34 and

Table 66 for propagation of error analysis approach and results. Generally, the process was broken down to identify sources of error, five being identified; 1. Sample preparation (milling and sieving), 2. Massing out samples, 3. Use of imperfect

correction factor to account for matrix (sweep gas) effects, 4. Experimental GC sample to sample signal variability, and 5. Analysis of results when comparing yield of a specific species across oxidative conditions. Error attributed to milling and sieving was the potential inconsistency of final particle size distribution, specifically average particle size. Earlier experiments, Figure 22, showed increasing particle size increased pyrolysis characteristic time, as did increased sample size, Figure 21. The deviation in product distribution, Figure 20, (quantified by average normalized deviance across oxidative condition) was quantified for sample size, normalized by change in characteristic time to determine a potential error from the sample size deviation which might be expected during normal operation. Because composition effects data was not available for particle size, the ratio of change in characteristic time to composition change, observed for sample size effects was applied to particle size's observed change in characteristic time, see Figure 34. Correction factor error was determined by taking coefficient of variation (average-normalized standard deviation) of the seven compounds' correction factors which it (the overage correction factor) was derived from. GC error was quantified by assessing sample to sample peak area variability of the three replications for each condition (these peak areas were sample size normalized to 100 μg and the oxidative peak areas had the correction factor applied). When comparing peak areas across oxidative condition, coefficient of variation (resultant from the propagation of error analysis), was applied to make the decision of statistically significant differences.

Table 66 shows how the results change when the propagation of error analysis is implemented.

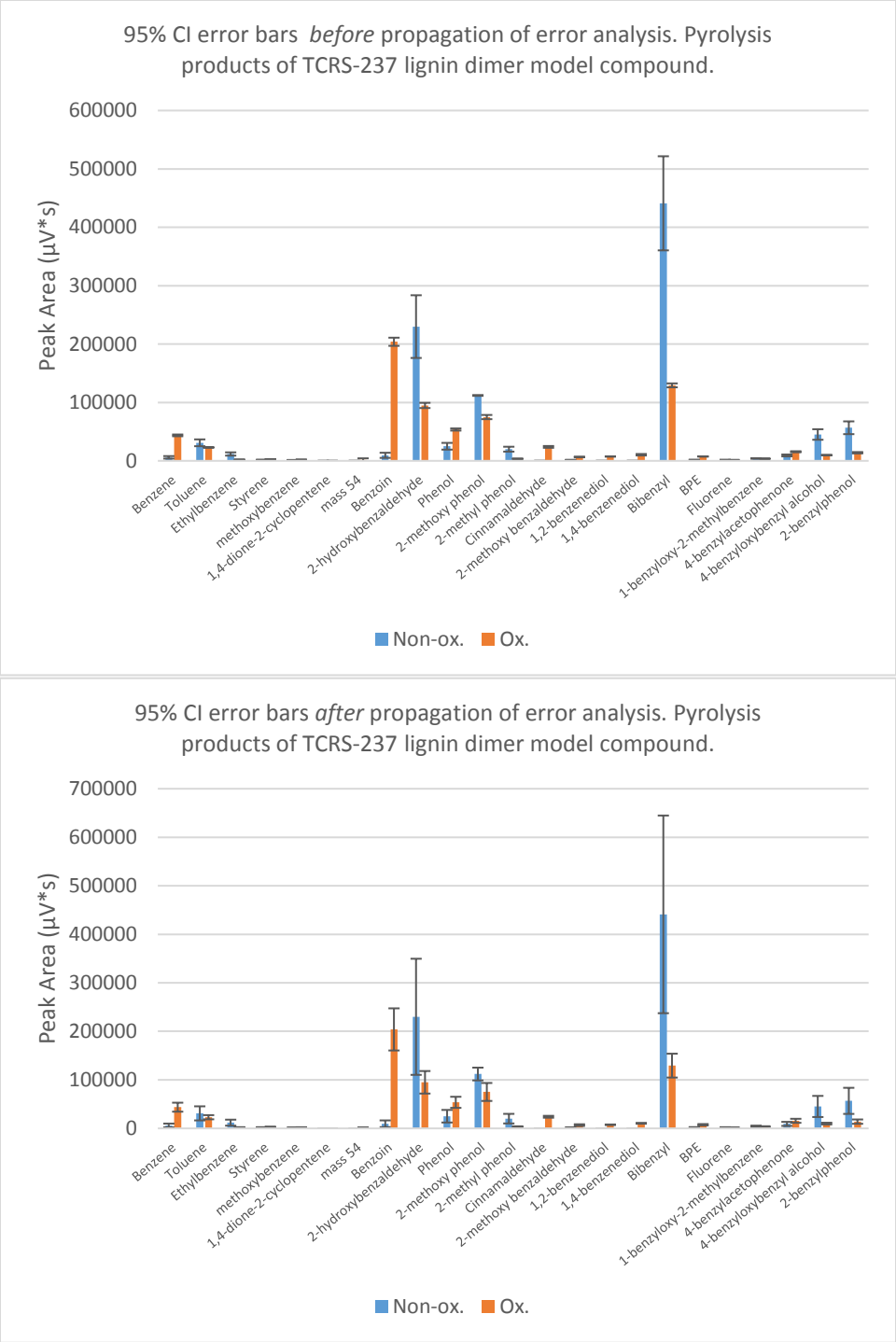

Figure 29. Propagation of error analysis nullifies many findings.

Pyrolytic Lignin Yield of Technical (isolated) Lignin

Experiments comparing Renmatix© switchgrass to Renmatix© switchgrass lignin supported the claim of isolated lignin having lesser pyrolytic lignin yield, Figure 30. Fumed silica was shown to increase the capability of lignin to volatilize (by reduced char yield and increased monophenolic yield). By preventing melt-phase coalescence, it was suggested the finer lignin particles experienced

a greater heating rate which would reduce extent of dehydration reactions and reduce time which lignin was in a thermal regime conducive of repolymerization reactions. Oxidative pyrolysis of lignin had inconclusive results due to prior-described limitations of oxidation in the micropyrolyzers, and due to prior complexities of quantifying increase in volatiles production since a portion is oxidized to light gases not quantified by GC/FID.

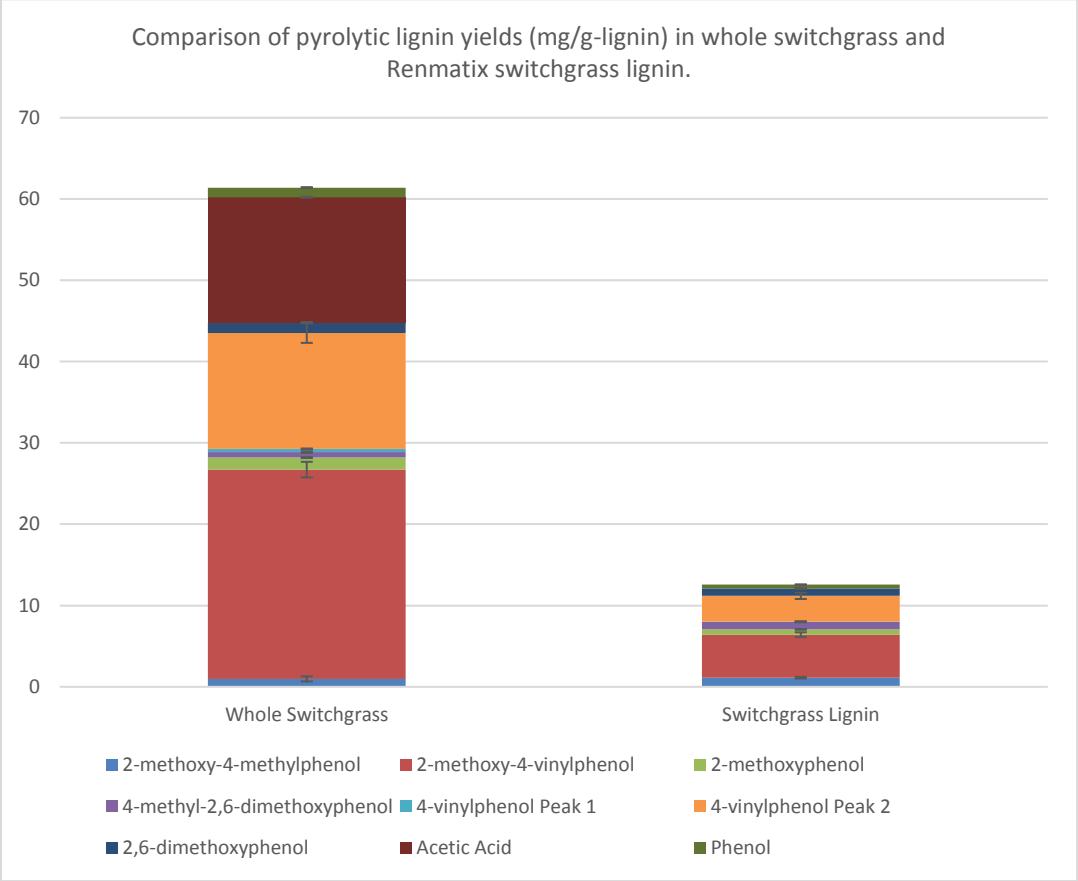

Figure 30. Isolated lignins produce lower yields of pyrolytic lignin than whole biomass. (Comparison of pyrolytic lignin yields (mg/g-lignin) in whole switchgrass and Renmatix© switchgrass lignin of select calibrated compounds (representative of ~23% of pyrolytic lignin yield in ADM organosolv lignin – as quantified by Patwardhan 2010 (dissertation)); yields normalized on a lignin-mass basis (assumed switchgrass is 22.5% lignin by mass); error bars represent 95% CI of three replicates.)

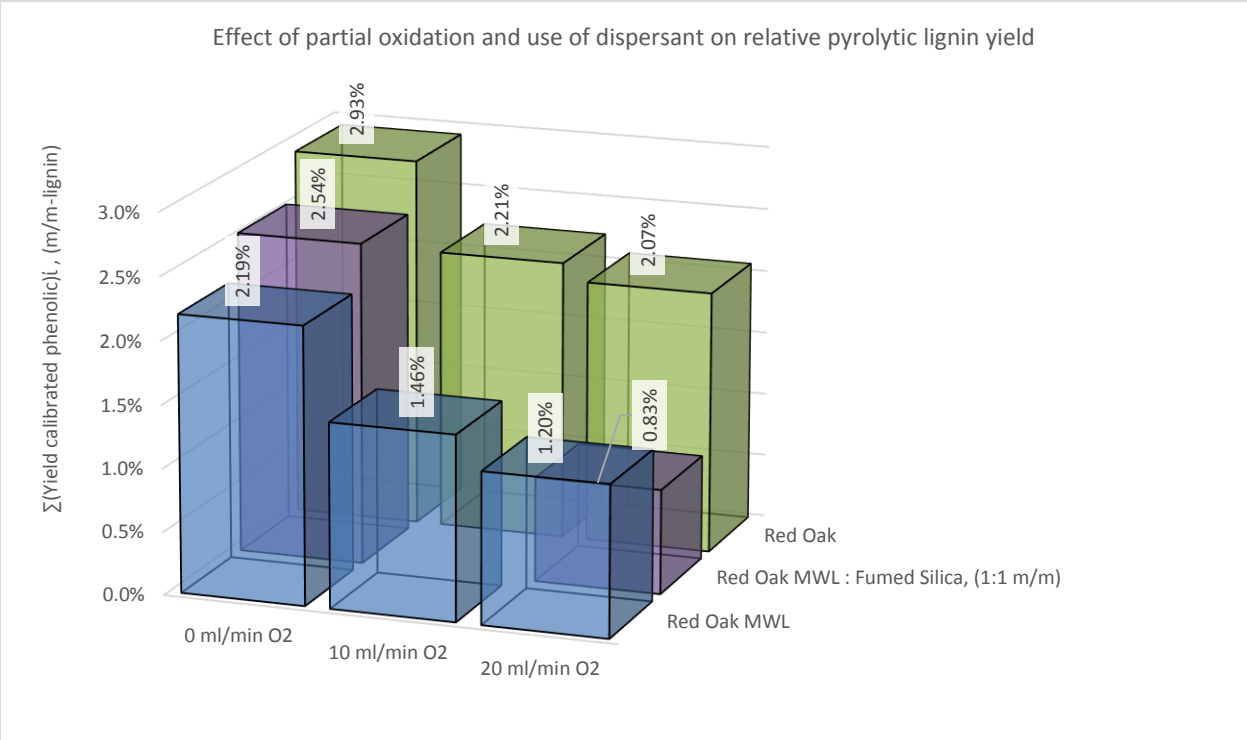

Figure 31. Dispersant increases pyrolytic lignin yield, while partial oxidation decreases it.
(Pyrolytic lignin yields quantified via GC-MS/FID calibration by compounds representative of ~23% of pyrolytic lignin, trials tested in triplicate)

CHAPTER 6.
GENERAL CONCLUSIONS

Autothermal pyrolysis is a variant of FP which has the potential to reduce capital costs, operating costs, and increase volume of marketable char (if no longer required for process heat applications). Although it has been shown possible to carefully control the process such that minimal desired product is oxidized (consumed), learning more about the underlying oxidation (exothermic) reactions occurring could assist in the decisions made when developing the process at larger scales.

In the instance that red oak is the process feedstock, admission of small sub-stoichiometric amounts of air into the reactor leads primarily to the oxidation of flammable gases, secondarily to that of the char particles, and minimally to the bio-oil (condensable) vapors and aerosols. The non-condensable gases likely oxidize by dehydration, decarbonylation, and decarboxylation reactions. Char particles likely react in gas-solid reactions with reactive oxygen species (various radical/reactive oxides, hydroxides, and peroxides), leading directly to CO and CO_2.

Although a smaller contribution to the process heat, oxidation of the bio-oil vapors and aerosols is chemically the most complex set of processes, was the focus of the review presented in Chapter 2. Sugar yields have been shown to increase; many of the carbohydrate oxidation reactions are involved in cleavage of interunit linkages or oxidation of side chains, yielding monosaccharides. Similar is likely exhibited in the lignin fraction; increased bio-oil water content is likely attributable to increase in dehydration reactions associated with hydrolytic depolymerization. Details of these reaction pathways are investigated in Chapter 2.

Total yield of aldehyde, ketone, and carboxylic acid-containing lignin-derived phenolics have been shown to increase. High temperature (500°C) oxygen in the vicinity of vapor phase pyrolysis intermediates has the potential for multiple step single-electron oxidations by molecular oxygen or ROS.

Future efforts might attempt to model the kinetics of autothermal pyrolysis. Utilization of oxygen isotope-labeled model compounds in oxidative pyrolysis could provide greater certainty about mode and extent of oxygen incorporation into product species, through NMR analysis. Pyrolysis experiments comparing thermodynamics of whole biomass and model feedstocks, should further inform about the source of heat during autothermal pyrolysis.

REFERENCES

[1] E. Weiss, in, Watwill, Switzerland, USPTO, 1941.

[2] J. Clark, in *Chemguide - Helping you Understand Chemistry*, 2013.

[3] J. McMurry, *Organic Chemistry*, Cengage Learning, Belmont, California, United States, 2012, p.

[4] J.G. Calvert, *Pure and Applied Chemistry, The Scientific Journal of IUPAC*, 62, (2009) 2167.

[5] P. Karen, P. McArdle and J. Takats, *Pure and Applied Chemistry - IUPAC Recommendations*, 88, (2016) 831.

[6] M.J. Moran, H.N. Shapiro, D.D. Boettner and M.B. Bailey, *Fundamentals of Engineering Thermodynamics*, John Wiley & Sons Inc., Hoboken, NJ, United States, 2014, p.

[7] E. Merzerbacher, *Quantum Mechanics*, John Wiley & Sons, Inc., Chapel Hill, NC, U.S., 1998, p.

[8] P. Atkins, J. de Paula and R. Friedman, *Quanta, matter and change. A molecular approach to physical chemistry*, W.H. Freeman and Company, NYC, NY, U.S., 2009, p.

[9] M.R. Leach, in *The Chemogenesis Web Book*, meta-synthesis1999-2016, Manchester, 2016.

[10] I.N. Levine, *Quantum Chemistry*, Prentice Hall, MCGraw Hill International, Englewood Cliffs, NJ, U.S., 1991, p.

[11] P. Klán and J. Wirz, *Photochemistry of Organic Compounds: From Concepts to Practice*, Wiley-Blackwell, Brno, Czech Republic 2009, p.

[12] A. Krieger-Liszkay, *Journal of Experimental Botany*, 56, (2004) 337.

[13] V.N. Kondratiev, in, Moscow, Russia, 2016.

[14] R. Zhao, E.L. Mungall, A.K.Y. Lee, D. Aljawhary and J.P.D. Abbatt, *Atmospheric Chemistry and Physics*, 14, (2014) 9695.

[15] R.C. Brown and T.R. Brown, *Biorenewable Resources: Engineering New Products from Agriculture, 2nd Edition*, Wiley-Blackwell, 2014, p.

[16] M. Bourguignon, K.J. Moore, R.C. Brown, K.H. Kim, B.S. Baldwin and R. Hintz, *BioEnergy Research*, (2016).

[17] J. Cobb, in *Hybrid Cars*, HybridCars.com, 2016.

[18] A. Davies, in *Wired.com*, Wired, 2016.

[19] R.D. Perlack and B.J. Stokes, in, U.S. Department of Energy, Oak Ridge, TN, 2011, p. 227.

[20] R.C. Brown and T.R. Brown, *Biorenewable Resources - Engineering New Products from Agriculture*, Wiley Blackwell, Ames, IA, U.S., 2014, p.

[21] S. Yokoyama and Y. Matsumura, *The Asian Biomass Handbook*, The Japan Institute of Energy, Tokyo, 2008, p.

[22] R.B. Bates and A.F. Ghoniem, *Bioresource Technology*, 124, (2012) 460.

[23] B. Acharya, I. Sule and A. Dutta, *Biomass Conversion and Biorefinery*, 2, (2012) 349.

[24] T. Bridgewater, in N. Carling (Ed.), Aston University, 2007.

[25] E. Beglinger, in *US Forest Service Technical Reports*, USDA Forest Service - Forest Products Lab, Madison, 1956.

[26] C.H. McMichael, M.W. Palace, M.B. Bush, B. Braswell, S. Hagen, E.G. Neves, M.R. Silman, E.K. Tamanaha and C. Czarnecki, *Proc Biol Sci*, 281, (2014) 20132475.

[27] D.A. Laird, R.C. Brown, J.E. Amonette and J. Lehmann, *Biofuels, Bioproducts and Biorefining*, 3, (2009) 547.

[28] M.K. Karmakar, J. Mandal, S. Haldar and P.K. Chatterjee, *Fuel*, 111, (2013) 584.

[29] A. Ghosh, R.C. Brown and X. Bai, *Green Chemistry*, (2016), (2015) 1023.

[30] M.R. Haverly, K.V. Okoren and R.C. Brown, *Energy & Fuels*, 30, (2016) 9419.

[31] M.M. Wright and R.C. Brown, *Biofuels, Bioproducts and Biorefining*, 1, (2007) 49.

[32] M.M. Wright, J.A. Satrio and R.C. Brown, in, U.S. Department of Energy, Ames, 2010, p. 62.

[33] W.J.A. Butterfield, *The Chemistry of Gas Manufacture - A Practical Handbook on the Production, Purification, and Testing of Illuminating and Fuel Gas, and on the Bye-products of Gas Manufacture*, Charles Griffin and Company Ltd., Exeter Street, Strand, London, 1907, p.
[34] D. Leckel, *Energy & Fuels*, 23, (2009) 2342.
[35] J.R. Rostrup-Nielsen, *Catalysis Today* 71, (2002) 243.
[36] D.E. Daugaard and R.C. Brown, *Energy & Fuels*, 17, (2003) 934.
[37] M.J. Spearpoint, in, NIST, Gaithersburg, MD, 1999, p. 382.
[38] F.P. Incropera, D.P. Dewitt, T.L. Bergman and A.S. Lavine, *Fundamentals of Heat and Mass Transfer*, John Wiley & Sons, Los Angeles, CA, U.S., 2007, p.
[39] C.A. Harper, *Handbook of Building Materials for Fire Protection*, McGraw-Hill, Lutherville, MD, U.S., 2004, p.
[40] K. Raveendran, A. Ganesh and K.C. Khilar, *Fuel*, 75, (1996) 987.
[41] J. Polin, L.E. Whitmer, R.G. Smith and R.C. Brown.
[42] I.W. Smith, *Symposium (International) on Combustion/The Comustion Institute*, 19, (1982) 1045.
[43] P.R. Solomon, M.A. Serio and E.M. Suuberg, *Progress in Energy Combustion Science*, 18, (1992) 133.
[44] D.J. Hucknall, *Chemistry of Hydrocarbon Chemistry*, Chapmand and Hall, Southhampton, New York, US, 1985, p.
[45] I. Glassman, R. Yetter and N. Gluman, *Combustion (Fifth Edition)*, Academic Press, 2014, p. 757.
[46] S.R. Collinson and W. Thielemans, *Coordination Chemistry Reviews*, 254, (2010) 1854.
[47] F.-X. Collard and J. Blin, *Renewable and Sustainable Energy Reviews*, 38, (2014) 594.
[48] D. Mohan, C.U. Pittman, Jr., M. Bricka, F. Smith, B. Yancey, J. Mohammad, P.H. Steele, M.F. Alexandre-Franco, V. Gomez-Serrano and H. Gong, *J Colloid Interface Sci*, 310, (2007) 57.
[49] T. Dickerson and J. Soria, *Energies*, 6, (2013) 514.
[50] M. Brebu and C. Vasile, *Cellulose Chemistry and Technology*, 44, (2010) 353.
[51] C. Crestini, M. Crucianelli, M. Orlandi and R. Saladino, *Catalysis Today*, 156, (2010) 8.
[52] M. Amutio, G. Lopez, R. Aguado, J. Bilbao and M. Olazar, *Energy & Fuels*, 26, (2012) 1353.
[53] I.P. Boukis, P. Grammelis, S. Bezergianni and A.V. Bridgwater, *Fuel*, 86, (2007) 1372.
[54] D.A.E. Butt, *Journal of Analytical and Applied Pyrolysis*, 76, (2006) 55.
[55] A. Garzon, I. Bravo, A.J. Barbero and J. Albaladejo, *J Agric Food Chem*, 62, (2014) 9705.
[56] K.H. Kim, R. Brown and X. Bai, *Fuel*, 130, (2014) 135.
[57] S. Lofti, D.C. Boffito and G.S. Patience, *ChemSusChem*, 8, (2015) 3424
[58] J.M. Mesa-Pérez, J.D. Rocha, L.A. Barbosa-Cortez, M. Penedo-Medina, C.A. Luengo and E. Cascarosa, *Applied Thermal Engineering*, 56, (2013) 167.
[59] N.E. Persson, S.D. Blass, C. Rosenthal, A. Bhan and L.D. Schmidt, *RSC Advances*, 3, (2013) 20163.
[60] M.J.T.J. Arts, G.R.M.M. Haenen, H.-P. Voss and A. Bast, *Food and Chemical Toxicology*, 42, (2004) 45.
[61] G. Rovero and A.P. Watkinson, *Fuel Processing Technology*, 26, (1990) 221.
[62] D.S. Scott, J. Piskorz, D. Radelin and P. Majerski, in, Ottowa, Canada, 1995.
[63] J.A. Suárez, P.A. Beaton, R. Zanzi and A. Grimm, *Energy Sources, Part A: Recovery, Utilization, and Environmental Effects*, 28, (2006) 695.
[64] M.-Y. Wey, B.-H. Liou, S.-Y. Wu and C.-H. Zhang, *Journal of the Air & Waste Management Association*, 45, (1995) 855.
[65] H.Y. Zhang, R. Xiao, Q.W. Pan, Q.L. Song and H. Huang, *Chemical Engineering & Technology*, 32, (2009) 27.
[66] D. Li, C. Briens and F. Berruti, *Biomass and Bioenergy*, 76, (2015) 96.
[67] M. Amutio, G. Lopez, R. Aguado, M. Artetxe, J. Bilbao and M. Olazar, *Fuel*, 95, (2012) 305.
[68] I.P. Boukis, S. Bezergianni, P. Grammelis and A.V. Bridgwater, *Fuel*, 86, (2007) 1387.

[69] D.A.E. Butt, *Journal of Analytical and Applied Pyrolysis*, 76, (2006) 38.
[70] D. Butt, *Journal of Analytical and Applied Pyrolysis*, 76, (2006) 48.
[71] K.H. Kim, X. Bai, M. Rover and R.C. Brown, *Fuel*, 124, (2014) 49.
[72] W. Jin, K. Singh and J. Zondlo, *Agriculture*, 3, (2013) 12.
[73] L.e. Jin, L. Wang, L. Su and Q. Cao, *International Journal of Green Energy*, 9, (2012) 719.
[74] M.K. Misra, K.W. Ragland and A.J. Baker, *Biomass and Bioenergy*, 4, (1992) 103.
[75] T.E. Amidon, B. Bujanovic, S. Liu and J.R. Howard, *Forests*, 2, (2011) 929.
[76] T.Q. Yuan, S.N. Sun, F. Xu and R.C. Sun, *J Agric Food Chem*, 59, (2011) 10604.
[77] Y. Zhou, H. Stuart-Williams, G.D. Farquhar and C.H. Hocart, *Phytochemistry*, 71, (2010) 982.
[78] J. Zhang, Y.S. Choi, C.G. Yoo, T.H. Kim, R.C. Brown and B.H. Shanks, *ACS Sustainable Chemistry & Engineering*, 3, (2015) 293.
[79] Z. Jin, K.S. Katsumata, T.B. Lam and K. Iiyama, *Biopolymers*, 83, (2006) 103.
[80] P. Bhaumik and P.L. Dhepe, (2015) 1.
[81] H.A. Khalil, M. Tehrani, Y. Davoudpour, A. Bhat, M. Jawaid and A. Hassan, *Journal of Reinforced Plastics and Composites*, 32, (2012) 330.
[82] A.R. War, M.G. Paulraj, T. Ahmad, A.A. Buhroo, B. Hussain, S. Ignacimuthu and H.C. Sharma, *Plant Signal Behav*, 7, (2012) 1306.
[83] P.R. Larson, *The Vascular Cambium, Development and Structure*, Springer-Verlag, Syracuse, NY, U.S., 1994, p.
[84] E.J. Mellerowicz, M. Baucher, B. Sundberg and W. Boerjan, *Plant Molecular Biology*, 47, (2001) 239.
[85] P. Kitin, Y. Sano and R. Funada, *Journal of Experimental Botany*, 53, (2002) 483.
[86] Y. Murakami, R. Funada, Y. Sano and J. Ohtani, *Annals of Botany*, 84, (1999) 429.
[87] N. Terashima, M. Okada and Y. Tomimura, *Mokuzai Gakkaishi (Journal of Wood Science)*, 25, (1979) 422.
[88] L.J. Gibson, *J R Soc Interface*, 9, (2012) 2749.
[89] M. Ashby, *Materials Selection in Mechanical Design*, Butterworth-Heinemann, Cambridge, UK, 2010, p.
[90] B.B. Hallac and A.J. Ragauskas, *Biofuels Bioproducts and Biorefining*, 5, (2011) 215.
[91] S. Youssefian and N. Rahbar, *Sci Rep*, 5, (2015) 11116.
[92] D. Klemm, H.-P. Schmauder and T. Heinze, in *Comprehensive Cellulose Chemistry: Functionalization of Cellulose*, 1998 Wiley-VCH Verlag GmbH, Weinheim, 2004, Chapter Ch. 10, p. 275.
[93] P. Zungenmaier, *Crystalline Cellulose and Cellulose Derivatives - Charaterization and Structures*, © 2008 Springer-Verlag Berlin Heidelberg, Syracuse, 2008, p.
[94] B. Lindman, G. Karlström and L. Stigsson, *Journal of Molecular Liquids*, 156, (2010) 76.
[95] T. Liebert and T. Heinze, *BioResources*, 3, (2008) 576.
[96] R.C. Sun and J. Thompkinson, *Carbohydrate Polymers*, 50, (2002) 263.
[97] X. Zhou, W. Li, R. Mabon and L.J. Broadbelt, *Energy Technology*, 5, (2017) 52.
[98] A. Ebringerová, Z. Hromádková and T. Heinze, 186, (2005) 1.
[99] G.O. Aspinall, *The Polysaccharides Volume 2*, Academic Press, New York, 1983, p. 783.
[100] J.S.G. Reid, M. Edwards and I.C.M. Dea, *European Journal of Lipid Science and Technology*, 44, (1988).
[101] L. Navarini, R. Gilli, V. Gombac, A. Abatangelo, M. Bosco and R. Toffanin, *Carbohydrate Polymers*, 40, (1999) 71.
[102] A.M. Stephen, G.O. Philips and P.A. Williams, *Food Polysaccharides and Their Applications*, Taylor and Francis, Boca Raton, 2006, p.
[103] V.D. Scherbukhin and O.V. Anulov, *Applied Biochemistry and Microbiology*, 35, (1999) 229.

[104] N.M. Packter, *The Biochemistry of Plants: A Comprehensive Treatise; Carbohydrates*, Academic Press, 1988, p.
[105] E. Sjöström, *Wood Chemistry: Fundamentals and Chemistry*, Academic Press, January 1, 1981, p.
[106] M. Pauly, P. Albersheim, A. Darvill and W.S. York, *The Plant Journal*, 20, (1999) 629.
[107] N.C. Carpita and D.M. Gibeaut, *The Plant Journal*, 3, (1993) 1.
[108] A. Grimm, E. Kruger and W. Burchard, *Carbohydrate Polymers*, 27, (1995) 205.
[109] T.S. Kahlon and C.L. Woodruff, *Cereal Chemistry*, 80, (2003) 260.
[110] J.W. Anderson and N.J. Gustafson, *The American Journal of Clinical Nutrition*, 48, (1988) 749.
[111] M.S. Izydorczyk, L.J. Macri and A.W. MacGregor, *Carbohydrate Polymers*, 35, (1997) 249.
[112] C. Altaner, A.I. Hapca, J.P. Knox and M.C. Jarvis, *Holzforschung*, 61, (2007).
[113] M.Y. Pillow and R.F. Luxford, in, USDA, Washinton, D.C., 1937, p. 32.
[114] W. Boerjan, J. Ralph and M. Baucher, *Annu Rev Plant Biol*, 54, (2003) 519.
[115] J. Zakzeski, P.C.A. Bruijnincx, A.L. Jongerius and B.M. Weckhuysen, *Chemical Reviews*, 110, (2010) 3552.
[116] A.J. Ragauskas, G.T. Beckham, M.J. Biddy, R. Chandra, F. Chen, M.F. Davis, B.H. Davison, R.A. Dixon, P. Gilna, M. Keller, P. Langan, A.K. Naskar, J.N. Saddler, T.J. Tschaplinski, G.A. Tuskan and C.E. Wyman, *Science*, 344, (2014) 1246843.
[117] H. Lange, S. Decina and C. Crestini, *European Polymer Journal*, 49, (2013) 1151.
[118] M.P. Pandey and C.S. Kim, *Chemical Engineering & Technology*, 34, (2011) 29.
[119] S. Kang, X. Li, J. Fan and J. Chang, *Renewable and Sustainable Energy Reviews*, 27, (2013) 546.
[120] P. de Wild, R. Van der Laan, A. Kloekhorst and E. Heeres, *Environmental Progress & Sustainable Energy*, 28, (2009) 461.
[121] O.Y. Abdelaziz, D.P. Brink, J. Prothmann, K. Ravi, M. Sun, J. Garcia-Hidalgo, M. Sandahl, C.P. Hulteberg, C. Turner, G. Liden and M.F. Gorwa-Grauslund, *Biotechnol Adv*, 34, (2016) 1318.
[122] G.T. Beckham, C.W. Johnson, E.M. Karp, D. Salvachua and D.R. Vardon, *Curr Opin Biotechnol*, 42, (2016) 40.
[123] K. Davis, M. Rover, R. Brown, X. Bai, Z. Wen and L. Jarboe, *Energies*, 9, (2016) 808.
[124] M.V. Galkin and J.S. Samec, *ChemSusChem*, 9, (2016) 1544.
[125] R.E. Key and J.J. Bozell, *ACS Sustainable Chemistry & Engineering*, 4, (2016) 5123.
[126] S.-H. Li, S. Liu, J.C. Colmenares and Y.-J. Xu, *Green Chem.*, 18, (2016) 594.
[127] J.G. Linger, D.R. Vardon, M.T. Guarnieri, E.M. Karp, G.B. Hunsinger, M.A. Franden, C.W. Johnson, G. Chupka, T.J. Strathmann, P.T. Pienkos and G.T. Beckham, *Proc Natl Acad Sci U S A*, 111, (2014) 12013.
[128] R. Rinaldi, R. Jastrzebski, M.T. Clough, J. Ralph, M. Kennema, P.C. Bruijnincx and B.M. Weckhuysen, *Angew Chem Int Ed Engl*, 55, (2016) 8164.
[129] P.J. de Wild, W.J.J. Huijgen and H.J. Heeres, *Journal of Analytical and Applied Pyrolysis*, 93, (2012) 95.
[130] D. Lee, V.N. Owens, A. Boe and P. Jeranyama, in, Sun Grant Initiative SDSU, Brookings, 2007, p. 17.
[131] D. Fengel and G. Wegener, *Wood : chemistry, ultrastructure, reactions*, De Gruyter, Berlin, Germany, 2011, p.
[132] M. Lahtinen, Reactivity and Reactions of Lignin Model Compounds with Laccasses, Dissertation University of Helsinki, Department of Chemistry, 2013, 100.
[133] B. Nanayakkara, M. Manley-Harris, I.D. Suckling and L.A. Donaldson, *Holzforschung*, 63, (2009).
[134] R. Smit, R.M. Ede and I.D. Suckling, *Quantification of condensed and uncondensed structures in Lignin*, at: Proceedings of the 53rd Appita Annual Conference, 773-780,
[135] I.D. Suckling, M.F. Pasco, B.R. Hortling and J. Sundquist, *Holzforschung*, 48, (1994) 501.
[136] J.C. Cushman, *Plant Physiology*, 127, (2001) 1439.

[137] J.A. Bassham, A.A. Benson and M. Calvin, *Journal of Biological Chemistry*, 185, (1950) 781.
[138] F.G. Pearce, *Biochem J*, 399, (2006) 525.
[139] K. Herrmann and L. Weaver, *Annual Review of Plant Physiology and Molecular Biology*, 50, (1999) 473.
[140] D.M. Guo, J.H. Ran and X.Q. Wang, *J Mol Evol*, 71, (2010) 202.
[141] E.L. Camm and G.H.N. Towers, *Phytochemistry*, 12, (1972) 961.
[142] J.R.M. Potts, R. Weklych and E.E. Conn, *The Journal of Biological Chemistry*, 249, (1974) 5019.
[143] R. Zhong, H. Morrison III, D.S. Himmelsbach, F.L. Poole II and Z.-H. Ye, *Plant Physiology*, 124, (2000) 563.
[144] R. Zhong, H. Morrison III, J. Negrel and Z.-H. Ye, *The Plant Cell*, 10, (1998) 2033.
[145] K. Meyer, J.C. Cusumano, C. Sommerville and C.C.S. Chappel, *PNAS - Biochemistry*, 93, (1996) 6869.
[146] G.G. Gross and M.H. Zenk, *European Journal of Biochemistry*, 42, (1974) 453.
[147] T. Kawasaki, H. Koita, T. Nakatsubo, K. Hasegawa, K. Wakabayashi, H. Takahashi, K. Umemura, T. Umezawa and K. Shimamoto, *Proc Natl Acad Sci U S A*, 103, (2006) 230.
[148] M.S. Yanez, B. Matsuhiro, C. Nunez, S. Pan, C.A. Hubbell, P. Sannigrahi and A.J. Ragauskas, *Polymer Degradation and Stability*, 110, (2014) 184.
[149] F. Asgari and D.S. Argyropoulos, *Candaian Journal of Chemistry*, 76, (1998) 1606.
[150] A. Guerra, I. Filpponen, A.L. Lucia and D.S. Argyropoulos, *Journal of Agricultural and Food Chemistry*, 54, (2006) 9696−9705.
[151] A.U. Buranov and G. Mazza, *Industrial Crops and Products*, 28, (2008) 237.
[152] D.Y. Min, H. Jameel, H.M. Chang, L. Lucia, Z.G. Wang and Y.C. Jin, *RSC Advances*, 4, (2014) 10845.
[153] M.Y. Balakshin, E.A. Capanema and H.-m. Chang, *Holzforschung*, 61, (2007) 1.
[154] F. Monlau, A. Barakat, E. Trably, C. Dumas, J.-P. Steyer and H. Carrère, *Critical Reviews in Environmental Science and Technology*, 43, (2013) 260.
[155] M. Balakshin, E. Capanema, H. Gracz, H.M. Chang and H. Jameel, *Planta*, 233, (2011) 1097.
[156] D. Ibarra, M.I. Chavez, J. Rencoret, J.C. Del Rio, A. Gutierrez, J. Romero, S. Camarero, M.J. Martinez, J. Jimenez-Barbero and A.T. Martinez, *Journal of Agricultural and Food Chemistry*, 55, (2007) 3477.
[157] J. Ralph, T. Akiyama, H. Kim, F. Lu, P.F. Schatz, J.M. Marita, S.A. Ralph, M.S. Reddy, F. Chen and R.A. Dixon, *J Biol Chem*, 281, (2006) 8843.
[158] L. Zhang and G. Gellerstedt, *Magn Reson Chem*, 45, (2007) 37.
[159] H.m. Chang, E.B. Cowling and W. Brown, *Holzforschung*, 29, (1975) 153.
[160] B.H. Davidson, J. Parks, M.F. Davis and B.S. Donohoe, in C.E. Wyman (Ed.), *Aqueous Pretreatment of Plant Biomass for Biological and Chemical Conversion to Fuels and Chemicals*, John Wiley & Sons, 1st Edition edn., 2013, Chapter Chapter 3, p. 23.
[161] J.H. Langenheim, *American Scientist*, 78, (1990) 16.
[162] Z. Chen, T.E. Kolb and K.M. Clancy, *Journal of Chemical Ecology*, 28, (2002) 897.
[163] W.L. Chameides, R.W. Lindsay, J. Richardson and C.S. Kiang, *Science*, 241, (1988) 1473.
[164] M. Kates, *Techniques of Lipidology: Isolation, Analysis, and Identification of Lipids*, Newport Somerville, 2010, p.
[165] S.F. O'Keefe, in C.C. Akoh and D.B. Min (Eds.), *Food Lipids: Chemistry, Nutrition, and Biotechnology*, CRC Press Taylor & Francis, Boca Raton, London, NY, 3rd Ed. edn., 2008, Chapter Chapter 1, p. 3.
[166] C. Burnett and M. Fiume, in, Washinton D.C., 2011.
[167] D.J. Murphy, *Progress in Lipid Research*, 33, (1994) 71.
[168] T. Akihisa, W.C.M.C. Kokke, Tamura and Toshitake, in *Physiology and Biochemistry of Sterols*, AOCS Publishing 1992, Tokyo, Japan, 1992, Chapter Chapter 7., p. 172.

[169] V. Piironen, D.G. Linday, T.A. Miettinen, J. Toivo and A.-M. Lampi, *Journal of the Science of Food and Agriculture*, 80, (2000) 939.
[170] R. Talati, D.M. Sobieraj, S.S. Makanji, O.J. Phung and C.I. Coleman, *J Am Diet Assoc*, 110, (2010) 719.
[171] P. Dutta and L.-Å. Appelqvist, *Grasas y Aceites*, 47, (1996) 841.
[172] S.D. Clouse, *Arabidopsis Book*, 9, (2011) e0151.
[173] Z.A. Wojciechowski, in *Physiology and Biochemistry of Sterols*, American Oil Chemists Society, Champaign, IL, U.S., 1991, Chapter Chapter 14.
[174] T. Verleyen, M. Forcades, R. Verhe, K. Dewettinick, A. Huyghebaert and W. De Greyt, *The Journal of the American Oil Chemists' Society*, 79, (2002) 117.
[175] G. Liu, M.M. Wright, Q. Zhao, R.C. Brown, K. Wang and Y. Xue, *Energy Conversion and Management*, 112, (2016) 220.
[176] H.F. Brinson and L.C. Brinson, *Polymer Engineering Science and Viscoelasticity - An Introduction*, Springer, New York, Heidelberg, Dordrecht, London, 2015, p. 482.
[177] A.V. Bridgwater, D. Meier and D. Radlein, *Organic Geochemistry*, 30, (1999) 1479.
[178] F. Abnisa and W.M.A. Wan Daud, *Energy Conversion and Management*, 87, (2014) 71.
[179] A.V. Bridgewater, *Biomass and Bioenergy*, 38, (2012) 68.
[180] D.A. Bulushev and J.R.H. Ross, *Catalysis Today*, 171, (2011) 1.
[181] C. Liu, H. Wang, A.M. Karim, J. Sun and Y. Wang, *Chem Soc Rev*, 43, (2014) 7594.
[182] D. Neves, H. Thunman, A. Matos, L. Tarelho and A. Gómez-Barea, *Progress in Energy and Combustion Science*, 37, (2011) 611.
[183] J.E. White, W.J. Catallo and B.L. Legendre, *Journal of Analytical and Applied Pyrolysis*, 91, (2011) 1.
[184] J.M.J. Antal, W.S.L. Mok, G. Varhegyi and T. Szekely, *Energy and Fuels*, 4, (1990) 221.
[185] C.A. Koufopanos and N. Papayannakos, *The Canadian Journal of Chemical Engineering*, 69, (1991) 907.
[186] C. Şerbănescu, *Chemical Papers*, 68, (2014).
[187] A.K. Galwey, *Thermochimica Acta*, 413, (2004) 139.
[188] J. Lédé, *Journal of Analytical and Applied Pyrolysis*, 94, (2012) 17.
[189] M. Garcia-Perez, A. Chaala and C. Roy, *Fuel* 81, (2002) 893.
[190] X. Bai, P. Johnston and R.C. Brown, *Journal of Analytical and Applied Pyrolysis*, 99, (2013) 130.
[191] P.M. Molton and T.F. Demmitt, in, Pacific Northwest Laboratories, 1977.
[192] Y.-C. Lin, J. Cho, G.A. Thompsett, P.R. Westmoreland and G.W. HJuber, *Journal of Physical Chemistry*, 113, (2009) 20097.
[193] V. Agarwal, P.J. Dauenhauer, G.W. Huber and S.M. Auerbach, *J Am Chem Soc*, 134, (2012) 14958.
[194] R. Vinu and L.J. Broadbelt, *Energy & Environmental Science*, 5, (2012) 9808.
[195] H.B. Mayes and L.J. Broadbelt, *J Phys Chem A*, 116, (2012) 7098.
[196] R.K. Agrawal, *The Canadian Journal of Chemical Engineering*, 66, (1988) 413.
[197] J. Zhang, M.W. Nolte and B.H. Shanks, *ACS Sustainable Chemistry & Engineering*, 2, (2014) 2820.
[198] H.B. Mayes, M.W. Nolte, G.T. Beckham, B.H. Shanks and L.J. Broadbelt, *ACS Sustainable Chemistry & Engineering*, 2, (2014) 1461.
[199] J.L. Komen, W. Bothell, A.S. Weerawarna and R.A. Jewell, in E.P. Office (Ed.), U.S., 2002, p. 17.
[200] L. Schoenfeldt and B. Nielsen, in USPTO (Ed.), U.S., 2003, p. 8.
[201] H. Yang and T.G.M. van de Ven, *Cellulose*, 23, (2016) 1791.
[202] S.A. Yuldoshov, A.A. Atakhanov, A.A. Sarymsakov and S.H. Rashidova, *Nano Science & Nano Technology: An Indian Journal*, 10, (2016) 106.
[203] P. Stenstad, M. Andresen, B.S. Tanem and P. Stenius, *Cellulose*, 15, (2007) 35.
[204] F. Shafizadeh and Y.L. Fu, *Carbohydrate Research*, 29, (1973) 113.

[205] R. Bura and R. Gustafson, in, College of Forest Resources, Seattle, Washington, U.S., 2010.
[206] H. Yang, R. Yan, H. Chen, D.H. Lee and C. Zheng, *Fuel*, 86, (2007) 1781.
[207] H. Chen, in *Biotechnology of Lignocellulose: Theory and Practice*, Chemical Industry Press, Springer Science & Business Media Dordrecht 2014, Beijing, XVIII edn., 2014, Chapter Chapter 2, p. 25.
[208] P.R. Patwardhan, R.C. Brown and B.H. Shanks, *ChemSusChem*, 4, (2011) 636.
[209] G.R. Ponder, J.N. Richards and T.T. Stevenson, *Journal of Analytical and Applied Pyrolysis*, 22, (1992) 217.
[210] D. Shen, L. Zhang, J. Xue, S. Guan, Q. Liu and R. Xiao, *Carbohydr Polym*, 127, (2015) 363.
[211] H.C. Yoon, P. Pozivil and A. Steinfeld, *Energy & Fuels*, 26, (2012) 357.
[212] J. Wetterling, Modelling of Hemicellulose Degradation during Softwood Kraft Pulping, Thesis Chalmers University of Technology, Division of Forest Products and Chemical Engineering, Department of Chemical and Biological Engineering, 2012,
[213] R.A. Young, K.V. Sarkanen, P.G. Johnson and G. Allan, *Carbohydrate Research*, 21, (1971) 111.
[214] S. Danielsson, Xylan Reactions in Kraft Cooking - Process and Product Considerations, Dissertation School of Chemical Sciences and Engineering, Royal Institute of Technology, Division of Wood Chemistry and Pulp Technology, Department of Fibre and Polymer Technology, 2007, 73.
[215] D. Watkins, M. Nuruddin, M. Hosur, A. Tcherbi-Narteh and S. Jeelani, *Journal of Materials Research and Technology*, 4, (2015) 26.
[216] J.A. Caballero, R. Font, A. Marcilla and J.A. Conesa, *Industrial & Engineering Chemistry Research*, 34, (1995) 806.
[217] R.W. Detroy, in I.S. Goldstein (Ed.), *Organic Chemicals from Biomass*, CRC Press, Rahleigh, 1981, Chapter Chapter 3, p. 19.
[218] N. Berkowitz, *Fuel*, 36, (1957) 355.
[219] J.J.M. Orfão, F.J.A. Antunes and J.L. Figueiredo, *Fuel*, 78, (1999) 349.
[220] W. Fiddler, W.E. Parker, A.E. Wasserman and R.C. Doerr, *Journal of Agricultural and Food Chemistry*, 15, (1967) 757.
[221] J.B. McDermott and M.T. Klein, *I&EC Process Design & Development*, 25, (1986) 885.
[222] R. Brezny, I. Surina and M. Kosik, *Holzforschung*, 34, (1984) 199.
[223] C. Branca and C. Di Blasi, *Industrial & Engineering Chemistry Research*, 45, (2006) 5891.
[224] M.R. Rover, P.A. Johnston, L.E. Whitmer, R.G. Smith and R.C. Brown, *Journal of Analytical and Applied Pyrolysis*, 105, (2014) 262.
[225] P.R. Patwardhan, R.C. Brown and B.H. Shanks, *ChemSusChem*, 4, (2011) 1629.
[226] Y.S. Choi, R. Singh, J. Zhang, G. Balasubramanian, M.R. Sturgeon, R. Katahira, G. Chupka, G.T. Beckham and B.H. Shanks, *Green Chem.*, 18, (2016) 1762.
[227] T. Nakamura, H. Kawamoto and S. Saka, *Journal of Analytical and Applied Pyrolysis*, 81, (2008) 173.
[228] A.M. Scheer, C. Mukarakate, D.J. Robichaud, M.R. Nimlos and G.B. Ellison, *J Phys Chem A*, 115, (2011) 13381.
[229] D.J. Robichaud, M.R. Nimlos and G.B. Ellison, in M. Schlaf and Z.C. Zhang (Eds.), *Reaction Pathways and Mechanisms in Thermocatalytic Biomass Conversion II - Homogeneously Catalyzed Transformations, Acrylics from Biomass, Theoretical Aspects, Lignin Valorization and Pyrolysis Pathways*, Springer, 2016, Chapter Ch. 8.
[230] E. van der Heidi, J. Schenk and A.W. Gerritsen, *Recueil des Travaux Chimiques des Pays-Bas*, 109, (1990) 93.
[231] S. Ozawa, K. Sasaki and Y. Ogino, *Fuel*, 65, (1986) 707.

[232] R.G.W. Norrish and G.W. Taylor, *Proceedings of the Royal Society of London. Series A, Mathematical and Physical Sciences*, 238, (1956) 143.
[233] R.G.W. Norrish and G.W. Taylor, *Proceedings of the Royal Society of London. Series A, Mathematical and Physical Sciences*, 234, (1956) 161.
[234] D.M. Newitt and J.H. Burgoyne, *Proceedings of the Royal Society of London. Series A, Mathematical and Physical Sciences*, 153, (1936) 448.
[235] J.A. Barnard and V.J. Ibberson, *Combustion and Flame*, 9, (1964) 149.
[236] D.S. Argyropoulos, *Oxidative Delignification Chemistry*, American Chemical Society, 2001, p.
[237] R.A. Northey, 785, (2001) 44.
[238] H.M. Chang and G. Allan, in K.V. Sarkanen and C.H. Ludwig (Eds.), *Lignins - Occurence, Formation, Structure and Reactions*, Wiley Interscience, Heidelberg, Germany, 1971, Chapter Chapter 11.
[239] H.D. Burgess, in *The Book and Paper Group Annual*, The American Institute for Conservation, 1982.
[240] H.-R. Bjorsvik and F. Minisci, *Organic Process Research & Development*, 3, (1999) 330.
[241] G.A. Smook, *Handbook for Pulp and Paper Technologists*, Angus Wilde Publications Inc., Bellingham, Washington, U.S., 2002, p.
[242] T.J. Blain, in, TAPPI Pulping Conference, 1998.
[243] T. Reitberger, J. Gierer, E. Yang and B.-H. Yoon, 785, (2001) 255.
[244] J. Ponomarenko, T. Dizhbite, M. Lauberts, A. Volperts, G. Dobele and G. Telysheva, *Journal of Analytical and Applied Pyrolysis*, 113, (2015) 360.
[245] C. Venkat, K. Brezinski and I. Glassman, *High Temperature Oxidation of Aromatic Hydrocarbons I - Reaction Mechanisms and Modeling*, at: Nineteenth Symposium (International) on Combustion, 143.
[246] R. Perazzini, R. Saladino, M. Guazzaroni and C. Crestini, *Bioorg Med Chem*, 19, (2011) 440.
[247] F.S. Chakar and A.J. Ragauskas, 785, (2001) 444.
[248] F. Guillén, C. Muñoz, V. Gómez-Toribio and A.T. Martínez, *Applied and Environmental Microbiology*, 66, (2000) 170.
[249] C. Crestini and D.S. Argyropoulos, in *Oxidative Delignification Chemistry*, American Chemical Society, Washington, D.C., 2001, Chapter 23, p. 373.
[250] K.G. Welinder, *Current Opinion in Structural Biology*, 2, (1992) 388.
[251] K.V. Fagerstedt, E.M. Kukkola, V.V. Koistinen, J. Takahashi and K. Marjamaa, *J Integr Plant Biol*, 52, (2010) 186.
[252] J.-C. Sigoillot, J.-G. Berrin, M. Bey, L. Lesage-Meessen, A. Levasseur, A. Lomascolo, E. Record and E. Uzan-Boukhris, 61, (2012) 263.
[253] J. Linden and L.-O. Öhman, *Journal of Pulp and Paper Science*, 24, (1998) 269.
[254] D.W. Wong, *Appl Biochem Biotechnol*, 157, (2009) 174.
[255] G.V.B. Reddy, M. Sridhar and M.H. Gold, *European Journal of Biochemistry*, 270, (2003) 284.
[256] G. Henriksson, G. Johansson and G. Pettersson, *Journal of Biotechnology*, 78, (2000) 93.
[257] G. Henriksson, L. Hildén, P. Ljungquist, P. Ander and B. Pettersson, 785, (2001) 456.
[258] O. Zaushitsyna, D. Berillo, H. Kirsebom and B. Mattiasson, *Topics in Catalysis*, 57, (2013) 339.
[259] C. Crestini, R. Perazzini and R. Saladino, *Applied Catalysis A: General*, 372, (2010) 115.
[260] S. Rodríguez Couto, J.F. Osma, V. Saravia, G.M. Gübitz and J.L. Toca Herrera, *Applied Catalysis A: General*, 329, (2007) 156.
[261] W. Herrmann, R.M. Kratzer and R.W. Fischer, *Angewandte Chemie International Edition*, 36, (1997) 2652.
[262] C. Crestini, P. Pro, V. Neri and R. Saladino, *Bioorg Med Chem*, 13, (2005) 2569.
[263] M. Crucianelli, R. Saladino and F. De Angelis, *ChemSusChem*, 3, (2010) 524.

[264] P.G. Cozzi, *Chem Soc Rev*, 33, (2004) 410.
[265] J. Odermatt, O. Kordsachia, R. Patt, L. Kühne, C.L. Chen and J.S. Gratzl, 785, (2001) 235.
[266] C. Canevali, F. Morazzoni, M. Orlandi, B. Rindone, R. Scotti, J. Sipila and G. Brunow, 785, (2001) 197.
[267] C. Díaz-Urrutia, B. Sedai, K.C. Leckett, R.T. Baker and S.K. Hanson, *ACS Sustainable Chemistry & Engineering*, 4, (2016) 6244.
[268] O. Delgado, A. Dress, A. Muller and M.T. Pope, in M.T. Pope and A. Muller (Eds.), *Polyoxometalates: From Platonic Solids to Anti-retroviral Activity*, 1994 Kluwer Academic Publishers, Springer Science + Business Media B. V. , 1994, Chapter 1, p. 7.
[269] A.R. Gaspar, J.A.F. Gamelas, D.V. Evtuguinb and C.P. Netob, *Green Chemistry*, 9, (2007) 717.
[270] V.A. Grigoriev, C.L. Hill and I.A. Weinstock, 785, (2001) 297.
[271] C.S. Thom, C.F. Dickson, D.A. Gell and M.J. Weiss, *Cold Spring Harb Perspect Med*, 3, (2013) a011858.
[272] C. Crestini and P. Tagliatesta, in *The Porphyrin Handbook*, Academic Press, Elsevier Science, Rome, Rome, Italy, 2003, Chapter 66, p. 161.
[273] P. Kumar, D.M. Barrett, M.J. Delwiche and P. Stroeve, *Industrial & Engineering Chemistry Research*, 48, (2009) 3713.
[274] M. Ghiaci, F. Molaie, M.E. Sedaghat and N. Dorostkar, *Catalysis Communications*, 11, (2010) 694.
[275] C. Crestini, A. Pastorini and P. Tagliatesta, *European Journal of Inorganic Chemistry*, 2004, (2004) 4477.
[276] D. Pattou, G. Labat, S. Defrance, J.-L. Seris and B. Meunier, *Bulletin de la Société chimique de France*, 131, (1994) 78.
[277] Q.-X. Wan and Y. Liu, *Catalysis Letters*, 128, (2008) 487.
[278] P.A. Watson, L.J. Wright and T.J. Fullerton, *Journal of Wood Chemistry and Technology*, 13, (2006) 411.
[279] Y. Liu, H.-J. Zhang, Y. Lu, Y.-Q. Cai and X.-L. Liu, *Green Chemistry*, 9, (2007) 1114.
[280] H. Wariishi, S.-i. Tsutsumi, T. Yamanaka, K. Uezu, M. Goto, S. Furusaki and H. Tanaka, 785, (2001) 226.
[281] J.F. Kadla and H.m. Chang, 785, (2001) 108.
[282] J.F. Kadla, H.m. Chang and H. Jameel, *Holzforschung*, 51, (1997) 428.
[283] G. Gellerstedt and R. Agnemo, *Acta Chemica Scandinavica*, 34B, (1980) 275.
[284] L. Jurasek, Y. Sun and D.S. Argyropoulos, 785, (2001) 130.
[285] A. Rahimi, A. Ulbrich, J.J. Coon and S.S. Stahl, *Nature*, 515, (2014) 249.
[286] N.D. Patil and N. Yan, *Tetrahedron Letters*, 57, (2016) 3024.
[287] B. Kurek, B.R. Hames, C. Lequart, K. Ruel, B. Pollet, C. Lapierre, F. Gaudard and B. Monties, 785, (2001) 272.
[288] K.V. Sarkanen, *IUPAC Pure and Applied Chemistry*, (1962) 219.
[289] J.-i. Azuma, T. Nomura and T. Koshijima, *Agricultural and Biological Chemistry*, 49, (1985) 2661.
[290] T. Watanabe, in *Wood research : bulletin of the Wood Research Institute Kyoto University*, Kyoto University, Kyoto, 1989, p. 59.
[291] N. Takahashi and T. Koshijima, *Wood Science and Technology*, 22, (1988) 231.
[292] T.W. Jeffries, *Biodegradation*, 1, (1990) 163.
[293] X.-F. Zhou, *Hemijska industrija*, 68, (2014) 541.
[294] M.T.T. Nguyen, Synthesis and Oxidation of Lignin-Carbohydrate Model Compounds, Dissertation University of Maine, Department of Chemistry, 2008, 105.
[295] T.-T. You, L.-M. Zhang, S.-K. Zhou and F. Xu, *Industrial Crops and Products*, 71, (2015) 65.
[296] A. Stolle, B. Ondruschka and H. Hopf, *Helvetica Chimica Acta*, 92, (2009) 1673.

[297] P.F. Britt, A.C. Buchanan and C.V. Owens, *Preprints of Papers- American Chemical Society, Division of Fuel Chemistry*, 49, (2004) 868.
[298] J.S. Tumuluru, S. Sokhansanj, J.R. Hess, C.T. Wright and R.D. Boardman, *Industrial Biotechnology*, 7, (2011) 384.
[299] S.C. Moldoveanu, *Pyrolysis of organic molecules with applications to health and environmental issues*, Elsevier, Great Britain, 2010, p. 744.
[300] P.F. Britt, A.C. Buchanan, M.M. Kidder, C.V. Owens, J.R. Ammann, J.T. Skeen and L. Luo, *Fuel*, 80, (2001) 1727.
[301] N.A. Porter, S.E. Caldwell and K.A. Mills, *Lipids*, 30, (1995) 277.
[302] E. Hovenkamp, I. Demonty, J. Plat, D. Lutjohann, R.P. Mensink and E.A. Trautwein, *Prog Lipid Res*, 47, (2008) 37.
[303] Y. Lin, D. Knol, I. Valk, V. van Andel, S. Friedrichs, D. Lutjohann, K. Hrncirik and E.A. Trautwein, *Chem Phys Lipids*, (2017).
[304] Y. Lin, D. Knol and E.A. Trautwein, *Eur J Lipid Sci Technol*, 118, (2016) 1423.
[305] T. Hosoya, H. Kawamoto and S. Saka, *Journal of Analytical and Applied Pyrolysis*, 84, (2009) 79.
[306] S. Wu, D. Shen, J. Hu, H. Zhang and R. Xiao, *BioResources*, 9, (2014) 2259.
[307] S. Wang, X. Guo, K. Wang and Z. Luo, *Journal of Analytical and Applied Pyrolysis*, 91, (2011) 183.
[308] S. Wang, H. Lin, Y. Zhao, J. Chen and J. Zhou, *Journal of Analytical and Applied Pyrolysis*, 118, (2016) 259.
[309] R.C. Brown (Ed.), Thermochemical processing of biomass: conversion into fuels, chemicals and power, Wiley, West Sussex, UK, 2011.
[310] Y.C. Lien and W.W. Nawar, *Journal of Food Science*, 39, (1974) 914.
[311] M.A. Ratcliff, E.E. Medley and P.G. Simmonds, *Journal of Organic Chemistry*, 39, (1973) 1481.
[312] K.D. Maher and D.C. Bressler, *Bioresource Technology*, 98, (2007) 2351.
[313] K. Wang and R.C. Brown, *Green Chemistry*, 15, (2013) 675.
[314] A. Quek and R. Balasubramanian, *Journal of Analytical and Applied Pyrolysis*, 101, (2013) 1.
[315] P.E. Savage, *Journal of Analytical and Applied Pyrolysis*, 54, (2000) 109.
[316] J.F. Mastral, C. Berrueco and J. Ceamanos, *Journal of Analytical and Applied Pyrolysis*, 80, (2007) 427.
[317] E. Butler, G. Devlin and K. McDonnell, *Waste and Biomass Valorization*, 2, (2011) 227.
[318] Y.C. Rotliwala and P.A. Parikh, *Waste Management Resources*, 29, (2011) 1251.
[319] Y. Xue, S. Zhou, R.C. Brown, A. Kelkar and X. Bai, *Fuel*, 156, (2015) 40.
[320] K.R. Millington, H. Ishii and G. Maurdev, *Amino Acids*, 38, (2010) 1395.
[321] J.R. Requena, C.C. Chao, R.L. Levine and E.R. Stadtman, *Proc Natl Acad Sci U S A*, 98, (2001) 69.
[322] D. Boguszewska-Mankowska, M. Nykiel and B. Zagdanska, (2015).
[323] A.J.S. Angelo, *Critical Reviews in Food Science and Nutrition*, 36, (1996) 175.
[324] F. Shahidi and Y. Zhong, (2005).
[325] K. Robards, A.F. Kerr and E. Patsalides, *Analyst*, 113, (1988) 213.
[326] J.M. Lee, J.S. Lee, J.R. Kim and S.D. Kim, *Energy*, 20, (1995) 969.
[327] J.-i. Hayashi, T. Nakahara, K. Kusakabe and S. Morooka, *Fuel Processing Technology*, 55, (1998) 265.
[328] X. Zhu, M. Elomaa, F. Sundholm and C.H. LochmuÈller, *Polymer Degradation and Stability*, 62, (1998) 487.
[329] D.S. Achilias, in D. Achilias (Ed.), *Material Recycling - Trends and Perspectives*, InTech Thessaloniki, 2012, Chapter Ch. 1, p. 3.
[330] K. Wang, J. Zhang, B.H. Shanks and R.C. Brown, *Applied Energy*, 148, (2015) 115.
[331] D. Dalluge, T. Daugaard, P.A. Johnston, N. Kuzhiyil, M.M. Wright and R.C. Brown, *Green Chemistry*, 16, (2014) 4144.

[332] N. Kuzhiyil, D. Dalluge, X. Bai, K.H. Kim and R.C. Brown, *ChemSusChem*, 5, (2012) 2228.
[333] H.F. Calcote, B. Olson and D.G. Keil, *ACS Division of Fuel Chemistry, Preprints.*, 32, (1987) 524.
[334] M. Dente, G. Bozzano, T. Faravelli, A. Marongiu, S. Pierucci and E. Ranzi, 32, (2007) 51.
[335] J. Li, M.C. Paul, P.L. Younger, I. Watson, M. Hossain and S. Welch, *Applied Energy*, 156, (2015) 749.
[336] A.G. Vlasenko, Ingrid J. and J.P.D. Abbatt, *Journal of Physical Chemistry A*, 112, (2008) 1552.
[337] L.H. Renbaum and G.D. Smith, *Phys Chem Chem Phys*, 11, (2009) 2441.
[338] J.H. Kroll, C.Y. Lim, S.H. Kessler and K.R. Wilson, *J Phys Chem A*, 119, (2015) 10767.
[339] M. Amutio, G. Lopez, R. Aguado, M. Artetxe, J. Bilbao and M. Olazar, *Energy and Fuels*, 26, (2012) 1353.
[340] A.S. Pollard, M.R. Rover and R.C. Brown, *Journal of Analytical and Applied Pyrolysis*, 93, (2012) 129.
[341] J. Proano-Aviles, J.K. Lindstrom, P. Johnston and R.C. Brown, in R.C. Brown (Ed.), *Thermal and Catalytic Sciences 2016*, TCS 2016, Chapel Hill, NC, 2016.
[342] J.K. Lindstrom, P. Gable and R.C. Brown, in R.C. Brown (Ed.), *Thermal and Catalytic Sciences 2016*, TCS 2016, Chapel Hill, NC, 2016.
[343] Frontier-Laboratories, in, 2016.
[344] J. Proano-Aviles, J.K. Lindstrom, P.A. Johnston and R.C. Brown, *Energy Technology*, 5, (2017) 189.
[345] A. Hosaka, C. Watanabe and S. Tsuge, *Journal of Analytical and Applied Pyrolysis*, 78, (2007) 452.
[346] M.S. Mettler, S.H. Mushrif, A.D. Paulsen, A.D. Javadekar, D.G. Vlachos and P.J. Dauenhauer, *Energy Environ. Sci.*, 5, (2012) 5414.
[347] C. Di blasi, *Progress in Energy and Combustion Science*, 34, (2008) 47.
[348] L. Yu and Z. Cheng, in *Wheat Antioxidants*, Wiley-Interscience, Hoboken, NJ, US, 2007, Chapter Chapter 5, p. 54.
[349] Z. Cheng, H. Zhou, J. Yin and L. Yu, *J Agric Food Chem*, 55, (2007) 3325.
[350] A. Urbaniak, M. Molski and M. Szeląg, *Computational Methods in Science and Technology*, 18, (2012) 117.
[351] Y. Chen, H. Xiao, J. Zheng and G. Liang, *PLoS One*, 10, (2015) e0121276.
[352] V.D. Kancheva, L. Saso, P.V. Boranova, A. Khan, M.K. Saroj, M.K. Pandey, S. Malhotra, J.Z. Nechev, S.K. Sharma, A.K. Prasad, M.B. Georgieva, C. Joseph, A.L. DePass, R.C. Rastogi and V.S. Parmar, *Biochimie*, 92, (2010) 1089.
[353] E. Dorrestijn, M. Kranenburg, M.V. Ciriano and P. Mulder, *Journal of Organic Chemistry*, 64, (1999) 3012.
[354] G. Cirillo, O.I. Parisi, D. Restuccia, F. Puoci and N. Picci, in *Phenolic Acids: Composition, Applications and Health Benefits*, Nova Science Publishers, Rende, Italy, 2012, Chapter Chapter 5, p. 73.
[355] P.F. Britt, A.C. Buchanan, K.B. Thomas and S.-K. Lee, *Journal of Analytical and Applied Pyrolysis*, 33, (1995) 1.
[356] L. Chen, X. Ye, F. Luo, J. Shao, Q. Lu, Y. Fang, X. Wang and H. Chen, *Journal of Analytical and Applied Pyrolysis*, 115, (2015) 103.
[357] S. Chu, A.V. Subrahmanyam and G.W. Huber, *Green Chem.*, 15, (2013) 125.
[358] M.J. Cooney, P.F. Britt and A.C. Buchanan, in, Oak Ridge National Lab, Oak Ridge, TN, June 1, 1997, p. 89.
[359] T. He, Y. Zhang, Y. Zhu, W. Wen, Y. Pan, J. Wu and J. Wu, *Energy & Fuels*, 30, (2016) 2204.
[360] M.T. Klein and P.S. Virk, *Industrial & Engineering Chemisty Fundamentals*, 22, (1983) 35.
[361] R. Parthasarathi, R.A. Romero, A. Redondo and S. Gnanakaran, *The Journal of Physical Chemistry Letters*, 2, (2011) 2660.
[362] K.H. Kim, X. Bai and R.C. Brown, *Journal of Analytical and Applied Pyrolysis*, 110, (2014) 254.

[363] V.B. Custodis, P. Hemberger, Z. Ma and J.A. van Bokhoven, *J Phys Chem B*, 118, (2014) 8524.
[364] K.-i. Kuroda, A. Nakagawa-izumi and D.R. Dimmel, *Journal of Agricultural and Food Chemistry*, 50, (2002) 3396.
[365] I. Miranda, J. Gominho, I. Mirra and H. Pereria, *Industrial Crops and Products*, 41, (2013) 299.
[366] W. Jin, K. Singh and J. Zondlo, *Agriculture*, 3, (2012) 12.
[367] R. Grana, A. Frassoldati, T. Faravelli, U. Niemann, E. Ranzi, R. Seiser, R. Cattolica and K. Seshadri, *Combustion and Flame*, 157, (2010) 2137.
[368] H.-H. Carstensen and A.M. Dean, in *Computational Modeling in Lignocellulosic Biofuel Production*, 2010 American Chemical Society, Golden, Colorado, US, 2010, Chapter Chapter 10, p. 201.

APPENDIX A: ANNOTATED BIBLIOGRAPHY OF RELEVANT WORKS

TCC, Pyrolysis Fundamentals, Composition of Biorenewable Resources

An Experimental Study on the Competing Processes of Evaporation and Polymerization of Levoglucosan in Cellulose Pyrolysis, X. Bai, P. Johnston and R.C. Brown, *Journal of Analytical and Applied Pyrolysis*, 99, (2013) 130.

This micropyrolyzer study sought to determine the effects of reactor operation conditions on the yield of the desirable monosaccharide levoglucosan, from the perspective of its mass balance (production and consumption). By theory, crystalline cellulose should pyrolyze to produce 100% levoglucosan (the monomer resultant from glycosidic cleavage of the cellulose polymer), if there were no processes actively consuming it. Although further degradation to furans, pyrans and light oxygenates occurs to some extent in many reactors, this study focused on other paths inhibiting its formation. Specifically, initial cellulose depolymerization and the two potential subsequent routes; evaporating from the condensed phase *and* repolymerization in the condensed phase to molecules too large to boil. Vapors from the condensed phase are assumed to become entrained in the sweep gas, meaning they are successfully collected. Condensed-phase polymers subsequently dehydrate to cellulose char.

The study showed that increasing sample size (increasing mass transfer limitations) decreased yield. Decreased ventilation lead to increased char production (increasing likelihood of multiple interactions of products and associated secondary reactions). Helium allowed for greater levoglucosan yield than did nitrogen, likely due to helium's greater diffusivity. The most interesting finding in this study was one counter-intuitive to the general rationale for *fast* pyrolysis, being that higher heating rates allow for rapid depolymerization to compounds light enough to boil (rather than slow heating which might lead to repolymerization and condensed carbon bonds; generally carbonization to a thermally-stable state)… the finding was that higher heating rates favor polymer formation because; "levoglucosan does not have sufficient time to evaporate, which favors polymerization…This question is subject to further research". A last relevant finding was initial dissolution of the cellulose in water increased levoglucosan yields.

Techno-economic Analysis of Biomass Fast Pyrolysis to Transportation Fuels, M.M. Wright, J.A. Satrio and R.C. Brown, in, U.S. Department of Energy, Ames, 2010, p. 62.

This paper described results of an updated TEA biofuel production study. The conversion process was the motivation for much of the work done by Dr. Robert Brown at the Bioeconomy Institute; that is, the potential for economically-feasible fuels from hydrotreated fast-pyrolysis bio-oil. The study concluded that the original TEA work made a few assumptions which underestimated MFSP. The original study predicted a MFSP of $2.11/gallon and the updated TEA predicted a MFSP of $2.57/gallon. The conclusion was that even though the prediction increased, this pathway should be market-competitive if oil market prices slightly rise.

Continuous Production of Sugars from Pyrolysis of Acid-infused Lignocellulosic Biomass, D. Dalluge, T. Daugaard, P.A. Johnston, N. Kuzhiyil, M.M. Wright and R.C. Brown, *Green Chemistry*, 16, (2014) 4144.

A publication that offers a problem and a solution. Biomass commonly has ash content, of which is predominantly comprised of alkaline and alkaline earth metals (AAEM's). These metals catalyze decomposition reactions at elevated temperatures, to the detriment of monosaccharides. Specifically, they catalyze ring scission of these sugars to light oxygenates, diminishing the yield of

the desired sugars. This study presents results of infusing the biomass with dilute sulfuric acid, resulting in stabilization of the metals into thermally-stable salts, with no catalytic degradation activity. Specifically the paper showed results of improved sugar yields (from 7.8% to 15.9% for red oak, and 4.5% to 16.2% for switchgrass) at the continuous fluidized bed scale. The major drawback with full passivation of AAEM's was increased char yield (increasing by 65% and 30% for red oak and switchgrass respectively).

Lignins - Occurrence, Formation, Structure and Reactions, K. Freudenberg, *Lignins - Occurrence, Formation, Structure and Reactions*, Wiley-Interscience, Heidelberg, Germany, 1971, p.

A classic text in the world of lignin literature, has a great set of introductory chapters and chapter on microbial degradation (oxidative).

Pyrolytic Sugars from Cellulosic Biomass, N. Kuzhiyil, D. Dalluge, X. Bai, K.H. Kim and R.C. Brown, *ChemSusChem*, 5, (2012) 2228.

An experimental study on the suitability of different acids for AAEM passivation in cellulose pyrolysis. Four feedstocks (switchgrass, corn stover, red oak, and loblolly pine) as well as six acids (acetic, formic, nitric, hydrochloric, phosphoric, and sulfuric) were tested. Sulfuric was the most effective at increasing the anhydrosugar yield, followed closely by phosphoric, which was followed by hydrochloric acid. Effect of acid concentration was also studied; for which all of the acids maximized their benefit at around 0.2-0.3 mmol/gram-biomass.

The Structural Changes of Lignin and Lignin-Carbohydrate Complexes in Corn Stover Induced by Mild Sodium Hydroxide Treatment, D.Y. Min, H. Jameel, H.M. Chang, L. Lucia, Z.G. Wang and Y.C. Jin, *RCS Adv.*, 4, (2014) 10845.

A study on the effect of mild alkaline hydrolysis of corn stover milled wood lignin and cellulolytic enzyme lignin-structure. They used C-NMR and HxC-HSQC-NMR to quantify linkages and relative Syringyl- and p-hydroxy-units. Milled wood lignins were demonstrated to contain a notable carbohydrate content in the form of LCC's, specifically phenyl-glycosides and benzyl-ethers and gamma-esters were attributed to LCC units (and have a decent graphic depicting these). They quantified that prior to the hydrolysis, there were ~18 LCC-linkages per 100 C9 units in the cob and stem. Important to note, is that LCC-linkages significantly decreased with the hydrolysis step, whereas of all the lignin linkages (beta-O-4, beta-5, beta-beta, gamma-acyl), only the gamma-acyl was significantly reduced while the beta-5 linkage content nearly doubled. The relative quantities of linkages and LCC's were notable in contribution to the mechanistic model development.

Product Distribution from the Fast Pyrolysis of Hemicellulose, P.R. Patwardhan, R.C. Brown and B.H. Shanks, *ChemSusChem*, 4, (2011) 636.

A micropyrolyzer study investigating pyrolysis mechanisms of the hemicellulose proxy, xylan. The study framed the mechanism with respect to the well-developed (or long-time investigated and disputed) cellulose pyrolysis mechanism, [195]. Notable differences with between xylan and hemicellulose were the lack of an anhydride product from xylan pyrolysis resultant from xylan's lack of a "sixth carbon and substituted oxygen at the fourth position" (in the ring). Also notably, the selectivity towards specific furans and anhydroxylopyranose species (AXP, DAXP1, DAXP2) in xylan pyrolysis, result from dehydrations of xylose. Important summative statements were made; "Levoglucosan –a single dehydration product of glucose –was the predominant product of pure cellulose pyrolysis, whereas, in the case of hemicellulose pyrolysis, DAXP2 –a double

dehydration product of xylose –was found to be the major product.", "In the case of cellulose glycosidic bond cleavage, a glucosyl cation intermediate is formed, which is stabilized by the formation of a 1,6-anhydride (dimer), and is available for subsequent cleavage of the remaining glycosidic linkage to form levoglucosan. In the case of xylan glycosidic bond cleavage, a xylosyl cation intermediate is formed, unable to form a stable anhydride due to lack of substituted ring oxygen and the missing sixth carbon, thus directly cleaves again and is dehydrated to DAXP1 and DAXP2". Also notably, hemicellulose pyrolysis forms greater amounts of acids and light oxygenates "attributed to the branched, amorphous structure, and low degree of polymerization of hemicellulose".

Understanding the Fast Pyrolysis of Lignin, P.R. Patwardhan, R.C. Brown and B.H. Shanks, *ChemSusChem*, 4, (2011) 1629.

A study investigating the mechanisms of pyrolytic lignin oligomer and aerosol formation. Two main competing theories exist for the formation of pyrolytic lignin aerosols; one, that uneven heating and high shear stresses induced by initiating boiling of the lignin melt phase lead to thermal ejection of small droplets of lignin (forming condensable aerosols). The second theory is that lignin pyrolyzes to monomers and small oligomers capable of evaporating and becoming entrained. Following evaporation, the units (often radicals) recombine to form aerosols. The paper is in favor of the later, due to observed repolymerization on very short time scales.

Lignin Valorization: Improving Lignin Processing in the Biorefinery, A.J. Ragauskas, G.T. Beckham, M.J. Biddy, R. Chandra, F. Chen, M.F. Davis, B.H. Davison, R.A. Dixon, P. Gilna, M. Keller, P. Langan, A.K. Naskar, J.N. Saddler, T.J. Tschaplinski, G.A. Tuskan and C.E. Wyman, *Science*, 344, (2014) 1246843.

A Science Magazine review, brief overview, of lignin biosynthesis, recovery and valorization. A takeaway from the biosynthesis section was the genetic research being done resulting in lignin structural modifications, citing a group generating lignins with shorter side chains and another increasing ratio of ester linkages to condensed linkages, both improving ease of depolymerization. Some biorefinery applications discussed were; carbon fiber (to replace PAN-based fiber), engineering polymers, thermoset plastic elastomers, polymeric foams, membranes, fuels and chemicals (of which 1,4-butanediol and adipic acid were introduced). The carbon fiber process described involves extrusion of isolated (possibly solvated) lignin melt, followed by oxidation then carbonization (under pyrolytic conditions) of the fiber. Oxypropylation was suggested as a pathway suitable for conversion of lignin to polyurethane feedstock polyols. One of the genetic modification groups used lignin rich in hydroxycinnamaldehydes to generate a formaldehyde-free resin, whose strength was attributed to aldehyde crosslinking. Much of the discussion on fuels involved catalytic pathways to reduce inherent methoxy and hydroxyl reactivity. Of interest to this paper is discussion of catalytic oxidation of side chains to less reactive species and ring-opening reactions to "potentially valuable" organic acids.

The Effect of Pyrolysis Temperature on Recovery of Bio-oil as Distinctive Stage Fractions, M.R. Rover, P.A. Johnston, L.E. Whitmer, R.G. Smith and R.C. Brown, *Journal of Analytical and Applied Pyrolysis*, 105, (2014) 262.

A study making use of the fractionated bio-oil collection system on the PPDU at the Bioeconomy Institute. Specifically investigating the effect of pyrolysis temperature (over the range of 350-550°C) on product composition, and distribution of products among the collection system's

six stage fractions, found increasing temperatures increase yield of methane and CO, while decreasing yield of CO_2, for the NCG's. Higher temperatures favored alkylated phenol production, while mono- and dimethoxyphenols had maximum yields at 400°C, and 350°C respectively. When summing all phenolics, temperature did not seem to have a significant effect on yield. Levoglucosan yield was maximized when acids were minimized, at 450°C. Although effect on *average* molecular weight was not reported, and is not clear from GPC chromatograms, lower temperatures had greater amounts of low-molecular weight compounds in the heavy-ends (stage fractions 1 and 2 (SF1 and SF2)).

Catalytic Pyrolysis of Individual Components of Lignocellulosic Biomass, K. Wang, K.H. Kim and R.C. Brown, *Green Chem.*, 16, (2014) 727.

A CFP study of biomass components, showing cellulose produced more aromatics than hemicellulose which both produced far greater amounts than lignin does. Coke was observed to comprise the majority of the solid carbonaceous residue resultant from conversion of the carbohydrate fraction, whereas char was major lignin-derived solid residue. Based on product distribution, relative extent of reaction mechanisms was inferred; although "below optimal", dehydration reactions were the predominant means for deoxygenation. Decarbonylation (responsible for CO production) occurred preferentially over decarboxylation (responsible for CO_2 production).

Catalytic Pyrolysis of Microalgae for Production of Aromatics and Ammonia, K. Wang and R.C. Brown, *Green Chemistry*, 15, (2013) 675.

A study investigating the catalytic (HZSM-5) FP of algae. Algae outperformed red oak in terms of aromatics yield (25% vs 16.7% on a carbon mass basis). Much of the nitrogen content was converted to ammonia, although a small fraction was converted to hydrogen cyanide. If scaled, HCN produced would need to be handled, impinging in a basic solution or passing through a metal hydroxide packed bed were amelioration measures suggested.

Influence of the Interaction of Components on the Pyrolysis Behavior of Biomass, S. Wang, X. Guo, K. Wang and Z. Luo, *Journal of Analytical and Applied Pyrolysis*, 91, (2011) 183.

A TGA and FTIR study which makes use of a lab-scale continuous reactor. Unfortunately neither written nor reviewed by individuals with full command of the English language, many statements are unclear. Some of the studies cited had mixed findings; "Alen et al. showed that pine behaved as the sum of its components", Raveendran et al. "with both a TGA and packed-bed pyrolyzer showed there were no detectable interactions … 14 species tested along with seven isolated fractions", "Yang et al. observed negligible interactions among three main components", "Wang et al. TGA work found lignin and hemicellulose affected pyrolysis characteristics of cellulose but not each other", in a gasification study Hosoya et al. identified cellulose-lignin interaction effects, Worasuwannarak et al. showed "yield of methyl- and vinyl-guaiacols enhanced in presence of cellulose".

The study itself found enhanced yields of 2,6-dimethoxyphenol in the presence of holocellulose, and enhanced yields of furfural and acetic acid when cellulose were pyrolyzed together.

Cellulose-Hemicellulose and Cellulose-Lignin Interactions during Fast Pyrolysis, J. Zhang, Y.S. Choi, C.G. Yoo, T.H. Kim, R.C. Brown and B.H. Shanks, *ACS Sustainable Chemistry & Engineering*, 3, (2015) 293.

A micropyrolyzer-GC-MS/FID experiment which rigorously investigated interaction effects in both hardwood and herbaceous biomass. The type specimen for indication of interaction effects, levoglucosan was shown to experience interactions in whole biomass due to inter-fraction bonding preventing formation of a levoglucosyl end group required for formation (due to oxygen at the C6 carbon covalently bonded to lignin). Overall findings included no observed interactions in red oak, and cellulose-lignin interactions in switchgrass (herbaceous).

Autothermal pyrolysis, partial oxidative pyrolysis

Biomass Oxidative Flash Pyrolysis: Autothermal Operation, Yields and Product Properties, M. Amutio, G. Lopez, R. Aguado, M. Artetxe, J. Bilbao and M. Olazar, *Energy and Fuels*, 26, (2012) 1353.

Oxidative FP of "pinewood wastes" was carried out in a conical spouted bed reactor under three conditions (oxygen concentrations covering an equivalence ratio of 0-0.25). Product yields as well as ultimate analyses were carried out on the char, non-condensable gases and bio-oil product streams to show the effect of increasing extent of oxidation on product composition. It is important to note that this study does not test a range near the autothermal equivalence ratio (ER ~ 0.06) with much resolution, rather only tested equivalence ratios of 0, 0.15, and 0.25.

Kinetic Study of Lignocellulosic Biomass Oxidative Pyrolysis, M. Amutio, G. Lopez, R. Aguado, M. Artetxe, J. Bilbao and M. Olazar, *Fuel*, 95, (2012) 305.

Partial oxidative TGA/DTG (i.e. slow pyrolysis) testing of "pinewood wastes" and representative biomass fractions at three oxygen concentrations was carried out to look at the kinetics of slow oxidative pyrolysis in order to build a kinetic model. The two stage, six step model was based on pyrolysis and heterogeneous oxidation (of gases, vapors and aerosols), followed by a char oxidation stage. These conditions were carried out for each of the three main biomass fractions. The TGA experiments were used to support the model by providing mass loss rates at various temperatures. The two-stage concept was arrived at from two distinct peaks present in each fraction's TGA curve. The model concluded that both hemicellulose volatiles and char oxidized primarily, followed by cellulose char. Oxidation of cellulose volatiles and lignin products was minor. Because it was not mechanistic in nature, this study's findings didn't notably contribute to the mechanistic framework developed here.

Autothermal Fast Pyrolysis of Birch Bark with Partial Oxidation in a Fluidized Bed Reactor, D. Li, F. Berruti and C. Briens, *Fuel*, 121, (2014) 27.

A slug-fed fluidized bed reactor study investigating effect of oxygen concentration on pyrolysis product properties. The study focused heavily on autothermal pyrolysis, from the adiabatic definition (i.e. autothermal not accounting for bed heat losses, supplying only heat equivalent to the heat of pyrolysis). For their system, autothermal pyrolysis "energy-neutrality" occurs at an ER of "slightly above 0.05 for both 500 and 550°C". Interestingly they report a major reduction in bio-oil yield at AT conditions, "22% of the dry bio-oil chemicals are lost at 500°C". This loss is notable because birch bark would be expected to have a higher lignin content than ground entire hardwood whole biomass (red oak heartwood for example), ~30% vs ~15%, respectively, [365,366] . Bio-oil analysis showed that of the eight highest-yielding birch bark-bio-oil compounds; acetic acid, acetol, levoglucosan, 4-(4-hydroxyphenyl)-2-butanone yields initially increased then decreased, while phenol, 2-methylphenol and 4-methylphenol yields increased then leveled off, with increasing oxygen content in the sweep gas. They claim phenol yields remain stable when far

exceeding autothermal oxygen due to its high "ignition point (715°C)". If lignin-derived monophenol yields increase, yet overall dry-bio-oil yield decreases more than others observed, [71], given birch bark has greater lignin content than red oak, light lignin product fragments could be more sensitive to oxidation than biomass carbohydrates. Overall their results agree with Zhou et al. [293]; claiming increased yield of viscous monomeric phenols with increase in oxygen content. Additionally, average molecular weight was shown to decrease with increasing oxygen content, yet 500°C pyrolysis consistently yielded lower molecular weight products than 550°C.

A Detailed Kinetic Study of Pyrolysis and Oxidation of Glycerol (Propane-1,2,3-triol), E. Barker-Hemings, C. Cavallotti, A. Cuoci, T. Faravelli and E. Ranzi, *Combustion Science and Technology*, 184, (2012) 1164.

A kinetic study complimented by pyrolysis experiments in a laminar flow quartz tube reactor. The kinetic study modeled the oxidative pyrolysis of glycerol and two oxidation products; acetol and a 3-hydroxypropanal. Glycerol has been shown to degrade by hydrogen abstraction reactions and dehydration reactions, as is common among most alcohols. The kinetic model evaluates all of the possible hydrogen abstractions (from the 4 primary alpha, the 1 secondary alpha, and the 3 hydroxyl-hydrogens). Barker-Hemmings cited two sources that experimentally derived rate laws for reactions for the three hydrogen types, showing hydroxyl hydrogens had greatest reaction rate, followed by primary, followed by secondary hydrogens (as would follow logic of relative bond strength and steric availability for attack), [367,368] . Dehydration reactions were shown to occur with the hydroxyl groups, thus having two main pathways. The first pathway (reaction with the hydroxyl on the 1 or 3-carbon), leads to 3-hydroxypropanal, which could be further dehydrated to prop-2-enal. The second pathway leading to the formation of 1-hydroxypropan-2-one, possibly further oxidized (by hydrogen abstraction) to acetaldehyde.

Formation of Phenols from the Low-temperature Fast Pyrolysis of Radiata Pine (Pinus radiata) Part I. Influence of Molecular Oxygen, D.A.E. Butt, *Journal of Analytical and Applied Pyrolysis*, 76, (2005) 38.

A "Bench-scale" fluidized bed low-temperature oxidative pyrolysis of oven dried or oven dried-and-ethanol extracted radiata pine experimental study. Oxygen fed at 0, 10, 20 % (v/v-sweep gas). Bio-oil was analyzed for monophenols with GC/MS. Monophenol yields increased from 0.09% (m/m-liquid product) to 11.98% as oxygen was increased from 0 to 20%. It seems important to note that they operated the fluid bed at 295°C, likely the reason non-oxidative pyrolysis yielded such little monophenols (the process might simply not been harsh enough to pyrolyze polyphenols into monophenols). The dramatic increase in monophenol yield could have been due to uncontrolled increase in bed temperature resultant from exothermic reactions attributable to the admission of 10 and 20% oxygen, thus creating more severe pyrolysis conditions. It should also be noted that for most of the conditions tested, the process had a char yield on the order of 90% (m/m-biomass fed). Interestingly, more than 75% of monophenolic products were comprised of seven phenols. Also what's more was how these phenols differ from phenols of high selectivity from 500°C pyrolysis, where many methoxy functionalities are present. In 295°C pyrolysis more methyl functionalities were observed.

Mechanistic and Kinetic Study on the Reactions of Coumaric Acids with Reactive Oxygen Species: A DFT Approach, A.s. Garzón, I.n. Bravo, A.J. Barbero and J. Albaladejo, *Journal of Agriculture and Food Chemistry*, 62, (2014) 9705.

A computational study (using density functional theory) on the oxidation of alkene-, aldehyde-, or carboxylic acid-side chain-containing phenolics by way of reactive oxygen species (denoted ·OX). The underlying mechanisms which the paper summarizes are hydrogen abstraction from aldehyde and carboxylic acid functionalities, and addition reactions with non-aromatic double bonds. They classify the relative reactivity of oxygenated functionalities as follows: $\cdot OH > \cdot OCH_3 > \cdot OOH > \cdot OOCH_3$.

Analytical Pyrolysis –A Tool for Revealing Lignin Structure- Antioxidant Activity Relationship, J. Ponomarenko, T. Dizhbite, M. Lauberts, A. Volperts, G. Dobele and G. Telysheva, *Journal of Analytical and Applied Pyrolysis*, 113, (2015) 360.

A analytical chemistry study investigating antioxidatant content of various lignins, predominantly using GC/MS, size-exclusion chromatography, and EPR to charactrize. Antioxidant contents were compared across various characteristics, generally finding similar trends to those presented for aromatic acids by biochemists. Phenolic hydroxyls, able to undergo hydrogen abstraction are the most significant indicator of aromatic activity. Following phenolic –OH was; relative G + S phenylpropane content, followed by α-CH_2 groups , followed by oxygenated phenylpropane side chains, followed lastly by the size of pi-conjugated systems (while the content of carbonyl content had a negative relationship with antioxidant activity.

Formic-acid-Induced Depolymerization of Oxidized Lignin to Aromatics, A. Rahimi, A. Ulbrich, J.J. Coon and S.S. Stahl, *Nature Research Letters*, (2014) 1.

A mechanistic experimental paper presenting H-NMR and GPC data showing how lignin is oxidatively depolymerized. Partial oxidation of pulp and paper mill wastes (lignosulfonates) in mild formic acid solution formed aromatics. The paper is based around an alcohol oxidation mechanism, where CHOH dehydrogenates to a carbonyl (in the form of a ketone), which destabilizes the β-O-4 bond leading to C-C or C-O cleavage, thus further depolymerizing the lignin fragments. The presented mechanisms contributed notably to the mechanistic framework presented below.

Fast Oxidative Pyrolysis of Sugar Cane Straw in a Fluidized Bed Reactor, J.M. Mesa-Pérez, J.D. Rocha, L.A. Barbosa-Cortez, M. Penedo-Medina, C.A. Luengo and E. Cascarosa, *Applied Thermal Engineering*, 56, (2013) 167.

A fluidized bed study looking at effect of equivalence ratio and temperature on product distribution. “Autothermal” equivalence ratios of 0.14-0.23 were tested. This high range was classified as autothermal due to the inclusion of bed heat losses in addition to the standard definition; enthalpy of pyrolysis. Because this range was tested, bio-oil and char become significantly consumed toward its upped end, whose yield both decreased by roughly 20 percentage points as they transitioned from 0.14-0.23. Aqueous-phase (“acid-extract”) and non-aqueous-phase species concentrations were reported by chromatogram area percent for only the 0.14 equivalence ratio case. These concentrations seem roughly comparable to other studies findings, although correct identification of phenolics is questionable because I had never before come across some of the names presented (in this application), and because of the non-descript method description; “gas chromatography was used to identify compounds”.

On-line Deoxygenation of Cellulose Pyrolysis Vapors in a Staged Autothermal Reactor, N.E. Persson, S.D. Blass, C. Rosenthal, A. Bhan and L.D. Schmidt, *RCS Adv.*, 2013, (2013) 20163.

An experimental study using a continuous minireactor for oxidative catalytic pyrolysis followed by *ex situ* zeolite catalytic upgrading. Five different *in situ* catalysts were investigated (followed by the *ex situ* zeolite bed). Although equivalence ratio was not calculated, the sweep was comprised of 2 standard liters per minute (SLPM) nitrogen, 1 SLPM hydrogen, and 0.2 SLPM oxygen, while cellulose was fed at 10 grams per hour. Due to the use of catalyst, the product stream was comprised of primarily olefins, light gases, and aromatics, with few oxygenates. Because this was a catalytic study, it is fundamentally different than this paper's topic of discussion.

A Two-Stage Spouted Bed Process for Autothermal Pyrolysis or Retorting, G. Rovero and A.P. Watkinson, *Fuel Processing Technology*, 26, (1990) 221.

A coal study using a spouted char combustor (heat source) in series with a spouted pyrolyzer. The effect of coal type and operation parameters on tar yield were presented. The reactor was operated between harsh pyrolysis and mild gasification conditions, where maximum observed liquid yields of 12 wt. % were observed, (other than in an experiment where very small particles were tested, in which case ~15 wt. % was achieved). A notable finding was that the char separation principle used (intended for low char-holdup spouted beds) did not work well with low rank (high-volatiles content) coals; tar yields decreased, hypothesized to result from ash-promoted decomposition of tar. Since not mechanistic in nature, this study did not contribute notably to the mechanistic framework presented here.

Autothemal Fluidized Bed Pyrolysis of Cuban Pine Sawdust, J.A. Suárez, P.A. Beaton, R. Zanzi and A. Grimm, *Energy Sources Part A*, 28, (2006) 695.

A fluidized bed study reportedly operating at equivalence ratios of 1.0, 1.5, and 2.0 (as in operating in an oxygen-*rich* environment). Liquids yields decreased from 14-2% with increase in ER from 1.0-2.0. Because the study operated at such a high equivalence ratio, its findings are not highly applicable to autothermal pyrolysis.

Hydrodynamics of a Novel Biomass Autothermal Fast Pyrolysis Reactor: Flow Pattern and Pressure Drop, H. Zhang, R. Xiao, Q. Pan, Q. Song and H. Huang, *Chemical Engineering Technology*, 32, (2009) 27.

Effects of operation parameters on hydrodynamics in a "novel" reactor consisting of internally-interconnected fluidized beds. The reactor consists of a draft tube and an internal dipleg which transported the spouted media down into the (surrounding annulus) combustor. The goal of the reactor was to extract, then catalytically upgrade and separate volatiles from other products which can be used to provide process heat. Because oxidation reactions occur separately from the pyrolysis reactions, and due to the physical nature of the study, its findings don't majorly contribute to the mechanistic framework presented here.

CFB Air-blown Flash Pyrolysis. Part II: Operation and Experimental Results, I.P. Boukis, S. Bezergianni, P. Grammelis and A.V. Bridgwater, *Fuel*, 86, (2007) 1387.

This study investigated effects of operation parameters on liquid yield in a circulating fluidized bed which had a char combustor located in what might be considered a plenum. It is assumed that all oxygen is consumed during the sweep gas's residence in the char combustor. A 60% wet-basis bio-oil yield was achieved. Similarly to Zhang et al. 2009, oxidation occurs in isolation of pyrolysis, and this paper was not highly mechanistic in nature, so did not notably contribute to the mechanistic framework presented here.

The Effect of Low-concentration Oxygen in Sweep Gas During Pyrolysis of Red Oak Using a Fluidized Bed Reactor, K.H. Kim, X. Bai, M. Rover and R.C. Brown, *Fuel*, 124, (2014) 49.

A fluidized bed partial oxidative pyrolysis study examining effect of oxygen content, varying from ER of 0.034-0.539 on bio-oil composition. The significant finding was that oxygen in the range of ER = 0.034-0.068, increased yield of monophenolics and hydrolysable sugars from that of non-oxidative pyrolysis. Even at ER = 0.539, bio-oil yield was not significantly diminished relative to non-oxidative pyrolysis. Kim showed that char morphology (specifically that surface pore size, and surface area increased) changes with increased oxygen concentration. Analysis showed increased yield of a few oxidized monophenol species, specifically; vanillin and 4-hydroxy-3,5-dimethoxybenzaldehyde (both of which contain aldehyde functionalities), as well as 4-hydroxy-3-methoxyacetophenone and 4-hydroxy-3,5-dimethoxyacetophenone (both of which contain ketone functionalities), while yield of vinyl-containing species decreased. Kim cited studies on lignin oxidation leading for vanillin formation, and selective oxidation of styrene's vinyl group to a ketone group, CITATIONS. Kim reports a decreased carboxylic (acetic) acid yield with increased oxygen, suggesting acetic acid decomposes to light oxygenates, and that these more readily oxidize to NCG than do the normally oligomeric lignin-derived products. Levoglucosan was showed to behave similarly to the acids (steadily decreasing in yield with increasing oxygen, suggesting oxidation to furans or light oxygenates). Another relevant point was that oxidation of AAEM's produces thermally stable oxides, hydroxides, and carbonates.

Partial Oxidative Pyrolysis of Acid Infused Red Oak Using a Fluidized Bed Reactor to Produce Sugar Rich Bio-oil, K.H. Kim, R. Brown and X. Bai, *Fuel*, 130, (2014) 135.

This study used the same experimental setup and range of oxidative operating conditions as did the prior Kim et al. [71] paper, but infused the biomass with acid (sulfuric acid) to passivate AAEM's, converting them into thermally stable salts. Kim showed that acid infusion leads to repolymerization and condensation reactions leading to char formation. He proposes that the oxidation of pyrolytic lignin counters this by breaking it down to volatile monophenols. Also concluded was that pyrolytic lignin is the main source of char agglomeration, and that oxidation reduces adhesive effect of lignin-derived char

Gas-phase Partial Oxidation of Lignin to Carboxylic Acids over Vanadium Pyrophosphate and Aluminum-Vanadium-Molybdenum, S. Lofti, D.C. Boffito and G.S. Patience, *ChemSusChem*, 8, (2015) 3424

A catalytic fluidized bed microreactor pyrolysis study of atomized alkaline lignin solution. Although many of the mechanisms presented don't directly apply since they are catalyzed, some behaviors can still apply. Cleavage products of lignin methyl or ethyl alkyl side chains form formic or acetic acid, respectively. Hydration of side chains containing double bonds can crack to form acetic acid. If able ring-open a phenolic ring (something which would possibly be almost entirely an artifact of catalysis), it is possible to form maleic anhydride as an intermediate, which could further decompose to maleic acid. The catalyst used was aluminum-vanadium-molybdenum, which had significant selectivity towards lactic acid. Some of the concepts presented contributed towards the mechanistic framework presented here.

Oxidative Pyrolysis of Integral Softwood Pellets, Olsson, Maria, J. Kjallstrand and G. Petersson, *Journal of Analytical and Applied Pyrolysis*, 67, (2003) 135.

A study on open combustion of wood pellets, not having to do with a controlled pyrolysis experiment. Their goal was to analyze the composition of the smoke. Interestingly their smoke contained the following lignin-derived compounds; 2-methoxy-4-vinylphenol (most predominantly), 2-methoxyphenol, two vinylphenol species, vanillin, phenol, and naphthalene, as well as the following carbohydrate derived compounds; 2-furaldehyde, levoglucosan. Also interestingly, these were only present during whole pellet flaming combustion. During glowing char combustion, only aromatics were given off. Because not a well-controlled experiment, and not mechanistic in nature, did not notably contribute to the mechanistic model.

Process for the Production of Anhydrosugars from Lignin and Cellulose Containing Biomass by Pyrolysis, D.S. Scott, J. Piskorz, D. Radelin and P. Majerski, in, Ottowa, Canada, 1995.

This is a patent which lays out a conversion process to go from lignocellulose to a purified levoglucosan stream as well as a fermentable sugar stream. The process (and its variants (claims)) roughly involves a low temperature "dilute" (5 wt. %) acid hydrolysis followed by a water wash then drying, followed by oxidative pyrolysis. The volatile pyrolysis products are condensed out in a two stage condenser, yielding aqueous and non-aqueous phases. The aqueous phase is activated carbon-filtered then dried (de-watered) "yielding levoglucosan" and the non-aqueous fraction is activated carbon-filtered then acid hydrolyzed to yield "fermentable sugars". What makes this 1995 patent interesting is the use of oxidative pyrolysis as an approach to effectively "preferentially delignify" the biomass. Even though it is claimed that the lignin is fully removed to non-condensable products, if there is a significant *non*-aqueous fraction formed then the lignin fraction is clearly not fully oxidized (but rather break it down to volatile, condensable fragments). They describe the activated carbon as being used to remove the phenolic components. Although not specified, I would presume a relatively high equivalence ratio is used if they are attempting to fully dignify the components to non-condensable. There are no mechanisms or references presented on oxygen-delignification in this work.

The Autothermal Pyrolysis of Waste Tires, M.-Y. Wey, B.-H. Liou, S.-Y. Wu and C.-H. Zhang, *Journal of the Air and Waste Management Association*, 45, (1995).

A 10 cm diameter fluidized bed catalytic oxidative pyrolysis study of shredded waste tire fed at 35 – 215 kg/hr. The bed was operated at ER = 0.07-0.35. The catalysts tested were a zeolite and calcium carbonate. They operated at nearly 10 times the minimum fluidization velocity. Because of the presence of catalyst and a polymeric hydrocarbon feedstock, the main proposed reactions pathways were; "isomerization, cyclization, aromatization, alkylation, hydrogenation, and disproportionation reactions… brought about from the formation of carbanions by proton addition to olefins and aromatics *or* the formation of alkyl-carbonium ions by the hydrogen addition to saturated alkyl-hydrocarbons and cyclized alkyl-hydrocarbons"

Partial Oxidation Mechanisms of Biomass Models, Role of the Condensed Phase

Effect of Pyrolysis Pressure and Heating Rate on Radiata Pine Char Structure and Apparent Gasification Reactivity, E. Cetin, R. Gupta and B. Moghtaderi, *Fuel*, 84, (2005) 1328.

Morphology and reactivity of char were measured over a range of pyrolysis heating rates and pyrolysis pressures, using SEM, digital cinematography, BET surface area analysis, and TGA (for "reactivity" quantification). Higher pressures decreased reactivity, decreased char particle swelling, and increased char yield. Higher heating rates led to melt-deformation, smoothing the outer surface, and increased void fraction and void volume.

Lignins Occurrence, Formation, Structure and Reactions – Chapter 11. – Oxidation, H.M. Chang and A.G. G., in K.V. Sarkanen and C.H. Ludwig (Eds.), Wiley Interscience, Heidelberg, Germany, 1971, Chapter 11.

This chapter does a general review of lignin oxidation, classified into three categories; degradation to aromatic carbonyl- and carboxylic acid-containing compounds (a behavior which applies to molecular oxygen, permanganate degradation of methylated lignins, and metal-oxides), degradation of aromatic rings (behavior applying to strong acids and chlorinated oxidizers), and oxidation limited to "specific groups" (generally applying to highly selective catalytic oxidation for structural/functional elucidation).

Nitrobenzene was used to investigate relative prevalence of S,G,H units in lignin, and to selectively convert Isoeugenol to vanillin (by the mechanism shown). "Nitrobenzene functions as a two-electron acceptor and undergoes conventional stepwise reduction to nitrosobenzene, phenyl hydroxylamine then to aniline". For metal oxides, "alkali solutions of some heavy metals also oxidatively degrade lignin materials *without destroying the aromatic nuclei*…aromatic aldehydes and or aromatic carboxylic acids are products". For cupric oxide, the relevance of oxidant strength is described, "A weak oxidant will tend to favor oxidative coupling while a stronger oxidant will further oxidize intermediate oxidation products… CuO has an oxidation potential to strike balance between these two factors". For other metal oxides in general, "lower valence increases yield of lignin acids, while higher valence augments production of ether-solubles". There is also a section on permanganate oxidation, where much of the behavior seems to be dictated by environment conditions (how the lignins were methylated, what base and how strong the alkaline solution is, etc.), as permanganate is referred to as a "mild oxidant"

Many insights are presented in the molecular oxygen section; "oxidative coupling which is of course characteristic of the oxidative treatment of phenolic compounds by one-electron transfer reagents…Kratzl, Gratzle and Claus have shown recently the primary step is in air oxidation of monohydric phenols… is the resonance-stabilized free phenoxy radicals". Additionally, "Reactions not involving peroxy radical include the coupling of two phenoxy radicals. For G-unit derivatives with an uncondensed 5-position, 5-5 coupling results, in S-derivatives coupling less likely due to substituent-blocked ortho and para positions…oxidation of methylguaiacol results in dimerization by phenyl radical coupling whereas alpha-carbonyl/carbinol derivatives experience side chain elimination trough Dakin-type reactions" (see mechanism below).

Single Particle Asphaltene Pyrolysis in a Drop-tube Furnace, S. Dhir, N. Mahapatra, V. Kurian, M. Alipour and R. Gupta, *Energy & Fuels*, 30, (2016) 6132.

An experimental study looking primarily into particle size effects on char yield, mass loss, and morphology. Additionaly, analyical chemistry was investigated using ICP-MS, XRF, and FTIR. They identified higher pyrolysis temperatures associated with the formation of cenosphere-resembling char particles. They also identified higher temperatures associated with loss of active sites, content of alkenes, and C-C linkages. Smaller particles were shown to exhibit behaviors, such as lesser char yield, lesser oxygen content, and and lesser activation energy; aligning with lesser heat and mass transfer limitations.

Gas phase oxidation of benzoic acid to phenol over nickel oxide catalysts, DumaCITATION, V. Duma, K.E. Popp, M.C. Kung, H. Zhou, S. Nguyen, S. Ohyama, H.H. Kung and C.L. Marshall, *Chemical Engineering Journal*, 99, (2004) 227.

An experimental study which presents oxidation of benzoic acid by mechanism of either a nucleophilic aromatic-hydrogen substitution by oxygen (yielding unobserved hydroxyoxobenzoic acid), *or* by formation of a peroxyacid intermediate followed by transfer of oxygen to the ortho position (was in better agreement with experimental findings). A general reaction scheme involved decarboxylation of benzoic acid to benzene and biphenyl, dehydration of benzoic acid to benzoate radical and phenol, which recombine to form a dibenzoate intermediate leading to xanthone, or fluorenone (if benzene replaced benzoate radical).

Chemical Sinks of Organic Aerosol: Kinetics and Products of the Heterogeneous Oxidation of Erythritol and Levoglucosan, S.H. Kessler, J.D. Smith, D.L. Che, D.R. Worsnop, K.R. Wilson and J.H. Kroll, *Environmental Science and Technology*, 44, (2010) 7005.

A study comparing mass loss kinetics of levoglucosan and erythritol (in the context of their existence as organic (atmospheric) aerosols). Due to the relatively low volatility, oxidation was proposed to play a substantial role in mass loss, to a much greater extent with erythritol than levoglucosan.

Effect of Temperature, Pressure, and Residence Time on Pyrolysis of Pine in an Entrained Flow Reactor, G. Newalkar, K. Iisa, A.D. D'Amico, C. Sievers and P. Agrawal, *Energy & Fuels*, 28, (2014) 5144.

A study making use of unique pressurized entrained flow reactor, in predominantly the gasification regime (in terms of temperature, residence time), at flash pyrolysis heating rates. Gasification products were characterized by a suite of analytical chromatrography applications. Low pressures and long residence times led to soot-precursor formation. High pressures led to cenosphere-like (large-void/highly-porous structures). Low temperatures yielded large meso- and macro-pore content.

Organic Chemical Structure and Structural Shrinkage of Chars, J. Pastor-Villegas, C.J. Duran-Valle, C. Valenzuela-Calahorro and V. Gomez-Serrano, *Carbon*, 36, (1998) 1251.

A char morphology study correlating chemical processes with morphological products. Three main observations included high temperature pyrolysis leading to inter-layer ether-bond cross-linking, porosity is closely related to the extent of devolatilization, and that char particle shrinkage is resultant from breakdown of interlayer C-O bonds.

The Influence of Partial Oxidation Mechanisms on Tar Destruction in TwoStage Biomass Gasification, J. Ahrenfeldt, H. Egsgaard, W. Stelte, T. Thomsen and U.B. Henriksen, *Fuel*, 112, (2013) 662.

A study investgating wood pellet oxidation mechanisms under air-blown gasification conditions, for the purpose of understanding tar destruction (analogous to bio-oil oxidation). Partial oxidation was shown to convert primary tars to soot precursors ("low-molecular weight PAH's"). Higher moisture content (in steam-blown operation) inhibited formation of PAH's, suggested through enhanced decomposition of monophenolics. Because described for the purposes of gasification (and thus very high equivalence ratios), has less relevance towards behaviors which might occur during autothermal pyrolysis.

Reaction Mechanisms for Pyrolysis of Benzaldehydes, M. Akazawa, Y. Kojima and Y. Kato, *新潟大学農学部研究報告*, 67, (2014) 57.

A Py-GC/MS study investigating secondary reactions occurring with four benzaldehydes; 4-hydroxybenzaldehyde, vanillin, syringaldehyde, and veratrumaldehyde. Using the pyrolysis product composition of the four, and existing published mechanisms, a number of pyrolysis mechanisms were proposed.

Multistep Mechanism for the Devolatilization of Biomass Fast Pyrolysis Oils, C. Branca and C. Di Blasi, *Industrial & Engineering Chemistry Research*, 45, (2006) 5891.

A study on bio-oil combustion mechanisms containing a detailed bio-oil composition comparison across a few scaled-pyrolysis examples with different biomass (bio-oil comparison across biomass type).

Partial oxidation of D-xylose to maleic anhydride and acrylic acid over vanadyl pyrophosphate, T. Ghaznavi, C. Neagoe and G.S. Patience, *Biomass and Bioenergy*, 71, (2014) 285.

A microfluidized bed catalytic pyrolysis study where a xylose solution was injected as a vaporized spray. The effects of catalyst on conversion was investigated. 50% maleic anhydride yield was achieved, and it was postulated if the bed could be operated in a more truly gas-solid reaction manner (where the injected solution fully evaporated prior to contacting bed), higher yields could be achieved (since carmelization would occur to a lesser extent).

The Gaseous Oxidation of Toluene II – The Analytical Results, J.A. Barnard and V.J. Ibberson, *Combustion and Flame*, 9, (1964) 149.

An experimental and mechanistic study on the gaseous oxidation of toluene, which proposes a mechanism that builds upon findings of similar studies carried out decades earlier. This study investigated oxidation, conveniently in the standard pyrolysis range of 500°C. The main finding of the study was that formaldehyde played a crucial role in the reaction sequence (particularly being "responsible" for the rate limiting degenerate branching step). Specifically, the concentration of formaldehyde was correlated with the reaction rate.

Pyrolysis-GC/MS of Sinapyl and Coniferyl Alcohol, A.E. Harman-Ware, M. Crocker, A.P. Kaur, M.S. Meier, D. Kato and B. Lynn, *Journal of Analytical and Applied Pyrolysis*, 99, (2013) 161.

Mixtures of sinapyl and coniferyl alcohol were pyrolyzed using Py-GC/MS in attempt to develop a predictive model for S:G ratio of native lignins, based off of pyrolysis product distribution. A small extent of demethoxylation of sinapyl alcohol was observed, although described as insignificant when assembling calibration curves. Peach-pit lignin S:G was accurately predicted using their linear pyrolysis product model.

A Critical Review of Cellobiose Dehydrogenases, G. Henriksson, G. Johansson and G. Pettersson, *Journal of Biotechnology*, 78, (2000) 93.

A chapter in a text on oxidative delignification focusing on the application of a cellobiose dehydrogenation enzyme for selective depolymerization of lignins. The study found that β-aryl-ether linkages were successfully cleaved using the enzyme, additionally that phenolic compounds can be made formed, which could further be oxidized by standard delignifying enzymes such as manganese peroxidases.

Mechanisms for the Formation of Monomers and Oligomers During Pyrolysis of a Softwood Lignin, T. Kotake, H. Kawamoto and S. Saka, *Journal of Analytical and Applied Pyrolysis*, 105, (2014) 309.

Pyrolysis of Japanese cedar and associated MWL; both alone and in the presence of either an aprotic solvent or H-donor was carried out for the purposes of learning about chemistry which might occur leading to observed product distribution. Presence of an aprotic solvent suppressed formation of a quinone-methide intermediate, normally supporting repolymerization, lead to increased coniferyl alcohol yields (in the case of whole biomass). Presence of a hydrogen donor increased yield of monophenolic and pyrolytic lignin yields from MWL. In-depth mechanistic discussion on all of these ensues.

Vapor-phase Cracking of 4-vinylguaiacol in a Laminar-flow Reactor: Kinetics and Effect of Temperature on Product Composition, E.B. Ledesma, J.N. Hoang, A.J. Solon, M.M.H. Tran, M.P. Nguyen, H.D. Nguyen, T. Hendrix-Doucette, J.V. Vu, C.K. Fortune and S. Batamo, *Industrial & Engineering Chemistry Research*, 53, (2014) 12527.

Entrained flow pyrolysis ("vapor-phase cracking") of 4-vinylguaiacol was investigated over a wide temperature range, showing majority of conversion occurring between 400-550ºC. Four possible radical reaction initiation mechanisms are proposed for 4-vinylguaiacol. Additionally a decomposition pathway, leading to the formation of furans is proposed.

Study of Guaiacol Pyrolysis Mechanism Based on Density Functional Theory, C. Liu, Y. Zhang and X. Huang, *Fuel Processing Technology*, 123, (2014) 159.

Following proposal of five guaiacol pyrolysis reaction pathways, centered around methoxy group homolysis (demethylation), demethoxylation, and rearrangement, kinetics were modeled in a DFT environment. A demethoxylation pathway was energetically preferred, and a rearrangement pathway lead to the pyrolysis intermediate (repolymerization precursor) quinone-methide intermediate.

Selective oxidation of styrene to acetophenone in the presence of ionic liquids, V.V. Namboodiri, R.S. Varma, E. Sahle-Demessie and U.R. Pillai, *Green Chemistry*, 4, (2002) 170.

An autoclave study with the goal of replacing the conventional Friedel-Crafts method (involving benzene acetylation) for the production of acetophenone, a paladium catalyzed oxidation of styrene (classically called the Waker reaction) in the presence of a cation-ionic liquid is investigated as a prospective replacement. The effects of time, temperature, pressure, catalyst ratios on acetophenone selectivity were investigated. Co-products dilluting acetophenone were benzaldehyde and benzoic acid.

Toward the Oxidation of the Phenyl Radical and Prevention of PAH Formation in Combustion Systems, D.S. Parker, R.I. Kaiser, T.P. Troy, O. Kostko, M. Ahmed and A.M. Mebel, *J Phys Chem A*, 119, (2015) 7145.

An experimental mechanistic study of the oxidation of phenyl radicals, and role this plays in soot precursor formation, at 873 and 1003K. A mechanism involving many pathways is proposed. Product composition is compared for both cases.

Cool Flames in the Combustion of Toluene and Ethylbenzene, R.G.W. Norrish and G.W. Taylor, *Proceedings of the Royal Society of London. Series A, Mathematical and Physical Sciences*, 238, (1956) 143.

A 1950's era combustion research study on the gaseous oxidation of toluene and ethylbenzene. The mechanistic proposal in this document was the association of the weak, low

temperature flame originating from the oxidation of these compounds with formaldehyde combustion spectra, thus the glow associated with side-chain oxidation (really oxidation of pyrolytically-cleaved side chain). This connection was made because these spectra were not observed with benzene oxidation in a prior study.

Larger products of these oxidations included; acetophenone, benzaldehyde, benzoic acid, phenol, and hydroquinone. The study also discussed acetophenone (a compound of more direct interest, a common constituent of pyrolytic bio-oil). It was remarked that it is relatively pyrolytically stable, thus requiring oxidation or reaction to form benzaldehyde, or benzoic acid. It was postulated that much benzaldehyde produced arises from acetophenone oxidation.

Three findings (juxtaposing oxidation of these aromatics with paraffin oxidation were, "upper and lower cool-flame limits were not sharp, appearance of glow is not associated with sudden increase in reaction rate, and pressure rise during the incubation period is significant relevant to that associated with appearance of glow".

The Oxidation of Benzene, R.G.W. Norrish and G.W. Taylor, *Proceedings of the Royal Society of London. Series A, Mathematical and Physical Sciences*, 234, (1956) 161.

A 1950's era combustion research study on the gaseous oxidation of benzene. Due to the resonance stability/aromaticity of a structure such as benzene, high temperatures are required even to oxidize this compound (no reaction observed below 873K). 953K was used for these experiments. The oxidation of benzene was proposed to initiate with a hydrogen abstraction yielding a phenyl radical (see mechanism below). Observed products involved CO, CO2, water, H2, C2-hydrocarbonds, phenol, 1,2-dihydroxybenzene, 1,4-benzoquinone, CH2O, formic acid, and small amounts of diphenyl and anthracene.

The Oxidation of Aromatic Hydrocarbons at High Pressures; I-Benzene, II-Toluene, III-Ethyl Benzene, D.M. Newitt and J.H. Burgoyne, *Proceedings of the Royal Society of London. Series A, Mathematical and Physical Sciences*, 153, (1936) 448.

One of the earlier mechanistic combustion era studies investigating gaseous oxidation of substituted aromatics. It was proposed that for toluene oxidation, "side chains undergo oxidation in a manner resembling paraffin oxidation" leading to formation of benzaldehyde and benzoic acid at atmospheric pressure, and benzyl alcohol at elevated pressures. At high pressures, side chains and the ring was suggested to occur simultaneously. Decomposition occurs by hydroxylation yielding phenol when the side chains are oxidized, or alcohols when the ring is oxidized.

A potentially applicable insight, "When excess hydrocarbon was present in the reacting medium, oxidation was partially arrested during earlier stages …considerable quantities of phenol found in products". The big-picture claim of the paper was "With substituted benzenes, it was found that oxygen attack occurred at the alpha-carbon atom of the side chain", [44].

Biomass Processing Over Gold Catalysts; Chapter 2 - Selective Oxidation/Dehydrogenation Reactions, O.A. Simakova, R.J. Davis and D.Y. Murzin, (2013) 11.

A textbook chapter reviewing gold-catalyzed (aqueous-phase) oxidations of numerous plant molecules (ethanol, 5-hydroxymethyl furfural, glucose, galactose, lactose, glycerol, glyceraldehyde, and others), the role of gold particle size, co-catalysts/support effects, and a summary of published kinetic data. Mechanisms presented throughout the literature for each of the reagents were presented here.

A Study of the Mechanisms of Vanillin Pyrolysis by Mass Spectrometry and Multivariate Analysis, E.-J. Shin, M.R. Nimlos and R.J. Evans, *Fuel*, 80, (2001) 1689.

A vanillin pyrolytic degradation study (over range of 500-800ºC), making use of molecular beam mass spectroscopy (i.e. a study in collaboration with NREL, where MS enables inline kinetic measurements of conversion to intermediates and product species. Specifically, anisole, phenol, and benzaldehyde published mechanisms were built upon from the perspectives of uni- and bimolecular reactions of vanillin.

The Reaction of Phenyl Radical with Molecular Oxygen: A G2M Study of the Potential Energy Surface, I.V. Tomakov, G.-S. Kim, V.M. Kislov, A.M. Mebel and M.C. Lin, *Journal of Physical Chemistry A*, 109, (2005) 6114.

A computational chemistry study evaluating a number of potential oxidation pathways. Energetically-favored products include furan, and ortho-benzoquinone (with associated pathway of aromatic ring degradation to cyclopentadienyl ring products).

The Fate of Lignin during Hydrothermal Pretreatment, H. Trajano, N.L. Engle, M. Foston, A.J. Ragauskas, T.J. Tschaplinski and C.E. Wyman, *Biotechnology for Biofuels*, 6, (2013) 1.

A GPC/NMR/HSQC cellulolytic enzyme lignin aqueous oxidation kinetic and mechanistic study, under hydrothermal liquefaction conditions. The study suggested that LCC interactions allowed for greater overall lignin extraction, and release of S- units moreso than G-units. Further, that depolymerization followed by repolymerization appeared to be the predomiant pathway of "lignin modification", and that presence of polysaccharides should assist depolymerization during this pretreatment.

High Temperature Oxidation of Aromatic Hydrocarbons, C. Venkat, K. Brezinski and I. Glassman, *High Temperature Oxidation of Aromatic Hydrocarbons I - Reaction Mechanisms and Modeling*, at: Nineteenth Symposium (International) on Combustion, 143.

One of the later classical experimental studies (being published in 1982) on hydrocarbon oxidation cited in Hucknall's text, investigating the oxidation of benzene, toluene, and ethylbenzene and proposing a mechanism for the oxidation of each. The main finding or claim of this paper is that the rate of reaction is primarily controlled by the oxidation of phenyl radical (an intermediate formed in the case of all three aromatics). The concept of side chain oxidation occurring first (or preferentially reacted with first while still remaining) was well established in earlier studies. The earlier studies noted that the concentration of formaldehyde was correlated with the reaction rate, but this must have been an artifact of the earlier phenyl oxidation limited reaction.

Aqueous-phase Photo-oxidation of Levoglucosan – a Mechanistic Study Using Time-of-flight Chemical Ionization Mass Spectrometry (Aerosol ToF-CIMS), R. Zhao, E.L. Mungall, A.K.Y. Lee, D. Aljawhary and J.P.D. Abbatt, *Atmospheric Chemistry and Physics*, 14, (2014) 9695.

The title describes this well, analysis from the perspective of organic (atmospheric) aerosol oxidation mechanisms. Use of the ToF-CIMS allowed for quasi-kinetic values to be determined for eluting species. A series of very nice graphics and mechanisms were presenting, which give a good sense of the photo-oxidation behavior (in terms of decomposition behaviors) during brief review of the article.

Depolymerization of Cellulose to Glucose by Oxidation-Hydrolysis, L. Zhou, X. Yang, J. Xu, M. Shi, F. Wang, C. Chen and J. Xu, *Green Chem.*, 17, (2015) 1519.

A study looking at the effect of various oxidizers on alpha-cellulose and micro-crystalline cellulose (in aqueous or condensed/gas phase reactions), where oxidation is being used as a pretreatment for hydrolysis. Hydrogen peroxide, KMnO4, HNO3, TEMPO-CaClO catalyst were tested in the aqueous phase, while NO2, O2, and air were used in tube furnace experiments. The experiment found that generally, the CH2-OH group was oxidized into a carbonyl and then a carboxylic acid.

Lignin Depolymerization via an Integrated Approach of Anode Oxidation and Electro-generated H2O2 Oxidation, H. Zhu, Y. Chen, T. Qin, L. Wang, Y. Tang, Y. Sun and P. Wan, *RSC Advances*, 4, (2014) 6232.

An aqueous phase electrochemical "oxidation" (oxidative depolymerization) of lignin in a graphitic cathode, Ru/Ti/IrO_2 anode, hydrogen peroxide solution system. Product compositions from this were compared to only electrochemical oxidation and only hydrogen peroxide oxidation. Three products of high selectivity were diethyl ether, 4'-(4-methoxyphenoxy)-acetophenone and vanillin (both on the order of 10 wt. %). A series of possible reaction pathways was presented as potential sources of all observed product classes.

Investigative Cleavage of Beta-O-4 Linkage in Lignin Model Compounds by Aerobic Oxidation of C-alpha and C-gamma Hydroxyl Groups, N.D. Patil and N. Yan, *Tetrahedron Letters*, 57, (2016) 3024.

A room temperature, lignin dimer model compound catalytic aerobic oxidation study. The group used TEMPO catalyst with a combination of CuCl and substances called bpy and NMI, which resulted in abstracting hydrogens from the ether-linkage-alcohol groups, turning them into carbonyl groups (forming an "1,3-dicarbonyl adduct"). By mixing with catalytic amounts of acid the adduct was cleaved into carboxylic acid-containing phenol and another phenolic monomer.

Metalloporphyrins in the Biomimetic Oxidation of Lignin and Lignin Model Compounds, C. Crestini and P. Tagliatesta, in *The Porphyrin Handbook*, Academic Press, Elsevier Science, Rome, Rome, Italy, 2003, Chapter 66, p. 161.

A review paper on the oxidation of lignin through the use of a class of catalysts called metalloporphyrins. This class of catalyst was selected because of how its activity could be considered biomimetic to that of lignin peroxidase and manganese peroxidase. Oxidation of phenolic monomers, dimers, isolated lignins as well as a pulp and paper waste liquor using two fungal enzymes (lignin peroxidase and manganese peroxidase), assisted by this type of catalyst, is reviewed. Lignin peroxidase seemed to oxidize veratryl alcohol to veratraldehyde (through side chain oxidation) as well as para-quinone (through a ring-opening reaction in the presence of air) via a "one-electron oxidation" to veratryl alcohol radical. While lignin peroxidase is able to oxidize non-phenolic lignin subunits (those not containing a phenolic hydroxyl), manganese peroxidase is described to oxidize the alpha-hydroxyl and alpha-oxo lignin units (keto acid groups). Manganese peroxidase does this by reduction of Mn(III) to Mn(II). The porphyrin-mediated oxidation is described to proceed via the same path to veratraldehyde as lignin peroxidase, but by "benzylic oxidation followed by C-5 hydroxylation then C-3 demethoxylation and oxidation to quinoids". When catalyzing cleavage of a beta-O-4 model, the porphyrin lead to alpha-beta cleavage (forming veratraldehyde) and alpha-1 cleavage (forming para-quinone). When testing a beta-1 model, similar occurred but yielding ortho-quinone rather than para. For the beta-alpha cleavage the

proposed mechanism involved a benzylic oxidation (ring electron attack) followed by resonance of the radical to the beta carbon which then leads to cleavage upon interaction with another radical fragment and kicking off of an alcohol-hydrogen to stabilize the ring's positive charge (see scheme 17). Additionally, beta-1 oxidation lead to small amounts of muconic acid derivatives forming from ring-opening. Workup of the porphyrin with 5-5' model compounds oxidized aldehyde functionalities to carboxylic acids and some extent of ring-opening occurred. In another 5-5' model (with methoxy functionalities rather than aldehydes), one of the rings oxidized to a quinone (without cleaving from the other). In a sentence, oxidation of lignins with porphyrins proceeded through side-chain oxidation, formation of ortho- and para-benzoquinones, and small amounts of aromatic ring cleavage to muconic acid derivatives.

APPENDIX B: ADDITIONAL GRAPHICS

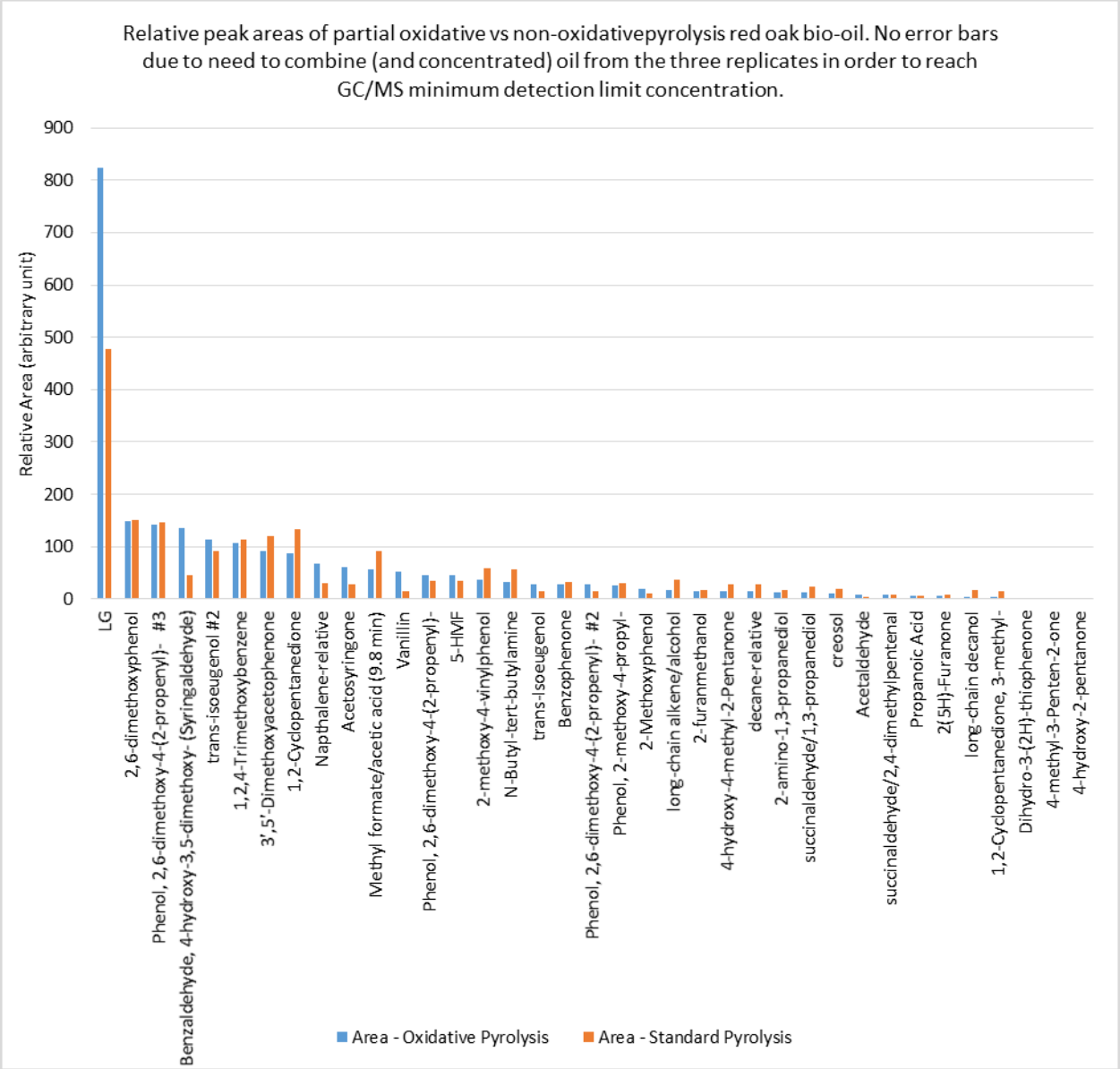

Figure 32. Bio-oil from oxidative and non-oxidative pyrolysis of red oak; composition compared. (Bio-oil generated by controlled pyrolysis duration quench micropyrolysis, followed by collection of oil from three sets of 30 samples for each condition; no error bars because all of replications were combined to achieve GC/MS minimum concentration detection limits.)

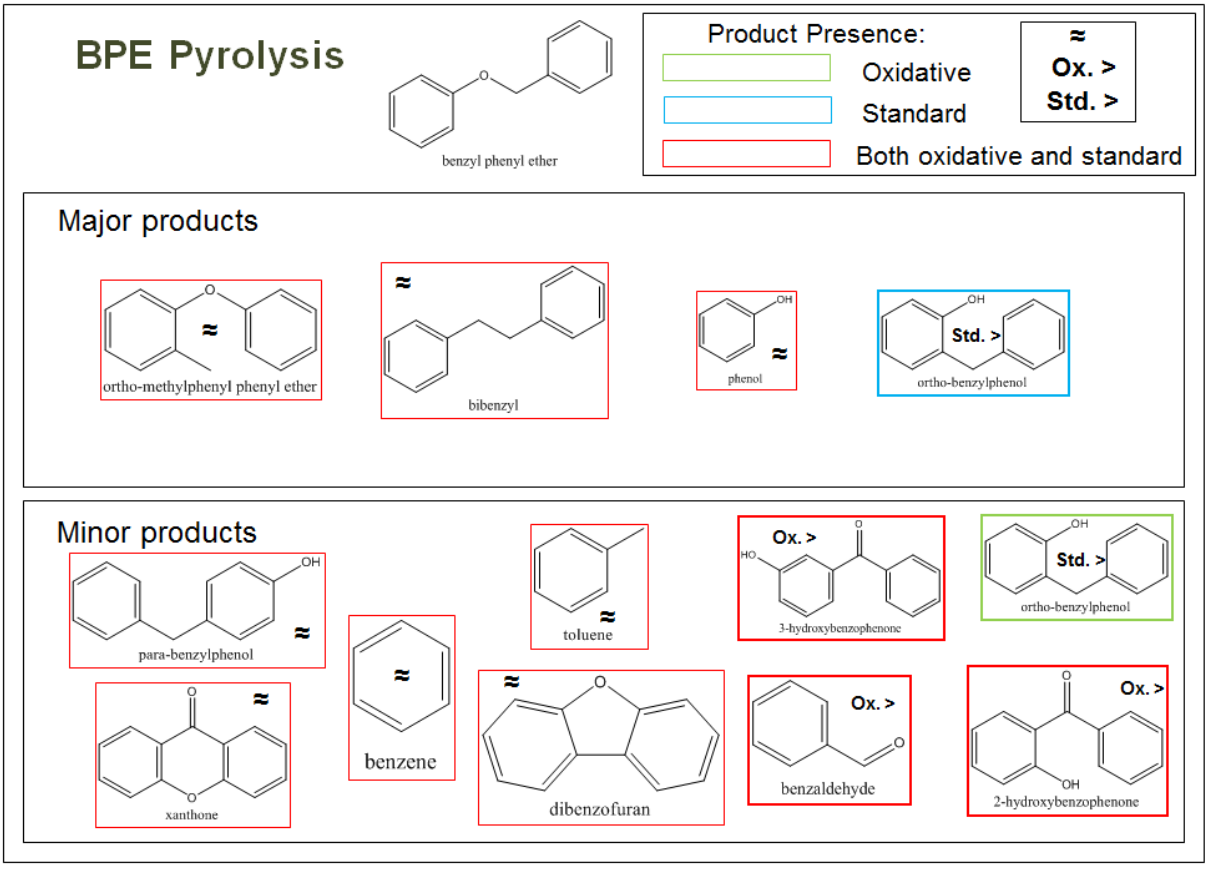
BPE Pyrolysis
benzyl phenyl ether
Product Presence:
Oxidative
Standard
Both oxidative and standard
≈
Ox. >
Std. >
Major products
ortho-methylphenyl phenyl ether
bibenzyl
phenol
Std. >
ortho-benzylphenol
Minor products
para-benzylphenol
toluene
Ox. >
3-hydroxybenzophenone
Std. >
ortho-benzylphenol
xanthone
benzene
dibenzofuran
Ox. >
benzaldehyde
Ox. >
2-hydroxybenzophenone

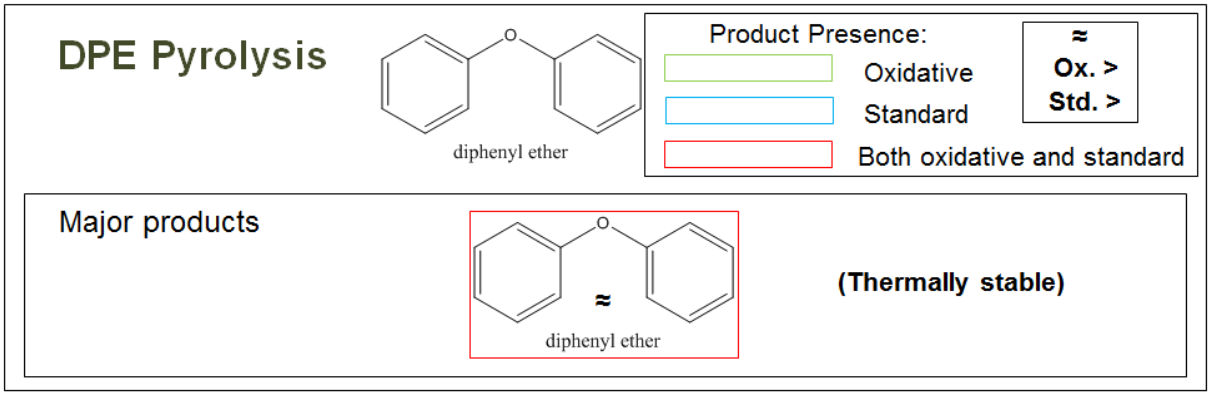
DPE Pyrolysis
diphenyl ether
Product Presence:
Oxidative
Standard
Both oxidative and standard
≈
Ox. >
Std. >
Major products
diphenyl ether
(Thermally stable)

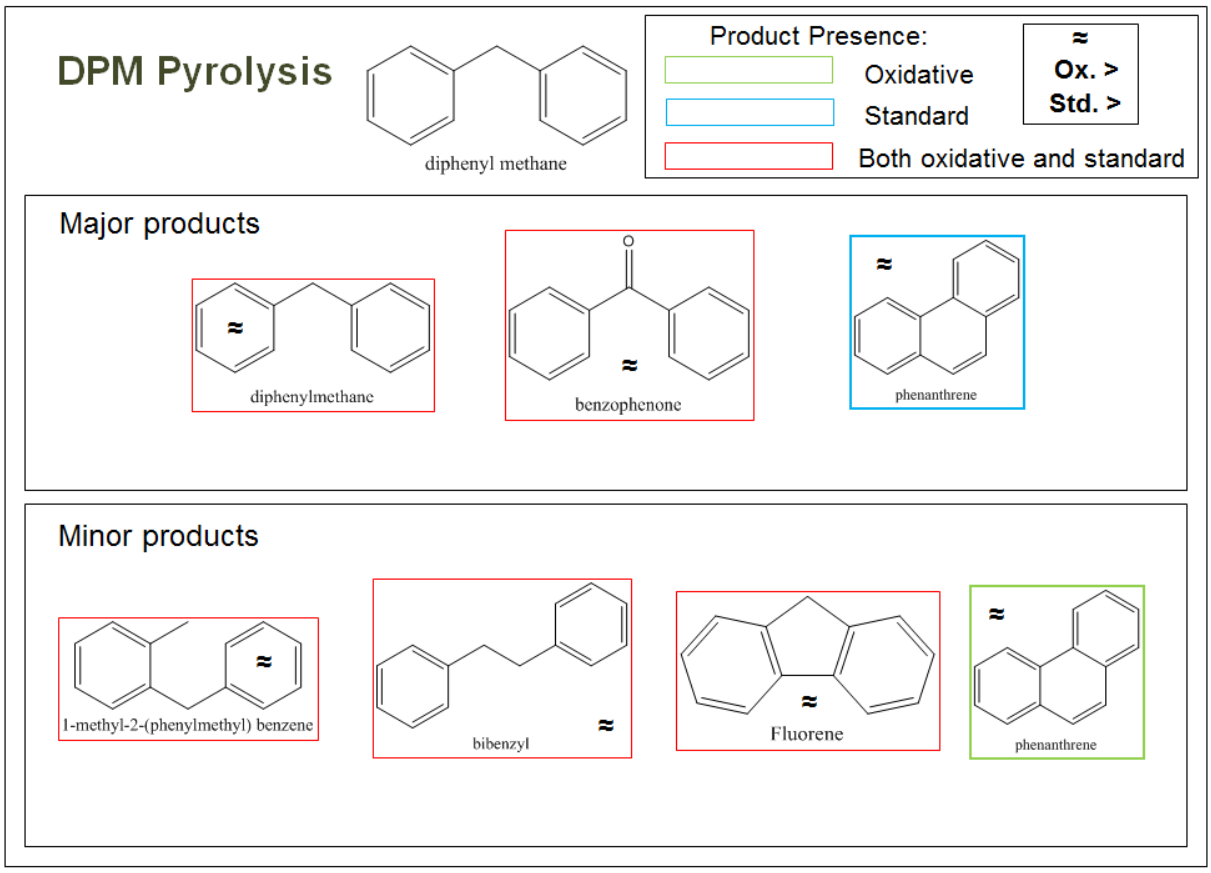
DPM Pyrolysis
diphenyl methane
Product Presence:
Oxidative
Standard
Both oxidative and standard
≈
Ox. >
Std. >
Major products
diphenylmethane
benzophenone
phenanthrene
Minor products
1-methyl-2-(phenylmethyl) benzene
bibenzyl
Fluorene
phenanthrene

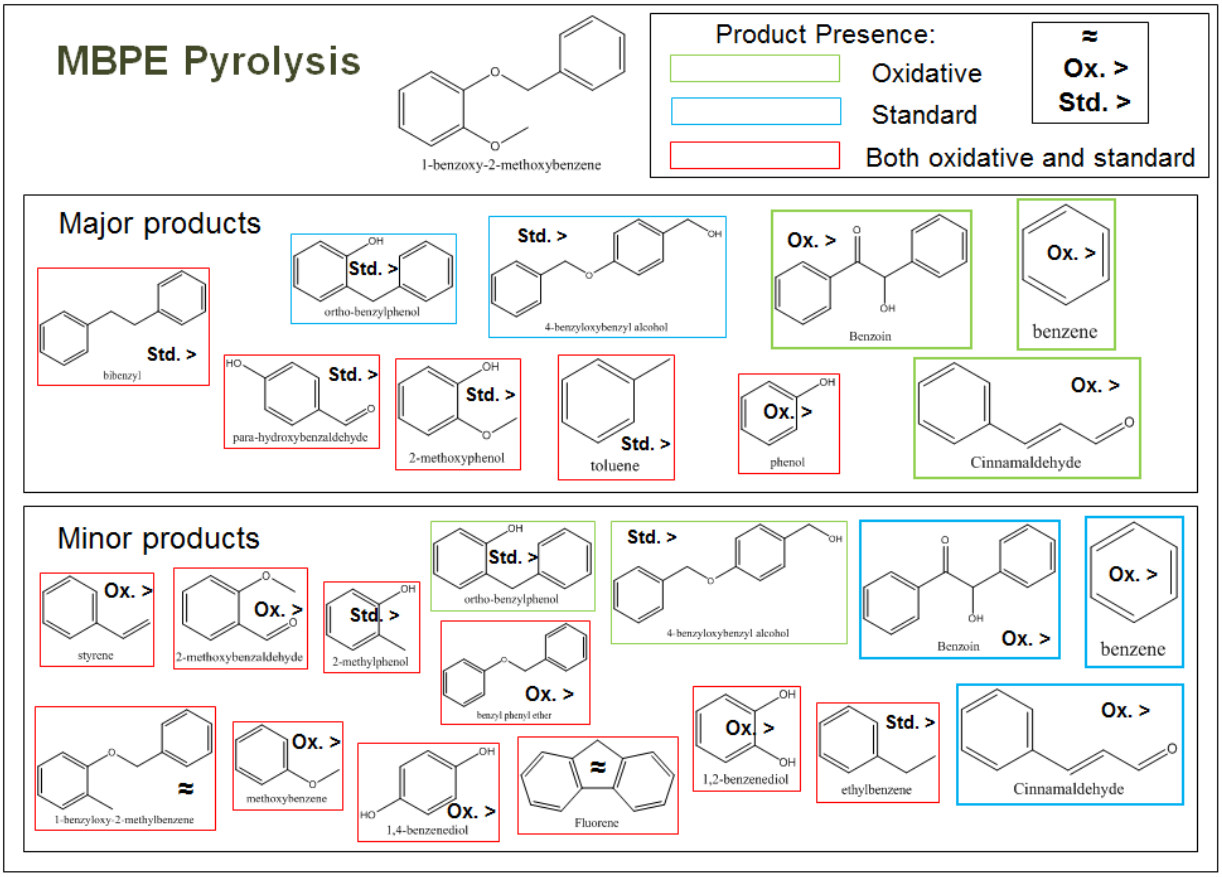
MBPE Pyrolysis
1-benzoxy-2-methoxybenzene
Product Presence:
Oxidative
Standard
Both oxidative and standard
≈
Ox. >
Std. >
Major products
bibenzyl
Std. >
ortho-benzylphenol
Std. >
4-benzyloxybenzyl alcohol
Std. >
Benzoin
Ox. >
benzene
Ox. >
para-hydroxybenzaldehyde
Std. >
2-methoxyphenol
Std. >
toluene
Std. >
phenol
Ox. >
Cinnamaldehyde
Ox. >
Minor products
styrene
Ox. >
2-methoxybenzaldehyde
Ox. >
2-methylphenol
Std. >
ortho-benzylphenol
Std. >
4-benzyloxybenzyl alcohol
Std. >
Benzoin
Ox. >
benzene
Ox. >
benzyl phenyl ether
Ox. >
1-benzyloxy-2-methylbenzene
≈
methoxybenzene
Ox. >
1,4-benzenediol
Ox. >
Fluorene
≈
1,2-benzenediol
Ox. >
ethylbenzene
Std. >
Cinnamaldehyde
Ox. >

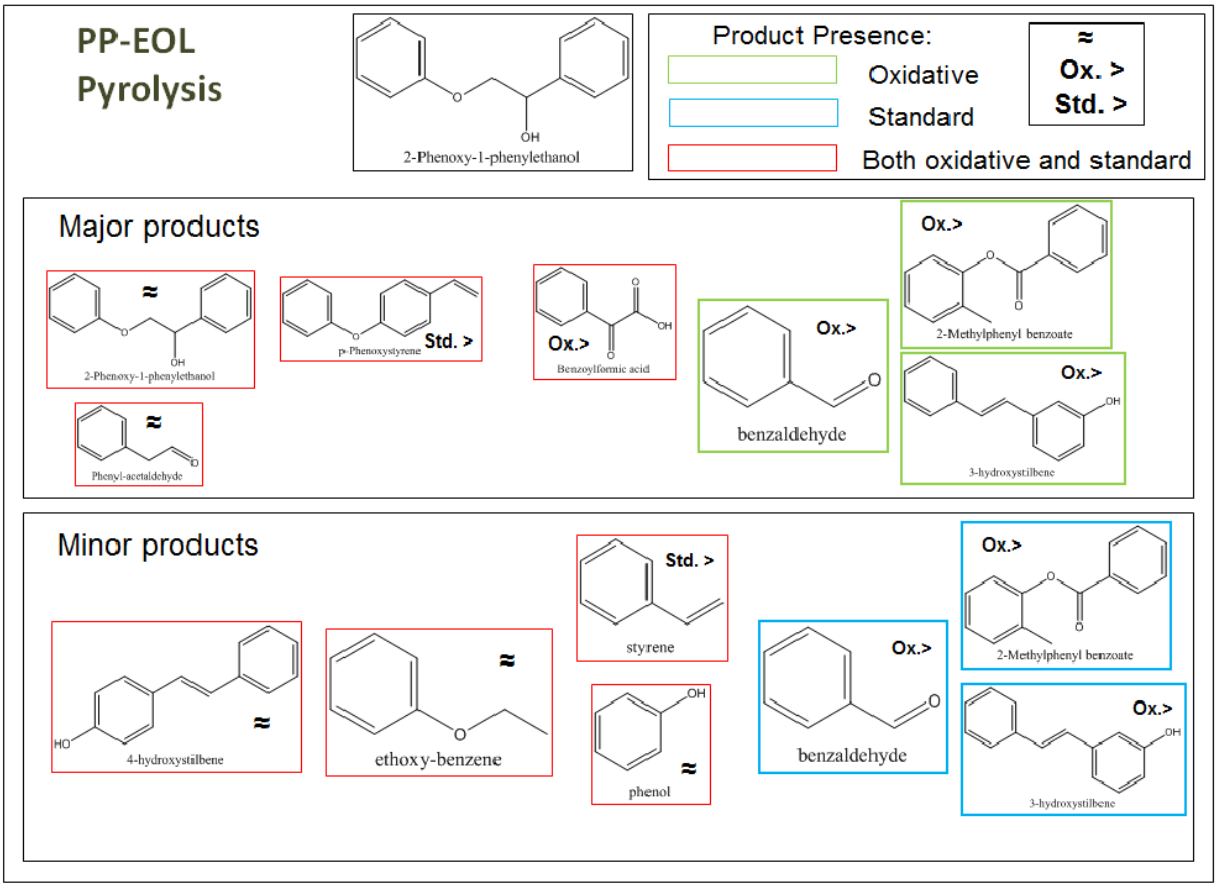
PP-EOL
Pyrolysis
2-Phenoxy-1-phenylethanol
Product Presence:
Oxidative
Standard
Both oxidative and standard
≈
Ox. >
Std. >
Major products
2-Phenoxy-1-phenylethanol
p-Phenoxystyrene
Std. >
Benzoylformic acid
Ox.>
benzaldehyde
Ox.>
2-Methylphenyl benzoate
Ox.>
3-hydroxystilbene
Phenyl-acetaldehyde
Minor products
4-hydroxystilbene
ethoxy-benzene
Std. >
styrene
phenol
Ox.>
benzaldehyde
Ox.>
2-Methylphenyl benzoate
Ox.>
3-hydroxystilbene

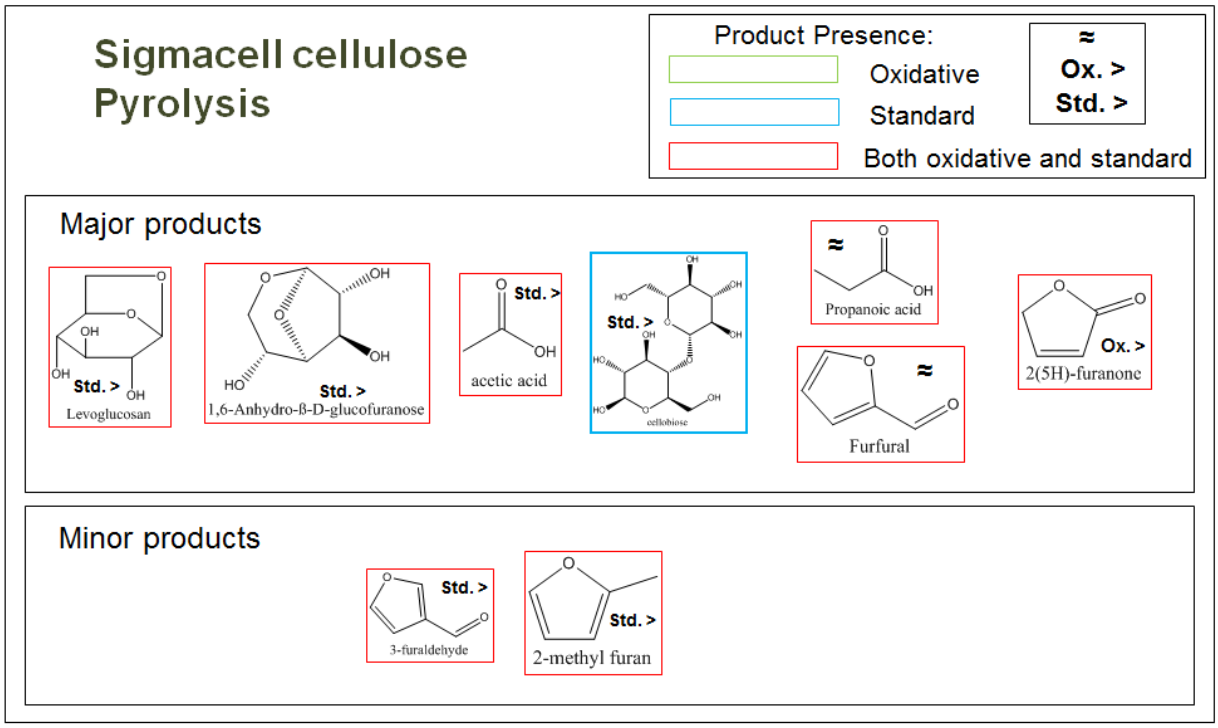
Sigmacell cellulose Pyrolysis
Product Presence:
Oxidative
Standard
Both oxidative and standard
≈
Ox. >
Std. >
Major products
Std. >
Levoglucosan
Std. >
1,6-Anhydro-ß-D-glucofuranose
Std. >
acetic acid
Std. >
cellobiose
≈
Propanoic acid
≈
Furfural
Ox. >
2(5H)-furanone
Minor products
Std. >
3-furaldehyde
Std. >
2-methyl furan

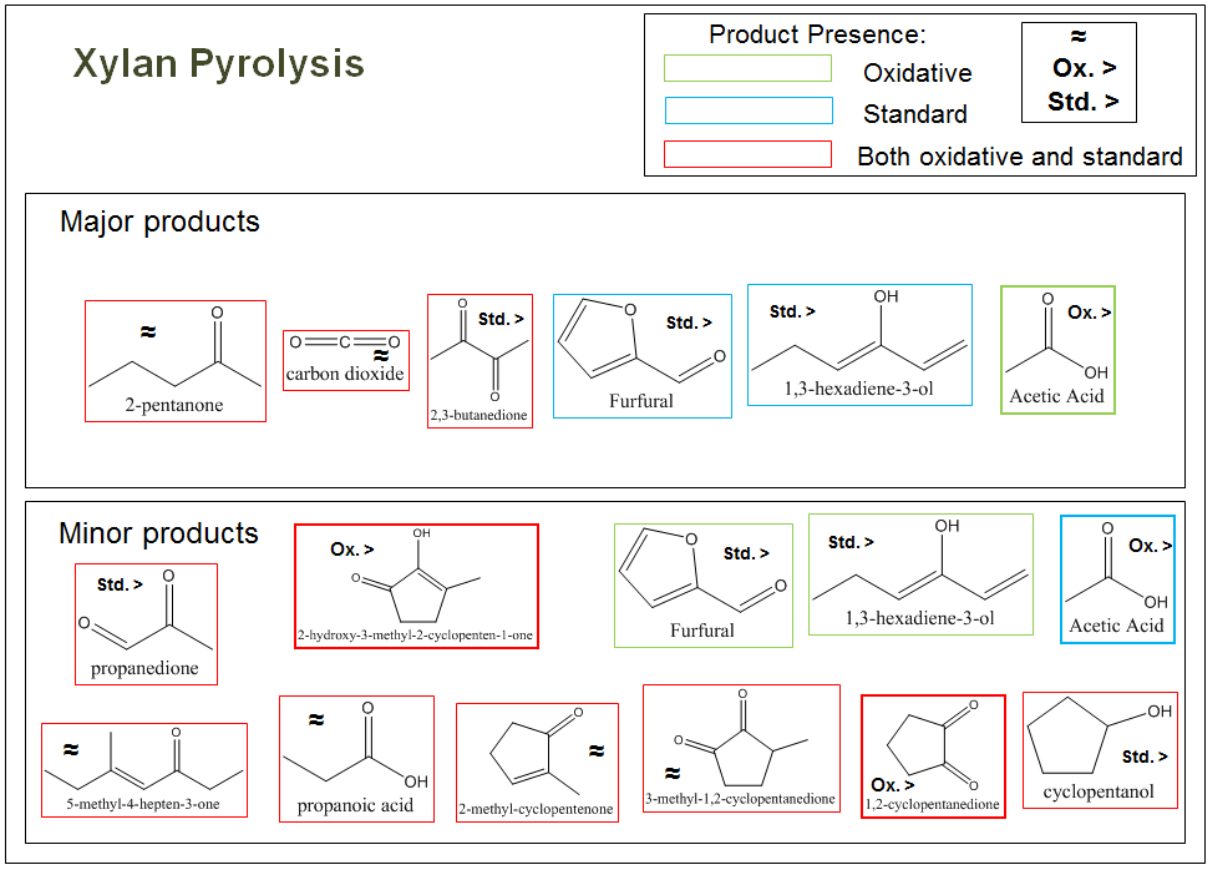
Xylan Pyrolysis
Product Presence:
Oxidative
Standard
Both oxidative and standard
≈
Ox. >
Std. >
Major products
≈
2-pentanone
carbon dioxide
Std. >
2,3-butanedione
Std. >
Furfural
Std. >
1,3-hexadiene-3-ol
Ox. >
Acetic Acid
Minor products
Std. >
propanedione
Ox. >
2-hydroxy-3-methyl-2-cyclopenten-1-one
Std. >
Furfural
Std. >
1,3-hexadiene-3-ol
Ox. >
Acetic Acid
≈
5-methyl-4-hepten-3-one
≈
propanoic acid
≈
2-methyl-cyclopentenone
≈
3-methyl-1,2-cyclopentanedione
Ox. >
1,2-cyclopentanedione
Std. >
cyclopentanol

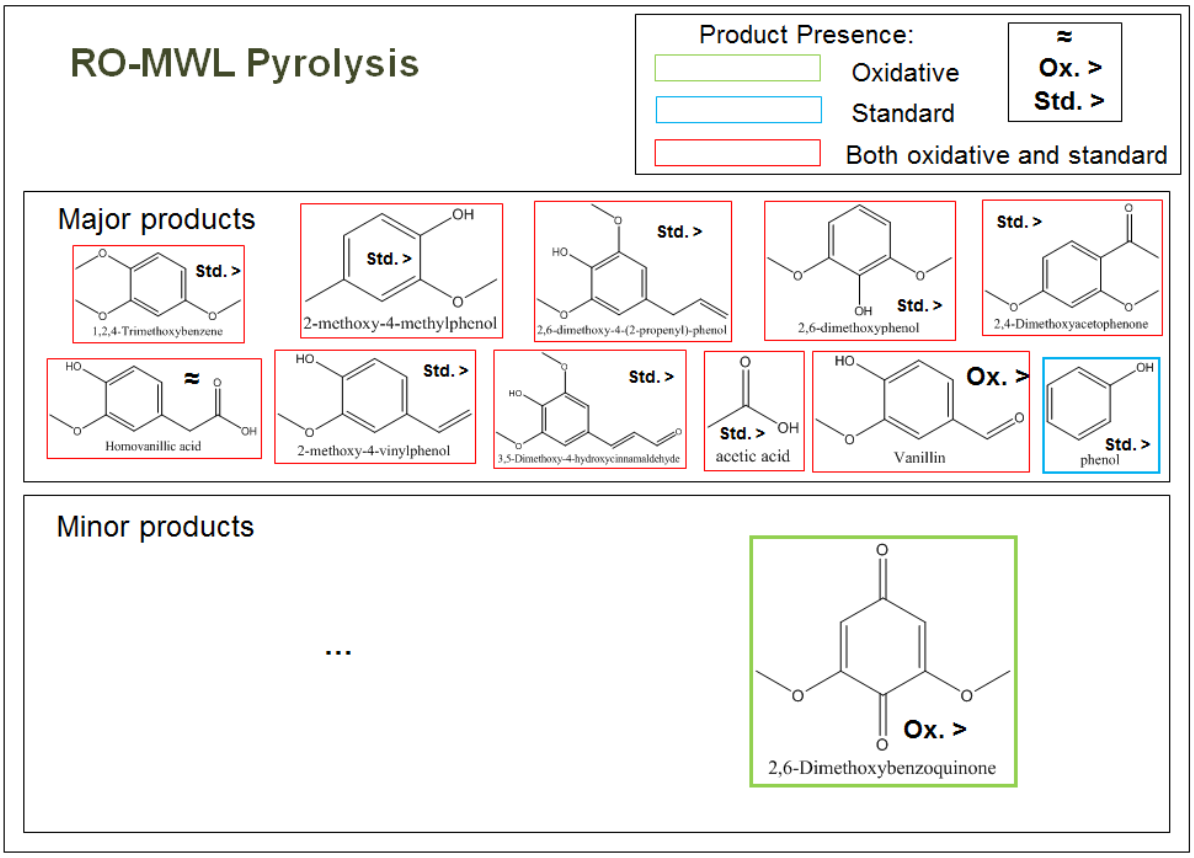

Figure 33. Series showing relative yields of products from lignin model dimer pyrolysis. (BPE = benzyl phenyl ether, DPE = diphenyl ether, MBPE = 1-benzyoxy-2-methoxybenzene, PP-EOL = 2-Phenoxy-1-phenylethanol, BB = Bibenzyl; green denotes product only present in oxidative condition, blue denotes only present in inert (standard pyrolysis) condition, Std. > denotes yield is greater in standard pyrolysis, vice versa for Ox. >, and ≈ denotes yields were comparable.)

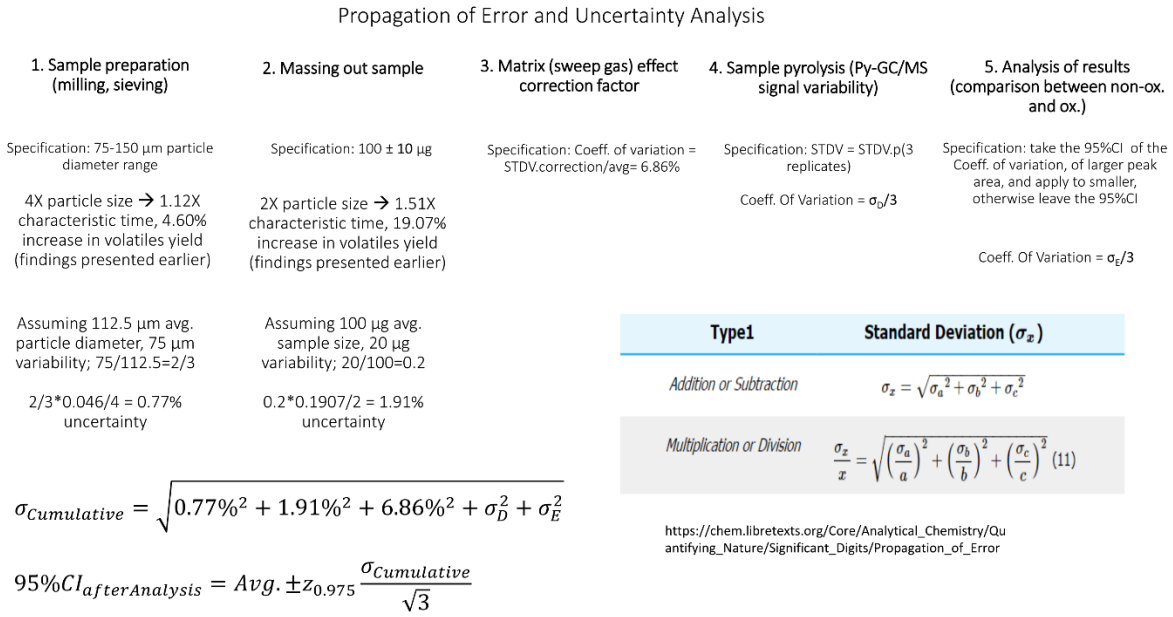

Figure 34. Propagation of error and uncertainty analysis approach.

APPENDIX C: ADDITIONAL TABLES

Table 1. Autothermal pyrolysis bio-oil composition data table recreated from Kim et al. [71].

The Properties of Bio-oils								
	Based On		Control	0.525% O_2	1.05% O_2	2.10% O_2	4.20% O_2	8.40% O_2
Water Content (wt.%)	SF1		6.41	6.78	6.46	5.37	6.04	8.71
	SF2		54.27	61.98	62.10	67.61	74.07	73.54
	Bio-oil (SF1 + SF2)		31.91	37.15	37.42	40.33	48.14	52.90
MAN (mg KOH/g)	SF1		29.79	31.99	32.15	30.65	25.95	33.05
	SF2		96.00	99.99	95.02	76.29	56.84	57.19
Elemental Composition (Wt.%)	SF1							
		C	57.61	57.62	56.40	56.05	56.85	53.58
		H	6.36	6.30	6.24	6.26	6.19	5.13
		O (diff.)	35.92	35.96	37.26	37.59	36.84	41.17
		N	0.11	0.12	0.10	0.11	0.12	0.11
	SF2							
		C	22.04	19.08	18.41	15.28	12.21	11.90
		H	9.15	9.24	9.24	9.47	9.77	9.87
		O (diff.)	68.81	71.38	72.35	75.25	78.02	78.23
		N	n.d.	n.d.	n.d.	n.d.	n.d.	n.d.
HHV (MJ/kg)	SF1		22.80	22.71	22.02	21.87	22.16	18.90
	SF2		9.80	8.50	8.18	7.01	5.98	5.99
Compositional analysis of bio-oils determined by IC and GC-FID								
g/100 g biomass			Control	0.525% O2	1.05% O2	2.10% O2	4.20% O2	8.40% O2
Carbohydrates								
Acetic acid			3.04 ± 0.42	2.72 ± 0.01	2.89 ± 0.21	2.26 ± 0.17	1.89 ± 0.09	1.97 ± 0.18
Glycolic acid			0.38 ± 0.11	0.29 ± 0.03	0.34 ± 0.05	0.3 ± 0.07	0.23 ± 0.01	0.2 ± 0.01
Formic acid			0.45 ± 0.12	0.43 ± 0.01	0.47 ± 0.01	0.43 ± 0.06	0.39 ± 0.04	0.42 ± 0.06
Propionic acid			0.27 ± 0.15	0.14 ± 0	0.21 ± 0.04	0.17 ± 0.08	0.11 ± 0.01	0.12 ± 0.04
Acetol			1.52 ± 0.46	1 ± 0.15	0.91 ± 0.05	0.83 ± 0.19	0.6 ± 0.04	0.45 ± 0.16
Dimethoxytetrahydrofuran			0.38 ± 0.16	0.16 ± 0.03	0.22 ± 0.01	0.25 ± 0.06	0.22 ± 0.01	0.18 ± 0.06
Furfural			0.35 ± 0.11	0.22 ± 0.04	0.19 ± 0.02	0.15 ± 0.04	0.12 ± 0.02	0.14 ± 0.06
2-Furanmethanol			0.1 ± 0.09	0.01 ± 0	0.01 ± 0	0.01 ± 0	0 ± 0	0.01 ± 0.01
5-Methyl furfural			0.06 ± 0.03	0.03 ± 0.01	0.03 ± 0	0.03 ± 0.01	0.02 ± 0	0.05 ± 0.03
2-(5H)Furanone			0.44 ± 0.17	0.33 ± 0.04	0.36 ± 0.05	0.31 ± 0.02	0.22 ± 0.02	0.23 ± 0.03
Methylcyclopentenolone			0.22 ± 0.08	0.11 ± 0.03	0.09 ± 0.01	0.08 ± 0.01	0.05 ± 0.01	0.03 ± 0.01
5-HMF			0.16 ± 0.02	0.2 ± 0.07	0.17 ± 0.02	0.17 ± 0.02	0.11 ± 0.01	0.07 ± 0.01
Levoglucosan			2.54 ± 0.08	3.37 ± 0.59	3.32 ± 0.18	3.43 ± 0.61	2.43 ± 0.28	2.36 ± 0.2
Sum of carbohydrate derivatives			9.88 ± 0.41	9.02 ± 0.96	9.18 ± 0.07	8.39 ± 0.53	6.37 ± 0.22	6.22 ± 0.41
Lignin								
Phenol			0.04 ± 0.03	0.02 ± 0	0.02 ± 0	0.02 ± 0.01	0.01 ± 0	0.03 ± 0
2-Methoxyphenol			0.15 ± 0.07	0.08 ± 0.02	0.09 ± 0.01	0.1 ± 0.02	0.09 ± 0	0.13 ± 0.05
2-Methoxy-4-methylphenol			0.09 ± 0.03	0.06 ± 0.01	0.06 ± 0.01	0.05 ± 0.01	0.04 ± 0	0.03 ± 0
4-Ethyl-2-methoxyphenol			0.02 ± 0.01	0.01 ± 0.01	0.01 ± 0	-	-	-
2-Methoxy-4-vinylphenol			0.16 ± 0.02	0.14 ± 0.02	0.13 ± 0.02	0.13 ± 0.01	0.12 ± 0.01	0.07 ± 0
Eugenol			0.04 ± 0.01	0.03 ± 0.01	0.03 ± 0	0.02 ± 0	0.02 ± 0	0.01 ± 0
2,6-Dimethoxyphenol			0.37 ± 0.07	0.36 ± 0.08	0.36 ± 0	0.29 ± 0.06	0.27 ± 0.02	0.16 ± 0.02
Isoeugenol			0.24 ± 0.08	0.2 ± 0.07	0.2 ± 0.03	0.21 ± 0.04	0.17 ± 0.05	0.11 ± 0.01
4-Methyl-2,6-dimethoxyphenol			0.26 ± 0.06	0.3 ± 0.09	0.27 ± 0.01	0.22 ± 0.04	0.21 ± 0	0.12 ± 0.01
Vanillin			0.1 ± 0.02	0.13 ± 0.04	0.13 ± 0	0.16 ± 0.05	0.16 ± 0.04	0.21 ± 0.02
4-Hydroxy-3-methoxyacetophenone			0.05 ± 0	0.08 ± 0.03	0.07 ± 0	0.09 ± 0.03	0.08 ± 0.01	0.07 ± 0.01
2,6-Dimethoxy-4-(2-propenyl) phenol			0.21 ± 0.02	0.2 ± 0.08	0.18 ± 0.02	0.14 ± 0	0.15 ± 0.02	0.07 ± 0
2,6-Dimethoxy-4-(1-propenyl) phenol			0.72 ± 0.05	0.91 ± 0.44	0.87 ± 0.02	0.64 ± 0.24	0.56 ± 0.02	0.24 ± 0.01
4-Hydroxy-3,5-dimethoxybenzaldehyde			0.24 ± 0.01	0.36 ± 0.13	0.4 ± 0.01	0.45 ± 0	0.6 ± 0.09	0.68 ± 0.02
4-Hydroxy-3,5-dimethoxyacetophenone			0.14 ± 0	0.19 ± 0.07	0.11 ± 0.05	0.18 ± 0.03	0.17 ± 0	0.03 ± 0.01
Sum of lignin derivatives			2.84 ± 0.37	3.05 ± 1.1	2.93 ± 0.02	2.69 ± 0.28	2.66 ± 0.16	1.94 ± 0.11
Sum of total			*12.7 ± 0.77*	*12.1 ± 2.05*	*12.1 ± 0.09*	*11.1 ± 0.81*	*9 ± 0.06*	*8.2 ± 0.53*
Sugars in bio-oil after acid hydrolysis.								
g/100 g biomass			Control	0.525% O2	1.05% O2	2.10% O2	4.20% O2	8.40% O2
Cellobiosan			0.1 ± 0	0.12 ± 0.04	0.09 ± 0	0.09 ± 0	0.09 ± 0.02	0.07 ± 0
Glucose			4.28 ± 0.06	4.62 ± 0.09	4.48 ± 0.26	4.28 ± 0.23	4.3 ± 0.05	3.39 ± 0.13
Xylose			1.47 ± 0.1	1.38 ± 0.01	1.36 ± 0	1.22 ± 0.01	1.27 ± 0.01	0.95 ± 0.04
Sorbitol			1.67 ± 0.24	2.72 ± 0.31	1.83 ± 0.35	1.92 ± 0.01	1.83 ± 0.07	1.61 ± 0.1
Levoglucosan			0.31 ± 0.02	0.24 ± 0.11	0.26 ± 0.1	0.25 ± 0.06	0.23 ± 0.01	0.27 ± 0.07
Total			7.83 ± 0.71	9.08 ± 0.56	8.03 ± 0.72	7.76 ± 0.32	7.72 ± 0.15	6.29 ± 0.35
Yield of Pyrolytic Lignin in Bio-oil								
g/100 g biomass			Control	0.525% O2	1.05% O2	2.10% O2	4.20% O2	8.40% O2
			15.75 ± 0.29	13.75 ± 1.32	12.30 ± 0.25	11.23 ± 0.23	10.94 ± 0.70	9.48 ± 0.94
The Properties of Biochars			Control	0.525% O2	1.05% O2	2.10% O2	4.20% O2	8.40% O2
Elemental composition (wt.%)	C		77.14	77.88	75.31	73.70	72.09	69.40
	H		3.44	3.32	3.32	3.18	2.90	2.92
	O (diff.)		19.20	18.59	21.17	22.88	24.74	27.40
	N		0.22	0.22	0.21	0.24	0.28	0.28
HHV (MJ/kg)			27.74	27.92	26.66	25.66	24.42	23.15

Table 2. Autothermal pyrolysis bio-oil composition data table recreated from Amutio et al. [52].

Compound			0	15	25
acids			2.73	3.72	3.84
	formic acid		0.17	0.31	0.28
	acetic acid		1.11	0.54	0.67
	propanoic acid		0.14	0.4	0.29
	dimethylbenzoic acids		0.26	0.38	0.62
alcohols			2	2.07	1.86
	methanol		0.69	0.47	0.49
	glycerin		1.11	1.36	1.09
aldehydes			1.93	2.21	1.7
	formaldehyde		0.35	0.82	0.72
	acetaldehyde		0.16	0.15	0.13
	2-propenal		0.12	0.05	0.05
	benzaldehydes		0.49	0.55	0.24
furans			3.32	3.46	2.89
	furan		0.71	0.42	0.2
	2-furanmethanol		0.75	1.27	1.16
	tetrahydro 2-furanmethanol		1.17	0.38	0.09
ketones			6.44	7.52	6.37
	acetone		0.67	0.02	0.02
	acetol		1.53	1.37	0.92
	cyclopentanediones		0.52	0.98	0.89
	cyclohexanone		1.23	0.95	0.68
	hydroxymethoxyphenyl ketones		1.09	1.51	1.6
phenols			16.49	13.45	15.31
	alkyl phenols		1.8	2.16	2.21
		phenol	0.4	0.26	0.26
		cresols	0.67	1.4	1.34
	catechols		7.16	4.5	3.93
		catechol	4.08	2.25	1.6
		methyl catechols	2.4	1.05	0.98
	guaiacols		7.48	6.65	9.04
		guaiacol	1.86	0.58	1.21
		eugenol	1.4	2.04	2.79
saccharides			4.46	0.37	0.35
	2,3-anhydro-d-mannosan		1.56	0	0
	levoglucosan		2.78	0.37	0.35
others			0.06	0.74	0.78
unidentified			12.61	16.35	15.13
total organic			49.97	48.33	46.93
water			25.36	35.97	43.22
bio-oil			75.33	84.3	90.15

Table 3. Autothermal pyrolysis bio-oil composition data table recreated from Amutio et al. Continued [52].

Model Compound Non-Oxidative vs. Oxidative Pyrolysis Peak Areas			*Non-Oxidative Pyrolysis*	*Oxidative Pyrolysis*	
Model	**Pyrolysis Product**	**MS-Elution Time (min)**	**FID Average Peak Area (μV*s)**	**FID Average Peak Area (μV*s)**	**Yield during Ox. Py.**
Benzylphenyl Ether (BPE)	Benzene	8-8.2	2990 ± 1076	3401 ± 791	Insig. Dif.
	Toluene	11.2-11.4	2731 ± 231	2820 ± 882	Insig. Dif.
	Benzaldehyde	21	15626 ± 2921	41811 ± 7929	Greater
	Phenol	24.8	64491 ± 4390	71294 ± 2757	Insig. Dif.
	Bibenzyl	36.15	82821 ± 5998	71361 ± 17675	Insig. Dif.
	Dibenzofuran	36.75	885 ± 534	1622 ± 233	Insig. Dif.
	o/p-methylphenyl phenyl ether	38	833952 ± 111715	824536 ± 63068	Insig. Dif.
	2/3-hydroxybenzophenone	38.6	0 ± 0	1065 ± 156	Greater
	2/3-hydroxybenzophenone	41.56	1577 ± 375	2876 ± 394	Greater
	o/p-benzylphenol	41.9	37809 ± 10692	11203 ± 1684	Less
	o/p-benzylphenol / 1-methyl-2-phenoxy-benzene	44	17397 ± 7123	10017 ± 566	Insig. Dif.
	Xanthone / 4-hydroxy-9-flourenone / p-phenoxystyrene	45	1417 ± 1181	2140 ± 434	Insig. Dif.
1-benzyoxy-2-methoxybenzene (TCRS-237)	CO2	4.5	1135 ± 168	4199 ± 896	Greater
	mass 43	4.9	0 ± 0	2944 ± 490	Greater
	mass 68	5.4	0 ± 0	3676 ± 167	Greater
	mass 55	5.8	0 ± 0	3187 ± 123	Greater
	Benzene	8.3	5967 ± 2211	43684 ± 1480	Greater
	Toluene	11.4	30909 ± 5845	22962 ± 574	Less
	Ethylbenzene	14.7	11759 ± 2801	1952 ± 94	Less
	Styrene	16.3	1717 ± 243	2818 ± 174	Greater
	methoxybenzene	17.7	1192 ± 327	1915 ± 62	Greater
	mass 54	20.1	0 ± 0	1666 ± 2666	Insig. Dif.
	Benzoin	20.83	9478 ± 4407	204031 ± 6989	Greater
	2/3/4-hydroxybenzaldehyde	23.4	229931 ± 53695	94982 ± 4472	Less
	Phenol	24.5	25023 ± 5771	53702 ± 1842	Greater
	2-methoxy phenol	25.1	112004 ± 715	75053 ± 3606	Less
	2-methyl phenol	26	19998 ± 4182	3538 ± 94	Less
	Unknown	26.6	0 ± 0	2678 ± 190	Greater
	3-phenyl-2-propenal = E-Cinnamaldehyde	29.8	0 ± 0	23913 ± 1563	Greater
	2-methoxy benzaldehyde	30.2	1381 ± 419	6676 ± 363	Greater
	1,2/4-benzenediol	31.3	0 ± 0	7429 ± 99	Greater
	1,2/4-benzenediol	33.1	0 ± 0	10450 ± 1277	Greater
	Bibenzyl	35.7	441061 ± 80588	129345 ± 3386	Less
	BPE	37.4	1658 ± 391	7441 ± 200	Greater
	Fluorene	38.24	1434 ± 556	1542 ± 66	Insig. Dif.
	1-benzyloxy-2-methylbenzene	39	4001 ± 554	3633 ± 122	Insig. Dif.
	4-benzylacetophenone (maybe)	40.4	9247 ± 1619	15583 ± 895	Greater
	4-benzyloxybenzyl alcohol	42.2	45139 ± 9014	9875 ± 222	Less
	2-benzylphenol	42.4	56684 ± 10948	13884 ± 1175	Less
Diphenyl Ether (DPE)	DPE	9.2	956565 ± 676741	1209137 ± 101989	Insig. Dif.
Bibenzyl (BB)	Benzaldehyde	20.4	0 ± 0	3733 ± 1623	Greater
	Bibenzyl	35.7	1573859 ± 179526	1382080 ± 48450	Insig. Dif.
	Stilbene (cis/trans)	40.6	3722 ± 437	7621 ± 3983	Insig. Dif.
	Phenanthrene/Anthracene	42.8	2519 ± 663	1510 ± 895	Insig. Dif.
Diphenyl Methane (DPM)	DPM	34	1151577 ± 799530	540430 ± 115786	Insig. Dif.
	BiBenzyl	36.25	957 ± 718	518 ± 145	Insig. Dif.
	1-methyl-2/3/4-(phenylmethyl) benzene	36.5	371 ± 264	213 ± 20	Insig. Dif.
	Benzophenone	40.2	52476 ± 7222	67374 ± 19016	Insig. Dif.
	Fluorenone	43.3	1173 ± 329	1013 ± 344	Insig. Dif.
	Phenanthrene	43.8	5676 ± 8143	149 ± 79	Insig. Dif.
2-Phenoxy-1-phenylethanol "PE Alcohol" (PP-EOL)	Styrene	16.5	14226 ± 4786	7635 ± 2545	Insig. Dif.
	Benzaldehyde	20.4	5489 ± 1780	23890 ± 9063	Greater
	ethoxy-benzene	20.6	0 ± 0	6332 ± 6937	Insig. Dif.
	Phenyl-acetaldehyde	23.4	32126 ± 2299	32863 ± 2114	Insig. Dif.
	Phenol	24.2	5225 ± 1504	7145 ± 2674	Insig. Dif.
	Benzoylformic acid/2,2-dihydroxy-1-phenyl-ethanone	24.3	42081 ± 6676	56857 ± 7612	Greater
	3/4-hydroxystilbene	39.4	11043 ± 977	16744 ± 646	Greater
	p-Phenoxystyrene/4-Hydroxystilbene	40.3	187145 ± 5591	136862 ± 10104	Less
	p-Phenoxystyrene/4-Hydroxystilbene	40.8	1501 ± 637	881 ± 194	Insig. Dif.
	2/4-Methylphenyl benzoate	44.3	11405 ± 2101	19309 ± 7446	Insig. Dif.
	2-Phenoxy-1-phenylethanol (PEA)	44.7	828119 ± 130891	771437 ± 40210	Insig. Dif.

Table 4. Autothermal pyrolysis bio-oil composition data table recreated from Amutio et al. continued [52].

	Dioxoloane	7.5	4251 ± 421	4036 ± 550	Insig. Dif.
	Acetic Acid	10	43792 ± 1468	39806 ± 2415	Less
	Acetic Anhydride/1-hydroxy-2-propanone/Acetaldehyde	14.4	2334 ± 682	1551 ± 183	Insig. Dif.
	Furfual/3-furaldehyde	16.6	2202 ± 127	2343 ± 305	Insig. Dif.
	Phenol	24.2	30391 ± 1428	13735 ± 1562	Less
	2-methoxyphenol	24.8	1765 ± 128	0 ± 0	Less
	2/3/4-methyl-phenol	26.9	3786 ± 324	1008 ± 43	Less
	2-methoxy-4-methylphenol	27.8	68090 ± 3339	29106 ± 3516	Less
	3,5-dimethoxy-toluene	29.2	2285 ± 118	1143 ± 39	Less
	3,4-dimethoxy-toluene	29.6	4847 ± 242	1353 ± 47	Less
	4-ethyl-2-methoxyphenol	30.1	12841 ± 558	5454 ± 50	Less
	2-methoxy-4-vinylphenol	31.6	50668 ± 2144	28287 ± 2366	Less
	Eugenol	32.2	9712 ± 427	5828 ± 331	Less
	2,6-dimethoxyphenol	33	58022 ± 3619	27000 ± 1550	Less
	2-methoxy-3/4-propenyl-phenol	33.6	7314 ± 275	5413 ± 278	Less
	3-(Hydroxymethyl)-5-methoxyphenol	34	6085 ± 377	2946 ± 281	Less
	2-methoxy-3/4-propenyl-phenol	35.1	38477 ± 1794	19867 ± 1374	Less
	1,2,4-Trimethoxybenzene	35.25	106721 ± 4776	43049 ± 3742	Less
RO-MWL	Vanillin	35.6	23979 ± 1169	28073 ± 1686	Greater
	2,5-dimethoxybenzoic acid	36.9	9718 ± 2248	5350 ± 3167	Insig. Dif.
	2-methoxy-4-propylphenol	37	16278 ± 769	6748 ± 1578	Less
	3-Methoxy-4-hydroxyacetophenone	37.6	15659 ± 797	11473 ± 833	Less
	2,4-Dimethoxyacetophenone	38.4	51296 ± 2297	22707 ± 3004	Less
	Methoxyeugenol	38.8	27177 ± 1047	11219 ± 1184	Less
	Coniferyl alcohol	39.8	12247 ± 982	8064 ± 1241	Less
	2,6-dimethoxy-4-(2-propenyl)-phenol	40	15542 ± 621	8432 ± 863	Less
	Coniferyl aldehyde	40.9	5660 ± 366	1535 ± 229	Less
	3-hydroxy-4-methoxy-2-(2-propenyl)-benzaldehyde	41.15	5672 ± 373	969 ± 202	Less
	2,6-dimethoxy-4-(2-propenyl)-phenol	41.4	67517 ± 4133	24910 ± 2755	Less
	Homovanillic acid/4-hydroxy-3,5-dimethoxybenzaldehyde	41.9	51297 ± 3923	45825 ± 3939	Insig. Dif.
	1-ethyl-3-(phenylmethyl)-benzene	43	16209 ± 3485	7427 ± 3409	Less
	4'-hydroxy-3',5'-dimethoxy-acetophenone	43.4	31147 ± 2793	20693 ± 2821	Less
	4-(3-hydroxy-1-propenyl)-2-methoxyphenol	43.9	5438 ± 1009	0 ± 0	Less
	2,5-dimethoxy-, acetate-benzenemethanol	44.2	29962 ± 3297	19177 ± 1733	Less
	4'-hydroxy-3',5'-dimethoxy-acetophenone	44.9	7539 ± 715	3918 ± 246	Less
	3,5-Dimethoxy-4-hydroxycinnamaldehyde	45.2	15583 ± 3492	8782 ± 2437	Less
	3,5-Dimethoxy-4-hydroxycinnamaldehyde	49.5	44742 ± 6159	23154 ± 3866	Less

Table 5. Data from lignin model and biomass fraction non-oxidative vs. oxidative py-GC.

Sigmacell Cellulose	Acetic Anhydride	5.4-std 5.8-ox	3340 ± 290	14575 ± 4663	Greater
	Propanoic acid	5.8-std 6.0-ox	7548 ± 520	9515 ± 1711	Insig. Dif.
	1-hydroxy-2-propyne	7.6	1164 ± 53	1903 ± 595	Greater
	Acetic Acid	10.1	12314 ± 1344	2818 ± 504	Less
	2-methyl furan	13	915 ± 42	622 ± 118	Less
	2-methyl-2-butenal	14.9	446 ± 27	569 ± 213	Insig. Dif.
	2(5H)-furanone	15.4	2393 ± 117	2802 ± 164	Greater
	3-furaldehyde	15.6	1044 ± 114	647 ± 98	Less
	Furfural	16.5	3416 ± 418	3371 ± 613	Insig. Dif.
	1,4-dione-2-cyclopentene/2H-Pyran-2-one/2-cyclohexen-1-one	19.5	584 ± 45	608 ± 107	Insig. Dif.
	3-pentyn-1-ol	19.8	0 ± 0	353 ± 115	Greater
	1,2-cyclopentadione/cyclohexanone	20.1	1484 ± 154	0 ± 0	Less
	2(5H)-furanone/2-methyl-2-butenal/3,4-dihydro-2H-Pyran-2-one	22	539 ± 16	1402 ± 287	Greater
	3-hydroxy-cyclohexanone	22.7	2007 ± 232	0 ± 0	Less
	2-cyclohexen-1-one	23.1	0 ± 0	550 ± 120	Greater
	2-hydroxy-3-methyl-2-cyclopenten-1-one/3,4-dihydro 2H-Pyran-2-one/3-methyl-1,2-cyclopentanedione/1,2 cyclohexanedione	23.4	350 ± 93	2292 ± 494	Greater
	2,5-dimethyl-4-hydroxy-3(2H)-Furanone	24.8	732 ± 160	0 ± 0	Less
	2,5-Furandicaroxaldehyde	26.4	329 ± 60	435 ± 118	Insig. Dif.
	2,3-anhydro-d-galactosan	30.3	5734 ± 454	2863 ± 731	Less
	3,4-andhydr-d-galactosan/1-(2,2-dimethylcyclopentyl)ethanone	30.6	522 ± 79	1354 ± 226	Greater
	2,3/3,4-anhydro-d-galactosan/mannosan	30.7	711 ± 115	2629 ± 217	Greater
	1,4:3,6-dianhydro-alpha-d-glucopyranose	31.1	1102 ± 79	1435 ± 228	Greater
	beta-lactose (cellobiose?)	31.9	0 ± 0	446 ± 119	Greater
	2,3/3,4-anhydro-d-galactosan/mannosan (not sure which)	32.5	2992 ± 488	1994 ± 343	Less
	beta-lactose (cellobiose?) (unsure which is it)	32.9	800 ± 168	748 ± 95	Insig. Dif.
	2,3/3,4-anhydro-d-galactosan/mannosan (unsure which)	33.8	1065 ± 281	680 ± 177	Insig. Dif.
	Trehalose	34.4	8085 ± 1023	485 ± 317	Less
	3,4-anhydro-d-galactosan/1,5-anhydro-d-mannitol	34.9	6324 ± 800	2527 ± 625	Less
	Vanillin lactoside	35.6	0 ± 0	298 ± 46	Greater
	Levoglucosan	41.1	376703 ± 51488	202818 ± 85542	Less
	2,7-anhydro-L-galactose-heptulofuranose/1,6-anhydro-alpha/beta-d-galatofuranose/maltose	44.2	25022 ± 2292	14390 ± 4481	Less
Xylan	CO2	4	6763 ± 906	6816 ± 646	Insig. Dif.
	2,3-butanedione	5.6	5050 ± 1676	1965 ± 53	Less
	propanedione	7.4	2423 ± 202	1495 ± 135	Less
	1,3-hexadiene-3-ol	7.8	3441 ± 378	1428 ± 115	Less
	Acetic Acid	9.9	2589 ± 435	3935 ± 571	Greater
	2-pentanone	11	6849 ± 561	6880 ± 157	Insig. Dif.
	propanoic acid	13.1	1304 ± 245	972 ± 156	Insig. Dif.
	cyclopentanol	13.5	1788 ± 20	1268 ± 50	Less
	Butanoic acid (possibly)	14.3	3021 ± 345	3116 ± 197	Insig. Dif.
	Furfural	16.5	3454 ± 139	2389 ± 173	Less
	2-methyl-cyclopentenone	18.3	568 ± 59	614 ± 50	Insig. Dif.
	1,2-cyclopentanedione	20	493 ± 26	873 ± 63	Greater
	3-methyl-1,2-cyclopentanedione	22	0 ± 0	507 ± 89	Greater
	2-hydroxy-3-methyl-2-cyclopenten-1-one	23.2	1092 ± 129	1750 ± 109	Greater
	5-hydroxy-2,3-dimethyl-cyclopenten-1-one	23.7	432 ± 44	262 ± 47	Less
	5-methyl-4-hepten-3-one	26.1	730 ± 37	762 ± 49	Insig. Dif.
	***None of the peaks beyond this are identifiable				

All tests run according to following: 500C, 20s, 500µg sample, triplicate

Oxidative Pyrolysis carried out using mixed sweep gas (10% O2, 90% He by vol.)

Standard Pyrolysis used pure helium sweep gas

Table 6. Propagation of error and uncertainty analysis leads to fewer significant differences in comparison.

Subsequent Propagation of Error Analysis
CV=Coefficient of Variation = STDV/avg
0.513% CV (that which will be added on prior to taking square root)

Non-ox.								Ox.							
Avg	STDV	95% CI	Avg	STDV	95% CI	Significant Difference?	Yield during Ox Py	initial-CV	Final-CV	Final-95%CI	initial-CV	Final-CV	Final-95%CI	Significant Difference?	Yield during Ox Py
5967.152	1953.933	2211.042	43665.84	1307.82	1479.91	Yes	Greater	32.745%	57.670%	3894.0649	2.995%	18.731%	9255.07	Yes	Less
30909.22	5165.539	5845.25	22953.07	507.0998	573.8269	Yes	Less	16.712%	41.503%	14516.374	2.209%	16.500%	4285.6519	No	Insignificant
11759.64	2475.926	2801.723	1951.482	83.91214	94.95378	Yes	Less	21.054%	46.441%	6179.9284	4.300%	21.939%	484.47181	Yes	Less
1717.974	214.9521	243.2367	2817.342	154.3308	174.6386	Yes	Greater	12.512%	36.090%	701.61133	5.478%	24.477%	780.33739	No	Insignificant
1192.556	289.8286	327.9659	1915.16	55.12329	62.37672	Yes	Greater	24.303%	49.816%	672.25773	2.878%	18.416%	399.10792	No	Insignificant
0	0	0	0	0	0	No	Insignificant	0.000%	7.164%	0	0.000%	7.164%	0	No	Insignificant
0	0	0	1665.576	2355.48	2665.428	No	Insignificant	0.000%	7.164%	0	0.000%	7.164%	135.02829	Yes	Less
9478.59	3895.226	4407.782	203944.5	6174.045	6986.462	Yes	Greater	41.095%	64.504%	6918.6442	3.027%	18.816%	43424.719	Yes	Less
229931.5	47451.25	53695.16	94941.48	3950.782	4470.649	Yes	Less	20.637%	45.990%	119658.95	4.161%	21.621%	23228.085	No	Insignificant
25023.49	5100.692	5771.87	53679.41	1627.437	1841.585	Yes	Greater	20.384%	45.713%	12944.227	3.032%	18.828%	11436.836	Yes	Less
112004.4	632.0293	715.1953	75021.75	3186.12	3605.367	Yes	Less	0.564%	10.381%	13156.589	4.247%	21.818%	18521.969	Yes	Greater
19998.25	3696.189	4182.555	3537.094	83.09537	94.02953	Yes	Less	18.483%	43.584%	9862.9899	2.349%	16.919%	677.18721	Yes	Less
0	0	0	23902.9	1380.7	1562.381	Yes	Greater	0.000%	7.164%	0	0.000%	7.164%	1937.809	Yes	Less
1381.629	370.706	419.4856	6673.866	320.7636	362.9715	Yes	Greater	26.831%	52.292%	817.54697	4.806%	23.064%	1741.8138	Yes	Less
0	0	0	7426.116	88.09688	99.68917	Yes	Greater	0.000%	7.164%	0	0.000%	7.164%	602.03546	Yes	Less
0	0	0	10445.8	1128.209	1276.665	Yes	Greater	0.000%	7.164%	0	0.000%	7.164%	846.84166	Yes	Less
441061.3	71216.92	80588.05	129290.1	2991.5	3385.139	Yes	Less	16.147%	40.817%	203715.34	2.314%	16.814%	24599.148	Yes	Less
1658.755	345.6164	391.0946	7438.397	177.2049	200.5225	Yes	Greater	20.836%	46.205%	867.28171	2.382%	17.016%	1432.2994	Yes	Less
1434.187	492.1389	556.8973	1542.231	58.30587	65.97809	No	Insignificant	34.315%	59.015%	957.7631	3.781%	20.722%	361.62823	No	Insignificant
4001.253	490.2994	554.8158	3631.729	108.261	122.5066	No	Insignificant	12.254%	35.731%	1617.8061	2.981%	18.693%	768.20597	No	Insignificant
9247.245	1430.918	1619.206	15576.96	791.3715	895.5046	Yes	Greater	15.474%	39.984%	4183.9533	5.080%	23.651%	4168.8705	No	Insignificant
45139.15	7966.636	9014.932	9870.875	196.4374	222.2858	Yes	Less	17.649%	42.617%	21768.407	1.990%	15.822%	1767.2708	Yes	Less
56684.56	9675.754	10948.95	13878.82	1038.448	1175.093	Yes	Less	17.069%	41.932%	26896.484	7.482%	28.276%	4440.8209	Yes	Less